Mesenchymal stem cells in peripheral nerve repair

Strain every nerve

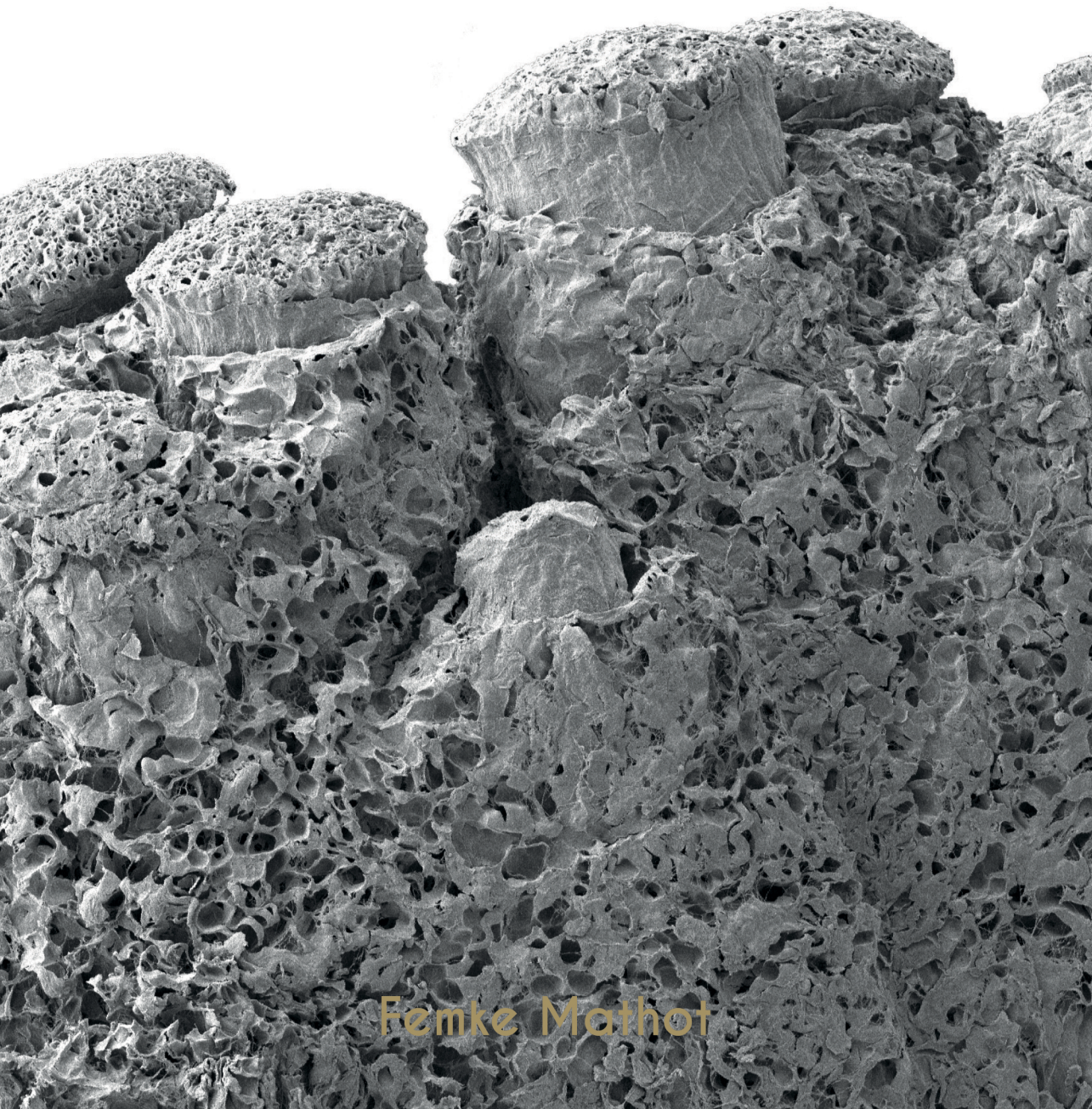

Femke Mathot

Mesenchymal Stem Cells in peripheral nerve repair

Strain every nerve

Femke Mathot

Colofon

Cover design: Design by Loes & Femke Mathot
Printing: Ridderprint BV - www.ridderprint.nl

ISBN: 978-94-6416-621-7

Mesenchymal Stem Cells in peripheral nerve repair

Strain every nerve

Doctoral Thesis

to obtain the degree of doctor

from Radboud University Nijmegen

on the authority of the Rector Magnificus prof. dr. J.H.J.M. van Krieken,

according to the decision of the Council of Deans

to be defended in public on

Friday, September 10, 2021

at 12.30 hours

by

Femke Mathot

born on November 5, 1991

in Boskoop (the Netherlands)

Supervisors:
Prof. dr. S.E.R. Hovius (Erasmus MC)
Prof. dr. D.J.O. Ulrich

Co-supervisor:
Dr. T.H.J. Nijhuis

Doctoral Thesis Committee:
Prof. dr. R.H.M.A. Bartels
Prof. dr. J.H. Coert (UMC Utrecht)
Dr. N. Van Alfen

Paranymphs:
L.J. Mathot
R. Mathot

Mesenchymal Stem Cells in peripheral nerve repair

Strain every nerve

Proefschrift

Ter verkrijging van de graad van doctor

aan de Radboud Universiteit Nijmegen

op gezag van de rector magnificus prof. dr. J.H.J.M. van Krieken,

volgens besluit van het college van decanen

in het openbaar te verdedigen op

vrijdag 10 september 2021

om 12.30 uur precies

door

Femke Mathot

geboren op 5 november, 1991

te Boskoop

Promotoren:
Prof. dr. S.E.R. Hovius (Erasmus MC)
Prof. dr. D.J.O. Ulrich

Copromotor:
Dr. T.H.J. Nijhuis

Manuscriptcommissie:
Prof. dr. R.H.M.A. Bartels
Prof. dr. J.H. Coert (UMC Utrecht)
Dr. N. Van Alfen

Paranimfen:
L.J. Mathot
R. Mathot

Strain every nerve

"To expand a maximum amount of effort to achieve something"

Voor mijn ouders

TABLE OF CONTENTS

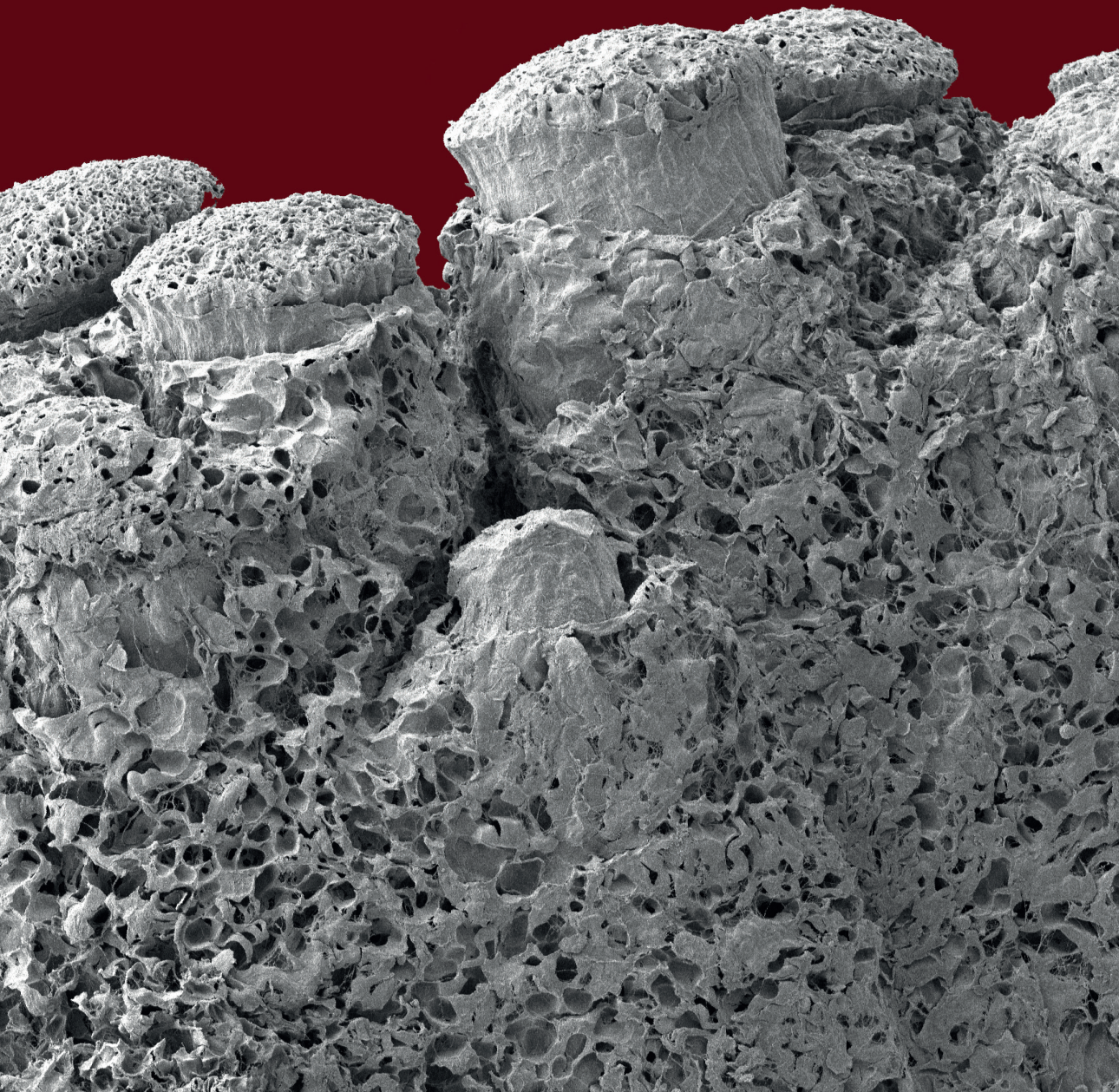

Chapter 1

General introduction and outline of this thesis

BACKGROUND

The brain and the spinal cord together fulfill the role of the central nervous system. In this system, incoming signals are processed and converted into concrete sensations like pain or touching. This system also forms and sends commands to their targets leading to desired actions like muscle contraction, enabling us to walk, talk or eat. The peripheral nervous system facilitates the transfer of the incoming and outgoing signals between the central nervous system and its target (organs). Accurate sensation and muscle control are therefore completely dependent on a fully functional peripheral nervous system.

Due to its crucial function, peripheral nerve injuries can be life-changing events, impacting a patients function, autonomy and quality of life.[1, 2] They occur in 3% of all extremity traumas, most commonly as a result of motor vehicle accidents and penetrating traumas.[3] The socio-economic impact of peripheral nerve injuries is so substantial that maximum efforts should be made to obtain maximal recovery rates.[4] This thesis aims to fulfill a role in the efforts to improve outcomes of peripheral nerve injuries.

ANATOMY

The peripheral nervous system is composed of an extensive network of peripheral nerves. The anatomy of a peripheral nerve is illustrated in **figure 1**. A peripheral nerve is a bundle containing a varying amount of fascicles that are held together by the epineurium, a layer of connective tissue. These fascicles intermingle with each other along the course of the nerve. Each fascicle consists of a bundle of axons, encompassed by layers of perineurial cells and collagen, the perineurium.[5] Each individual axon is surrounded by endoneurium.[6] These extracellular matrix components (epineurium, perineurium and endoneurium) are pivotal in axon guidance and triggering intracellular signals, which should be taken into account when restoring peripheral nerve injuries.[7]

Axons are long, tubular offshoots of nerve cell bodies (neurons). Most neurons have multiple other cytoplasm-protrusions besides the axon, which are much shorter than axons. These so called dendrites receive stimuli from other cells and if stimuli are strong enough, they are converted in the cell body to an electrical stimulus (action potential) which is transmitted by the axon. Most axons branch towards their ends (axon terminals), making connections with other neurons or target cells by synaptic junctions. Action potentials are transmitted through these junctions by the release of neurotransmitters. At a neuromuscular junction this release causes activation of muscle fibers, resulting in muscle contraction. The location of the neuron cell-body and the synaptic junctions of its axon determines its function.[6, 8]

Oxygen and other essential nutrients for the cells and their processes in the peripheral nervous system are provided by diffusion from intrinsic and extrinsic vessels, the vasa nervorum. The extrinsic vasculature runs along the surface of the nerve, supplying the epineural and perineural regions. The internal vasculature is located inside the fascicles, the endoneurial compartment.[9,

[10] Considering its function, optimization of revascularization of repaired peripheral nerves hypothetically forms an opportunity to improve nerve regeneration outcomes.

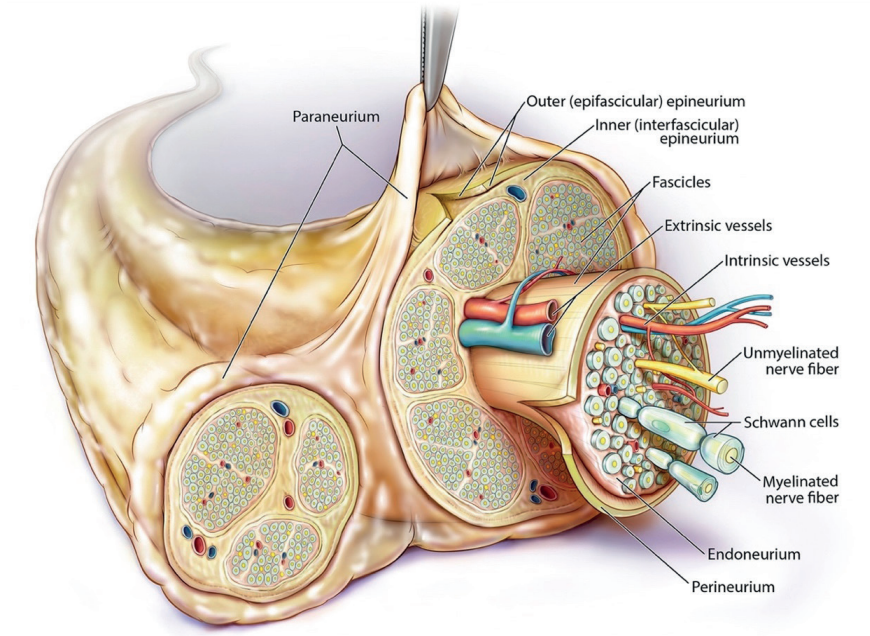

Figure 1. *Cross sectional anatomy of a peripheral nerve.* *(Used with permission of the American Society of Regional Anesthesia and Pain Medicine. All rights reserved.)*

NERVE SUBDIVISIONS

Besides sensory, motor and mixed nerves, the peripheral nervous system can be subdivided in multiple other ways. When studying the direction of the transmitted stimuli, one can distinguish either afferent (towards the central nervous system) and efferent (away from the central nervous system) nerve fibers. Motor fibers are classified as efferent, sensory fibers are mostly afferent. The somatic versus autonomic nervous system are distinguished based on their control mechanism. The somatic system comprises voluntary actions that we can control like the movement of skeletal muscles. Actions of internal organs like cardiac contraction and digestive movements of the colon are involuntary and belong to the autonomic nervous system.[11]

On a axonal level, axon fibers can be subdivided into either myelinated and unmyelinated axons. Myelin, which consist for approximately 80% of lipids, is formed by Schwann cells in the peripheral nervous system. Each Schwann cell wraps around one segment of an axon many times to form a myelin sheet: an internode.[12] The amount of myelin that is formed by the Schwann cells is related to the diameter and the function of the axon and neuron.[13] The gaps between each of the internodes are called nodes of Ranvier and contain many sodium and

potassium channels.[14] As a response to an action potential that is send off from the neuron, these sodium channels open, causing an influx of positive sodium ions that rejuvenate the action potential. Through this mechanism, myelin helps to prevent action potentials from decaying during their travel down the entire length of the axon.[15] The transmitted action potentials are also accelerated by the presence of myelin. Because nodes of Ranvier are not myelinated, the action potentials only slow down at each node, leading to saltatory conduction; 'jumping' propagation of the action potential from node to node.[16] Unmyelinated axons lack the insulating layer of myelin, resulting in less rapid and less efficient transmission of action potentials.[17, 18]

Based on the level of myelination and the conduction velocity, nerve fibers can be divided into three classes by Erlanger and Gasser[19]: group A) heavily myelinated fibers, group B) moderately myelinated fibers, group C) unmyelinated fibers. Group A fibers contain fibers responsible for somatic motoric control, proprioception, vibration, light touch and fast pain. Autonomic nerve fibers belong to group B. Pressure, slow pain, crude touch and temperature are transmitted by group C fibers. The thicker the axon, the thicker the myelin sheath and the faster the nerve conduction velocity.[20] The importance of adequate levels of myelin for each type of nerve fiber is emphasized by diseases like multiple sclerosis, which is caused by demyelination of the central nervous system.[21] Presence of myelinating cells (Schwann cells) at the site of a nerve injury is therefore hypothesized to be crucial for adequate peripheral nerve regeneration.

PATHOPHYSIOLOGY OF NERVE REGENERATION

Seddon, later supplemented by Sunderland, refined a classification concerning the severity of peripheral nerve injury. Grade I, neuropraxia, includes the loss of the myelin sheath, without damage to the axon. When the myelin sheath and the axon are damaged but the nerve casings (endoneurium, perineurium, epineurium) are still intact, one speaks of a grade II nerve injury, axonotmesis. In grade III, (endoneurium) and grade IV (endoneurium and perineurium), the connective tissues surrounding the axons are additionally injured. Grade V is a complete transection of the nerve (myelin, axon, endoneurium, perineurium, epineurium), neurotmesis.[22, 23] Grade VI is a later proposed addition to the classification and describes different grades of injury along the course of the nerve.[24]

In large axon injuries or injuries close to the neuron cell body, neuron death can occur. In cases with axonal injury distant from the neuron, axons are able to regenerate. Considering their complex composition, injured peripheral nerves require complex recovery processes to restore their function. This starts with Wallerian degeneration; damaged cells die by apoptosis and axonal and myelin debris distal to the injury is phagocytosed by activated macrophages.[25] Part of the damaged and nearby lying Schwann Cells change their gene and protein expression, resulting in non-myelinating, proliferating Schwann Cells.[26, 27] Wallerian degeneration blends into nerve regeneration when the neurons, macrophages and Schwann

cells start secreting trophic factors as a response to the injury.[13, 28, 29] A so called growth cone is formed at the proximal nerve stump.[30, 31] Angiogenic trophic factors (like VEGF-a) stimulate angiogenesis, which provides the needed oxygen and nutrients to align the proliferating Schwann cells in 'Bands of Büngner'.[32, 33] These bands guide regenerating axons, enhanced by neurotrophic factors (like NGF, BDNF, GDNF) that are produced by Schwann cells and neurons, in the right direction.[34] Extracellular matrix components are rebuild as a result of the expression and secretion of extracellular matrix proteins by Schwann cells.[28] Eventually, remyelination and reinnervation occurs and the phenotype of Schwann cells is reversed back to a myelinating phenotype.[35] This process is illustrated in **figure 2**. Presence of angiogenic trophic factors, neurotrophic factors and extracellular matrix proteins at the regenerating nerve stump facilitates axon regeneration and should therefore be considered as target to improve outcomes of nerve injuries.

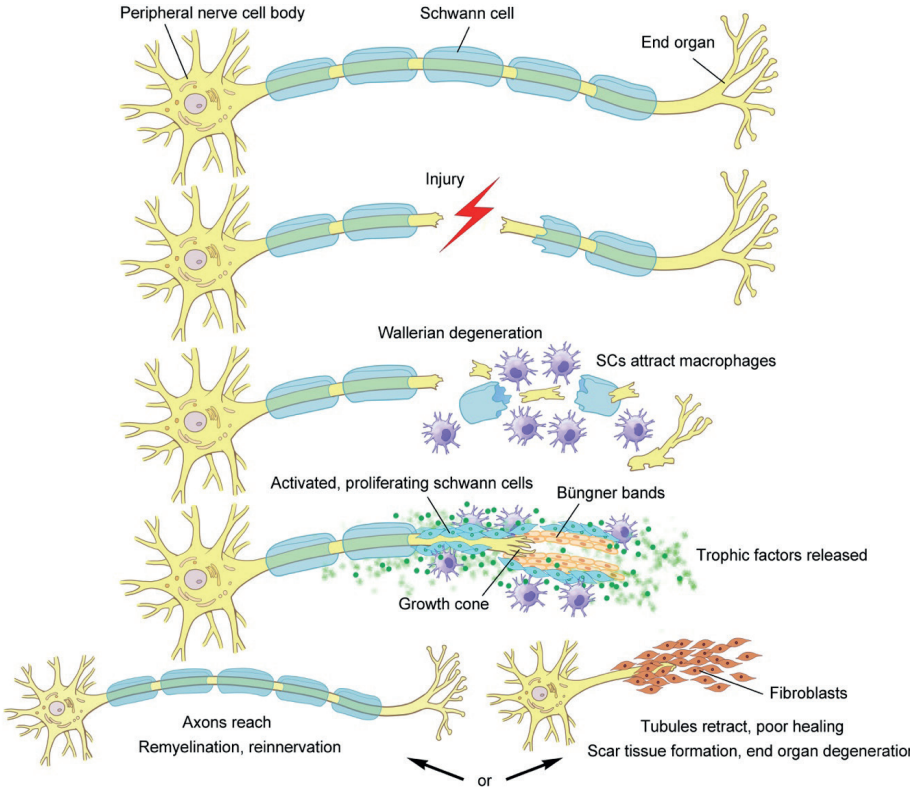

Figure 2. The process of Wallerian degeneration and nerve regeneration. After nerve injury, activated macrophages phagocytose the axonal and myelin debris. Activated Schwann cells, macrophages and neurons secrete trophic factors that initiate the formation of Bands of Bügner, resulting in axon regeneration. Absence of those essential factors can lead to poor nerve regeneration, scar tissue formation and end organ degeneration. (Used with permission of Mayo Foundation for Medical Education and Research, all rights reserved.)

NERVE RECONSTRUCTION OPTIONS & SHORTCOMINGS

The described process occurs in the first days to weeks after peripheral nerve injury. With a regeneration speed of 1-3mm per day, axon regeneration in proximal nerve injuries can take up to months before the target muscle is reached.[36, 37] The critical time frame for nerve regeneration to occur is 12-18 months after the nerve injury.[38] Delayed regeneration leads to worse or absent functional outcomes, which is attributed to 1) degeneration of synaptic acetylcholine receptors which leads to less receptiveness of muscle fibers for reinnervation, 2) difficulty to recover from muscle denervation atrophy that increases as denervation time extends [39] and 3) deterioration of the endoneurial tubes in the distal nerve stumps, leading to less guidance and less axons that successfully reach the denervated muscle fibers.[40, 41] Maximal nerve regeneration efficiency/speed should be pursued to obtain maximal functional outcomes.

Spontaneous successful reinnervation after a peripheral nerve injury depends on the severity of nerve injury, representing the degree of internal disorganization. Neuropraxia, axonotmesis and incomplete nerve lesions have good prospects for axon regeneration when treated conservatively.[38] More extensive lesions or complete transections most often do not spontaneously lead to acceptable outcomes. Therefore, spontaneous nerve regeneration is sometimes awaited in closed, blunt trauma cases, while sharp transection nerve injuries are preferably surgically restored within 72 hours.[38, 42] The severity of the nerve injury, the time elapsed since the injury and the distance between the proximal nerve stump and the target muscle should all be considered when deciding to operate on a peripheral nerve injury.

Direct coaptation of both nerve ends by suturing the epineurium is the preferred surgical restoration technique, but only if this can be obtained in a tension-free manner. When this condition cannot be met, one can use nerve grafts (autologous or allogenous) or conduits (natural or synthetic) to bridge the nerve gap.

Autografts

Nerve autografts are currently used as the gold standard in peripheral nerve repair.[43] They are readily available, provide Schwann Cells and other important neurotrophic factors, contain the desired ultrastructure to guide regenerating axons and are immunologically inert. Unfortunately, autografts require the sacrifice of autologous nerves which are limited available and can result in donor side morbidity like loss of sensation or painful neuroma formation.[44, 45] Especially in big nerve branch injuries or multiple injured nerves, autograft sources fall short to restore all defects, emphasizing the need for autograft substitutes that result in equal functional outcomes.

Allografts

Efforts to replace the role of autografts have led to the development of allogenous nerve grafts, currently the second-best option in cases with extensive peripheral nerve injuries.[46, 47] To eliminate immune rejection of the allograft, techniques to decellularize the donor nerves have been studied. This decellularization process leads to the loss of Schwann cells

and important neurotrophic factors, but retains the ultrastructure of the nerve. Since 2007, only one decellularized nerve allograft has been FDA approved and is currently readily available in daily clinical practice. Although sensory nerve gaps have been successfully repaired with these Avance® Nerve Grafts, reported outcomes of long segment, large diameter and mixed and motor nerve gaps are consistently inferior to that of autografts.[43, 46, 48] Absence of Schwann cells, intrinsic angiogenic trophic factors, neurotrophic factors and extracellular matrix proteins are hypothesized to cause the inferiority of allografts.

Conduits

Natural conduits like veins have been used to bridge peripheral nerve gaps in the past, but synthetic conduits have gained more scientific and clinical interest over the years. The NeuraGen® Nerve Guide is a collagen type 1 conduit that was FDA approved in 2001.[49] Conduits lack Schwann cells, a guiding ultrastructure and angiogenic and neurotrophic factors. They have only led to satisfactory outcomes in small-caliber sensory nerve gaps up to 3cm.[50, 51]

MESENCHYMAL STEM CELLS

Schwann cells, the guiding ultrastructure (particularly in conduits), angiogenic and neurotrophic factors are removed in nerve allografts and conduits. Replacing these components is logically suggested as the solution to enhance outcomes of allografts and conduits to a level equal to that of autografts. As described, Schwann cells fulfill a key role in multiple processes during Wallerian degeneration, axon regeneration and stimulus transmission, by producing neurotrophic, angiogenic and extracellular matrix factors and by forming myelin.[32] Therefore Schwann cells are considered as the obvious required supplementation to the listed autograft substitutes. Although Schwann cells did demonstrate potential as nerve regeneration catalysts, they need to be derived from nerve tissue. Thus their use requires the sacrifice of an autologous nerve; exactly what is intended to be prevented when using nerve autograft substitutes.[52, 53] Mesenchymal stem cells (MSCs) are precursor cells used in numeral medical fields due to their trophic characteristics and differentiation capacities. Environmental signals influence MSCs to produce trophic factors or to differentiate into specific cell types, tailored to the surrounding regenerating tissue.[52, 54, 55] The use of these MSCs as a supplementation to the previously described nerve autograft substitutes is a hopeful research topic.[56, 57] Differentiation of MSCs into Schwann cell-like cells prior to implementation in peripheral nerve injuries is also a suggested strategy to replace the missing Schwann cells. Although this concept is supported by several in vitro studies, in vivo outcomes still need to show if this strategy is cost- and time-efficient.[52, 58, 59] Mesenchymal stem cells can be obtained from mesenchymal tissues like dental pulp, bone marrow and adipose tissue. In contradiction to dental pulp and bone marrow, adipose tissue is easily and less invasively accessible. Higher MSC-yields and rapid proliferation in culture are additional benefits of adipose derived MSCs.[60-63]

PREVIOUS RESEARCH

Optimization of processed nerve allografts

In studies performed prior to this thesis, the focus first was on optimization of nerve allograft processing/decellularization techniques. Histological analysis of Avance® nerve grafts revealed remaining cellular debris in the grafts, potentially leading to immunologic responses or blockage of ingrowing axons. In an effort to improve these aspects, elastase was added to the decellularization protocol. Elastase demonstrated to significantly reduce the amount of cellular debris and immunogenicity of nerve allografts. Subsequently, cold storage (4°C) of decellularized nerve allografts resulted in a less damaged ultrastructure of the grafts compared to frozen storage (-80°C) techniques.[64] Elastase-processed, cold stored allografts demonstrated improved functional outcomes in a rodent model compared to frozen stored allografts that were decellularized without elastase. In a bigger nerve defect model (rabbit) however, autografts still outperformed these optimized decellularized nerve allografts.[65]

Mesenchymal stem cells

To be able to test if MSCs can supplement decellularized allografts and conduits, a delivery technique needed to be defined that would not be traumatic to either the MSCs or the nerve substitute, in contradiction to previously described injection techniques.[66] Even distribution of MSCs and an efficient method were additional requirements. Dynamic seeding, by which MSCs are rotated in the presence of a decellularized nerve allograft, led to a nontraumatic, homogenously distributed attachment of MSCs to the surface of nerve allografts.[67] The process of decellularizing allografts and seeding them with MSCs in a rat model is illustrated in figure 3. The interaction between MSCs and the extracellular matrix of the nerve allografts led to enhanced expressions of multiple trophic genes in vitro, which was partly confirmed by quantification of the produced trophic factors.[68] Taking this seeding strategy to an in vivo rodent model, it was shown that the seeded MSCs survived up to 29 days and that the MSCs did not migrate to surrounding tissues.[69] It also led to enhanced expressions of angiogenic factors.[70] It would therefore be interesting to not only study the long term functional outcomes after nerve repair with MSC-seeded allografts, but also to analyze if the MSCs improve vascularization of the nerve allografts.

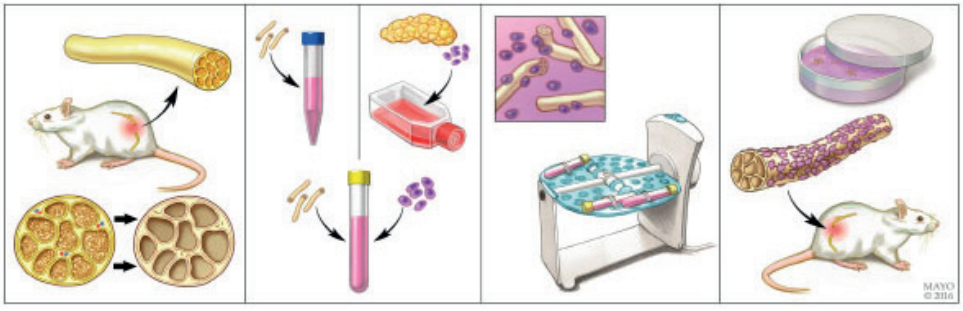

Figure 3. *Nerve harvest, decellularization and seeding techniques.* *(Used with permission of Mayo Foundation for Medical Education and Research, all rights reserved.)*

Evaluation methods

Many different evaluation techniques have been described to quantify the level of nerve regeneration. Histology enables us to analyze the inside of the nerve. Stained ultrathin sections of nerves reveal information about the number of axons, the axon area, the myelinated fiber area and the total nerve area. The N-ratio, which is composed of the total myelinated fiber area divided by the total nerve area, is an often used measure to express the amount of sprouting axons.[71]

Nerve conduction capacities can be quantified by electrophysiology, compound muscle action potentials (CMAP). An artificial action potential is evoked proximal to the nerve graft. The amplitude of that signal is measured in the muscle distal to the nerve graft. The bigger the amplitude of the distally measured signal, the better the nerve regeneration process has occurred.[65, 72]

Although one could argue if histology and electrophysiology measurements are direct or indirect measures of nerve regeneration, muscle function represents the most relevant outcome factor for motion. Isometric tetanic force has been described to most reliably represent muscle function and has been validated in rodent models. A stimulus is introduced to the nerve graft, and the resulting muscle contraction force is quantified.[73]

As denervation of a muscle will result in muscle atrophy and shrinking of the muscle, the size and mass of a muscle after nerve reconstruction also provide information on successful reinnervation. Although the muscle mass is easy to obtain, it does require the sacrifice of the animal. Ultrasound measurements of the cross-sectional area of (re)innervated muscles can be obtained non-invasively and can therefore be used to study nerve regeneration over time.[74, 75]

GENERAL AIMS AND OUTLINE OF THIS THESIS

The ideal future perspective is an off-the-shelf nerve substitute that can be used in peripheral nerve injuries, resulting in functional outcomes equal to those of autograft nerves. The specific aim of this thesis was to examine whether the in vivo outcomes of nerve allografts and conduits can be improved by the addition of adipose derived Mesenchymal Stem Cells, either undifferentiated or differentiated into Schwann cell-like cells. If so, MSC seeding might have clinical potential in peripheral nerve injury cases with shortage or inadequate autologous nerve graft material. As part of this objective we aimed to get more insight through which mechanisms these cells potentially influence nerve regeneration. We first intended to examine in vitro if and how differentiated MSCs could be dynamically seeded on nerve grafts and then we aimed to study the gene expression profiles of the seeded MSCs. Subsequently, we set the goal to analyze the in vivo effects of MSCs regarding vascularity and functionality. This hopefully would give us the opportunity to be able to explain if and how MSCs affect nerve regeneration. In order to evaluate if the described techniques can be applicable to a clinical setting, we eventually aimed to dynamically

seed human MSCs on human nerve grafts or on clinically available nerve substitutes and to analyze their gene expression profiles after seeding; hopefully setting the stage for clinical application somewhere in the near future.

As preliminary step for the other chapters, the current knowledge on differentiation of MSCs into Schwann cell-like cells is summarized in **chapter 2**. It sets the fundament of why differentiated MSCs deserve to be studied in the perspective of peripheral nerve repair, besides undifferentiated MSCs. The ability of differentiated MSCs to be dynamically seeded onto processed nerve allografts like undifferentiated MSCs is examined and described in **chapter 3**, enabling a fair comparison of the in vitro and in vivo potential of both cell types. Gene expression profile changes of differentiated and undifferentiated MSCs after seeding on nerve allografts, affected by the extracellular matrix of the nerve allograft, are studied at various time points after seeding in **chapter 4**. As revascularization is hypothesized to be an essential factor for successful nerve regeneration, we first tested and validated new evaluation strategies for nerve vascularization in **chapter 5**. In **chapter 6**, this is extrapolated to an in vivo study in which the level of vascularization in nerve allografts seeded with differentiated and undifferentiated MSCs is quantified and compared to the vascularization of unseeded allografts, autografts and normal nerves. The potential of differentiated and undifferentiated stem cell seeding to improve functional outcomes after peripheral nerve repair is studied in a rat sciatic nerve defect model in **chapter 7**. Functional results of MSC-seeded nerve allografts are compared to unseeded allografts and autografts over time and at two long term end points. To translate the described strategies to a more clinically applicable model, the study in **chapter 8** focuses on the potential of human MSCs to be seeded onto clinically available nerve graft substitutes. The consequences of the interaction between the MSCs and the extracellular matrix of the nerve graft substitutes on a gene expression level are studied and described in **chapter 9**. In **chapter 10**, the acquired results of all chapters are related to each other, discussed and placed in a broader perspective. An English and a Dutch summary are provided in **chapter 11**.

REFERENCES

1. Landers ZA, Jethanandani R, Lee SK, et al. The Psychological Impact of Adult Traumatic Brachial Plexus Injury. J Hand Surg Am 2018: 43: 950.e1-50.e6.
2. Wojtkiewicz DM, Saunders J, Domeshek L, et al. Social impact of peripheral nerve injuries. Hand (N Y) 2015: 10: 161-7.
3. Noble J, Munro CA, Prasad VS, Midha R. Analysis of upper and lower extremity peripheral nerve injuries in a population of patients with multiple injuries. J Trauma 1998: 45: 116-22.
4. Hong TS, Tian A, Sachar R, et al. Indirect Cost of Traumatic Brachial Plexus Injuries in the United States. J Bone Joint Surg Am 2019: 101: e80.
5. Stewart JD. Peripheral nerve fascicles: anatomy and clinical relevance. Muscle Nerve 2003: 28: 525-41.
6. King R. Microscopic anatomy: normal structure. Handb Clin Neurol 2013: 115: 7-27.
7. Chen P, Cescon M, Bonaldo P. The Role of Collagens in Peripheral Nerve Myelination and Function. Mol Neurobiol 2015: 52: 216-25.
8. Muzio MR, Cascella M. Histology, Axon. In StatPearls. Treasure Island (FL): StatPearls Publishing StatPearls Publishing LLC., 2020.
9. Muangsanit P, Shipley RJ, Phillips JB. Vascularization Strategies for Peripheral Nerve Tissue Engineering. Anat Rec (Hoboken) 2018: 301: 1657-67.
10. Best TJ, Mackinnon SE. Peripheral nerve revascularization: a current literature review. J Reconstr Microsurg 1994: 10: 193-204.
11. Menorca RM, Fussell TS, Elfar JC. Nerve physiology: mechanisms of injury and recovery. Hand Clin 2013: 29: 317-30.
12. Salzer JL. Schwann cell myelination. Cold Spring Harb Perspect Biol 2015: 7:a020529.
13. Kidd GJ, Ohno N, Trapp BD. Biology of Schwann cells. Handb Clin Neurol 2013: 115: 55-79.
14. Hernandez Fustes OJ, Kay CSK, Lorenzoni PJ, et al. 140 Years of the Lecons sur l'histologie du systeme nerveux: the pioneering description of the nodes of Ranvier. Arq Neuropsiquiatr 2019: 77: 749-51.
15. Suminaite D, Lyons DA, Livesey MR. Myelinated axon physiology and regulation of neural circuit function. Glia 2019: 67: 2050-62.
16. Huxley AF, Stampfli R. Evidence for saltatory conduction in peripheral myelinated nerve fibres. J Physiol 1949: 108: 315-39.
17. Seidl AH. Regulation of conduction time along axons. Neuroscience 2014: 276: 126-34.
18. Carroll SL. The Molecular and Morphologic Structures That Make Saltatory Conduction Possible in Peripheral Nerve. J Neuropathol Exp Neurol 2017: 76: 255-57.
19. Perl E. The 1944 Nobel Prize to Erlanger and Gasser. Faseb j 1994: 8: 782-3.
20. Michailov GV, Sereda MW, Brinkmann BG, et al. Axonal neuregulin-1 regulates myelin sheath thickness. Science 2004: 304: 700-3.
21. Pollock M, Calder C, Allpress S. Peripheral nerve abnormality in multiple sclerosis. Ann Neurol 1977: 2: 41-8.
22. Sunderland S. A classification of peripheral nerve injuries producing loss of function. Brain 1951: 74: 491-516.
23. Seddon HJ. A Classification of Nerve Injuries. Br Med J 1942: 2: 237-9.
24. Dellon AL, Mackinnon SE. Basic scientific and clinical applications of peripheral nerve regeneration. Surg Annu 1988: 20: 59-100.
25. Chen P, Piao X, Bonaldo P. Role of macrophages in Wallerian degeneration and axonal regeneration after peripheral nerve injury. Acta Neuropathol 2015: 130: 605-18.
26. Stoll G, Muller HW. Nerve injury, axonal degeneration and neural regeneration: basic insights. Brain Pathol 1999: 9: 313-25.
27. Parkinson DB, Bhaskaran A, Arthur-Farraj P, et al. c-Jun is a negative regulator of myelination. J Cell Biol 2008: 181: 625-37.

28. Bosse F. Extrinsic cellular and molecular mediators of peripheral axonal regeneration. Cell Tissue Res 2012: 349: 5-14.
29. Fu SY, Gordon T. The cellular and molecular basis of peripheral nerve regeneration. Mol Neurobiol 1997: 14: 67-116.
30. Lowery LA, Van Vactor D. The trip of the tip: understanding the growth cone machinery. Nat Rev Mol Cell Biol 2009: 10: 332-43.
31. Geraldo S, Gordon-Weeks PR. Cytoskeletal dynamics in growth-cone steering. J Cell Sci 2009: 122: 3595-604.
32. Jessen KR, Mirsky R. The repair Schwann cell and its function in regenerating nerves. J Physiol 2016: 594: 3521-31.
33. Cattin AL, Burden JJ, Van Emmenis L, et al. Macrophage-Induced Blood Vessels Guide Schwann Cell-Mediated Regeneration of Peripheral Nerves. Cell 2015: 162: 1127-39.
34. Gordon T. The role of neurotrophic factors in nerve regeneration. Neurosurg Focus 2009: 26: E3.
35. Caillaud M, Richard L, Vallat JM, Desmouliere A, Billet F. Peripheral nerve regeneration and intraneural revascularization. Neural Regen Res 2019: 14: 24-33.
36. Wujek JR, Lasek RJ. Correlation of axonal regeneration and slow component B in two branches of a single axon. J Neurosci 1983: 3: 243-51.
37. Buchthal F, Kuhl V. Nerve conduction, tactile sensibility, and the electromyogram after suture or compression of peripheral nerve: a longitudinal study in man. J Neurol Neurosurg Psychiatry 1979: 42: 436-51.
38. Campbell WW. Evaluation and management of peripheral nerve injury. Clin Neurophysiol 2008: 119: 1951-65.
39. Li L, Yokoyama H, Kaburagi H, et al. Remnant neuromuscular junctions in denervated muscles contribute to functional recovery in delayed peripheral nerve repair. Neural Regen Res 2020: 15: 731-38.
40. Fu SY, Gordon T. Contributing factors to poor functional recovery after delayed nerve repair: prolonged denervation. J Neurosci 1995: 15: 3886-95.
41. Scheib J, Hoke A. Advances in peripheral nerve regeneration. Nat Rev Neurol 2013: 9: 668-76.
42. Bassilios Habre S, Bond G, Jing XL, et al. The Surgical Management of Nerve Gaps: Present and Future. Ann Plast Surg 2018: 80: 252-61.
43. Rbia N, Shin AY. The Role of Nerve Graft Substitutes in Motor and Mixed Motor/Sensory Peripheral Nerve Injuries. J Hand Surg Am 2017: 42: 367-77.
44. FF IJ, Nicolai JP, Meek MF. Sural nerve donor-site morbidity: thirty-four years of follow-up. Ann Plast Surg 2006: 57: 391-5.
45. Hallgren A, Bjorkman A, Chemnitz A, Dahlin LB. Subjective outcome related to donor site morbidity after sural nerve graft harvesting: a survey in 41 patients. BMC Surg 2013: 13: 39.
46. Whitlock EL, Tuffaha SH, Luciano JP, et al. Processed allografts and type I collagen conduits for repair of peripheral nerve gaps. Muscle Nerve 2009: 39: 787-99.
47. Brooks DN, Weber RV, Chao JD, et al. Processed nerve allografts for peripheral nerve reconstruction: a multicenter study of utilization and outcomes in sensory, mixed, and motor nerve reconstructions. Microsurgery 2012: 32: 1-14.
48. Leckenby JI, Furrer C, Haug L, Juon Personeni B, Vogelin E. A Retrospective Case Series Reporting the Outcomes of Avance Nerve Allografts in the Treatment of Peripheral Nerve Injuries. Plast Reconstr Surg 2020: 145: 368e-81e.
49. Meek MF, Coert JH. US Food and Drug Administration /Conformit Europe- approved absorbable nerve conduits for clinical repair of peripheral and cranial nerves. Ann Plast Surg 2008: 60: 466-72.
50. Rbia N, Bulstra LF, Saffari TM, Hovius SER, Shin AY. Collagen Nerve Conduits and Processed Nerve Allografts for the Reconstruction of Digital Nerve Gaps: A Single-Institution Case Series and Review of the Literature. World Neurosurg 2019: 127: e1176-e84.
51. Moore AM, Kasukurthi R, Magill CK, et al. Limitations of conduits in peripheral nerve repairs.

Hand (N Y) 2009: 4: 180-6.
52. Tomita K, Madura T, Sakai Y, et al. Glial differentiation of human adipose-derived stem cells: implications for cell-based transplantation therapy. Neuroscience 2013: 236: 55-65.
53. Keilhoff G, Goihl A, Stang F, Wolf G, Fansa H. Peripheral nerve tissue engineering: autologous Schwann cells vs. transdifferentiated mesenchymal stem cells. Tissue Eng 2006: 12: 1451-65.
54. Caplan AI, Hariri R. Body Management: Mesenchymal Stem Cells Control the Internal Regenerator. Stem Cells Transl Med 2015: 4: 695-701.
55. Caplan AI. Adult Mesenchymal Stem Cells: When, Where, and How. Stem Cells Int 2015: 2015: 628767.
56. Kingham PJ, Kolar MK, Novikova LN, Novikov LN, Wiberg M. Stimulating the neurotrophic and angiogenic properties of human adipose-derived stem cells enhances nerve repair. Stem Cells Dev 2014: 23: 741-54.
57. Liu Y, Zhang Z, Qin Y, et al. A new method for Schwann-like cell differentiation of adipose derived stem cells. Neurosci Lett 2013: 551: 79-83.
58. Ladak A, Olson J, Tredget EE, Gordon T. Differentiation of mesenchymal stem cells to support peripheral nerve regeneration in a rat model. Exp Neurol 2011: 228: 242-52.
59. Orbay H, Uysal AC, Hyakusoku H, Mizuno H. Differentiated and undifferentiated adipose-derived stem cells improve function in rats with peripheral nerve gaps. J Plast Reconstr Aesthet Surg 2012: 65: 657-64.
60. Strioga M, Viswanathan S, Darinskas A, Slaby O, Michalek J. Same or not the same? Comparison of adipose tissue-derived versus bone marrow-derived mesenchymal stem and stromal cells. Stem Cells Dev 2012: 21: 2724-52.
61. Kingham PJ, Kalbermatten DF, Mahay D, et al. Adipose-derived stem cells differentiate into a Schwann cell phenotype and promote neurite outgrowth in vitro. EXP NEUROL 2007: 207: 267-74.
62. Yoshimura H, Muneta T, Nimura A, et al. Comparison of rat mesenchymal stem cells derived from bone marrow, synovium, periosteum, adipose tissue, and muscle. Cell Tissue Res 2007: 327: 449-62.
63. di Summa PG, Kingham PJ, Raffoul W, et al. Adipose-derived stem cells enhance peripheral nerve regeneration. J Plast Reconstr Aesthet Surg 2010: 63: 1544-52.
64. Hundepool CA, Nijhuis TH, Kotsougiani D, et al. Optimizing decellularization techniques to create a new nerve allograft: an in vitro study using rodent nerve segments. Neurosurg Focus 2017: 42.
65. Hundepool CA, Bulstra LF, Kotsougiani D, et al. Comparable functional motor outcomes after repair of peripheral nerve injury with an elastase-processed allograft in a rat sciatic nerve model. Microsurgery 2018: 38: 772-79.
66. Jesuraj NJ, Santosa KB, Newton P, et al. A systematic evaluation of Schwann cell injection into acellular cold-preserved nerve grafts. J Neurosci Methods 2011: 197: 209-15.
67. Rbia N, Bulstra LF, Bishop AT, van Wijnen AJ, Shin AY. A simple dynamic strategy to deliver stem cells to decellularized nerve allografts. Plast Reconstr Surg 2018.
68. Rbia N, Bulstra LF, Lewallen EA, et al. Seeding decellularized nerve allografts with adipose-derived mesenchymal stromal cells: An in vitro analysis of the gene expression and growth factors produced. J Plast Reconstr Aesthet Surg 2019: 72: 1316-25.
69. Rbia N, Bulstra LF, Thaler R, et al. In Vivo Survival of Mesenchymal Stromal Cell-Enhanced Decellularized Nerve Grafts for Segmental Peripheral Nerve Reconstruction. J Hand Surg Am 2019: 44: 514.e1-14.e11.
70. Rbia N, Bulstra LF, Friedrich PF, et al. Gene expression and growth factor analysis in early nerve regeneration following segmental nerve defect reconstruction with a mesenchymal stromal cell-enhanced decellularized nerve allograft. Plast Reconstr Surg Glob Open 2020: 8: e2579.
71. Vleggeert-Lankamp CL. The role of evaluation methods in the assessment of peripheral nerve regeneration through synthetic conduits: a systematic review. Laboratory investigation. J

Neurosurg 2007: 107: 1168-89.
72. Giusti G, Lee JY, Kremer T, et al. The influence of vascularization of transplanted processed allograft nerve on return of motor function in rats. Microsurgery 2016: 36: 134-43.
73. Shin RH, Vathana T, Giessler GA, et al. Isometric tetanic force measurement method of the tibialis anterior in the rat. Microsurgery 2008: 28: 452-7.
74. Hundepool CA, Nijhuis TH, Rbia N, et al. Noninvasive Ultrasound of the Tibial Muscle for Longitudinal Analysis of Nerve Regeneration in Rats. Plast Reconstr Surg 2015: 136: 633e-9e.
75. Bulstra LF, Hundepool CA, Friedrich PF, et al. Motor Nerve Recovery in a Rabbit Model: Description and Validation of a Noninvasive Ultrasound Technique. J Hand Surg Am 2016: 41: 27-33.

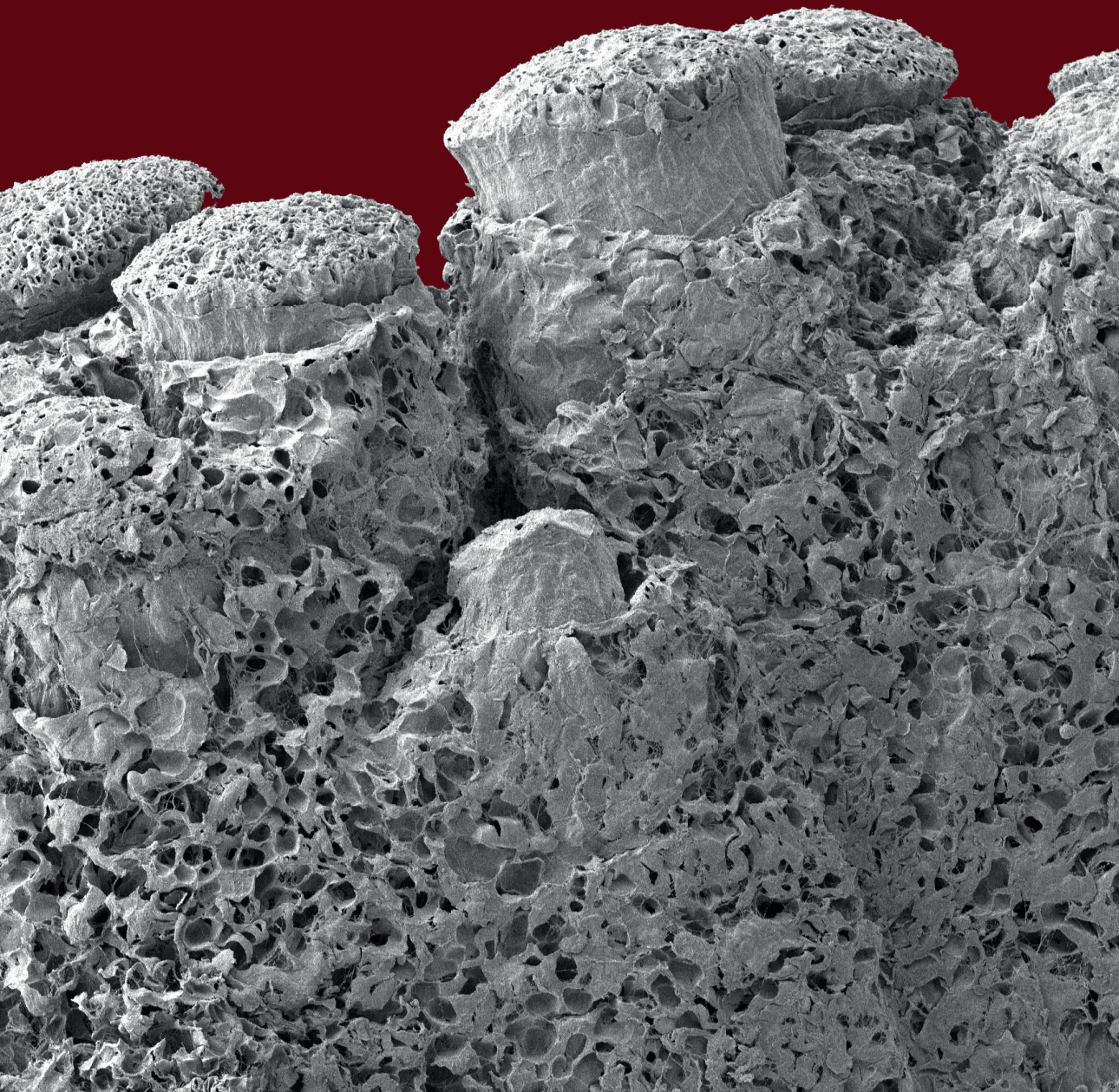

Chapter 2

Targeted stimulation of mesenchymal stem cells in peripheral nerve repair

Femke Mathot, Alexander Y. Shin, Andre J. van Wijnen

Gene. 2019 August;710:17-23

ABSTRACT

Mesenchymal stem cells (MSCs) have considerable translational potential in a wide variety of clinical disciplines and are the cellular foundation of individualized treatments of auto-immune, cardiac, neurologic and musculoskeletal diseases and disorders. While the cellular mechanisms by which MSCs exert their biological effects remain to be ascertained, it has been hypothesized that MSCs are supportive of local tissue repair through secretion of essential growth factors. Therapeutic applications of MSCs in peripheral nerve repair have recently been reported. This review focuses on how MSCs can promote nerve regeneration by conversion into Schwann-like cells, and discusses differentiation methods including delivery and dosing of naive or differentiated MSCs, as well as in vitro and in vivo outcomes. While MSC-based therapies for nerve repair are still in early stages of development, current progress in the field provides encouragement that MSCs may have utility in the treatment of patients with peripheral nerve injury.

INTRODUCTION

To achieve successful repair of peripheral nerve segmental defects, nerve autografts still supersede the results of all commercially available nerve graft substitutes (bioabsorbable conduits, vessels or processed allografts).[1] Nerve autografts are limited in availability and their harvest from patients automatically generates donor side morbidity. The application of MSCs has been actively considered for in vitro and in vivo studies seeking to improve outcomes of peripheral nerve reconstruction. MSCs potentially provide the necessary biological support for nerve substitutes to equate results obtained by autografts.[2, 3] Prior studies have also evaluated the application of Schwann cells to nerve graft substitutes and have demonstrated active expression of neurotrophic factors with encouraging outcomes. [4] However, clinical application of this technology is impractical, as it would require harvest of autologous nerve tissue to obtain autologous Schwann cells and extensive time to culture and grow the requisite number of Schwann cells for adequate seeding of the nerve graft substitutes. Alternatives to autologous Schwann cells would be the differentiation of autologous MSCs from the patient into Schwann-like cells. In vitro targeted stimulation of autologous MSCs has resulted in differentiation into Schwann-like cells without having to sacrifice autologous nerves.[4, 5] Hence, autologous MSCs can be harvested from the patient, differentiated into Schwann-like cells and be delivered to the site of nerve repair or seeded onto nerve graft substitutes to improve the regenerative environment. Important topics addressed in this review include methods for how to differentiate MSCs into Schwann-like cells, how to deliver naive or differentiated MSCs and the regenerative potential of differentiated MSCs compared to undifferentiated MSCs.

MESENCHYMAL STEM CELLS

MSCs can be isolated from a variety of tissues from the stromal vascular fraction that are extrinsic to blood vessels. They are most frequently obtained from either bone marrow or adipose tissue. Multiple studies have compared bone marrow and adipose MSCs and both sources yield viable MSCs that comply with minimal criteria for MSCs as defined in 2006 by the International Society for Cellular Therapy.[6] Key properties of MSCs include that they are plastic adherent, multi-potent and express canonical mesenchymal stem cell markers (CD44 and CD90), while other markers are absent (CD34 and CD45).[6, 7] In contrast to bone marrow, adipose tissue is more easily accessible and requires only minimally invasive methods (liposuction vs bone marrow harvest) to obtain adequate quantities of MSCs, while having a similar effect on nerve regeneration.[8, 9] MSCs that are derived from the stromal vascular fraction of adipose tissue are easily expanded and differentiated.[10, 11] These properties render adipose derived MSCs of particular interest for clinical applications compared to less accessible bone marrow derived MSCs.

A well-established method to derive MSCs from adipose tissue consists of mechanically disrupted and enzymatically digested tissues. The fat tissue obtained by liposuction is minced and enzymatically digested using collagenase type I. The undigested tissue is removed by filtration and the filtered solution is suspended in standard culture media containing a-MEM.

For clinical applications, this media is supplemented with platelet lysate (PL) to obtain zoonotic free clinical grade MSCs. We note that although Fetal Bovine Serum (FBS) suffices for research applications, the cell populations that emerge upon proliferative expansion in PL versus FBS may differ in their molecular properties and these differences may result in functional differences in cell therapy applications. Upon centrifugation, low density adipocytes emerge at the top of the tube, while stromal cells from the vasculature of fat tissue are collected as a pellet. The pellet can be re-suspended in MEM containing growth supplements (e.g., PL or FBS) and antibiotics (e.g., penicillin/streptomycin solution) for subsequent culture as adherent MSCs.[7, 11] Overall, deriving MSCs from adipose tissue is well-described and technically simple to perform making it advantageous for clinical applications.

MECHANISM OF ACTION

There are two major hypotheses on how MSCs establish tissue regeneration. The first proposes that the exogenously administered MSCs have a structural function in tissue injury and thus differentiate in vivo into tissue that requires repair. Growth factors and other paracrine molecules produced by the surrounding tissue stimulate the MSCs to differentiate into the requisite cell type. Supportive studies at best only infer this mechanism. Orbay and colleagues labeled undifferentiated MSCs and reported that they were still detected after 3 months and expressed Schwann cell proteins in a rat-model.[12] Tomita and colleagues reported in a rat-model that a small fraction of their GFP-labeled MSCs were still present after 8 weeks and expressed myelin protein, suggesting that some trans-differentiation into Schwann cells occurred.[4] In this model, MSCs may be able to both repair and replace injured tissue. However, to date this model for MSC function remains largely untested. While there is no question that cellular differentiation is required for neuronal development, it is not clear whether therapies relying on MSCs replicate the normal differentiation of Schwann cells.

The second hypothesis for MSCs has more recently emerged and this concept poses that MSCs have trophic functions that are important for extracellular matrix remodeling and tissue regeneration.[13] At least a subset of MSCs are derived from pericytes, which are released upon tissue damage or disease. The proteins and molecules produced by the MSCs can enhance angiogenesis, inhibit scar formation and stimulate tissue regeneration.[14] In addition to maximizing the intrinsic regenerative capacity of the tissue, MSCs have key immunomodulatory roles. After the initial immunologic response to injury, pro-inflammatory cytokines produced by NK cells and T lymphocytes 'activate' the MSCs. MSCs subsequently prevent the inappropriate and overaggressive activation of T lymphocytes and decrease the cytotoxic activity of NK cells through feedback loops.[15, 16] This 'trophic' concept has been corroborated by findings in multiple in vitro and in vivo studies of enhanced gene expression and growth factor production after the introduction of MSCs to damaged tissue.[17, 18] Overall, MSCs most likely have a trophic function and their role in enhancing nerve regeneration is to maximize the intrinsic regenerative capacity of the nerve and minimize the inappropriate

inflammatory response after nerve-injury. A dual function, in which a small fraction of the MSCs has a structural function by replacing injured tissue-cells, while the remaining part of the MSCs maximizes the intrinsic regenerative capacity of the injured tissue by producing growth factors and cytokines, is not inconceivable. The described different functions of MSCs are shown in **figure 1**.

In light of the hypotheses for the mechanisms of action of MSCs, several key questions need to be addressed prior to clinical implementation. These include the role of differentiation of MSCs prior to administration, the optimal dosing and time frame of application of differentiated versus undifferentiated MSCs and how MSCs need to be administered regardless of differentiation status.

APPLICATION OF MSCS

An important aspect for the clinical application of MSCs is that outside factors like local anesthetics or contrast medium can influence the viability of MSCs and should be taken into account in studies on the potential of MSCs for clinical applications. [19, 20] Although the outcomes of preclinical and clinical research on the use of MSCs have been promising in a wide variety of clinical disciplines, further research to determine the optimal doses and time points of implantation, the long-term risks and the long-term efficacy are needed to optimize outcomes of MSC-supported tissue regeneration.[21, 22]

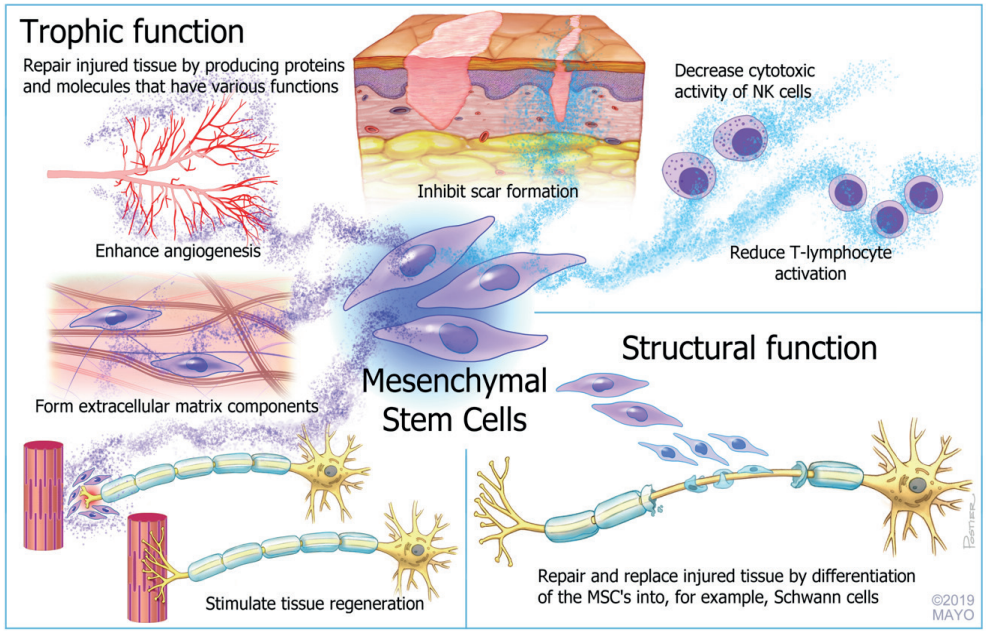

Figure 1. Schematic overview of the (hypothesized) subset of functions of mesenchymal stromal cells.

MSCS IN PERIPHERAL NERVE REPAIR

Differentiation of MSCs into Schwann-like cells

The neural induction of MSCs by chemicals combined with growth factors is the most established method to obtain Schwann cell-like differentiation. The induction protocol by Kingham and colleagues is widely used and includes two preparation steps with ß-mercaptoethanol (for 24 hours) and all-trans-retinoic acid (for 72 hours). Subsequently the cells are placed in growth medium enriched with a differentiation cocktail containing Platelet-derived growth factor (PDGF-AA), basis fibroblast growth factor (bFGF), Forskolin and a member of the Neuregulin family (Neuregulin-1 ß1, Glial growth factor-2 or Heregulin- ß1). After 2 weeks in differentiation medium, the morphology of MSCs is altered into an elongated spindle shape, characteristic of Schwann cells. Immunohistochemistry and Western blot analysis after differentiation has revealed expression of several phenotype-specific surface markers, including GFAP, S100 and p75-NTR. [2, 4, 5, 11, 17, 23-25] Studies have demonstrated this protocol is also suitable for human MSCs and that the function of those differentiated cells is analogous to Schwann cells. [4, 26] Regardless of the fact that the effect of differentiated MSCs needs to be further examined and confirmed, these findings imply that research on targeted stimulation of MSCs could be applied in humans in the future and therefore has a serious clinical relevancy. The additional timing and cost of differentiation need to be justified prior to human trials.

The components of Kingham's induction protocol each have specific biological functions. Forskolin activates adenylyl cyclase which increases the level of intracellular cyclic adenosine monophosphate (cAMP). cAMP causes an increase in the mitogenic responses of Schwann cells[27], in response to the mitogenic actions of the growth factors PDGF and bFGF/FGF2.[28] The neuregulin-1 family plays a crucial role in the actual development and evolution of Schwann cells. Their presence activates cascades promoting Schwann cell differentiation and expansion. The level of Neuregulin-1 (NRG1) determines differentiation of Schwann cells into myelinating or non-myelinating cells that are responsible for the development of group C nerve fibers. NRG1 levels determines axon size, which enables the myelinating Schwann cells to optimize myelin sheath thickness.[29, 30] Kingham's protocol is currently the preferred method to obtain Schwann-like cells from adipose derived MSCs. The effect of altering the dosages of the different components of the differentiation protocol on the ultimate function of the Schwann-like cells is an interesting prospect for future research.

As targeted neurogenic stimulation to induce differentiation of MSCs is an expensive, time-consuming and inefficient process requiring several weeks of laboratory-based preparation time, efforts have been made to find alternative approaches. Safford and colleagues used a chemical induction medium with butylated hydroxyanisole, potassium chloride, valproic acid, Forskolin, hydrocortisone and insulin to differentiate murine and human MSCs. Within 5-6 hours following neuronal induction, they observed dramatic cell morphological changes in cytoskeletal organization and membrane appearance in MSC cultures which persisted up to 5 days. Beyond 5 days however, the differentiated MSCs lost viability and perished within 14 days of culture.[10] The induction protocol of Anghileri involves the culturing of MSCs for 72 hours in growth medium with exogenous bFGF (FGF2) and human epithelial

growth factor as mitogenic factors to facilitate formation of cellular spheres. The spheres were induced to differentiate in media containing BDNF and all-trans-retinoic acid. After four weeks of culture, only half of the MSCs demonstrated the characteristic neuronal morphology, which expressed nestin and neuronal markers MAP-2 and NeuN, but lacked the expression of glial markers S100 and GFAP.[31] Ahmadi and colleagues compared the method of Anghileri to the chemical induction protocol of Woodburry and colleagues. Woodburry included an optimization step in which MSCs are initially induced by addition of ß-mercaptoethanol (BME) for 24 hours followed by induction of neural differentiation using dimethylsulfoxide (DMSO), BME and butylated hydroxyanisole for 1 to 5 days. Ahmadi noted the differentiation protocol of Anghileri significantly improved MSC survival and increased MSC viability, indicating the use of potentially toxic substances (e.g., DMSO and BME) may not be necessary and could be avoided for MSC differentiation.[32, 33] Thaler and colleagues confirmed the toxic effect of DMSO by demonstrating DMSO can initiate epigenetic changes which increased cell apoptosis.[34] Despite the attempts to equal the efficiency of Kingham's differentiation protocol by alternative chemical induction methods, none have resulted in high percentages of viable Schwann-like cells. In an ideal scenario, MSCs can be differentiated by natural, non-toxic compounds that are largely available, cost-effective and which do not influence the viability of MSCs.

In an effort to find a method meeting the requirements listed above, studies have been performed on the effect of nerve tissue/nerve leachate to cell cultures, co-culture of MSCs with Schwann cells and the electrical stimulation of MSCs. The induction culture medium of Liu and colleagues consisted of 1cm fragments of rat sciatic nerves soaked in normal growth medium (i.e., DMEM and 10% FBS). After 2 days, nerve fragments were removed and adipose tissue derived MSCs were further cultured in the sciatic nerve leachate for another 3 days. Cells adopted a spindle-shape within 48 hours and reflected by expression of S100 and GFAP proteins as was confirmed by immunohistochemistry and western blot analysis, but the nerve autografts required for this protocol would not create a clinically viable therapeutic solution.[18] Liao compared three methods to induce adipose tissue derived MSCs, including (I) neural induction with chemicals only (i.e., media with 2% DMSO for 5 hours), (II) neural induction by chemicals combined with growth factors (i.e., NGF, bFGF/FGF2 and BDNF, as well as the cAMP-related drug Forskolin) for 2 weeks, and (III) neural induction by co-culture of MSCs with Schwann cells. Immunohistochemistry and gene expression analysis showed higher mRNA levels for S100, nestin and GFAP in method II and III compared to method I. Similar to Liu and others, autologous Schwann cells would pose a practical problem for the clinical implementation of method III.[35] Das and colleagues differentiated MSC into Schwann-like cells by electrical stimulation to alter cellular membrane potential. The majority of electrically induced MSCs (>80%) showed Schwann cell markers S100 and p75 and enhanced secretion of NGF compared to chemically induced MSCs or undifferentiated MSCs.[36] Although electrical differentiation is promising and may mimic aspects of normal neuronal cell differentiation, physical methods for differentiation have remained largely unexplored and it remains unclear whether electrical stimulation will have practical benefits compared to differentiation with growth factors.

Methods of administration and cell dosage

The desired method of cell delivery depends on the intended mechanism of action of MSCs. MSCs need to be delivered within the ultrastructure of nerves to fulfill a structural function or need to be able to migrate to the site of injury. Micro-injection of the MSCs has been described, but the consequences of injection to cell viability and the resulting ultrastructural trauma to the nerve are potential concerns. Jesuraj and colleagues reported the pressure build-up in the syringe and needle during injection reduces viability of cells after needle passage. (46) In contrast, Onishi and colleagues reported that adipose derived MSCs were fairly robust within a range of fluid pressures within the syringe upon expulsion. [37, 38] Studies that examined the viability of bone marrow derived MSCs post-injection have various conclusions ranging from no viability changes to a temporarily affected viability, to a reduced viability. [39-41] Increasing the needle gauge may intuitively reduce cell damage, but inserting a larger needle in a processed nerve graft is practically almost impossible and can easily cause tearing of the epineurium. In addition, uncontrolled micro-injection leads to a non-uniform distribution of cells and may result in local accumulation of clusters of MSCs that potentially block the ingrowth of the regenerating nerve rather than enhancing it.[38] The calibers of myelinated axon fibers (2 to 22μm) in proportion to the average diameter of MSCs (17.9 – 30.4μm) also may be problematic when MSCs are injected in the nerve allograft.[42-44] In case of using hollow nerve conduits, injection of MSCs will not harm the conduit itself, but it can still cause decreased viability of the cells and might obstruct axonal ingrowth. Furthermore, leakage of cells out of the nerve substitute is a recognized problem; the study by Jesuraj and colleagues showed only 10% of cells were successfully transferred after one million cells were injected.[38] The injection of MSCs in nerve substitutes is not clinically applicable due to low and uncontrollable delivery efficiencies and the potential damage to the cells and the nerves. Hence, future studies may consider alternative delivery methods for both differentiated and undifferentiated MSCs.

Intravenous injection of MSCs has been investigated as an alternative to MSC-injection that prevents nerve-damage and cell-leakage and focuses on the more likely trophic function of MSCs. Although the vasculature potentially delivers a subset of MSCs to the area of injury, the cells may not accumulate to a critical mass to enhance nerve regeneration. In addition, the relatively large size of MSCs causes entrapment in capillaries.[45] MSCs can also be administered by intramuscular injection which delivers cells locally with preservation of the nerve. Intramuscular injection of MSCs in the gastrocnemius muscle resulted in a significantly improved functional recovery and neuro-conduction velocity compared to intravenous injection of MSCs or sham injection.[46] It has been reported that intramuscular injection of MSCs leads to enhanced nerve regeneration.[47] Even though these findings are promising, the described techniques still require injection of cells which potentially decreases the viability of the cells. The enhanced outcomes after intravenous and intramuscular injection of MSCs, do confirm the previously suggested trophic function of MSCs.

Soaking nerve grafts in MSC-solutions is another described method of cell delivery. Thompson and colleagues compared the injection of cells to a soaking technique in which the nerve samples were pretreated with a micro-needle roller. Injection led to a higher number of cells in the inner and middle zones of the nerves, while soaking delivered a higher number of cells

in the outer zone.[48] Dynamic seeding has been successful in vascular tissue engineering and resulted in a more efficient and uniform distribution of cells compared to static seeding with seeding efficiencies ranging from 38% to 90%.[49] This strategy was applied to a nerve-model by Rbia and colleagues. They non-traumatically seeded MSCs on the surface of a processed nerve allograft with the use of a bioreactor. This resulted in a uniform distribution of MSCs that were adhered to the nerve graft.[50] The cells did not migrate into the nerve allograft and the interaction between the MSCs and the nerve surface resulted in an upregulation of neurotrophic factors that potentially enhance nerve regeneration within the nerve graft.[50] Overall, dynamic seeding results in a uniform distribution of MSCs on nerve allografts that enables the cells to interact with the nerve ultrastructure with a high efficiency without harming the cells nor the nerve ultrastructure. To date, this is the most promising delivery method of MSCs to allograft nerves and might form the bridge towards individualized peripheral nerve repair in clinical practice.

Jesuraj and colleagues used a concentration of 1 x10^5 cells/5uL to inject and compared it to a concentration of 10^6 cells/5uL. Their analysis revealed an injection efficiency of 10% for the 1x10^6 cells (100.000 cells) and 40% for the 1x10^5 cells (40.000 cells) of which only the larger dose was trackable by in vivo fluorescence. [38] Thompson and colleagues also soaked or injected their 10mm allograft segments with 1x10^6 cells/5uL, but did not report a total efficiency. [48] Rbia and colleagues used 1x10^6 cells to dynamically seed their nerve segments and reported a seeding efficiency of 89.2%, suggesting that almost 900.000 cells were attached to the surface of the 10mm nerve segment before in vivo implementation. [50] Wang and colleagues also used 1x10^6 MSCs, diluted in 1mL fluid, to inject in the gastrocnemius muscle.[46] Despite the wide variety of delivery efficiencies, there seems to be consensus that at least 1x10^6 MSCs need to be presented to the nerve graft to generate noticeable biological effects. However, no studies on the optimal dosing of MSCs have been reported. Dynamic seeding of MSCs appears to be a reliable, effective and well-studied delivery method (see **table 1**).

None of the methods of administration reported to date have been specifically tested on differentiated MSCs, so direct comparisons between undifferentiated and differentiated MSCs with respect to their delivery efficiency are lacking. This could be a potential decisive factor as it has been emphasized that differentiation of MSC may decrease their potential to attach to surfaces.[51] It is essential that delivery methods are tested on differentiated MSCs as well as undifferentiated MSCs as the impact on clinical application is significant with respect to cost and time.

Differentiated MSCs versus undifferentiated MSCs in vitro

The in vitro capabilities of differentiated MSCs in peripheral nerve repair have been extensively evaluated. Kingham and colleagues found that differentiated MSCs significantly extended the number and the length of formed neurites by motor neuron-like cells compared to undifferentiated MSCs.[11] In another study of Kingham, enhanced expression was observed for nerve growth factor (NGF), brain-derived neurotrophic factor (BDNF), glial cell-derived neurotrophic factor (GDNF), vascular endothelial growth factor-A (VEGF-A) and angiopoietin-1 in differentiated MSC compared to undifferentiated MSCs.[17] ELISA analysis demonstrated enhanced secretion

of BDNF, GDNF, angiopoietin-1 and VEGF-A upon differentiation of MSCs. These increased levels of growth factors resulted in higher total neurite outgrowth, longer neurites and a better angiogenic potency after removal of the factors that stimulate differentiation from the growth medium.[17] Tomita found similar results and showed differentiated human MSCs produced higher levels of neurotrophic factors like BDNF, NGF and GDNF compared to undifferentiated MSCs. The secretion of these neurotrophic factors resulted in a significantly increased percentage of neuron-bearing neurites, and a significant increase in both neurite length and number of neurons.[4] Ladak also demonstrated that co-culture of differentiated MSCs with dorsal root ganglion neurons led to longer and more arborous neurite outgrowth than undifferentiated MSCs.[23] As described previously, the same result was found with differentiated human MSCs.[26] In vitro studies that examined the interaction between undifferentiated and differentiated MSCs with a processed nerve allograft showed persistent enhanced expression of neurotrophic genes that subsequently led to the secretion of neurotrophic growth factors.[52, 53] In general, differentiated MSCs enhance the expression of neurotrophic genes and the secretion of neurotrophic proteins, resulting in increased neurite outgrowth in vitro. These in vitro results are promising and support the hypothesis that differentiated MSCs have a trophic function in nerve regeneration. The remark needs to be made that any agent or growth factor added to the growth medium may become embedded in the extracellular matrix (ECM) and might not be completely washed out after removal of the differentiation media. Thus, the enhanced gene expressions and the increased neurite outgrowth could still be the effect of direct stimulation by the added growth factors instead of being positively influenced by the differentiated MSCs. In vivo research could eliminate this discrepancy.

Delivery method	Efficiency	Pros	Cons
Injection into nerve grafts	10-40%	• Delivers a high number of MSCs in the inner and middle nerve zones	• Reduced viability of MSCs • Damage to the ultrastructure of the nerve • Leakage of cells (conduits) • Local accumulation of MSCs
Intravenous injection	100%	• No damage to the ultrastructure of the nerve • No cell leakage	• Reduced viability of cells • Entrapment of MSCs in capillaries • Low number of MSCs at regeneration site
Intramuscular injection	100%	• Locally delivers MSCs • No damage to the ultrastructure of the nerve • No cell leakage	• Reduced viability of cells • Low number of MSCs at regeneration site
Soaking	Unknown	• Delivers MSCs in the outer nerve zones • Preserved viability of MSCs	• Damage to the nerve (micro-needle roller)
Seeding	89.2%	• Uniform distribution of MSCs • Preserved viability of MSCs • No damage to the ultrastructure of the nerve • No cell leakage	• Interaction between MSCs and extracellular matrix is required

Table 1. Overview of the pros and cons of the described delivery methods of MSCs.

Differentiated MSCs versus undifferentiated MSCs in vivo

When seeded on a conduit and transplanted in a rat-model, differentiated MSCs characterized by Kingham and colleagues increased the distance of axon regeneration and enhanced vascularity in nerve conduits compared to undifferentiated MSCs. These findings show that neurotrophic and angiogenic factors produced by differentiated MSCs interact with regenerative mechanisms that support repair of injured nerves by enhancing vascularization and improved nerve regeneration.[17] Ladak and colleagues found in vivo that differentiated MSCs seeded in a nerve conduit resulted in an equal number of regenerating axons across the nerve gap compared to seeded Schwann cells. However, the improved axon regeneration did not translate into improved electrodiagnostic parameters or increased muscle weight.[23] Keilhoff and colleagues compared the outcomes of Schwann cells, undifferentiated MSCs and differentiated MSCs injected in a devitalized muscle. The authors found both Schwann cells and differentiated MSCs contribute to appropriate regeneration while undifferentiated MSCs did not exhibit the ability to improve nerve repair.[47] Kappos showed in a rat sciatic nerve gap model that the addition of differentiated human MSCs to a nerve conduit led to functional outcomes (sciatic functional index and gastrocneumius muscle mass) that exceeded the results of undifferentiated human MSCs and Schwann cells.[54] In contrast, other studies showed low potential of the Schwann-like cells. Fox and colleagues demonstrated in a rat model that primary Schwann cells did not have a beneficial effect on nerve regeneration after 4 weeks when injected into nerve grafts.[55] Orbay and colleagues evaluated the effects of differentiated and undifferentiated MSCs when seeded in silicone tubes and compared the outcomes to empty silicone tubes and nerve grafts. Although the functional outcomes of both MSC-groups were significantly better than those of the other groups, there were no significant differences between differentiated or control MSCs.[24] Watanabe compared undifferentiated MSCs, differentiated MSCs and Schwann cells in a rat facial nerve gap model and came to similar conclusions in that all groups had a comparable amount of nerve regeneration and all cell based strategies gave functional results close to that of autografts.[56]

The advantages and disadvantages of differentiated versus undifferentiated MSCs in vitro and in vivo are presented in **table 2**. Although the majority of in vitro studies demonstrated a larger trophic potential of differentiated MSCs compared to undifferentiated MSCs, the in vivo outcomes were less unanimous. These conflicting results may be due to the embedded growth agents in the ECM that is generated in cell culture. Differences in differentiation methods, dosing and efficiency of cell delivery methods, and the composition of the nerve substitutes could affect the persistence of differentiation in vivo in the absence of the differentiation medium and could account for different outcomes. Further careful studies are required to confirm differentiated MSCs preserve their described enhanced trophic function in vivo.

CONCLUSION

Adipose derived MSCs are easy to access, deFfigrive, expand and can be successfully differentiated into Schwann-like cells. Therefore, adipose derived MSCs, and in particular adipose derived MSCs differentiated into Schwann-like cells have been broadly studied in

the effort to improve the outcomes of peripheral nerve repair/reconstruction. The neural induction of MSCs by chemicals combined with growth factors (PDFG-AA, bFGF/FGF2, Forskolin, neuregulin-1/NRG1) remains the preferred method to obtain Schwann cell-like differentiation and has been validated for human MSCs differentiation. To obtain the putative trophic effect of MSCs, they should be delivered in a timely and non-traumatic method. Dynamic seeding of MSCs on nerve grafts meets these criteria. Despite the wide interest in the use of both differentiated and undifferentiated MSCs in peripheral nerve repair, the optimal delivery and dosing of differentiated MSCs is a rather under-explored research topic. The advantages of using undifferentiated versus differentiated MSCs remain to be further defined. In vitro studies have shown that differentiated MSCs permit enhanced expression of neurotrophic genes and the secretion of neurotrophic proteins, resulting in increased neurite outgrowth when compared to undifferentiated MSCs. The beneficial effect of differentiated MSCs has not yet been convincingly confirmed in in vivo studies. Future studies are needed to determine the ideal method of delivery and optimal dosages of differentiated and undifferentiated MSCs to nerve allografts to ascertain their regenerative potential for peripheral nerve reconstruction. These studies should consider the ultimate goal of clinical applications, as well as be cognizant of the time and cost issues of peripheral nerve reconstruction/repair.

Cell type	In vitro		In vivo	
	Pros	Cons	Pros	Cons
Undifferentiated MSCs	• No extended preparation time • No extra preparation costs	• Less expression of neurotrophic genes • Less production of neurotrophic growth factors	• No extended preparation time • No extra preparation costs • Functional outcomes comparable to differentiated MSCs	• Histologically less axon regeneration
Differentiated MSCs	• Enhanced expression of neurotrophic genes • Enhanced production of neurotrophic growth factors • Extended number and length of neurites • Suitable for human MSCs	• Extended preparation time • Extra preparation costs	• Increased axon regeneration distance • Enhanced vascularity	• Inconsistency about functional outcomes • Extended preparation time • Extra preparation costs

Table 2. Overview of the pros and cons of the use of undifferentiated versus differentiated MSCs in vitro and in vivo for peripheral nerve repair. MSCs = mesenchymal stem cells.

REFERENCES

1. Rbia N, Shin AY. The Role of Nerve Graft Substitutes in Motor and Mixed Motor/Sensory Peripheral Nerve Injuries. J Hand Surg Am 2017: 42: 367-77.
2. Georgiou M, Golding JP, Loughlin AJ, Kingham PJ, Phillips JB. Engineered neural tissue with aligned, differentiated adipose-derived stem cells promotes peripheral nerve regeneration across a critical sized defect in rat sciatic nerve. Biomaterials 2015: 37: 242-51.
3. Hundepool CA, Nijhuis TH, Mohseny B, Selles RW, Hovius SE. The effect of stem cells in bridging peripheral nerve defects: a meta-analysis. J Neurosurg 2014: 121: 195-209.
4. Tomita K, Madura T, Sakai Y, et al. Glial differentiation of human adipose-derived stem cells: implications for cell-based transplantation therapy. Neuroscience 2013: 236: 55-65.
5. Caddick J, Kingham PJ, Gardiner NJ, Wiberg M, Terenghi G. Phenotypic and functional characteristics of mesenchymal stem cells differentiated along a Schwann cell lineage. Glia 2006: 54: 840-9.
6. Dominici M, Le Blanc K, Mueller I, et al. Minimal criteria for defining multipotent mesenchymal stromal cells. The International Society for Cellular Therapy position statement. Cytotherapy 2006: 8: 315-7.
7. di Summa PG, Kingham PJ, Raffoul W, et al. Adipose-derived stem cells enhance peripheral nerve regeneration. J Plast Reconstr Aesthet Surg 2010: 63: 1544-52.
8. Mahmoudifar N, Doran PM. Mesenchymal Stem Cells Derived from Human Adipose Tissue. Methods Mol Biol 2015: 1340: 53-64.
9. Yoshimura H, Muneta T, Nimura A, et al. Comparison of rat mesenchymal stem cells derived from bone marrow, synovium, periosteum, adipose tissue, and muscle. Cell Tissue Res 2007: 327: 449-62.
10. Safford KM, Hicok KC, Safford SD, et al. Neurogenic differentiation of murine and human adipose-derived stromal cells. Biochem Biophys Res Commun 2002: 294: 371-9.
11. Kingham PJ, Kalbermatten DF, Mahay D, et al. Adipose-derived stem cells differentiate into a Schwann cell phenotype and promote neurite outgrowth in vitro. Exp Neurol 2007: 207: 267-74.
12. Orbay H, Uysal AC, Hyakusoku H, Mizuno H. Differentiated and undifferentiated adipose-derived stem cells improve function in rats with peripheral nerve gaps. J Plast Reconstr Aesthet Surg 2011.
13. Caplan AI, Hariri R. Body Management: Mesenchymal Stem Cells Control the Internal Regenerator. Stem Cells Transl Med 2015: 4: 695-701.
14. Caplan AI. Adult Mesenchymal Stem Cells: When, Where, and How. Stem Cells Int 2015: 2015: 628767.
15. Castro-Manrreza ME, Montesinos JJ. Immunoregulation by mesenchymal stem cells: biological aspects and clinical applications. J Immunol Res 2015: 2015: 394917.
16. Ma S, Xie N, Li W, et al. Immunobiology of mesenchymal stem cells. Cell Death Differ 2014: 21: 216-25.
17. Kingham PJ, Kolar MK, Novikova LN, Novikov LN, Wiberg M. Stimulating the neurotrophic and angiogenic properties of human adipose-derived stem cells enhances nerve repair. Stem Cells Dev 2014: 23: 741-54.
18. Liu Y, Zhang Z, Qin Y, et al. A new method for Schwann-like cell differentiation of adipose derived stem cells. Neurosci Lett 2013: 551: 79-83.
19. Wu T, Smith J, Nie H, et al. Cytotoxicity of Local Anesthetics in Mesenchymal Stem Cells. Am J Phys Med Rehabil 2018: 97: 50-55.
20. Wu T, Nie H, Dietz AB, et al. Cytotoxic Effects of Nonionic Iodinated Contrast Agent on Human Adipose-Derived Mesenchymal Stem Cells. Pm r 2018.
21. Karussis D, Petrou P, Kassis I. Clinical experience with stem cells and other cell therapies in neurological diseases. J Neurol Sci 2013: 324: 1-9.
22. Gogel S, Gubernator M, Minger SL. Progress and prospects: stem cells and neurological

diseases. Gene Ther 2011: 18: 1-6.
23. Ladak A, Olson J, Tredget EE, Gordon T. Differentiation of mesenchymal stem cells to support peripheral nerve regeneration in a rat model. Exp Neurol 2011: 228: 242-52.
24. Orbay H, Uysal AC, Hyakusoku H, Mizuno H. Differentiated and undifferentiated adipose-derived stem cells improve function in rats with peripheral nerve gaps. J Plast Reconstr Aesthet Surg 2012: 65: 657-64.
25. di Summa PG, Kalbermatten DF, Raffoul W, Terenghi G, Kingham PJ. Extracellular matrix molecules enhance the neurotrophic effect of Schwann cell-like differentiated adipose-derived stem cells and increase cell survival under stress conditions. Tissue Eng Part A 2013: 19: 368-79.
26. Brohlin M, Mahay D, Novikov LN, et al. Characterisation of human mesenchymal stem cells following differentiation into Schwann cell-like cells. Neurosci Res 2009: 64: 41-9.
27. Kim HA, Ratner N, Roberts TM, Stiles CD. Schwann cell proliferative responses to cAMP and Nf1 are mediated by cyclin D1. J Neurosci 2001: 21: 1110-6.
28. Davis JB, Stroobant P. Platelet-derived growth factors and fibroblast growth factors are mitogens for rat Schwann cells. J Cell Biol 1990: 110: 1353-60.
29. Nave KA, Salzer JL. Axonal regulation of myelination by neuregulin 1. Curr Opin Neurobiol 2006: 16: 492-500.
30. Garratt AN, Britsch S, Birchmeier C. Neuregulin, a factor with many functions in the life of a schwann cell. Bioessays 2000: 22: 987-96.
31. Anghileri E, Marconi S, Pignatelli A, et al. Neuronal differentiation potential of human adipose-derived mesenchymal stem cells. Stem Cells Dev 2008: 17: 909-16.
32. Ahmadi N, Razavi S, Kazemi M, Oryan S. Stability of neural differentiation in human adipose derived stem cells by two induction protocols. Tissue Cell 2012: 44: 87-94.
33. Woodbury D, Schwarz EJ, Prockop DJ, Black IB. Adult rat and human bone marrow stromal cells differentiate into neurons. J Neurosci Res 2000: 61: 364-70.
34. Thaler R, Spitzer S, Karlic H, Klaushofer K, Varga F. DMSO is a strong inducer of DNA hydroxymethylation in pre-osteoblastic MC3T3-E1 cells. Epigenetics 2012: 7: 635-51.
35. Liao D, Gong P, Li X, Tan Z, Yuan Q. Co-culture with Schwann cells is an effective way for adipose-derived stem cells neural transdifferentiation. Arch Med Sci 2010: 6: 145-51.
36. Das SR, Uz M, Ding S, et al. Electrical Differentiation of Mesenchymal Stem Cells into Schwann-Cell-Like Phenotypes Using Inkjet-Printed Graphene Circuits. Adv Healthc Mater 2017: 6.
37. Onishi K, Jones DL, Riester SM, et al. Human Adipose-Derived Mesenchymal Stromal/Stem Cells Remain Viable and Metabolically Active Following Needle Passage. Pm r 2016: 8: 844-54.
38. Jesuraj NJ, Santosa KB, Newton P, et al. A systematic evaluation of Schwann cell injection into acellular cold-preserved nerve grafts. J Neurosci Methods 2011: 197: 209-15.
39. Garvican ER, Cree S, Bull L, Smith RK, Dudhia J. Viability of equine mesenchymal stem cells during transport and implantation. Stem Cell Res Ther 2014: 5: 94.
40. Agashi K, Chau DY, Shakesheff KM. The effect of delivery via narrow-bore needles on mesenchymal cells. Regen Med 2009: 4: 49-64.
41. Mamidi MK, Singh G, Husin JM, et al. Impact of passing mesenchymal stem cells through smaller bore size needles for subsequent use in patients for clinical or cosmetic indications. J Transl Med 2012: 10: 229.
42. Sunderland S, Lavarack JO, Ray LJ. The caliber of nerve fibers in human cutaneous nerves. J COMP NEUROL 1949: 91: 87-101.
43. Ryu YJ, Cho TJ, Lee DS, Choi JY, Cho J. Phenotypic characterization and in vivo localization of human adipose-derived mesenchymal stem cells. Mol Cells 2013: 35: 557-64.
44. Ge J, Guo L, Wang S, et al. The size of mesenchymal stem cells is a significant cause of vascular obstructions and stroke. Stem Cell Rev 2014: 10: 295-303.
45. Schrepfer S, Deuse T, Reichenspurner H, et al. Stem cell transplantation: the lung barrier. Transplant Proc 2007: 39: 573-6.
46. Wang P, Zhang Y, Zhao J, Jiang B. Intramuscular injection of bone marrow mesenchymal stem

cells with small gap neurorrhaphy for peripheral nerve repair. Neurosci Lett 2015: 585: 119-25.
47. Keilhoff G, Goihl A, Stang F, Wolf G, Fansa H. Peripheral nerve tissue engineering: autologous Schwann cells vs. transdifferentiated mesenchymal stem cells. Tissue Eng 2006: 12: 1451-65.
48. Thompson MJ, Patel G, Isaacs J, et al. Introduction of neurosupportive cells into processed acellular nerve allografts results in greater number and more even distribution when injected compared to soaking techniques. Neurol Res 2017: 39: 189-97.
49. Villalona GA, Udelsman B, Duncan DR, et al. Cell-seeding techniques in vascular tissue engineering. Tissue Eng Part B Rev 2010: 16: 341-50.
50. Rbia N, Bulstra LF, Bishop AT, van Wijnen AJ, Shin AY. A simple dynamic strategy to deliver stem cells to decellularized nerve allografts. Plast Reconstr Surg 2018.
51. Fairbairn NG, Meppelink AM, Ng-Glazier J, Randolph MA, Winograd JM. Augmenting peripheral nerve regeneration using stem cells: A review of current opinion. World J Stem Cells 2015: 7: 11-26.
52. Zhao Z, Wang Y, Peng J, et al. Repair of nerve defect with acellular nerve graft supplemented by bone marrow stromal cells in mice. Microsurgery 2011: 31: 388-94.
53. Zhang Y, Luo H, Zhang Z, et al. A nerve graft constructed with xenogeneic acellular nerve matrix and autologous adipose-derived mesenchymal stem cells. Biomaterials 2010: 31: 5312-24.
54. Kappos EA, Engels PE, Tremp M, et al. Peripheral Nerve Repair: Multimodal Comparison of the Long-Term Regenerative Potential of Adipose Tissue-Derived Cells in a Biodegradable Conduit. Stem Cells Dev 2015: 24: 2127-41.
55. Fox IK, Schwetye KE, Keune JD, et al. Schwann-cell injection of cold-preserved nerve allografts. Microsurgery 2005: 25: 502-7.
56. Watanabe Y, Sasaki R, Matsumine H, Yamato M, Okano T. Undifferentiated and differentiated adipose-derived stem cells improve nerve regeneration in a rat model of facial nerve defect. J Tissue Eng Regen Med 2017: 11: 362-74.

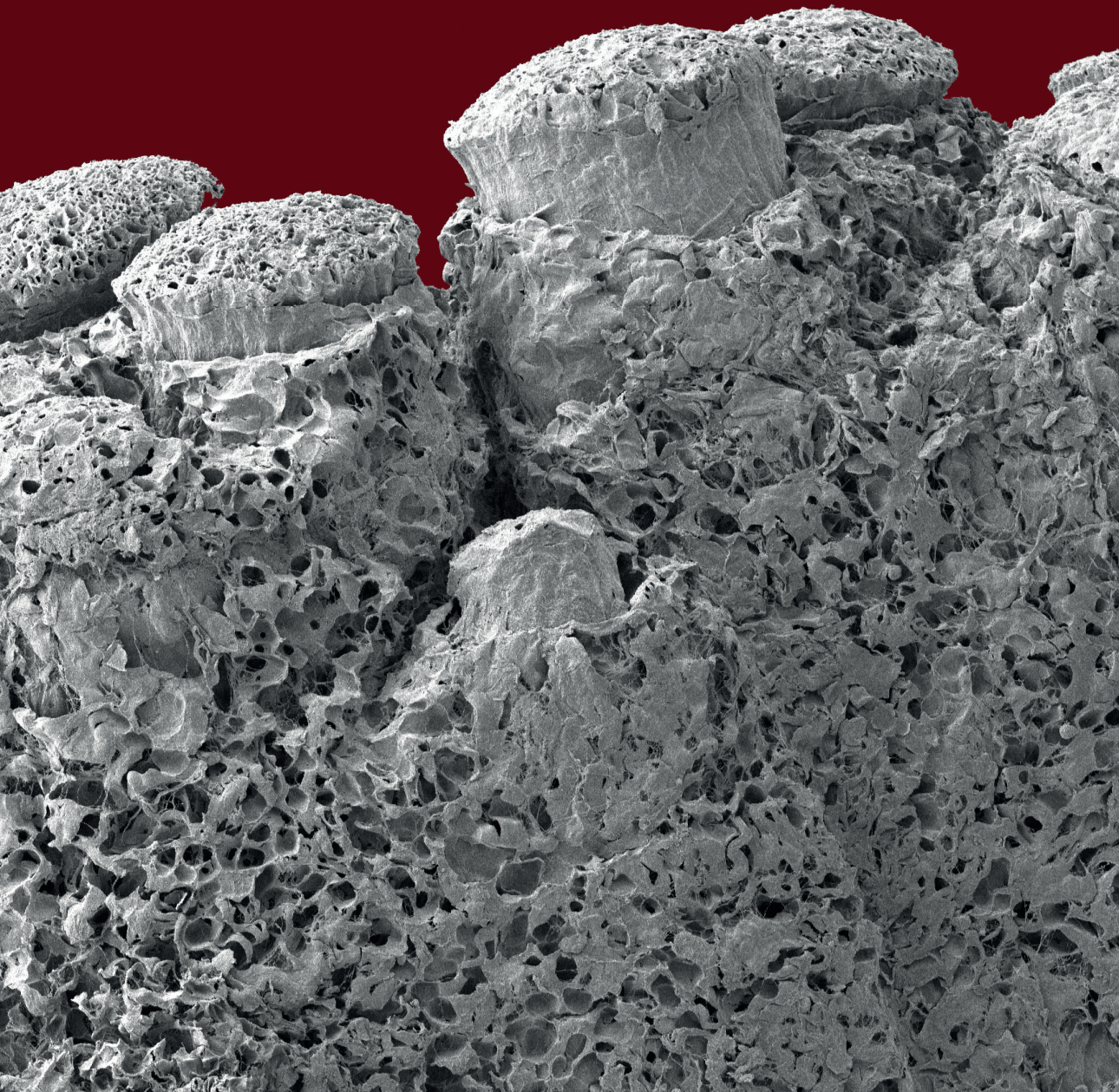

Chapter 3

Adhesion, distribution and migration of differentiated and undifferentiated mesenchymal stem cells (MSCs) seeded on nerve allografts

Femke Mathot, Nadia Rbia, Allen T. Bishop,
Steven E.R. Hovius, Andre J. van Wijnen, Alexander Y. Shin

Journal of plastic, reconstructive & aesthetic surgery: JPRAS.
2020 January; 73(1):81-89.

ABSTRACT

Background

Although undifferentiated MSCs and MSCs differentiated into Schwann-like cells have been extensively compared in vitro and in vivo, studies on the ability and efficiency of differentiated MSCs for delivery to nerve allografts are lacking. As this is essential for their clinical potential, the purpose of this study was to determine the ability of MSCs differentiated into Schwann-like cells to be dynamically seeded on decellularized nerve allografts and to compare their seeding potential to that of undifferentiated MSCs.

Methods

Fifty-six sciatic nerve segments from Sprague-Dawley rats were decellularized and MSCs were harvested from Lewis rat adipose tissue. Control and differentiated MSCs were dynamically seeded on the surface of decellularized allografts. Cell viability, seeding efficiencies, cell adhesion, distribution and migration were evaluated.

Results

The viability of both cell types was not influenced by the processed nerve allograft. Both cell types achieved maximal seeding efficiency after 12 hours of dynamic seeding, albeit that differentiated MSCs had a significantly higher mean seeding efficiency than control MSCs. Dynamic seeding resulted in a uniform distribution of cells among the surface of the nerve allograft. No cells were located inside the nerve allograft after seeding.

Conclusion

Differentiated MSCs can be dynamically seeded on the surface of a processed nerve allograft, in a similar fashion as undifferentiated MSCs. Schwann-like differentiated MSCs have a significantly higher seeding efficiency after 12 hours of dynamic seeding. We conclude that differentiation of MSCs into Schwann-like cells may improve the seeding strategy and the ability of nerve allografts to support axon regeneration.

INTRODUCTION

When it is impossible to repair an injured peripheral nerve by direct coaptation of the nerve ends, there are several options that can be used to restore the nerve's function. These include interposition nerve autografts, processed nerve allografts or bio-absorbable hollow conduits. While many studies have compared these options, the autologous nerve remains the gold standard in clinical practice, especially for restoration of major motor nerves.[1, 2] The limited availability and length of autografts requires the development of a replacement nerve that results in equal functional outcomes.[3] Although their regenerating potency still needs to be improved, processed allografts have shown to be a promising option.[2, 4-6]

Stem cells are believed to be an important control element in tissue regeneration by producing proteins and molecules that enhance angiogenesis, inhibit scar formation, stimulate tissue regeneration and have immunomodulatory effects.[7, 8] Their use has demonstrated potential to provide the needed extra biological support to processed nerve allografts.[9-13] Adipose tissue is a valuable source for mesenchymal stem cells (MSCs) from the stromal vascular fraction as it is easily accessible and contains relatively large amounts of rapidly proliferating MSCs.[14-18]

Schwann cells, the original facilitators of nerve regeneration, have been confirmed as even better providers of biological support to processed nerve allografts than MSCs.[19] However, their harvest requires the sacrifice of autologous nerve tissue. Another option to obtain Schwann-like cells is to chemically differentiate MSCs into Schwann-like cells.[20-23] Several in-vitro studies have demonstrated the potential of differentiated Schwann-like MSCs in peripheral nerve repair, resulting in increased neurite outgrowth of motor neurons compared to undifferentiated MSCs.[19, 24, 25]

The trophic function of MSCs that results in enhanced gene expression and production of neurotrophic growth factors[24, 26], does not require delivery of MSCs inside the nerve allograft. Because microinjection and soaking of MSCs damage both the cells and the allograft while reducing the number of uniformly attached cells, dynamic seeding offers a promising cell delivery strategy that has not been evaluated for differentiated MSCs.[27-29]

The purpose of this study was to determine the ability of MSCs differentiated into Schwann-like cells to be dynamically seeded on decellularized nerve allografts and to compare their seeding potential to that of control MSCs. This was investigated by three different sub-studies that aimed to evaluate (I) the influence of processed nerve grafts on the viability of differentiated MSCs, (II) the seeding potential of Schwann-like MSCs on processed nerve grafts and temporal optimization of seeding duration, and (III) the survivability, distribution and migration of differentiated MSCs after seeding.

MATERIALS AND METHODS

This study was approved by the IACUC institutional review committee and the Institutional

Review Board (IACUC protocol A3053-16).

Mesenchymal stem cell collection and characterization

Rat MSCs were obtained from the inguinal fat pad from Lewis rats and derived as previously published.[18] The obtained MSCs were previously characterized by plastic adherence and pluripotency toward mesodermal lineages.[29] For flow cytometric assessment of stem cell surface markers, MSCs in passage five were used. The expression of MSC surface markers (CD29 and CD90) and hemapoetic cell surface markers (CD34 and CD45) were tested and compared with three control samples. Cell suspensions were pre-incubated with Fc block (Purified Mouse Anti-Rat CD32, 0.5uG per 500uL; BD PharmingenTM, CA, USA) to avoid unspecific binding. Thereafter, CD29 antibody (CD29 antibody | HM beta 1-10; Bio-rad-antibodies, CA, USA), CD90 antibody (CD90 Antibody | OX-7; Bio-rad-antibodies, CA, USA), CD45 antibody (CD45 antibody | OX-1; Bio-rad-antibodies, CA, USA) and CD34 (Mouse/Rat CD34 antibody; R&D systems Inc, MN, USA) were introduced to different samples. For the CD34-sample, the appropriate secondary reagent was added as well (Donkey Anti-Sheep IgG Fluorescein-conjugated antibody; R&D systems Inc, MN, USA). Cells were washed twice in flow cytometry buffer and centrifuged at 300g for five minutes after each wash. Finally, 7-AAD staining was added to each sample to exclude dead cells. Flow cytometry was performed with a BD FACScan flow cytometer.

Mesenchymal Stem Cell differentiation into Schwann-like cells

MSC differentiation into Schwann-like cells was accomplished according to the extensively tested protocol of Kingham and colleagues.[18] Briefly, after two preparatory steps with ß-mercaptoethanol (Sigma-Aldrich corp., MO, USA) and all-trans-retinoic acid (Sigma-Aldrich Corp., MO, USA), the growth medium was replaced by differentiation medium containing Forskolin (Sigma-Aldrich corp., MO, USA), basic fibroblast growth factor (bFGF; PeproTech, NJ, USA), platelet-derived growth factor (PDGF-AA; PeproTech, NJ, USA) and Neuregulin-1 ß1 (NRG1-b1; R&D systems Inc, MN, USA). Successful MSC differentiation was verified by immunocytochemistry for Schwann cell marker S100 (Rabbit anti-S100; ThermoFisher Scientific, MA, USA), glial cell marker GFAP (Glial fibrillary acidic protein, mouse anti-GFAP; ThermoFisher Scientific, MA, USA) and Neurotrophin Receptor p75 (p75 NTR, rabbit anti-p75 NTR; ThermoFisher Scientific, MA, USA). Goat anti-rabbit FITC and goat anti-mouse Cyanine-3 (CY3) (both ThermoFisher Scientific, MA, USA) were used as secondary antibodies. Cell nuclei were labeled with DAPI (4',6-diamindino-2-phenylindole, ThermoFisher Scientific, MA, USA). The fluorescent expression of the differentiated MSCs was compared to the expression of undifferentiated MSCs and Schwann cells.

Nerve allograft processing

Fifty-six sciatic nerves were obtained from 28 Sprague-Dawley rats weighing 250-350 grams and were decellularized according to the protocol of Hundepool and colleagues.[30] In this 5-day protocol, the nerve allografts are exposed to elastase, resulting in less cellular debris with preservation of the ultrastructure of the nerve. Sprague-Dawley rats were specifically selected as there is a known histocompatibility mismatch to Lewis rats.[31, 32] The nerves were

sterilized using γ-irradiation and stored at 4° Celsius after processing.

Analysis of Cell viability

To assess the influence of chemical products used to process the allografts on the MSC-viability and to compare the vulnerability of differentiated MSCs and control MSCs, (3-(4,5-dimethylthiazol-2-yl)-5-(3-carboxymethoxyphenyl)-2-(4-sulfophenyl)-2H-tetrazolium) (MTS) assays (CellTiter 96® Aqueous One Solution Cell Proliferation Assay; Promega Corporation, WI, USA) were carried out according to the manufacturer's protocol.[33] This assay is a colorimetric method to determine the number of viable cells. Living cells in culture have metabolic activity and will convert the added reagent in formazan. Formazan quantity is directly correlated to the amount of 490nm absorbance and can therefore be measured with an Infinite® 200 Pro TECAN Reader (Tecan Trading AG, Switzerland).

Undifferentiated and differentiated MSCs (5,000 in 100µL growth medium per well) were transferred to a p-HEMA (Poly 2-hydroxyethyl methacrylate; Sigma-Aldrich Corp., MO, USA) coated 96-well plate, to prevent cells from migrating to the plastic surface of the well. After soaking in growth medium for two hours, 48 2mm-segments of processed nerve allografts were divided among the wells containing the cells. The medium was changed every 72 hours; undifferentiated MSCs were cultured in normal growth medium, differentiated MSCs were cultured in differentiation medium. The metabolic activity of undifferentiated MSCs (undifferentiated MSCs + pHEMA + allograft) was compared to differentiated MSCs (differentiated MSCs + pHEMA + allograft) on four estimated time points (T = 1, 2, 3 and 7 days). The remaining groups represented normal cell viability (pHEMA + undifferentiated MSCs and pHEMA + differentiated MSCs) and negative controls (no cells). For each group, the metabolic activity of three replicates per sample was tested twice on each time point. Colorimetric assays were performed with the Infinite® 200 Pro TECAN Reader (Tecan Trading AG, Switzerland) at an absorbance wavelength of 490nm. The metabolic activity of undifferentiated MSCs and differentiated MSCs in the vicinity of an allograft was expressed as a ratio of the metabolic activity of undifferentiated MSCs and differentiated MSCs without an allograft. The experimental design is shown in **table 1**.

Group	Description	Time points	N	Outcome measurements
I	Undifferentiated MSCs + allograft	T1 = 1 day T2 = 2 days T3 = 3 days T4 = 7 days	3 samples per group for each time point	Metabolic activity (MTS assay)
II	Differentiated MSCs + allograft			
III	Undifferentiated MSCs			
IV	Differentiated MSCs			

Table 1. *Experimental design experiment 1.*
MSCs: Mesenchymal Stem Cells
MTS assay: (3-(4,5-dimethylthiazol-2-yl)-5-(3-carboxymethoxyphenyl)-2-(4-sulfophenyl)-2H-tetrazolium assay

Seeding efficiency, cell adhesion, distribution and migration

A dynamic seeding strategy that was previously described for undifferentiated MSCs was used in this study.[29] In total, 36 processed nerve graft segments of 10mm in length were soaked in growth medium for two hours to remove any toxic decellularization agents and divided among conical tubes containing 10mL growth medium with one million undifferentiated MSCs or differentiated MSCs per nerve. These tubes were placed on a rotating system which was rotated for six, 12 or 24 hours at 37°C (n = 6 per group per seeding duration). Seeding efficiency on each time point was determined by cell counts in the cell supernatant of all the different samples; this provided the average number of free floating cells in the tubes and the average number of cells that were adherent to the nerve. Two supernatant samples (10μL) were taken out of each of the conical tubes after the seeding duration had passed. Subsequently, one investigator performed three cell counts on each of the supernatant samples. So for each nerve sample (n=6 per group per time point), 6 cell counts were averaged for final analysis in order to minimize potential error.

The viability and distribution of the cells seeded on the nerve grafts was studied by live/dead Cell Viability Assays (Invitrogen, Life Technologies Corporation, NY, USA) and Hoechst stain (Hoechst stain solution; Sigma-Aldrich Corp., MO, USA) and visualized using a confocal microscope (Zeiss LSM 780 confocal microscope). The live/dead and Hoechst stain assays were prepared by one investigator. Both the Live/dead stain and the Hoechst stain were obtained according to standardized protocols; incubation of the samples with live/dead stain (Invitrogen, Life Technologies Corporation, NY, USA) or Hoechst stain mixture (Hoechst stain solution; Sigma-Aldrich Corp., MO, USA) for 20 minutes after which the samples were washed with PBS. Both stains were performed on three samples per group per seeding duration.
Cell shape and distribution was evaluated by Scanning Electron Microscopy (SEM) of the three remaining seeded samples per group per time point. To obtain SEM images, the samples were transferred to 2% Trump's fixative solution (37% formaldehyde and 25% glutaraldehyde) overnight, washed in phosphate buffer, and rinsed in water and dehydrated through a graded series of ethanol. Subsequently, the samples were critical point dried using carbon dioxide, mounted on an aluminum stub and sputter-coated for 60 seconds using gold-palladium. The samples were imaged in a Hitachi S-4700 cold field emission scanning electron microscope (Hitachi High Technologies America, Inc., IL, USA) at 5kV accelerating voltage. The preparation and the imaging of the SEM samples were performed by the Microscopy and Cell analysis core lab of the Mayo Clinic. The distribution of cells on the outer surface was only assessed and described subjectively and were therefore not blinded. An overview of the experimental design is depicted in **table 2**.

Two extra processed nerves per group were seeded with the previously estimated optimal seeding duration and transferred to 10% formalin and processed and embedded in paraffin to evaluate the migration of cells into the nerve grafts. Three 5μM sections of the proximal- and mid-nerve segment were sectioned and Hoechst stained. The Hoechst-stained cross-sectional segments of the nerves were blinded for the objective assessment of present cells on the inner surface of the samples (present versus absent). The cells were visualized with a confocal microscope (Zeiss LSM 780 confocal microscope; Zeiss, Germany).

Group	Description	Time points (seeding duration)	Number of samples	Outcome measurements
I	Undifferentiated MSCs + nerve allograft	T1 = 6 hours T2 = 12 hours T3 = 24 hours	6 samples per group per time point	• Cell counts (n=6) • Live/dead + Hoechst stains (n=3) • SEM (n=3)
II	Differentiated MSCs + nerve allograft			

Table 2. Experimental design experiment 2. MSCs: Mesenchymal Stem Cells, SEM: Scanning Electron Microscopy

Statistical analysis

Seeding efficiencies are displayed ± Standard Error of the Mean. Significance of the interaction between cell type, time and outcome were analyzed with two-way ANOVA. If the interaction was significant, the within and between group comparisons were analyzed with the Kruskal-Wallis test, followed by pairwise comparisons using Wilcoxon rank-sum tests with Bonferroni correction. A value of $p < 0.05$ was considered statistically significant.

RESULTS

Mesenchymal stem cell collection

Flow cytometric analysis showed that the cultured rat MSCs were positive for mesenchymal stem cell markers CD29 (88.2%) and CD90 (88.3%) and negative for the hematopoetic cell markers CD34 (91.1%) and CD45 (86.0%), demonstrating that MSCs were definitively the cell lineage utilized in this study.

Mesenchymal stem cell differentiation into Schwann-like cells

The morphology of differentiated MSCs changed in vitro in a more spindle-like shape, typical for Schwann cells. In contrast to undifferentiated MSCs, Schwann cells and differentiated MSCs showed positive immunofluorescence for Schwann cell surface markers S100 Calcium Binding Protein B (S100B), Glial Fibrillary Acidic Protein (GFAP) and Nerve Growth Factor Receptor (NGFR/P75NTR), which verified successful differentiation into Schwann-like cells (**figure 1**).[18]

Cell viability

The cell viability of undifferentiated and differentiated MSCs were equal and remained constant during the first three time points, after which the viability of both cell types slightly decreased. No decrease in cell viability was observed upon co-culture of MSCs with the processed nerve allograft. The viability of differentiated MSCs in the vicinity of an allograft approaches the viability of differentiated MSCs alone over time ($p=0.270$), while the viability of undifferentiated MSCs with the allograft increased over time compared to undifferentiated MSCs alone; the increased viability ratio between 2 and 3 days of culture was statistically significant ($p=0.025$).

The differences between both cell-group ratios after 3 and 7 days of culture were statistically significant as well (p=0.009 and p=0.026). These results imply that chemical processing of nerve allografts does not generate a surface that decreases cell-viability. Interestingly, the demonstrated ratios suggest that the processed allograft stimulates the viability of undifferentiated MSCs, while this effect is not as obvious for differentiated MSCs. The absorbance ratios, and thus the viability ratios of the different cell cultures over time are shown in **figure 2**.

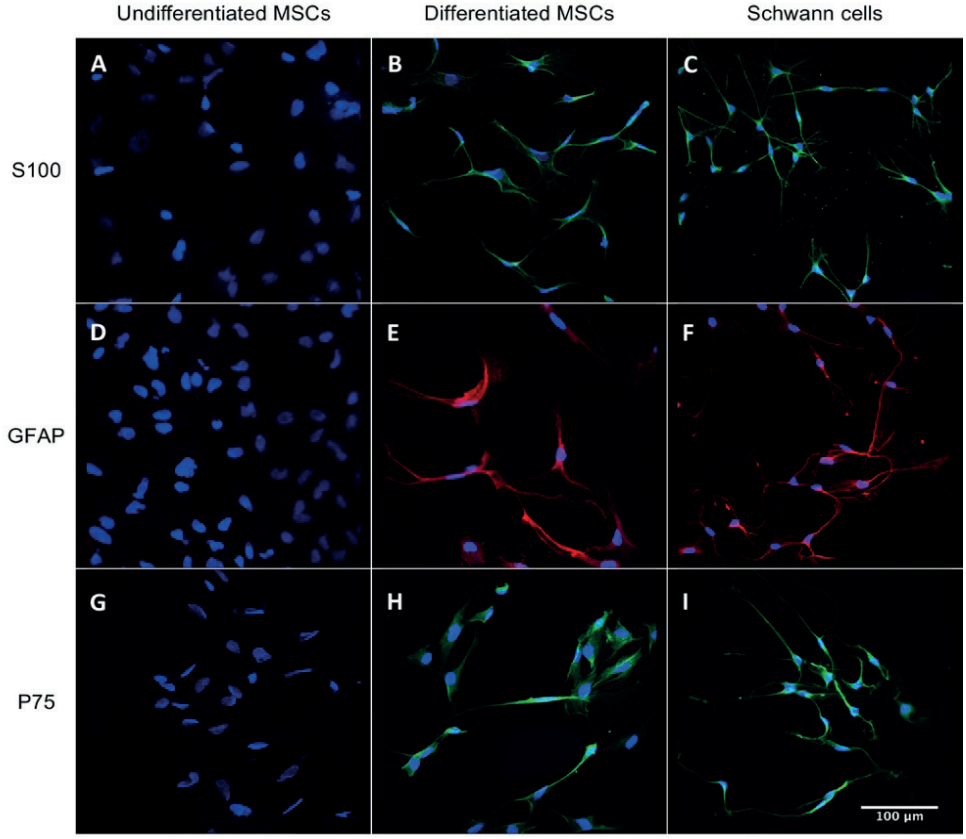

Figure 1. *Differentiation of MSCs into Schwann-like cells. Immunocytochemical comparison between undifferentiated MSCs (a, d, g), differentiated MSCs (b, e, h) and Schwann cells (c, f, i). Cells are tested for the presence of Schwann cell marker S100 (a, b, c, green), glial cell marker GFAP (d, e, f, red) and neurotrophin Receptor p75 (g, h, i, green). Cell nuclei are DAPI-stained (blue).*

Cell adhesion

After six hours of seeding, only 24.38% (±6.34) of undifferentiated MSCs and 43.33% (±3.02) of differentiated MSCs were attached to the processed nerve allografts. Subsequently, these percentages increased to 80.00% (±1.73) (undifferentiated MSCs) and 94.54% (±1.50) (differentiated MSCs) after 12 hours of dynamic seeding and changed to 82.00% (±5.92) (undifferentiated MSCs) and 77.50% (±6.67) (differentiated MSCs) after 24 hours. 'Between

group' analyses did not show any significant differences. 'Within group' analyses showed a significant interaction between seeding efficiency and seeding duration for undifferentiated MSCs (p=0.021) and differentiated MSCs (p=0.007). Pairwise comparisons revealed that the increase between 6 and 12 hours of seeding (p=0.029) undifferentiated MSCs was statistically significant, but not between 12 and 24 hours (p=0.486). The increased seeding efficiency between 6 and 12 hours and the decrease between 12 and 24 hours of seeding of differentiated MSCs were statistically significant (both p=0.029). Considering a shorter seeding duration is more cost effective and time efficient, the optimal dynamic seeding duration was determined to be 12 hours for both groups. The seeding efficiencies at different time points are shown in **figure 3**.

Cell distribution and migration

Dynamic seeding resulted in a layer of viable cells on the surface of the processed nerve allograft with no major differences in distribution between the cell-types and different seeding durations. Virtually no dead cells were apparent on the processed nerve allograft during dynamic seeding, which suggests that only viable cells are able to attach to the nerve. Although subjective, the differentiated MSCs seem to seed in a more clustered fashion than undifferentiated MSCs (**figure 4a-b**). Hoechst stain (not shown) and SEM of the surface of the seeded nerve grafts showed a similar distribution and illustrated that the cells retain their typical shapes during dynamic seeding (**figure 4c-f**). None of the cross-sectional segments of the proximal and mid-portion of the nerves showed migration of both undifferentiated MSCs and differentiated MSCs into the nerve graft (**figure 4g-h**).

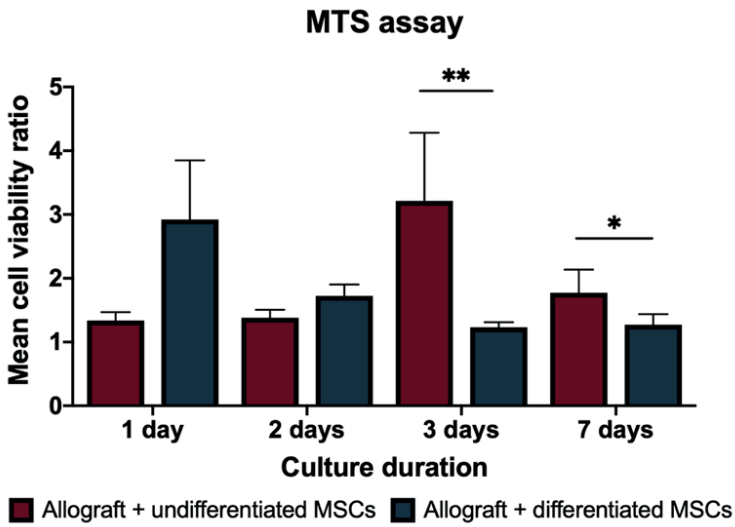

*Figure 2. Metabolic activity of undifferentiated and differentiated MSCs after a processed nerve allograft was introduced to their well. The activity is expressed as a ratio of the metabolic activity of MSCs without a processed nerve allograft. Undifferentiated MSCs had a significantly higher metabolic ratio after 3 (p=0.009) and 7 (p=0.026) days of culture. Error bars = SEM. **=p<0.01, *=p<0.05*

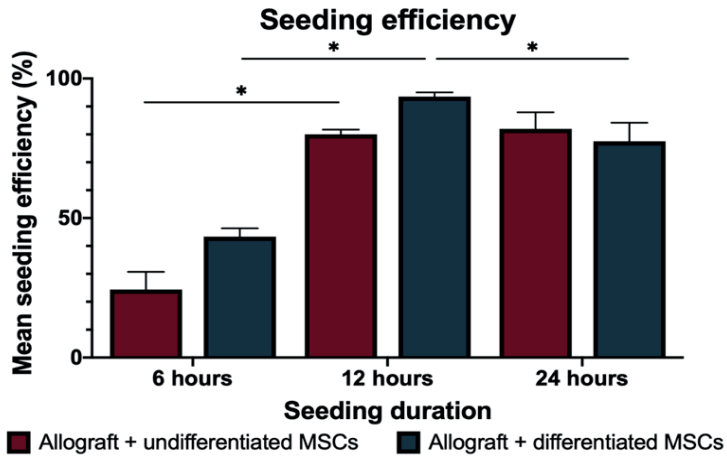

Figure 3. *Seeding efficiency of three different seeding durations. The efficiency is expressed as a percentage of the cells provided per nerve (1 million cells). The increase between 6 and 12 hours of seeding (p=0.029) undifferentiated MSCs was statistically significant. The increased seeding efficiency of differentiated MSCs between 6 and 12 hours and the decrease between 12 and 24 hours were also statistically significant (both p=0.029). Error bars = SEM. *=statistical significance, p<0.05*

DISCUSSION

The overall purpose of this study was to determine (I) the influence of processed nerve grafts on the viability of differentiated MSCs, (II) the seeding potential and optimal seeding duration of differentiated MSCs on processed nerve grafts, and (III) the survivability, distribution and migration of differentiated MSCs after seeding. The reagents used to process the nerve allografts in this study[30] did not influence the metabolic activity of either differentiated MSCs or undifferentiated MSCs. Similar to undifferentiated MSCs, the differentiated MSCs were successfully seeded on a processed nerve allograft using a previously reported dynamic seeding strategy[29], without compromising the quality of the inner nerve ultrastructure. The optimal dynamic seeding time for both groups was 12 hours, which led to the attachment of viable undifferentiated MSCs and differentiated MSCs to the surface of the processed nerve allograft. Both types of MSCs distributed among the nerve allograft in a uniform manner and did not migrate into the ultrastructure of the nerve allograft.

In vitro, Schwann-like MSCs support superior neurite outgrowth when co-cultured with motor-neurons and express higher levels of neurotrophic and angiogenic genes compared to undifferentiated MSCs.[18, 19, 24, 25] The potential for uncontrolled proliferation or differentiation of MSCs into non-neural lineages is another argument to differentiate MSCs before implementation. The pluripotency of undifferentiated MSCs makes them difficult to control in vivo. The concern that their potential to promote neoangiogenesis and to regulate the immune response may lead to tumor growth or metastasis has been described, but has not been confirmed yet.[34, 35] The disadvantages of differentiating MSCs into Schwann-like cells include the additional effort and extended preparation time which may delay the period between

nerve-injury and surgery. In vivo studies demonstrating no differences in functional outcomes compared to undifferentiated MSCs also favor the use of undifferentiated MSCs in the clinical setting.[36, 37] The absence of in vivo differences is potentially caused by the hypothesized limited survivability of differentiated cells[10] or an inefficient delivery of differentiated MSCs. Published delivery methods vary widely, while none of the delivery methods has specifically been tested on differentiated MSCs. Thus, to date there is no compelling evidence for the use of either undifferentiated MSCs or differentiated MSCs for seeded nerve allografts used for segmental motor nerve reconstruction.

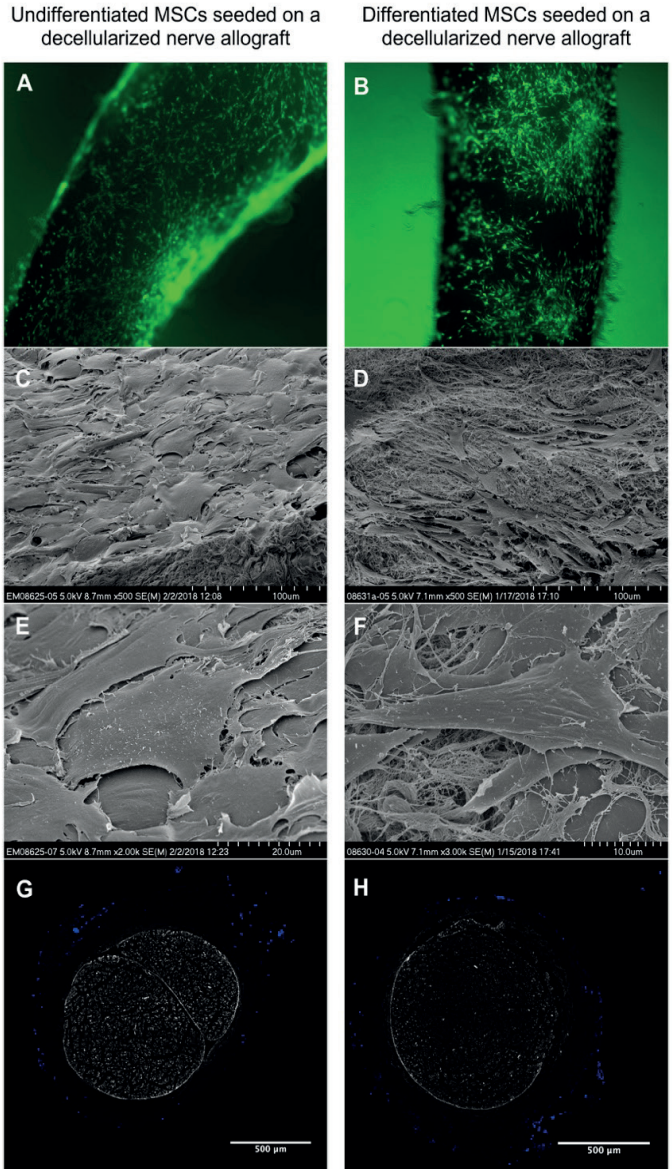

Figure 4.
Undifferentiated MSCs (left) and differentiated MSCs (right) seeded on a nerve allograft. 4a-b. Viable cells are visualized in green, dead cells in red (not present). 4c-f. Scanning Electron Microscopy images of undifferentiated MSCs seeded onto a nerve allograft (left) and differentiated MSCs seeded on a nerve allograft (right) in multiple magnifications (500X, 2000X and 3000X), showing the different morphology of the cells when seeded on the nerve allograft. 4g-h. Cross-sectional images of the mid-portions of processed nerve allografts seeded with undifferentiated (left) and differentiated (right) MSCs. Cell nuclei are Hoechst-stained (bright blue). The inner ultrastructure of the nerve does not contain any cells.

Cell-injection and nerve-

soaking in cell-solutions are used as delivery methods of MSCs with the rationale that they have a structural function as Schwann cells that need to be delivered within the nerve allograft itself. Injection may be traumatic to both MSCs and the ultrastructure of the nerve allograft and results in an unequal distribution of the delivered cells.[27, 38-40] The average diameter of MSCs exceeds the calibers of myelinated axon fibers, suggesting that MSCs can block axon ingrowth when delivered inside the nerve graft.[41-43] Soaking techniques deliver lower number of cells in a nonuniform distribution.[28]

It has been recently reported that growth factors and cytokines produced by MSCs may enhance nerve regeneration, while not necessitating intraneural placement of the MSCs.[7, 44] The straightforward dynamic seeding strategy of Rbia and colleagues successfully attaches large numbers of undifferentiated MSCs to the surface of a processed nerve allograft without harming the inner ultra-structure of the allograft.[29] The same technique resulted in the same optimal seeding duration for undifferentiated MSCs in this study, indicating a high reproducibility of the Rbia method. The seeding of differentiated MSCs is less well established and differentiation of cells may decrease their potential to attach to processed nerve allografts, possibly due to their changes in cellular morphology (e.g., spindle-like shape).[10] This study demonstrated there was no decrease in attachment efficiency when MSCs are differentiated. Based on our experience, dynamic seeding of differentiated MSCs onto a processed nerve allograft is possible and results in a uniform distribution of large amounts of differentiated MSCs (and undifferentiated MSCs) on the surface of the nerve allograft which has not been accomplished by other previously described methods.

Both cell types have previously shown to produce neurotrophic and angiogenic factors and have been allocated an immunomodulatory role. [7, 18, 19, 24, 25, 44] The porous epineurium of the processed nerve allografts (demonstrated in **figure 3**) allows for these factors to both regulate the immune response and angiogenesis in the surroundings of the regenerating nerve, and stimulate nerve regeneration inside the nerve allograft, while the cells remain on the outer surface of the graft. The seeded MSCs form an addition to the circulating stem cells normally attracted to the regenerating nerve, also functioning from outside the epineurium.

A limitation of this study is the in vitro setting, which may not translate into results expected for an in vivo setting. In vitro studies permit testing of the seeding potential of undifferentiated MSCs and differentiated MSCs without having to sacrifice extra animals. With the described strategy, it would approximately take up two to five weeks after nerve injury to obtain a processed allograft seeded with patient's own (undifferentiated or differentiated) MSCs. Although peripheral nerve injuries are ideally repaired as soon as possible after injury, a two- or five-week delay that eventually leads to the desirable improved nerve regeneration would be clinically applicable. Furthermore, the utility of methods to deliver undifferentiated MSCs and differentiated MSCs to the surface of a nerve graft relies on the idea that MSCs at least have a partly trophic function and that growth factors and cytokines produced by them will migrate through the epineurium and enhance nerve regeneration. This hypothesis needs to be confirmed both in vitro and in vivo. The current study is the essential first step in testing this hypothesis.

CONCLUSION

We successfully differentiated MSCs into Schwann-like cells and dynamically seeded them onto a processed nerve allograft. The viability of undifferentiated MSCs and differentiated MSCs was not influenced by the processed nerve allograft. Both cell types distributed equally among the nerve allograft, remained on the surface of the allograft and did not migrate into the graft. Thus, seeding of nerve allografts with Schwann-like MSCs can be further considered for in vivo studies for nerve repair.

Conflict of interest statement
None of the authors has a conflict of interest. This study was funded by the NIH R01, 'Bridging the gap: angiogenesis and stem cell seeding of processed nerve allograft'. 1 RO1 NS102360-01A1

Acknowledgements
We thank Patricia F. Friedrich for assistance with the preparations of the experiments.

REFERENCES

1. Rbia N, Shin AY. The Role of Nerve Graft Substitutes in Motor and Mixed Motor/Sensory Peripheral Nerve Injuries. J Hand Surg Am 2017: 42: 367-77.
2. Giusti G, Willems WF, Kremer T, et al. Return of motor function after segmental nerve loss in a rat model: comparison of autogenous nerve graft, collagen conduit, and processed allograft (AxoGen). J Bone Joint Surg Am 2012: 94: 410-7.
3. FF IJ, Nicolai JP, Meek MF. Sural nerve donor-site morbidity: thirty-four years of follow-up. Ann Plast Surg 2006: 57: 391-5.
4. Cho MS, Rinker BD, Weber RV, et al. Functional outcome following nerve repair in the upper extremity using processed nerve allograft. J Hand Surg Am 2012: 37: 2340-9.
5. Moore AM, MacEwan M, Santosa KB, et al. Acellular nerve allografts in peripheral nerve regeneration: A comparative study. MUSCLE NERVE 2011: 44: 221-34.
6. Whitlock EL, Tuffaha SH, Luciano JP, et al. Processed allografts and type I collagen conduits for repair of peripheral nerve gaps. MUSCLE NERVE 2009: 39: 787-99.
7. Caplan AI. Adult Mesenchymal Stem Cells: When, Where, and How. Stem Cells Int 2015: 2015: 628767.
8. Cao F, Liu T, Xu Y, Xu D, Feng S. Culture and properties of adipose-derived mesenchymal stem cells: characteristics in vitro and immunosuppression in vivo. Int J Clin Exp Pathol 2015: 8: 7694-709.
9. Moattari M, Kouchesfehani HM, Kaka G, et al. Chitosan-film associated with mesenchymal stem cells enhanced regeneration of peripheral nerves: A rat sciatic nerve model. J Chem Neuroanat 2017: 88: 46-54.
10. Fairbairn NG, Meppelink AM, Ng-Glazier J, Randolph MA, Winograd JM. Augmenting peripheral nerve regeneration using stem cells: A review of current opinion. World J Stem Cells 2015: 7: 11-26.
11. Zhao Z, Wang Y, Peng J, et al. Repair of nerve defect with acellular nerve graft supplemented by bone marrow stromal cells in mice. Microsurgery 2011: 31: 388-94.
12. Wang Y, Zhao Z, Ren Z, et al. Recellularized nerve allografts with differentiated mesenchymal stem cells promote peripheral nerve regeneration. Neurosci Lett 2012: 514: 96-101.
13. Hundepool CA, Nijhuis TH, Mohseny B, Selles RW, Hovius SE. The effect of stem cells in bridging peripheral nerve defects: a meta-analysis. J Neurosurg 2014: 121: 195-209.
14. Strioga M, Viswanathan S, Darinskas A, Slaby O, Michalek J. Same or not the same? Comparison of adipose tissue-derived versus bone marrow-derived mesenchymal stem and stromal cells. Stem Cells Dev 2012: 21: 2724-52.
15. Mahmoudifar N, Doran PM. Mesenchymal Stem Cells Derived from Human Adipose Tissue. Methods Mol Biol 2015: 1340: 53-64.
16. Yoshimura H, Muneta T, Nimura A, et al. Comparison of rat mesenchymal stem cells derived from bone marrow, synovium, periosteum, adipose tissue, and muscle. Cell Tissue Res 2007: 327: 449-62.
17. Safford KM, Hicok KC, Safford SD, et al. Neurogenic differentiation of murine and human adipose-derived stromal cells. Biochem Biophys Res Commun 2002: 294: 371-9.
18. Kingham PJ, Kalbermatten DF, Mahay D, et al. Adipose-derived stem cells differentiate into a Schwann cell phenotype and promote neurite outgrowth in vitro. Exp Neurol 2007: 207: 267-74.
19. Ladak A, Olson J, Tredget EE, Gordon T. Differentiation of mesenchymal stem cells to support peripheral nerve regeneration in a rat model. Exp Neurol 2011: 228: 242-52.
20. di Summa PG, Kingham PJ, Raffoul W, et al. Adipose-derived stem cells enhance peripheral nerve regeneration. J Plast Reconstr Aesthet Surg 2010: 63: 1544-52.
21. Ao Q, Fung CK, Tsui AY, et al. The regeneration of transected sciatic nerves of adult rats using chitosan nerve conduits seeded with bone marrow stromal cell-derived Schwann cells. Biomaterials 2011: 32: 787-96.
22. Chen X, Wang XD, Chen G, et al. Study of in vivo differentiation of rat bone marrow stromal cells into schwann cell-like cells. Microsurgery 2006: 26: 111-15.
23. Tomita K, Madura T, Mantovani C, Terenghi G. Differentiated adipose-derived stem cells promote

myelination and enhance functional recovery in a rat model of chronic denervation. J Neurosci Res 2012: 90: 1392-402.
24. Kingham PJ, Kolar MK, Novikova LN, Novikov LN, Wiberg M. Stimulating the neurotrophic and angiogenic properties of human adipose-derived stem cells enhances nerve repair. Stem Cells Dev 2014: 23: 741-54.
25. Tomita K, Madura T, Sakai Y, et al. Glial differentiation of human adipose-derived stem cells: implications for cell-based transplantation therapy. Neuroscience 2013: 236: 55-65.
26. Liu Y, Zhang Z, Qin Y, et al. A new method for Schwann-like cell differentiation of adipose derived stem cells. Neurosci Lett 2013: 551: 79-83.
27. Jesuraj NJ, Santosa KB, Newton P, et al. A systematic evaluation of Schwann cell injection into acellular cold-preserved nerve grafts. J Neurosci Methods 2011: 197: 209-15.
28. Thompson MJ, Patel G, Isaacs J, et al. Introduction of neurosupportive cells into processed acellular nerve allografts results in greater number and more even distribution when injected compared to soaking techniques. Neurol Res 2017: 39: 189-97.
29. Rbia N, Bulstra LF, Bishop AT, van Wijnen AJ, Shin AY. A simple dynamic strategy to deliver stem cells to decellularized nerve allografts. Plast Reconstr Surg 2018.
30. Hundepool CA, Nijhuis TH, Kotsougiani D, et al. Optimizing decellularization techniques to create a new nerve allograft: an in vitro study using rodent nerve segments. Neurosurg Focus 2017: 42.
31. Hudson TW, Zawko S, Deister C, et al. Optimized acellular nerve graft is immunologically tolerated and supports regeneration. Tissue Eng 2004: 10: 1641-51.
32. Kumta S, Yip K, Roy N, Lee SK, Leung PC. Revascularisation of bone allografts following vascular bundle implantation: an experimental study in rats. Arch Orthop Trauma Surg 1996: 115: 206-10.
33. Cory AH, Owen TC, Barltrop JA, Cory JG. Use of an aqueous soluble tetrazolium/formazan assay for cell growth assays in culture. Cancer Commun 1991: 3: 207-12.
34. Volarevic V, Markovic BS, Gazdic M, et al. Ethical and Safety Issues of Stem Cell-Based Therapy. Int J Med Sci 2018: 15: 36-45.
35. Lazennec G, Jorgensen C. Concise review: adult multipotent stromal cells and cancer: risk or benefit? Stem Cells 2008: 26: 1387-94.
36. Orbay H, Uysal AC, Hyakusoku H, Mizuno H. Differentiated and undifferentiated adipose-derived stem cells improve function in rats with peripheral nerve gaps. J Plast Reconstr Aesthet Surg 2012: 65: 657-64.
37. Watanabe Y, Sasaki R, Matsumine H, Yamato M, Okano T. Undifferentiated and differentiated adipose-derived stem cells improve nerve regeneration in a rat model of facial nerve defect. J Tissue Eng Regen Med 2017: 11: 362-74.
38. Garvican ER, Cree S, Bull L, Smith RK, Dudhia J. Viability of equine mesenchymal stem cells during transport and implantation. Stem Cell Res Ther 2014: 5: 94.
39. Agashi K, Chau DY, Shakesheff KM. The effect of delivery via narrow-bore needles on mesenchymal cells. Regen Med 2009: 4: 49-64.
40. Mamidi MK, Singh G, Husin JM, et al. Impact of passing mesenchymal stem cells through smaller bore size needles for subsequent use in patients for clinical or cosmetic indications. J Transl Med 2012: 10: 229.
41. Sunderland S, Lavarack JO, Ray LJ. The caliber of nerve fibers in human cutaneous nerves. J COMP NEUROL 1949: 91: 87-101.
42. Ryu YJ, Cho TJ, Lee DS, Choi JY, Cho J. Phenotypic characterization and in vivo localization of human adipose-derived mesenchymal stem cells. Mol Cells 2013: 35: 557-64.
43. Ge J, Guo L, Wang S, et al. The size of mesenchymal stem cells is a significant cause of vascular obstructions and stroke. Stem Cell Rev 2014: 10: 295-303.
44. Caplan AI, Hariri R. Body Management: Mesenchymal Stem Cells Control the Internal Regenerator. Stem Cells Transl Med 2015: 4: 695-701.

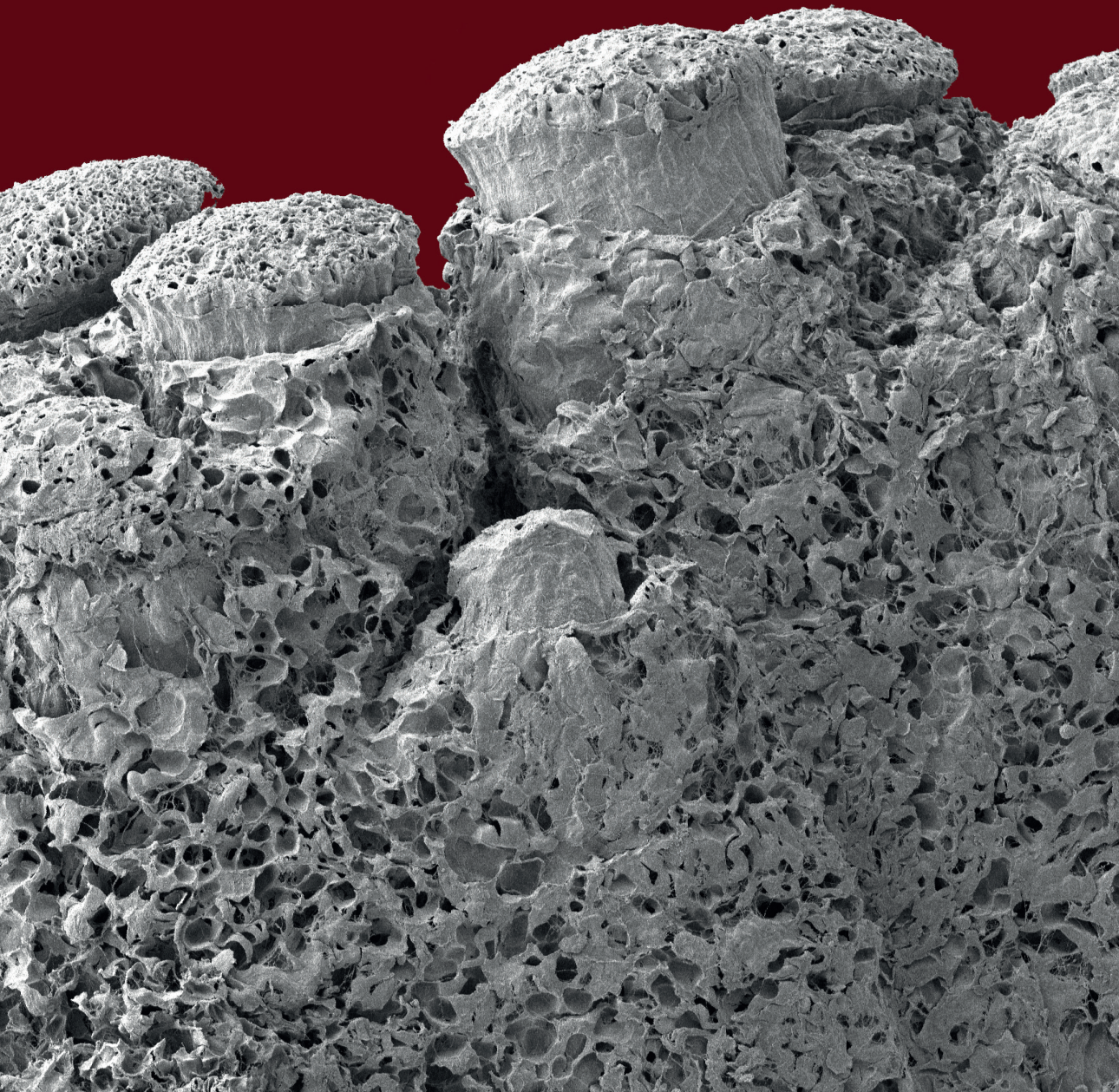

Chapter 4

Gene expression profiles of differentiated and undifferentiated adipose derived mesenchymal stem cells dynamically seeded onto a processed nerve allograft

Femke Mathot, Nadia Rbia, Roman Thaler, Allen T. Bishop, Andre J. van Wijnen, Alexander Y. Shin

Gene. 2020 January;724:144151

ABSTRACT

Background

Differentiation of mesenchymal stem cells (MSCs) into Schwann-like cells onto processed nerve allografts may support peripheral nerve repair. The purpose of this study was to understand the biological characteristics of undifferentiated and differentiated MSCs before and after seeding onto a processed nerve allograft by comparing gene expression profiles.

Methods

MSCs from Lewis rats were cultured in maintenance media or differentiated into Schwann-like cells. Both treatment groups were dynamically seeded onto decellularized nerve allografts derived from Sprague-Dawley rats. Gene expression was quantified by quantitative polymerase chain reaction (qPCR) analysis of representative biomarkers, including neurotrophic (*GDNF, PTN, GAP43, PMP22*), angiogenic (*CD31, VEGF1*), extracellular matrix (ECM) (*COL1A1*, *COL3A1*, *FBLN1*, *LAMB2*) or cell cycle (*CAPS3*, *CCBN2*) genes. Gene expression values were statistically evaluated using a 2-factor ANOVA with repeated measures.

Results

Baseline gene expression of undifferentiated and differentiated MSCs was significantly altered upon interaction with processed nerve allografts. Interaction between processed allografts and undifferentiated MSCs enhanced expression of neurotrophic (*NGF*, *GDNF*, *PMP22*), ECM (*FBLN1*, *LAMB2*) and regulatory cell cycle genes (*CCNB2*) during a 7-day time course. Interactions of differentiated MSCs with nerve allografts enhanced expression of neurotrophic (*NGF*, *GDNF*, *GAP43*), angiogenic (*VEGF1*), ECM (*FBLN1*) and regulatory cell cycle genes (*CASP3*, *CCNB2*) within one week.

Conclusions

Dynamic seeding onto processed nerve allografts modulates temporal gene expression profiles of differentiated and undifferentiated MSCs. These changes in gene expressions may support the reparative functions of MSCs in supporting nerve regeneration in different stages of axonal growth.

INTRODUCTION

Although many efforts have been made to find a neural tissue substitute equivalent to nerve autografts, autografts currently remain the gold standard in the reconstruction of critical nerve defects. [1-5] Nerve allografts are a promising option, but decellularization is required to prevent an immune response in the recipient. While necessary for successful transplantation, decellularization removes all cellular components including Schwann cells from allograft nerve tissues.[6, 7] Schwann cells are fundamental for peripheral nerve formation and play a critical role in peripheral nerve regeneration by producing axonotrophic factors and providing remyelination.[8, 9] It has been postulated that direct or indirect addition of growth factors may enhance nerve regeneration in processed nerve allografts, replacing or mimicking the function of the absent Schwann cells. Yet, direct delivery of growth factors has not resulted in improved outcomes [10-12], suggesting that cellular mechanisms are necessary for the growth factors to be functional.

Indirect delivery of growth factors could be provided by mesenchymal stromal cells (MSCs). MSCs are biologically important for tissue repair and regeneration by influencing the immune system, enhancing angiogenesis and inhibiting scar formation.[13, 14] MSCs are mostly obtained from either bone marrow or adipose tissue. Adipose tissue can be easily harvested and contains large amounts of MSCs that proliferate rapidly in optimized cell culture medium.[15-18] When added to decellularized nerve allografts, adipose-derived MSCs produce growth factors that support tissue repair in response to interactions with the extracellular matrix (ECM) of the allograft nerve.[19-24]

The interaction between the ECM of the decellularized nerve allograft and the MSCs influences the differentiation state of MSCs and their growth factor production.[25, 26] It has been proposed that inducing neural differentiation of MSCs prior to the addition to a decellularized allograft, may enhance nerve regeneration when compared to undifferentiated MSCs. Multiple studies have shown that it is possible to differentiate adipose derived MSCs into Schwann-like cells [18, 27-29] and in vitro studies demonstrated increased neurite outgrowth of motor neurons when exposed to differentiated MSCs compared to undifferentiated MSCs.[22, 30-36] While it is plausible that the biological properties of differentiated MSCs may be altered upon interaction with the ECM of nerve allografts, there is a paucity of molecular data that characterizes these putative differences. The purpose of this study was to evaluate temporal profiles of gene expression in undifferentiated and differentiated MSCs at multiple time points after dynamic seeding [37, 38] onto a decellularized nerve allograft. Determination of differences in gene expression may provide mechanistic insight into pathways that could be further leveraged to improve peripheral nerve repair.

MATERIALS AND METHODS

General design

This study was approved by the IACUC institutional review committee and the Institutional Review Board (IACUC protocol A3053-16). The experimental design is shown in **table 1**.

Group	Description	Time points	N	Outcome measurements

I	Undifferentiated MSCs + nerve allograft	T- = processed nerve allografts only
		Tc = cells only
		T0 = directly after seeding
		T1 = 1 day after seeding
		T2 = 3 days after seeding
		T3 = 7 days after seeding
		T4 = 14 days after seeding
		T5 = 21 days after seeding
			5 samples per group for each time point	qPCR analysis
				• Neurotrophic genes
				  • *NGF, GDNF, PTN, GAP43, PMP22*
				• Angiogenic genes
				  • *CD31, VEGF1*
				• ECM genes
				  • *COL1A1, COL3A1, FBLN1, LAMB2*
				• Regulatory cell cycle genes
				  • *CASP3, CCBN2*
				• Reference gene
				  • *GAPDH*

II	Differentiated MSCs + nerve allograft			

Table 1. *Experimental design.*
MSCs = mesenchymal stromal cells
qPCR analysis = quantitative polymerase chain reaction analysis

Mesenchymal stromal cell collection and characterization

Rat mesenchymal stromal cells were obtained from the inguinal fat pad of isogenic Lewis rats and derived as previously described.[16] Lewis rat MSCs were previously characterized by adherence to plastic, pluripotency towards mesodermal lineages, the presence of stem cell surface markers CD29 and CD90 and the absence of hemapoetic cell surface markers CD34 and CD45.[37, 38] MSCs were cultured in normal growth medium consisting of α-MEM (Advanced MEM (1x); Life Technologies Corporation, NY, USA), 5% platelet lysate (PLTMax®; Mill Creek Life Sciences, MN, USA), 1% Penicillin/Streptomycin (Penicillin-Streptomycin (10.000 U/mL; Life Technologies Corporation, NY, USA), 1% GlutaMAX (GlutaMAX Supplement 100X; Life Technologies Corporation, NY, USA) and 0.2% Heparin (Heparin Sodium Injection, USP, 1.000 USP units per mL; Fresenius Kabi, IL, USA).

Mesenchymal Stem Cell differentiation into Schwann-like cells

The differentiation protocol of Kingham and colleagues was used to differentiate MSCs into Schwann-like cells.[16] This protocol describes MSC-culture in differentiation medium that consists of 70 μL forskolin (Sigma-Aldrich corp., MO, USA), 5 μL of basis Fibroblastic Growth Factor (bFGF; PeproTech, NJ, USA), 2.5μL of Platelet Derived Growth Factor (PDGF-AA; PeproTech, NJ, USA), and 10 μLof Neuregulin 1-β1 (NRG1-b1; R&D systems Inc, MN, USA) per 50mL normal growth medium. In accordance with the protocol, differentiation of MSCs was confirmed by immunocytochemistry for Schwann cell markers S100 (Rabbit anti-S100; ThermoFisher Scientific, MA, USA), GFAP (Glial fibrillary acidic protein, mouse anti-GFAP; ThermoFisher Scientific, Waltham, MA, USA) and neurotrophin Receptor p75 (p75 NTR, rabbit anti-p75 NTR; ThermoFisher Scientific, Waltham, MA, USA). Differentiation markers were visualized with two different secondary antibodies (goat anti-mouse Cyanine-3 and goat anti-rabbit FITC; ThermoFisher Scientific, Waltham, MA, USA) and cell nuclei were labeled with DAPI (4',6-diamindino-2-phenylindole, ThermoFisher Scientific, Waltham, MA, USA). Immuno-

signals reflection protein expression in differentiated MSCs was compared to expression in Schwann cells and undifferentiated MSCs.

Nerve allograft decellularization

65 sciatic nerves were obtained from 33 Sprague-Dawley rats (Envigo, Madison, WI, USA) weighing 250-350 grams and were processed according to the protocol of Hundepool and colleagues.[7] Sprague-Dawley rats were specifically selected, because there is a known histocompatibility mismatch with Lewis rats.[39, 40] The nerves were sterilized using γ-irradiation and stored at 4°C for a maximum of 24 hours.

Dynamic MSC seeding

The 65 processed nerve allografts of 10mm in length were dynamically seeded for 12 hours with either 1x106 undifferentiated or differentiated MSCs from Lewis rats. This method has been previously demonstrated to be successful for both cell types.[37, 38] Once the seeding was completed, the seeded nerve allografts were placed in normal growth medium in 6-well plates. The growth medium was changed every 72 hours.

Real Time Reverse Transcriptase Quantitative Polymerase Chain Reaction (qPCR) analysis

Gene expression of decelllularized allografts dynamically seeded with undifferentiated and differentiated MSCs was measured for 5 duplicates per group at 6 different time points. Cells were harvested directly after seeding (T0) and 1 (T1), 3 (T2), 7 (T3), 14 (T4) and 21 (T5) days after seeding. Baseline gene expression (Tc) of both cell groups was obtained from 5 samples of undifferentiated and differentiated MSCs, while 5 unseeded decellularized allograft samples served as negative controls (T-).

At each time point, nerve tissues where frozen at -80°C in Qiazol. Each sample was minced with a sterile needle to enable ribonucleic acid (RNA) extraction according to the manufacturer's protocol (Direct-zolTM RNA MiniPrep Kit; Zymo Research, Irvine, CA, USA). After measuring RNA concentration with the NanoDropTM 2000/2000c Spectrophotometer (ThermoFisher Scientific, Waltham, MA, USA), complementary deoxyribonucleic acid (cDNA) was obtained in a concentration of 10ng/μL. Expression of mRNAs was determined by qPCR analysis for the neurotrophic markers nerve growth factor (NGF), glial cell line-derived neurotrophic factor (GDNF), pleiotrophin (PTN), growth associated protein 43 (GAP43) and peripheral protein 22 (PMP22); for the angiogenic markers platelet endothelial cell adhesion molecule 1 (PECAM1/CD31) and vascular endothelial cell growth factor alpha (VEGF1); for extracellular matrix (ECM) markers collagen type I (COL1A1), collagen type III (COL3A1), Fibulin 1 (FBLN1) and laminin subunit beta 2 (LAMB2); and for regulatory cell cycle markers caspase 3 (CASP3) and Cyclin B2 (CCBN2). Glyceraldehyde-3-Phosphate Dehydrogenase (GAPDH) served as reference gene. Primers were manufactured by Sigma and are listed in **table 2**. Function descriptions for the evaluated genes are provided in **table 3**. After preparing the reactions containing primers, real time-qPCR master mix (Qiagen, MD, USA) and cDNA, the reactions were amplified by real time-qPCR using a thermocycler (Bio-rad Laboratories, Inc., CA, USA) with the following

parameters: an initial step at 95oC for 15 min followed by 50 cycles of 95oC for 20s, 60oC for 35s and 72Co for 35s. All mRNA levels were calculated using the 2-ΔΔCT method and expressed relative to GAPDH as housekeeping gene.

Statistical analysis

The results of qPCR measurements of both undifferentiated and differentiated MSCs over time were analyzed per gene using a 2-factor Analysis Of Variance (ANOVA) with repeated measures on one factor. Post-hoc multiple comparisons were evaluated by the Mann Whitney-U test with Bonferroni correction. Data are expressed as the mean difference plus or minus the standard error of the mean (SEM). Significance was set at α=0.05. The interaction between the cell-types and the ECM was estimated by comparing the baseline gene-expression of both cell types (Tc) to the gene-expression of both groups immediately after seeding onto the processed nerve graft (T0). Relative differences in gene expression between undifferentiated and differentiated MSCs were also calculated.

Gene ID	Biology	Forward primer	Reverse primer
GAPDH	Household gene	TACCAGGGCTGCCTTCTCTTG	GGATCTCGCTCCTGGAAGATG
CYCA	Household gene	AGGATTCATGTGCCAGGGTG	CTCAGTCTTGGCAGTGCAGA
PGK1	Household gene	CGTGATGAGGGTGGACTTCA	GCAGCAACTGGCTCTAAGGA
NGF	Neurotropic marker	CACTCTGAGGTGCATAGCGT	CTATTGGTTCAGCAGGGGCA
GDNF	Neurotropic marker	CTGACCAGTGACTCCAATATGC	TTAAGACGCACCCCCGATTT
PTN	Neurotropic marker	GCCGAGTGCAAACAAACCAT	TGATTCCGCTTGAGGCTTGG
GAP43	Neurotropic marker	GATAACTCGCCGTCCTCCAA	CTACAGCTTCTTTCTCCTCCTCA
PMP22	Neurotropic marker	GTCTGGTCTGCTGTGAGCAT	GCCATTGGCTGACGATGGTG
VEGF	Angiogenic marker	AGAAAGCCCATGAAGTGGTGA	GCTGGCTTTGGTGAGGTTTG
CD31	Angiogenic marker	TTGTGACCAGTCTCCGAAGC	TGGCTGTTGGTTTCCACACT
COL1A1	ECM protein	AAGTCTCAAGATGGTGGCCG	TCGATCCAGTACTCTCCGCT
COL3A1	ECM protein	CCCGGCAACAATGGTAATCC	GACCTCGTGCTCCAGTTAGC
FBLN1	ECM protein	GCAGACACCTTTCGCCAAGA	CGTGACAGCCCTCAGAAAGA
LAMB2	ECM protein	AGTACCCACACGGATGGAGTG	CTCGAGAACAGCCAGGTACA
CASP3	Cell apoptosis protein	GGAGCTTGGAACGCGAAGAA	ACACAAGCCCATTTCAGGGT
CCNB2	Cell cycle component	ACCAGTGCAGATGGAGACAC	GACTGCAAAGCCTCAAGCTG

Table 2. mRNA primer sequences.

Genes	Functional description
NGF	Guides axonal growth and promotes Schwann cell activity.[41, 42]
GDNF	Promotes survival of neurons and axonal sprouting. [41, 43]
PTN	Neuronal protection and axon regeneration.[44]
GAP43	Prominent component in axonal growth cones.[45-47] Plays a key role in the formation of new connections at the neuromuscular junction.[48, 49]
PMP22	Important component of myelin and promotes Schwann cell growth and differentiation.[40, 51]
VEGF	Induces proliferation and migration of vascular endothelial cells, plays a key role in angiogenesis.[52, 53] Neuronal growth stimulator and neuroprotector.[52, 54-56]
CD31	Involved in the formation and stabilization of the lateral junctions between adjacent endothelial cells, maintaining the vascular permeability barrier and angiogenesis. [57-59]
COL1A1	Encodes for a major component of type I collagen, which influences axonal growth. Component of the ECM of nerves that enables Schwann cell adhesion, growth and differentiation.[9, 60, 61]
COL3A1	Encodes for a major component of type III collagen, which influences axonal growth. Component of the ECM of nerves that enables Schwann cell adhesion, growth and differentiation.[9, 60, 61]
FBLN1	Prominent in the matrix of the perineurium of peripheral nerves.[62]
LAMB2	Component of the basement membrane of muscles at the neuromuscular junctions.[63, 64]
CASP3	Crucial mediator in cell apoptosis of Schwann cells.[65, 66]
CCNB2	Forms mitosis promotic factor complexes with Cyclin-dependent kinase (Cdk).[67, 68]

Table 3. Function descriptions of the evaluated genes.

RESULTS

Adipose Derived Mesenchymal stem cell differentiation into Schwann-like cells

Similar to Schwann cells, the differentiated MSCs showed positive immunofluorescence for Schwann cell surface markers S100, GFAP and NTR p75 and morphologically changed to a spindle-like shape. Undifferentiated MSCs showed no expression of the tested markers (**figure 1**). Thus, the Schwann cell differentiation protocol we used induces the expected phenotypic changes under our experimental conditions.

Quantitative PCR analysis

QPCR analysis of unseeded decellularized nerve allografts did not result in detectable levels of mRNA. Hence, decellularization effectively prevented detection of RNA as expected, and indicates that any expression values obtained with nerve allografts are directly derived from the MSCs that were seeded.

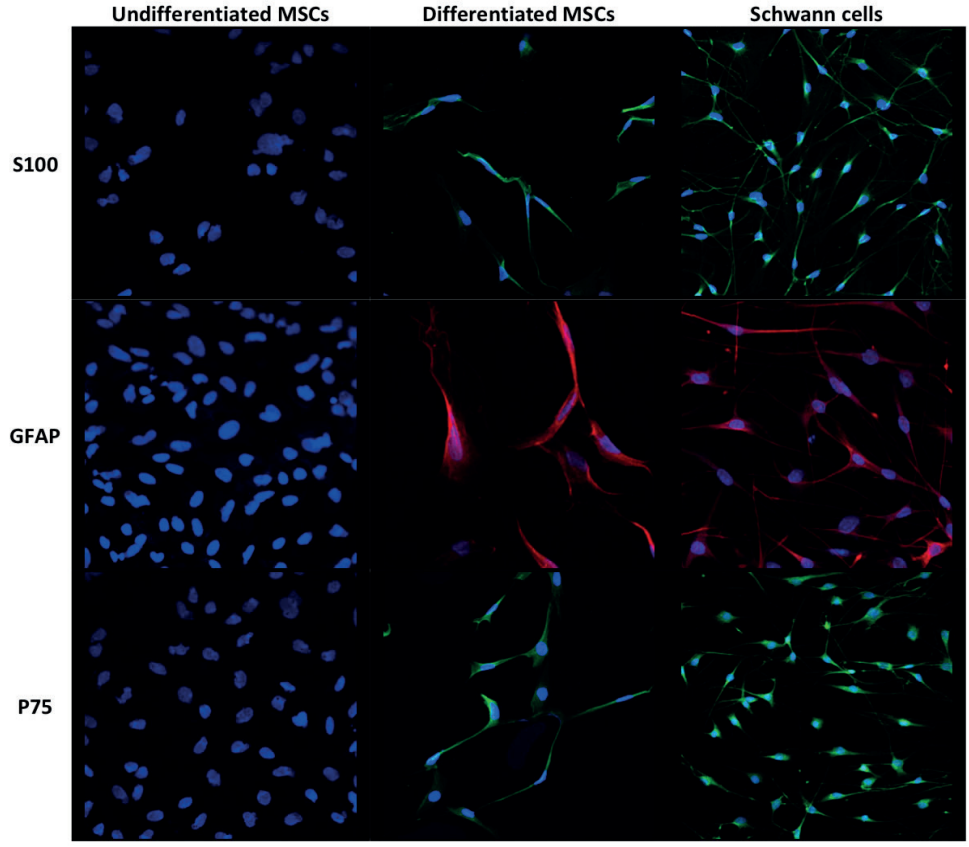

Figure 1. Differentiation of MSCs into Schwann-like cells. Immunocytochemical comparison between undifferentiated MSCs (A-D-G), differentiated MSCs (B-E-H) and Schwann cells (C-F-I). Cells are tested for the presence of Schwann cell marker S100 (A-B-C, green), glial cell marker GFAP (D-E-F, red) and neurotrophin Receptor p75 (G-H-I, green). Cell nuclei are DAPI-stained (blue). Magnification: 40X.

Neurotrophic gene expression

Baseline gene expression

Expression of *NGF* (0.987 ±0.071, p<0.001) and *GDNF* (0.312 ±0.031, p<0.001) was significantly higher in undifferentiated MSCs than in differentiated MSCs. The *GAP43* expression did not significantly differ between the cell types (p=0.127). Expression of *PMP22* (0.009 ±0.004, p=0.049) and *PTN* (2.044 ±0.278, p=0.002) was significantly elevated in differentiated MSCs.

Interaction

Compared to gene-expression before seeding, seeding of undifferentiated MSCs led to a significant decrease in *NGF* (-0.62 ±0.151; p=0.002) and *GDNF* expression (-0.403 ±0.034; p<0.001), but no significant changes in the expression of *GAP43*, *PTN* and *PMP22*. Seeding of differentiated MSCs caused a significant upregulation of *NGF* (+1.154 ±0.151; p<0.001) and *GDNF* expression (+0.159 ±0.034; p<0.001), a significant decrease in *GAP43* expression

(-0.111 ±0.019; p<0.001) and no significant changes in the expression of *PMP22* and *PTN*.

Gene expression over time
In general, expression of *NGF*, *GDNF* and *PMP22* in undifferentiated MSCs appeared to increase after 3 days of culture and remained elevated over the subsequent days until day 7, while expression of *GAP43* and *PTN* remained low. In differentiated MSCs, expression of *NGF*, *GDNF* and *GAP43* was especially high during the first 3 days after seeding, while the *PTN* and *PMP22* expression in differentiated MSCs increased after 7 days of culture. All neurotrophic expression curves are displayed in **figure 2** with asterisks demonstrating significant differences between groups.

Angiogenic gene expression

Baseline gene expression
Baseline *CD31* expression did not significantly differ between undifferentiated and differentiated MSCs (p=0.414). *VEGF1* expression was significantly higher in differentiated MSCs than in undifferentiated MSCs before seeding (19.351 ±3.138, p=0.003).

Interaction
Seeding the different cell-groups on a decellularized nerve allograft led to enhanced expression of *CD31* but this trend in mRNA levels was not statistically significant. Enhanced *VEGF1* expression for both undifferentiated MSCs (+67.121 ±9.064; p<0.001) and differentiated MSCs (+36.522 ±9.064; p=0.004) after seeding was statistically significant.

Gene expression over time
Generally, *CD31* expression in undifferentiated and differentiated MSCs peaked 24 hours after seeding and declined to minimal expression at 7 days after which the expression remained low. ANOVA analysis did not demonstrate a significant interaction between culture duration, cell type and *CD31* expression (p=0.094). ANOVA analysis showed a significant interaction between cell-type, time and *VEGF1* expression (p=0.001). The *VEGF1* expression curve followed the same pattern in both groups: it peaked directly after seeding and reached a plateau phase from 7 days onwards. All angiogenic expression curves are depicted in **figure 3**.

Extracellular matrix gene expression

Baseline gene expression
The baseline expression of *COL1A1* (p=0.134) and *LAMB2* (p=0.232) did not significantly differ between undifferentiated and differentiated MSCs. Differentiated MSCs had a significantly higher expression of *COL3A1* (13.119 ±5.492, p=0.049), while undifferentiated MSCs showed significantly higher *FBLN1* expression (1.767 ±0.446, p=0.013).

Interaction
The interaction with the ECM of decellularized nerve allografts led to significantly enhanced

expression of *COL3A1* in undifferentiated MSCs (+186.328 ±50.264; p=0.011), but did not appreciably alter expression of *COL1A1*, *FBLN1* and *LAMB2*. For differentiated MSCs, the interaction resulted in a significant enhanced expression of *FBLN1* (1.918 ±0.386; <0.001) but no changes in the *COL1A1*, *COL3A1* and *LAMB2* gene expression.

Gene expression over time

The temporal expression of extracellular matrix genes exhibited significant differences between cell type (**figure 4**). In general, the temporal expression profiles of *COL1A1* and *COL3A1* in undifferentiated and differentiated MSCs did not differ substantially from each other. ANOVA analysis only demonstrated a significant interaction between and within groups for *COL3A1* expression over time (p=0.027). For undifferentiated MSCs, a significant decrease in *COL3A1* between 3 days and 7 days after seeding (p=0.050) was observed, while for differentiated MSCs a significant increase between 14 and 21 days after seeding (p=0.007) was measured. There was a significant interaction between and within groups for *FBLN1* expression (p<0.001). The *FBLN1* expression in both groups started high, slowly decreased in the first week and increased from 7 days onwards. A significant interaction between cell-types (p=0.001) was found for the *LAMB2* expression, while no within-group differences were found over time. Overall, the *LAMB2* expression in undifferentiated MSCs slowly seemed to climb, reaching maximal levels at 21 days after seeding, while the expression of *LAMB2* in differentiated MSCs appeared to decline slowly.

Cell regulatory gene expression

Baseline gene expression

The baseline expression of *CCBN2* (1.613 ±0.580, p=0.049) and *CASP3* (0.867 ±0.081, p<0.001) in undifferentiated MSCs was significantly higher than in differentiated MSCs.

After seeding

After seeding, the gene expression in undifferentiated MSCs of *CASP3* was significantly enhanced (0.983 ±0.279; p=0.018), while *CCBN2*-expression significantly decreased (-1.638 ±0.501; p=0.040). Seeding of differentiated MSCs resulted in a significant enhanced expression of *CASP3* (2.501 ±0.279; p<0.001) and *CCBN2* (1.796 ±0.501; p<0.001).

Gene expression over time

Overall, *CASP3* expression of both cell-groups was high directly after seeding, but decreased afterwards and mRNA levels remained steady from 7 days onwards. ANOVA analysis showed a significant interaction between culture duration and the mean *CASP3* expression (p<0.001), but no significant differences between groups (p=0.404). *CCNB2* expression had a significant interaction with the cell-type and culture duration (p<0.001). In general, *CCBN2* expression of undifferentiated MSCs was low during the first 3 days after seeding and then slowly increased, reaching a peak after 21 days. In differentiated MSCs there was a peak measured after 1 day and then the expression slowly decreased. All expression values for cell cycle regulatory genes are presented in **figure 5** with significant differences between groups as indicated.

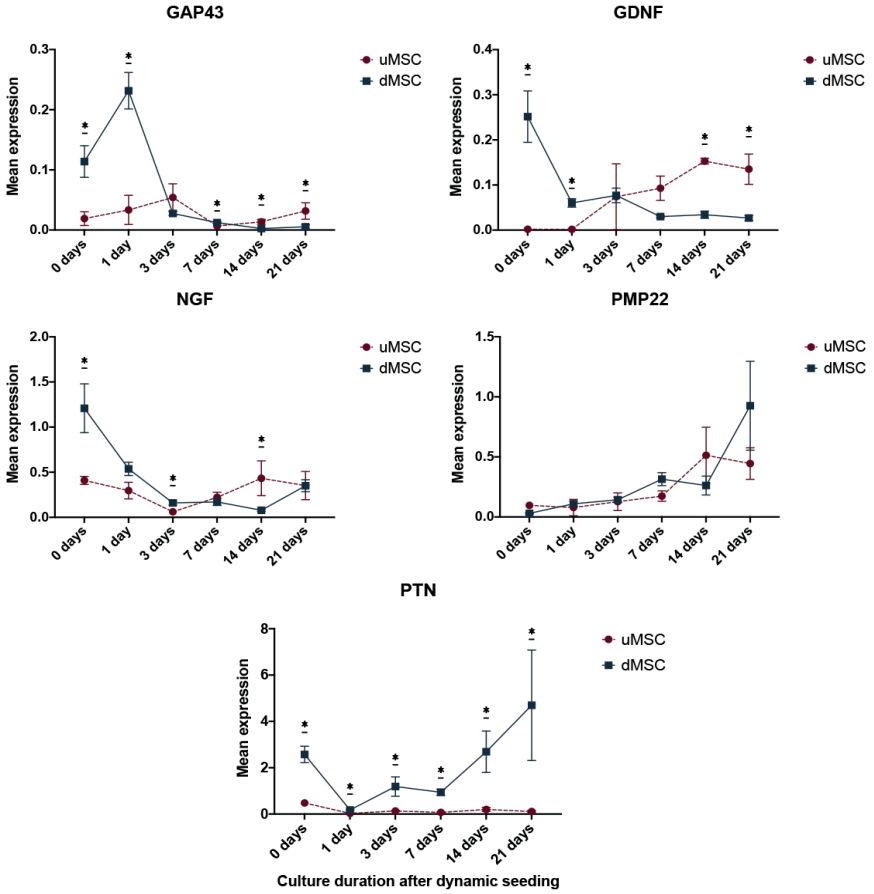

*Figure 2. Graphs of mean measured gene expressions of neurotrophic markers GAP43, GDNF, NGF, PMP22 and PTN in undifferentiated and differentiated MSCs over a time period of 21 days after dynamically seeding both cell-types on a processed nerve allograft. Error bars = Standard Error of the Mean. * = significant difference between groups (p<0.05).*

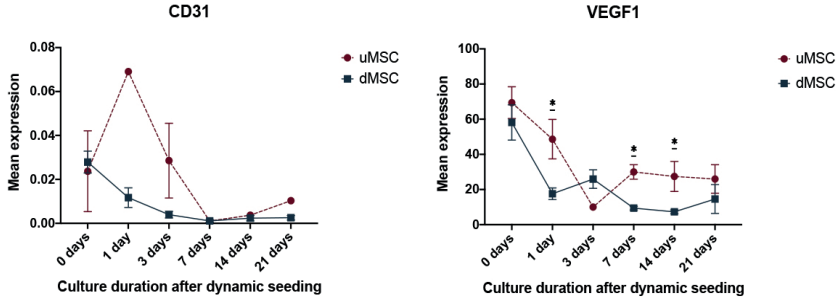

*Figure 3. Graphs of mean measured gene expressions of angiogenic markers platelet endothelial cell adhesion molecule 1 (PECAM1/CD31) and vascular endothelial cell growth factor alpha (VEGF1) in undifferentiated and differentiated MSCs over a time period of 21 days after dynamically seeding both cell-types on a processed nerve allograft. Error bars = Standard Error of the Mean. * = significant difference between groups (p<0.05).*

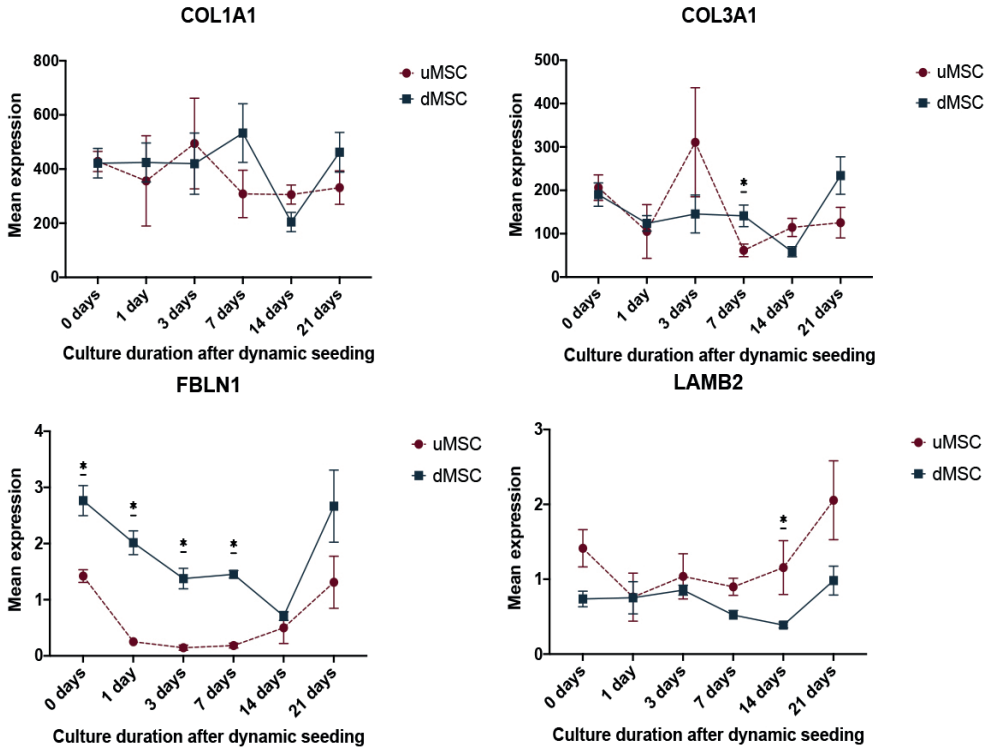

*Figure 4. Graphs of mean measured gene expressions of extracellular matrix markers collagen type I (COL1A1), collagen type III (COL3A1), Fibulin 1 (FBLN1) and laminin subunit beta 2 (LAMB2) in undifferentiated and differentiated MSCs over a time period of 21 days after dynamically seeding both cell-types on a processed nerve allograft. Error bars = Standard Error of the Mean. * = significant difference between groups (p<0.05).*

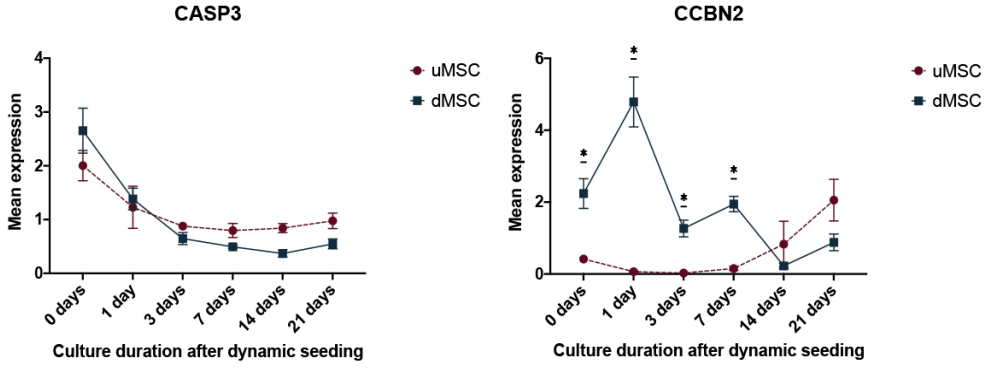

*Figure 5. Graphs of mean measured gene expressions of regulatory cell cycle markers caspase 3 (CASP3) and Cyclin B2 (CCBN2) in undifferentiated and differentiated MSCs over a time period of 21 days after dynamically seeding both cell-types on a processed nerve allograft. Error bars = Standard Error of the Mean. * = significant difference between groups (p<0.05).*

DISCUSSION

In this study, the gene expression profiles of undifferentiated and differentiated MSCs before and after seeding on a decellularized nerve allograft were analyzed. There is little consensus about which stem cell types are most optimal for use in clinical human peripheral nerve regeneration studies due to the ambiguity in their mechanism of action. We examined the expression of a large panel of genes that have a known role in nerve regeneration and compared their expression in undifferentiated MSCs to differentiated MSCs, before and after they interacted with the ECM of decellularized nerve allografts.

Interaction between MSCs and the nerve allograft

Compared to undifferentiated MSCs, the differentiation of MSCs into Schwann-like cells led to significantly enhanced mean expressions of the neurotrophic genes *PMP22* and *PTN*, the angiogenic gene *VEGF1* and extracellular matrix gene *COL3A1*. Expression of other neurotrophic genes (i.e., *NGF* and *GDNF*), the extracellular matrix gene *FBLN1*, and cell growth and survival related genes *CCBN2* and *CASP3* was significantly decreased after differentiation. When comparing the gene expression of both undifferentiated and differentiated cell states before and after the introduction to the ECM of decellularized nerve allografts, it was demonstrated that the interaction initially led to enhanced expression of *VEGF1*, *COL3A1* and *CASP3* in undifferentiated MSCs and increased mRNA levels of *NGF*, *GDNF*, *VEGF1*, *FBLN1*, *CASP3* and *CCBN2* in differentiated MSCs.

Our results corroborate studies that describe interactions between the ECM and MSCs which led to significant changes in their gene expression profiled and the observation that differentiation of MSCs leads to enhanced expression of *VEGF1*.[26, 69] Possible explanations for the reduced expression of *NGF* and *GDNF* in undifferentiated MSCs directly after seeding may include the lack of surgical host factors and the original (motor) function of the nerves used.[70, 71]

Gene expression over time

The short-term measurements (immediate post seeding, 1 day and 3 days after seeding) indicate differentiated MSCs express high levels of neurotrophic (*NGF*, *GDNF*, *GAP43*), angiogenic (*VEGF1*), tissue supportive (*FBLN1*) and cell regulatory genes (*CASP3*, *CCNB2*) which decrease over time. Undifferentiated MSCs appear to have a smaller role in the short term and only express high levels of *VEGF1* and *CASP3*. The effect of undifferentiated MSCs are seen in the long term (7, 14 and 21 days after seeding) by expressing enhanced levels of neurotrophic (*NGF*, *GDNF*, *PMP22*), extracellular matrix (*FBLN1*, *LAMB2*) and cell regulatory genes (*CCNB2*). In this later phase, the expression of factors from differentiated MSCs is less than undifferentiated MSCs. The expression of tissue supportive genes *COL1A1* and *COL3A1* remained stable over time in both cell types. The gene expression cascades presented here suggest that a combination of both differentiated and undifferentiated cells would lead to an optimal regenerative micro-environment for decellularized nerve allografts, by providing growth factors that stimulate axon ingrowth after implementation.

When considering whether differentiated or undifferentiated cells should be used upon translation into future human clinical studies, the extra costs and preparation time required for the differentiation of MSCs should be taken into account. Clinically, differentiation would lead to an extended period of 3 weeks between injury and repair. This must also be balanced with the hypothetical malignant potential of differentiated MSCs compared to undifferentiated MSCs.[72, 73]

Limitations

A limitation of the current in vitro setting is the lack of an effective tissue repair environment which is present in an in vivo setting.[70] However, an in vitro setting lends itself perfectly to evaluate the mechanisms in a thorough manner while limiting the number of animals used. Future in vivo animal studies are needed to corroborate these in vitro findings. Rat tissues were exclusively used in order to easily correlate the results to functional outcomes of nerve allografts seeded with undifferentiated and differentiated MSCs in an in vivo rat-model, which is the logical next step prior to the translation to human tissue. The current rat-model enables us to explore the underlying mechanism of action of differentiated versus undifferentiated MSCs in peripheral nerve repair, before these studies are translated to a more clinically applicable model.

We did not examine the effect of changed gene expression profiles on secreted growth factors. Although ELISA analysis could have contributed to our findings, it is a costly technique and attempts to correlate mRNA expression to protein secretion have had variable success.[74]

The gene expression levels of many different genes that are relevant for nerve regeneration have been examined and compared. The disadvantage of testing many genes at many different time points is that a statistical type I error is more likely to occur. Corrections were used to adjust for multiple comparisons, limiting the power of our findings. This numerical consideration emphasizes the significance of the findings that were statistically significant.

We found several significant differences within and between groups over time. As expected, extracellular matrix genes like *COL1A1* and *COL3A1* were highly expressed, while the expression of most other genes was a hundredfold less. However, due to the different cellular function of the genes we examined, these differences do not define the relevance of the findings. All genes have their basic level of expression that was (significantly) influenced by the ECM of the decellularized nerve allograft. To make a valid expression comparison between differentiated versus undifferentiated cells, we deliberately displayed expression levels only as a ratio of our housekeeping gene (GAPDH), instead of calculating a ratio of their baseline gene expression (cells only).

These limitations notwithstanding, gene expression profiles of cell types before and after interacting with the ECM of decellularized nerve allografts have not been described and compared to this extent before. The evaluation to three weeks after seeding enabled us to describe a potential expression cascade of both cell-types when used in combination with

an decellularized nerve allograft.[7] The validated dynamic seeding strategy that ensures the atraumatic delivery of viable MSCs on the surface of processed allografts is an additional strength of this study.[37, 38]

As indicated above, the in-vitro set up should first be translated to an in-vivo model to confirm the stimulatory effects of different MSC states on peripheral nerve regeneration. A repetition of the current study with human undifferentiated and differentiated MSCs with clinically available nerve graft substitutes (collagen conduits or decellularized allograft nerve) would be a logical next step for clinical translation.

CONCLUSION

Differentiation of MSCs in Schwann cell-like cells changes their baseline gene expression profile. The gene expression profile of both differentiated MSCs and undifferentiated MSCs changes when the MSCs interact with the ECM of a decellularized nerve allograft after being dynamically seeded on their surface. Differentiated MSCs are likely to play a major role on the short-term nerve regeneration by expressing high gene-levels in the first 72 hours after seeding, while the effect of undifferentiated MSCs appears a week after seeding. The differences in gene-profile and effective phases suggests that both cell-types can affect nerve regeneration in different ways and at different time points.

Acknowledgements

We thank Patricia F. Friedrich for assistance with the preparations of the experiments, as well as the members of the Shin, Bishop and van Wijnen laboratories for stimulating discussions, as well as generous sharing of ideas and reagents.

Funding

This study was funded by the NIH R01 NS102360. None of the authors has a conflict of interest.

REFERENCES

1. Rbia N, Shin AY. The Role of Nerve Graft Substitutes in Motor and Mixed Motor/Sensory Peripheral Nerve Injuries. J Hand Surg Am 2017: 42: 367-77.
2. Giusti G, Willems WF, Kremer T, et al. Return of motor function after segmental nerve loss in a rat model: comparison of autogenous nerve graft, collagen conduit, and processed allograft (AxoGen). J Bone Joint Surg Am 2012: 94: 410-7.
3. Brooks DN, Weber RV, Chao JD, et al. Processed nerve allografts for peripheral nerve reconstruction: A multicenter study of utilization and outcomes in sensory, mixed, and motor nerve reconstructions. MICROSURGERY 2012: 32: 1-14.
4. Cho MS, Rinker BD, Weber RV, et al. Functional outcome following nerve repair in the upper extremity using processed nerve allograft. J Hand Surg Am 2012: 37: 2340-9.
5. Moore AM, MacEwan M, Santosa KB, et al. Acellular nerve allografts in peripheral nerve regeneration: A comparative study. MUSCLE NERVE 2011: 44: 221-34.
6. Szynkaruk M, Kemp SW, Wood MD, Gordon T, Borschel GH. Experimental and clinical evidence for use of decellularized nerve allografts in peripheral nerve gap reconstruction. Tissue Eng Part B Rev 2013: 19: 83-96.
7. Hundepool CA, Nijhuis TH, Kotsougiani D, et al. Optimizing decellularization techniques to create a new nerve allograft: an in vitro study using rodent nerve segments. Neurosurg Focus 2017: 42.
8. Kidd GJ, Ohno N, Trapp BD. Biology of Schwann cells. Handb Clin Neurol 2013: 115: 55-79.
9. Chernousov MA, Carey DJ. Schwann cell extracellular matrix molecules and their receptors. Histol Histopathol 2000: 15: 593-601.
10. Hoyng SA, De Winter F, Gnavi S, et al. A comparative morphological, electrophysiological and functional analysis of axon regeneration through peripheral nerve autografts genetically modified to overexpress BDNF, CNTF, GDNF, NGF, NT3 or VEGF. Exp Neurol 2014: 261: 578-93.
11. Lee JY, Giusti G, Friedrich PF, Bishop AT, Shin AY. Effect of Vascular Endothelial Growth Factor Administration on Nerve Regeneration after Autologous Nerve Grafting. J Reconstr Microsurg 2016: 32: 183-8.
12. Piquilloud G, Christen T, Pfister LA, Gander B, Papaloizos MY. Variations in glial cell line-derived neurotrophic factor release from biodegradable nerve conduits modify the rate of functional motor recovery after rat primary nerve repairs. Eur J Neurosci 2007: 26: 1109-17.
13. Caplan AI. Adult Mesenchymal Stem Cells: When, Where, and How. Stem Cells Int 2015: 2015: 628767.
14. Cao F, Liu T, Xu Y, Xu D, Feng S. Culture and properties of adipose-derived mesenchymal stem cells: characteristics in vitro and immunosuppression in vivo. Int J Clin Exp Pathol 2015: 8: 7694-709.
15. Strioga M, Viswanathan S, Darinskas A, Slaby O, Michalek J. Same or not the same? Comparison of adipose tissue-derived versus bone marrow-derived mesenchymal stem and stromal cells. Stem Cells Dev 2012: 21: 2724-52.
16. Kingham PJ, Kalbermatten DF, Mahay D, et al. Adipose-derived stem cells differentiate into a Schwann cell phenotype and promote neurite outgrowth in vitro. Exp Neurol 2007: 207: 267-74.
17. Yoshimura H, Muneta T, Nimura A, et al. Comparison of rat mesenchymal stem cells derived from bone marrow, synovium, periosteum, adipose tissue, and muscle. Cell Tissue Res 2007: 327: 449-62.
18. di Summa PG, Kingham PJ, Raffoul W, et al. Adipose-derived stem cells enhance peripheral nerve regeneration. J Plast Reconstr Aesthet Surg 2010: 63: 1544-52.
19. Moattari M, Kouchesfehani HM, Kaka G, et al. Chitosan-film associated with mesenchymal stem cells enhanced regeneration of peripheral nerves: A rat sciatic nerve model. J Chem Neuroanat 2017: 88: 46-54.
20. Fairbairn NG, Meppelink AM, Ng-Glazier J, Randolph MA, Winograd JM. Augmenting

peripheral nerve regeneration using stem cells: A review of current opinion. World J Stem Cells 2015: 7: 11-26.
21. Zhao Z, Wang Y, Peng J, et al. Repair of nerve defect with acellular nerve graft supplemented by bone marrow stromal cells in mice. Microsurgery 2011: 31: 388-94.
22. Wang Y, Zhao Z, Ren Z, et al. Recellularized nerve allografts with differentiated mesenchymal stem cells promote peripheral nerve regeneration. Neurosci Lett 2012: 514: 96-101.
23. Hundepool CA, Nijhuis TH, Mohseny B, Selles RW, Hovius SE. The effect of stem cells in bridging peripheral nerve defects: a meta-analysis. J Neurosurg 2014: 121: 195-209.
24. Rbia N, Bulstra LF, Lewallen EA, et al. Seeding decellularized nerve allografts with adipose-derived mesenchymal stromal cells: An in vitro analysis of the gene expression and growth factors produced. J Plast Reconstr Aesthet Surg 2019: 72: 1316-25.
25. Armstrong SJ, Wiberg M, Terenghi G, Kingham PJ. ECM molecules mediate both Schwann cell proliferation and activation to enhance neurite outgrowth. Tissue Eng 2007: 13: 2863-70.
26. di Summa PG, Kalbermatten DF, Raffoul W, Terenghi G, Kingham PJ. Extracellular matrix molecules enhance the neurotrophic effect of Schwann cell-like differentiated adipose-derived stem cells and increase cell survival under stress conditions. Tissue Eng Part A 2013: 19: 368-79.
27. Ao Q, Fung CK, Tsui AY, et al. The regeneration of transected sciatic nerves of adult rats using chitosan nerve conduits seeded with bone marrow stromal cell-derived Schwann cells. Biomaterials 2011: 32: 787-96.
28. Chen X, Wang XD, Chen G, et al. Study of in vivo differentiation of rat bone marrow stromal cells into schwann cell-like cells. Microsurgery 2006: 26: 111-15.
29. Tomita K, Madura T, Mantovani C, Terenghi G. Differentiated adipose-derived stem cells promote myelination and enhance functional recovery in a rat model of chronic denervation. J Neurosci Res 2012: 90: 1392-402.
30. Kingham PJ, Kolar MK, Novikova LN, Novikov LN, Wiberg M. Stimulating the neurotrophic and angiogenic properties of human adipose-derived stem cells enhances nerve repair. Stem Cells Dev 2014: 23: 741-54.
31. Tomita K, Madura T, Sakai Y, et al. Glial differentiation of human adipose-derived stem cells: implications for cell-based transplantation therapy. Neuroscience 2013: 236: 55-65.
32. Ladak A, Olson J, Tredget EE, Gordon T. Differentiation of mesenchymal stem cells to support peripheral nerve regeneration in a rat model. Exp Neurol 2011: 228: 242-52.
33. Orbay H, Uysal AC, Hyakusoku H, Mizuno H. Differentiated and undifferentiated adipose-derived stem cells improve function in rats with peripheral nerve gaps. J Plast Reconstr Aesthet Surg 2012: 65: 657-64.
34. Watanabe Y, Sasaki R, Matsumine H, Yamato M, Okano T. Undifferentiated and differentiated adipose-derived stem cells improve nerve regeneration in a rat model of facial nerve defect. J Tissue Eng Regen Med 2017: 11: 362-74.
35. Keilhoff G, Goihl A, Stang F, Wolf G, Fansa H. Peripheral nerve tissue engineering: autologous Schwann cells vs. transdifferentiated mesenchymal stem cells. Tissue Eng 2006: 12: 1451-65.
36. Kappos EA, Engels PE, Tremp M, et al. Peripheral Nerve Repair: Multimodal Comparison of the Long-Term Regenerative Potential of Adipose Tissue-Derived Cells in a Biodegradable Conduit. Stem Cells Dev 2015: 24: 2127-41.
37. Rbia N, Bulstra LF, Bishop AT, van Wijnen AJ, Shin AY. A simple dynamic strategy to deliver stem cells to decellularized nerve allografts. Plast Reconstr Surg 2018.
38. Mathot F, Rbia N, Bishop AT, et al. Adhesion, distribution, and migration of differentiated and undifferentiated mesenchymal stem cells (MSCs) seeded on nerve allografts. J Plast Reconstr Aesthet Surg 2019.
39. Hudson TW, Zawko S, Deister C, et al. Optimized acellular nerve graft is immunologically tolerated and supports regeneration. Tissue Eng 2004: 10: 1641-51.
40. Kumta S, Yip K, Roy N, Lee SK, Leung PC. Revascularisation of bone allografts following vascular bundle implantation: an experimental study in rats. Arch Orthop Trauma Surg 1996: 115: 206-10.

41. Caseiro AR, Pereira T, Ivanova G, Luis AL, Mauricio AC. Neuromuscular Regeneration: Perspective on the Application of Mesenchymal Stem Cells and Their Secretion Products. Stem Cells Int 2016: 2016: 9756973.
42. Mnich K, Carleton LA, Kavanagh ET, et al. Nerve growth factor-mediated inhibition of apoptosis post-caspase activation is due to removal of active caspase-3 in a lysosome-dependent manner. Cell Death Dis 2014: 5: e1202.
43. Gordon T. The role of neurotrophic factors in nerve regeneration. Neurosurg Focus 2009: 26: E3.
44. Jin L, Jianghai C, Juan L, Hao K. Pleiotrophin and peripheral nerve injury. Neurosurg Rev 2009: 32: 387-93.
45. Schreyer DJ, Skene JH. Fate of GAP-43 in ascending spinal axons of DRG neurons after peripheral nerve injury: delayed accumulation and correlation with regenerative potential. J Neurosci 1991: 11: 3738-51.
46. Skene JH. Axonal growth-associated proteins. Annu Rev Neurosci 1989: 12: 127-56.
47. Yuan Q, Hu B, Su H, et al. GAP-43 expression correlates with spinal motoneuron regeneration following root avulsion. J Brachial Plex Peripher Nerve Inj 2009: 4: 18.
48. Benowitz LI, Routtenberg A. GAP-43: an intrinsic determinant of neuronal development and plasticity. Trends Neurosci 1997: 20: 84-91.
49. Aigner L, Arber S, Kapfhammer JP, et al. Overexpression of the neural growth-associated protein GAP-43 induces nerve sprouting in the adult nervous system of transgenic mice. Cell 1995: 83: 269-78.
50. Jetten AM, Suter U. The peripheral myelin protein 22 and epithelial membrane protein family. Prog Nucleic Acid Res Mol Biol 2000: 64: 97-129.
51. Naef R, Suter U. Many facets of the peripheral myelin protein PMP22 in myelination and disease. Microsc Res Tech 1998: 41: 359-71.
52. Ferrara N, Gerber HP, LeCouter J. The biology of VEGF and its receptors. Nat Med 2003: 9: 669-76.
53. Goodsell DS. The molecular perspective: VEGF and angiogenesis. Stem Cells 2003: 21: 118-9.
54. Pan Z, Fukuoka S, Karagianni N, Guaiquil VH, Rosenblatt MI. Vascular endothelial growth factor promotes anatomical and functional recovery of injured peripheral nerves in the avascular cornea. Faseb j 2013: 27: 2756-67.
55. Jin K, Mao XO, Greenberg DA. Vascular endothelial growth factor stimulates neurite outgrowth from cerebral cortical neurons via Rho kinase signaling. J Neurobiol 2006: 66: 236-42.
56. Zachary I. Neuroprotective role of vascular endothelial growth factor: signalling mechanisms, biological function, and therapeutic potential. Neurosignals 2005: 14: 207-21.
57. Jackson DE. The unfolding tale of PECAM-1. FEBS Lett 2003: 540: 7-14.
58. Cao G, O'Brien CD, Zhou Z, et al. Involvement of human PECAM-1 in angiogenesis and in vitro endothelial cell migration. Am J Physiol Cell Physiol 2002: 282: C1181-90.
59. Woodfin A, Voisin MB, Nourshargh S. PECAM-1: a multi-functional molecule in inflammation and vascular biology. Arterioscler Thromb Vasc Biol 2007: 27: 2514-23.
60. Koopmans G, Hasse B, Sinis N. Chapter 19: The role of collagen in peripheral nerve repair. Int Rev Neurobiol 2009: 87: 363-79.
61. Hubert T, Grimal S, Carroll P, Fichard-Carroll A. Collagens in the developing and diseased nervous system. Cell Mol Life Sci 2009: 66: 1223-38.
62. Miosge N, Gotz W, Sasaki T, et al. The extracellular matrix proteins fibulin-1 and fibulin-2 in the early human embryo. Histochem J 1996: 28: 109-16.
63. Maselli RA, Ng JJ, Anderson JA, et al. Mutations in LAMB2 causing a severe form of synaptic congenital myasthenic syndrome. J Med Genet 2009: 46: 203-8.
64. Engel AG. Genetic basis and phenotypic features of congenital myasthenic syndromes. Handb Clin Neurol 2018: 148: 565-89.
65. Porter AG, Janicke RU. Emerging roles of caspase-3 in apoptosis. Cell Death Differ 1999: 6: 99-104.

66. Tsuda Y, Kanje M, Dahlin LB. Axonal outgrowth is associated with increased ERK 1/2 activation but decreased caspase 3 linked cell death in Schwann cells after immediate nerve repair in rats. BMC Neurosci 2011: 12: 12.
67. Houtgraaf JH, Versmissen J, van der Giessen WJ. A concise review of DNA damage checkpoints and repair in mammalian cells. Cardiovasc Revasc Med 2006: 7: 165-72.
68. Latif C, Harvey SH, O'Connell MJ. Ensuring the stability of the genome: DNA damage checkpoints. ScientificWorldJournal 2001: 1: 684-702.
69. Georgiou M, Golding JP, Loughlin AJ, Kingham PJ, Phillips JB. Engineered neural tissue with aligned, differentiated adipose-derived stem cells promotes peripheral nerve regeneration across a critical sized defect in rat sciatic nerve. Biomaterials 2015: 37: 242-51.
70. Clements MP, Byrne E, Camarillo Guerrero LF, et al. The Wound Microenvironment Reprograms Schwann Cells to Invasive Mesenchymal-like Cells to Drive Peripheral Nerve Regeneration. Neuron 2017: 96: 98-114 e7.
71. Hoke A, Redett R, Hameed H, et al. Schwann cells express motor and sensory phenotypes that regulate axon regeneration. J Neurosci 2006: 26: 9646-55.
72. Volarevic V, Markovic BS, Gazdic M, et al. Ethical and Safety Issues of Stem Cell-Based Therapy. Int J Med Sci 2018: 15: 36-45.
73. Lazennec G, Jorgensen C. Concise review: adult multipotent stromal cells and cancer: risk or benefit? Stem Cells 2008: 26: 1387-94.
74. Greenbaum D, Colangelo C, Williams K, Gerstein M. Comparing protein abundance and mRNA expression levels on a genomic scale. Genome Biol 2003: 4: 117.

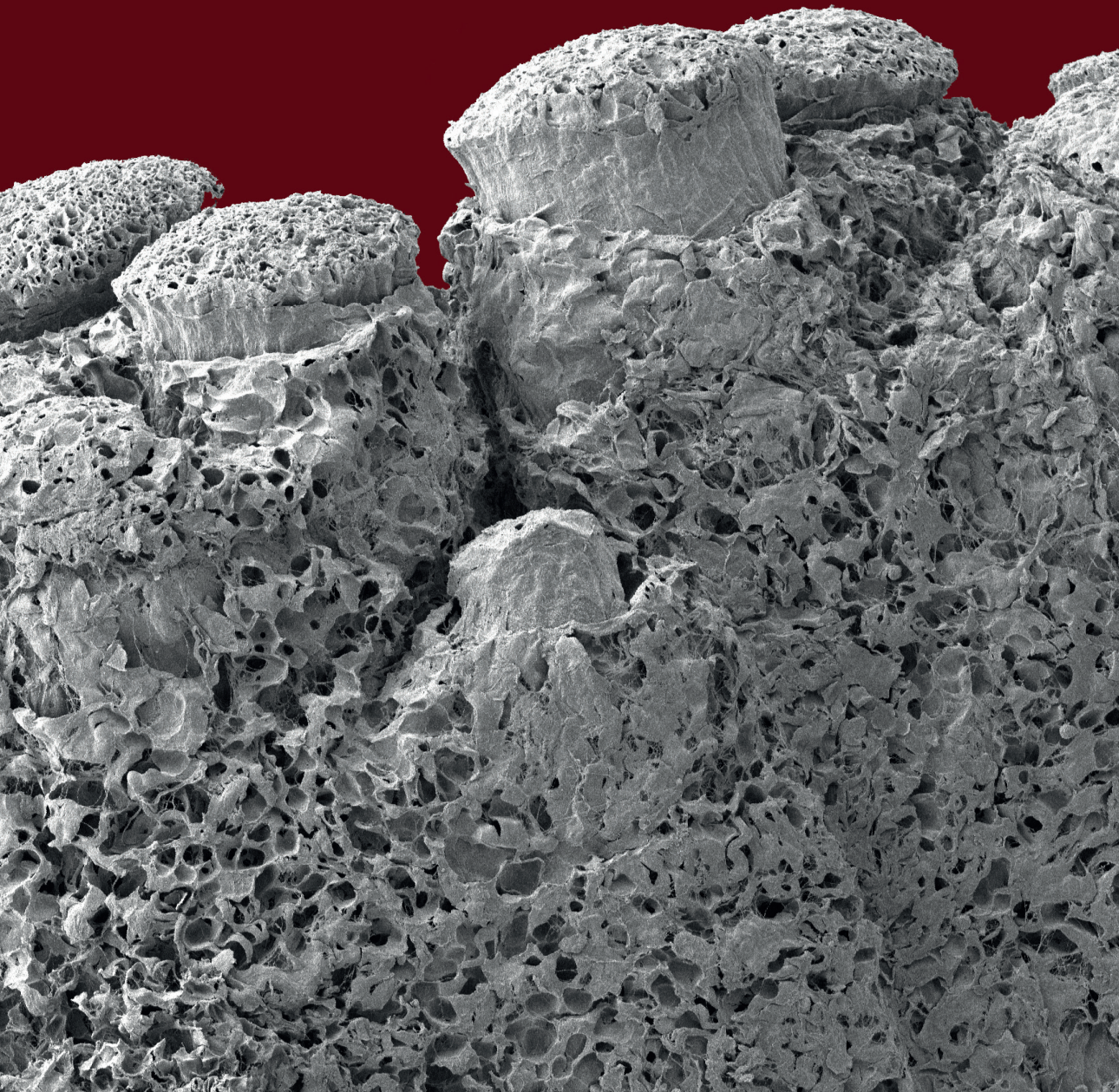

Chapter 5

New methods for objective angiogenesis evaluation of rat nerves using microcomputed tomography scanning and conventional photography

Tiam M. Saffari, Femke Mathot, Allen T. Bishop, Alexander Y. Shin

Microsurgery. 2020 March;40(3): 370-376

ABSTRACT

Introduction

Nerve regeneration involves multiple processes which enhance blood supply that can be promoted by growth factors. Currently, tools are lacking to visualize the vascularization patterns in transplanted nerves in vivo. The purpose of this study was to describe three-dimensional visualization of the vascular system in the rat sciatic nerve and to quantify angiogenesis of nerve reconstruction.

Materials and Methods

In 12 Lewis rats (weighing 250 – 300 grams), 10 mm sciatic nerve gaps were repaired with ipsilateral reversed autologous nerve grafts. At 12 and 16 weeks of sacrifice, Microfil® contrast compound was injected in the aorta. Nerve autografts (N=12) and contralateral untreated nerves (N=12) were harvested and cleared while preserving the vasculature. The amount of vascularization was measured by quantifying the vascular surface area using conventional photography (two dimensional) and the vascular volume was calculated with micro-computed tomography (three dimensional). For each measurement, a vessel/nerve area ratio was calculated and expressed in percentages (vessel%).

Results

The vascular volume measured 3.53 ± 0.43% in autografts and 4.83 ± 0.45% vessels in controls at 12 weeks and 4.95 ± 0.44% and 6.19 ± 0.29% vessels at 16 weeks, respectively. The vascular surface area measured 25.04 ± 2.77 % in autografts and 26.87 ± 2.13% vessels in controls at 12 weeks, and 28.11 ± 3.47% and 33.71 ± 2.60% vessels at 16 weeks respectively. The correlation between both methods was statistically significant (P=0.049).

Conclusions

Both methods are considered to successfully reflect the degree of vascularization. Application of this technique could be used to visualize and objectively quantify angiogenesis of the transplanted nerve graft. Moreover, this simple method is easily reproducible and could be extrapolated to any other desired target organ ex vivo in small animals to investigate the vascular network.

INTRODUCTION

It has been postulated that blood supply affects nerve regeneration[1-7], as it is reported that vascular endothelial cells directly guide the regeneration of peripheral nerve axons.[7] Angiogenesis can be enhanced through growth factors[8], in particular angiopoietin-1 (Ang-1); an important angiogenic factor that promotes vascular stabilization[9] and vascular endothelial growth factor (VEGF) which enhances intraneural angiogenesis.[2] To quantify blood vessels in nerve grafts or conduits, previous studies have focused on immunohistochemical staining.[10-12] Unfortunately, the amount of (neo)angiogenesis was not evaluated in these studies.

Histomorphometric analyses are used to describe angiogenesis, but are limited in the ability to identify the three-dimensional interconnectivity of the vasculature in serial histological sections [13, 14] and focuses on representing superficial blood flow.[15]. Connectivity defines the maximal number of branches that may be cut without separating the structure.[15] Insight in the connectivity of the vascular tree may contribute to crucial description of neovascularization patterns. Therefore, two-dimensional measures of vasculature deliver incomplete information.[13] Three-dimensional reconstruction of blood vessels in sciatic nerves of the rat has been technically difficult because the average diameter of the small endoneural vessels in the rat is 8.8 mm.[16]

Micro-computed tomography (micro CT) facilitates the visualization of contrast enhanced microvessels and could separate vessels from surrounding tissues, such as bone, fat tissue or nerve.[17] It provides three-dimensional volume imaging with spatial resolution at the micrometer scale and is applied in many fields, for instance in tumor visualization, cardiovascular plaque imaging[15, 17] and evaluation of surgical angiogenesis in bone allotransplantation models.[18-20]

As technology continues to evolve, modern micro CT systems are more commonly available and are capable of generating very small voxels with short scan acquisition times allowing both ex vivo and in vivo scanning.[15] Moreover, due to voxels as small as 1 µm, the vascular system in rat and even mice could now be visualized.[13, 14, 21, 22] As perfusion with a radiopaque contrast agent is the only requirement to delineate the vascular tree, a closer-meshed network of smaller vessels, contrast enhanced micro CT can become a powerful tool in quantifying angiogenesis.[13]

Information collected from conventional photography may complement the micro CT. Photographs could be analyzed by measuring the ratio of vessel area and total nerve area digitally.[23] More conventional methods such as manual vessel counts per sub-segment of the nerve, providing a vessel density per mm2, have also been described.[24] These techniques have never been verified and are questionably representative for the entire quantification of the nerve vasculature when used solely. However, with evolving technology, the quality of conventional photography has improved and there are numerous photo editing software programs available providing a cost-effective way to measure vessel and nerve surface areas.

The purpose of this study was to describe three-dimensional visualization of the vascular

system in the rat sciatic nerve and to quantify angiogenesis of nerve reconstruction. The micro CT and conventional photography were used to objectively quantify vascular volume and vascular surface area, respectively, as measurements of angiogenesis in rat nerve.

MATERIALS AND METHODS

Animal experiments were approved by our Institutional Animal Care and Use Committee (IACUC A3348-18). For this study, male Lewis rats (Envigo, USA) were used, weighing between 250 – 300 grams. All animals were housed with ad libitum access to food and water, with a 12-hour light-dark cycle after surgery.

Experimental design

In 12 Lewis rats, unilateral 10 mm sciatic nerve gaps were repaired with ipsilateral reversed autologous nerve grafts to create a mismatch in the alignment of the nerve fibers.[25, 26] This group was considered the gold standard for nerve repair. Rats survived for either 12- or 16 weeks. At the time of the sacrifice, autograft nerves (N=6 per time point) and the contralateral nerve samples as untreated, control samples (N=6 per time point) were harvested. The nerve vasculature was preserved to obtain the vascular volume and vascular surface area measurements.

Surgical procedure

After anesthesia in an isoflurane chamber, rats were shaved, prepped and positioned in the nosecone to maintain anesthesia throughout the procedure. Preoperatively the following were administrated subcutaneously; infection prophylaxis provided by Enrofloxacin (Baytril, Bayer, Germany, 10mg/kg), 5 ml of NaCl 0.9% solution to prevent dehydration and Buprenorphine SR (Buprenorphine SR-LAB, ZooPharm pharmacy, 0.6mg/kg) for pain control. During surgery, body temperature was maintained at 37°C with a heating pad.

The sciatic nerve was fully exposed proximally from the inferior margin of the piriformis muscle to approximately 5 mm distal to the bifurcation, under an operating microscope (Zeiss OpMi 6, Carl Zeiss Surgica, Oberkochen, Germany). A 10 mm segment of the sciatic nerve was excised by sharp transection with microsurgical scissors. The nerve graft was reversed and reconstructed with six 10-0 nylon (Ethilon, Ethicon Inc., Sommerville, NJ, USA), epineural interrupted sutures on either side of the anastomosis. Wounds were closed in layers, approximating muscle with two 5-0 absorbable interrupted sutures (5-0 Vicryl Rapide, Ethicon Inc., Sommerville, NJ, USA). The skin was closed subcutaneously, using the same suture. Postoperatively, the rats were kept warm with towels. The rats were observed weekly until completion of the experiment.

Perfusion of contrast

Twelve and 16 weeks postoperatively, rats were sacrificed. Access for aortic infusion catheter placement was achieved via the abdomen. A large midline incision was made in the abdomen to expose the aorta and vena cava. A small retractor was used to retract the digestive organs providing stable exposure of the aorta and vena cava throughout the experiment. The fat

surrounding the thoracic aorta and vena cava was cleaned using cotton tip applicators taking care not to harm the vascular structures. The thoracic aorta and vena cava were ligated proximally with a 5-0 Vicryl suture (5-0 Vicryl Rapide, Ethicon Inc., Sommerville, NJ, USA) which was kept long to act as grip sutures. The ligation was placed as proximal as possible and distal to any large hepatic bifurcations, depending on the anatomic variation. The aorta was dissected from the vena cava distally using cotton tip applicators. This was performed approximately 1 cm proximal to the iliac bifurcation. A loose 5-0 Vicryl suture was placed under the aorta. To facilitate the passage of contrast, a 24 Gauge catheter (Jelco IV Catheter Radiopaque, Smiths Medical International, UK) connected to an IV tubing system, was introduced in the aorta just distally to the proximally placed grip sutures, while keeping the aorta on tension by slightly pulling the grip sutures (**figure 1**). After the catheter was fixated with the previously placed suture around the aorta distally, 2-3 ml of saline (NaCl 0.9%) was infused through the tubing system to evaluate the patency of the aorta. The needle was removed off the cannula, while maintaining the cannula in the artery. Care was taken that the tip of the cannula would still be proximal to the iliac bifurcation, so that the contrast would reach both limbs. A yellow-colored (MV-122) Microfil® compound (MV 8ml, diluent 15 ml, and curing agent 1.2 ml, Flow Tech, Inc., Carver, MA, USA) in a 50 cc syringe was connected to the tubing system to be infused in the aorta. While putting pressure on the insertion site using gauze, the perfusion was performed with constant perfusion of approximately 100 mmHg. The perfusion was continued until the syringe was empty and yellow nailbeds on either paw were observed. After the perfusion was completed, a clamp was placed on the cannula to prevent leakage of the infused contrast. The rat was kept at room temperature while the agents cured for at least 90 minutes.

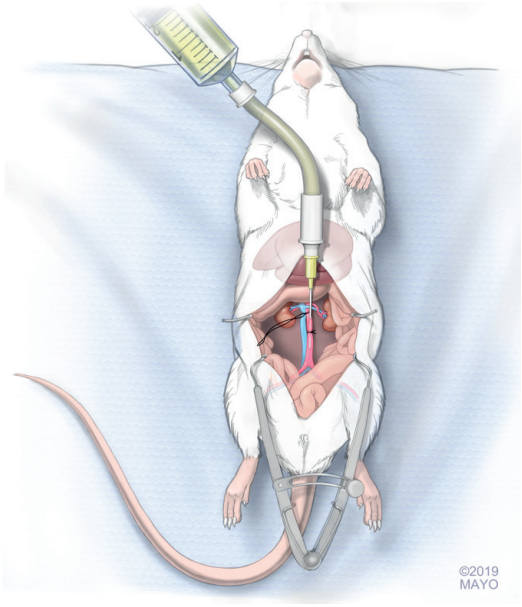

Figure 1. *Schematic drawing of the insertion of the catheter into the rat aorta. Long sutures indicate the grip sutures that have ligated the aorta and vena cava proximally. Short cut suture serves to hold catheter in place while injecting the Microfil® contrast compound into both common iliac arteries of the rat. (with permission of the Mayo Foundation, Copyright Mayo Foundation 2019)*

Sample collection

After the vascular bed was perfused successfully and the contrast had cured, the sciatic nerve was exposed and harvested extending to approximately 3 mm on either side of the anastomoses. Nerve samples were collected in phosphate buffered saline (PBS) and cleared for five days by immersion in graded series of ethyl alcohol as follows: the samples were first placed in 25% ethyl alcohol and at successive 24-48 hour intervals the concentration was raised to 50%, 75%, 95% and 100%. As the final step, the samples were immersed in methyl salicylate. If tissue had not cleared, a second clearing starting from 95% ethyl alcohol stage was performed to repeat the final steps of the clearing procedure. This procedure allowed clearing of all structures, with exception of the opacified microvascular structures that were filled with contrast.

Micro CT for calculating the vascular volume

After clearing had taken place, the samples were scanned in a SkyScan 1276 micro CT (Bruker Corporation, Billerica, MA, USA) at 40 kV voltage, 200 μA current and 10 μm resolution to calculate vascular volume. Three samples were scanned at a time, taking approximately 26 minutes per scan with frame averaging set at three in order to reduce noise. Three-dimensional images of the samples were reconstructed using Hierarchical InstaRecon software (NRecon, 1.7.4.2., InstaRecon, 2.0.4.0. InstaRecon). This software was used to adjust the following parameters while reconstructing the images; Beam Hardening Correction (%) was set at 51, Ring Artifact Correction at 9, Smoothing at 1, Post alignment compensation and Histogram windows were manually adjusted for each scan. After obtaining reconstruction of the images, AnalyzePro software (AnalyzeDirect, Inc., Overland Park, KS, USA) was used to measure the volume of the vasculature and the volume of the total nerve. A vessel/nerve area ratio was calculated and expressed in percentages (vessel%).

Photography for calculating the vascular surface area

After micro CT scanning was completed, the nerve samples were stretched by suturing both nerve ends onto a solid holder. Detailed pictures of the samples were obtained using a Canon 5D Mark IV camera, (Manual Mode, ISO 200, 1/200th of a sec, f/16), a Canon MP-E 65mm Macro lens and a Canon MT-26-RT Twin Lite Macro strobe light source. During photography, samples were placed in a petri dish with methyl salicylate in order to obtain clean photographs allowing for the specimen to be separated from the background for better measurement. The petri dish was placed on a black background to achieve maximum contrast with the yellow vessels in the nerve samples. Polarized light was used to reduce reflections and a 1:1 magnification was used to ensure consistency of the pictures. To correct for the surface area that altered depending on the angle of the image, two pictures of each nerve sample were obtained; one of the front whereafter the holder was flipped and the picture of the other side was obtained. With NIS-Elements software (NIS-Elements BR 4.51.01), the total vessel area and the total nerve area in the graft were measured in a blinded fashion. For each image, a vessel/nerve area ratio was calculated and expressed in percentages. The ratios of the two images (front and back) were averaged per sample.

Statistical analysis

The vascular volume and the vascular surface area were analyzed and compared to the

untreated side (control). A nonpaired student t-test for comparisons between groups was used for statistical investigation. Correlations were analyzed using Pearson's correlation test. Results were reported as the mean and standard error or the mean (SEM), and the level of significance was set at $\alpha \leq 0.05$.

RESULTS

Macroscopic appearance of the vessels in nerve samples

After the clearing process, the nerve samples were transparent and vessels were filled with Microfil®. For 3D imaging, the micro CT was used and allowed visualization of the vessels in space (**figure 2**). The size and position of the vessels were visualized. **Figure 3** shows the macroscopic images of the nerve autografts at 12- and 16 weeks and a control sample at 12 weeks obtained with a conventional digital camera. Sutures are clearly visible and were used to set the borders of the analysis frame. As demonstrated, the microvasculature was clearly visualized. The smallest diameter of blood vessels detected was 9.3 µm using micro CT and 7.4 µm using conventional photography.

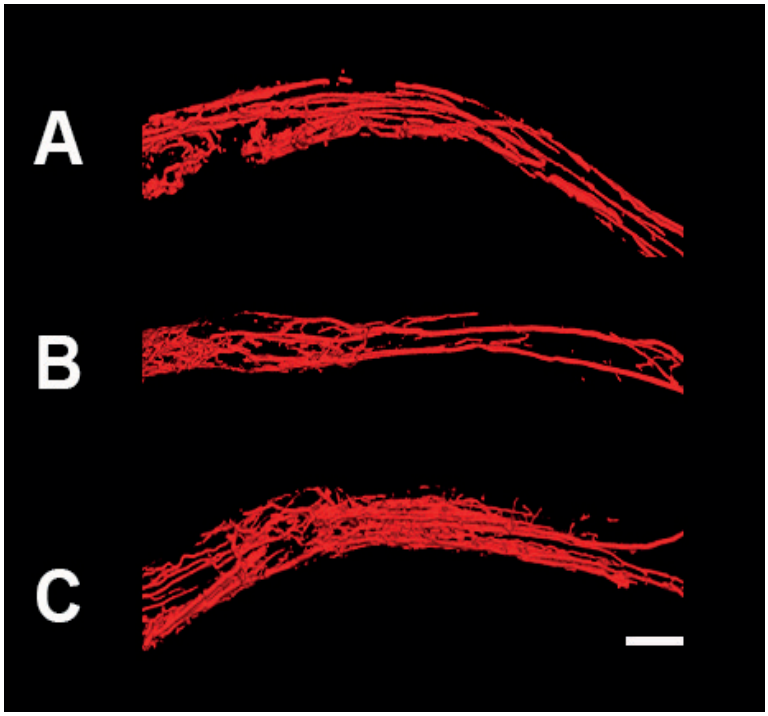

Figure 2. *Micro computed tomography (micro CT) images of nerve samples. Micro CT images of the same samples visualized in Figure 2. Control nerve at 12 weeks (A), nerve autograft at 12 weeks (B) and nerve autograft at 16 weeks (C). Nerve samples are positioned from proximal to distal (left to right respectively). Scale bar is set a 1 millimeters (mm).*

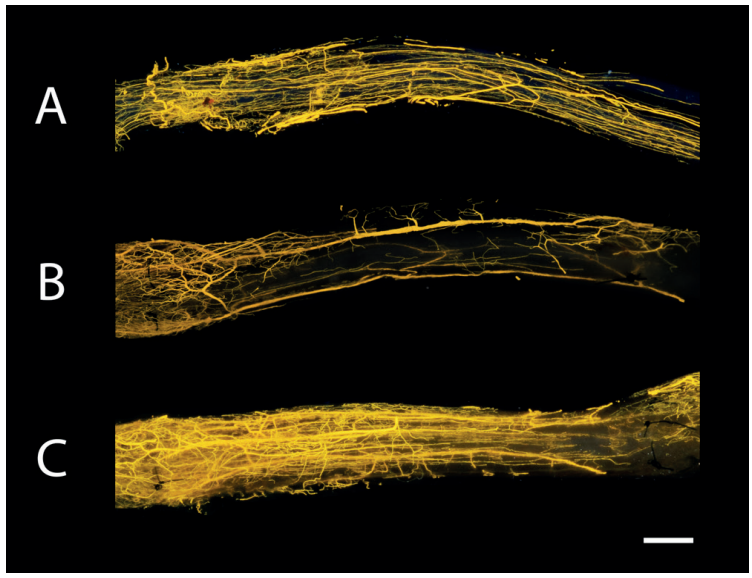

Figure 3. Macroscopic images of nerve samples obtained with conventional digital photography. Microvessels could be clearly seen in the control nerve at 12 weeks (A), nerve autograft at 12 weeks (B) and nerve autograft at 16 weeks (C). Sutures that are used to repair the graft are visible in nerve autograft groups (B+C) and depict the border of the analyzed frame. Nerve samples are positioned from proximal to distal (left to right respectively). Scale bar is set at 1 millimeters (mm).

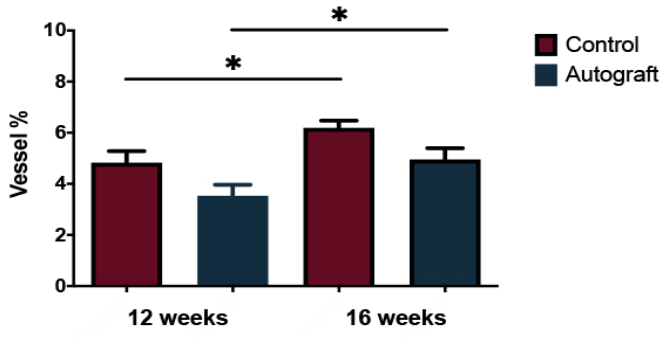

*Figure 4. Vascular volume of control and nerve autograft samples at 12 and 16 weeks using micro CT. Results are expressed as a percentage (vessel %) of the total nerve area and are given as the mean ±SEM. *Indicates significance at p<0.05.*

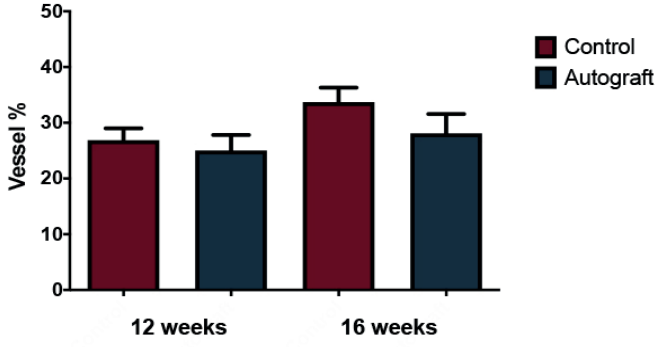

Figure 5. Vascular surface area of control and nerve autograft samples at 12 and 16 weeks using digital photography. Results are expressed as a percentage (vessel %) of the total nerve area and are given as the mean ±SEM.

Vascular volume measured with micro CT

The vascular volume was successfully measured using the micro CT. At 12 weeks, autograft nerves measured 3.53 ± 0.43% and control nerve samples measured 4.83 ± 0.45% vessels. At 16 weeks, this was 4.95 ± 0.44% and 6.19 ± 0.29% vessels for autografts and controls, respectively. These outcomes are depicted in **figure 4**.

Vascular surface area measured with conventional photography

After 12 weeks, the vascular surface area was 25.04 ± 2.77% and 26.87 ± 2.13% vessels for autografts and control nerves, respectively. At 16 weeks, photography measured 28.11 ± 3.47% vessels for autografts and 33.71 ± 2.60% vessels for controls (**figure 5**).

Correlations

The vascular volume and vascular surface area were significantly correlated with both time points and groups (r=0.951, p=0.049).

DISCUSSION

In this study, the authors successfully measured the vasculature of the sciatic nerve in rats to provide more insight in the amount of angiogenesis and the patterns of neoangiogenesis occurring in nerve regeneration. The limited options available to visualize the small vessels of the rat had previously impeded the understanding of the underlying neoangiogenesis patterns after nerve graft reconstruction.

The utility of the methods described in the current study is two-fold. First, it provides an objective quantification of the amount of angiogenesis, independently from the size of the vessels, in relation to the size of the nerve. Second, it eminently demonstrates the patterns of angiogenesis in (transplanted) nerves. Nerve revascularization is postulated to be composed of angiogenesis and neoangiogenesis; vessels that sprout into the existing vascular tree and vessels that create new pathways.[27] However, this theory has yet to be objectively described. Angiogenesis is the growth of blood vessels from existing vasculature. Angiogenesis occurs throughout development and forms transvascular tissue pillars that expand with overall growth resulting in the increase in vascularity over time.[28] This process could also be seen in our study, when comparing time points. The vascularization of nerves and in particular, the alignment of vessels in nerves is attributed to a directional role for regenerating axons.[29, 30] Applying the described techniques at several time points after nerve graft implementation may provide insight to the ratio between revascularization components. These techniques may demonstrate the relationship between vessel alignment and the level of nerve regeneration. Thus, allowing us to improve our understanding of the process and the importance of vascular development in nerve grafts.

As blood vessels provide little inherent contrast, viscosity is one of the most important properties of the implemented vehicle.[15] With viscosity levels around 20-30, Microfil® is the best available compound that injects both the arterial and venous system and reaches even

the smallest angiogenic vessels to allow complete study of the vascular network.[15] The injected Microfil® does not directly interact with the histology but could influence the proportion of axon and nerve areas during the analysis. Therefore, we would suggest harvesting other tissue prior to Microfil® injection to secure reliable histologic analysis.

There are a few considerations associated with these techniques. Although micro CT systems become more commonly available with improving quality[15], costs could add up and it is still conceivable that micro CT devices with small effective voxel size are not available for all researchers. In this case, solely the described conventional photography strategy could be used, as it is cost-effective, simple to perform and correlates with micro volume measurements. However, the limitation of conventional photography is that it does not describe vascularization in space and lacks detailed information. As only two sides of the nerve sample are measured and the surface area could not be corrected for the thickness of the nerve (i.e. depth of the obtained photo), representation of the amount of angiogenesis using vascular surface area may be questionable. The difference between various groups of nerve samples, however, could be described with conventional photography. The use of Microfil® to fill the complete vascular bed including the smallest arterial and venous branches allows visualization of the desired vascular system but limits any other histological examination in the same samples, as processing is different. The micro CT has the advantage of precisely measuring vessel volume in relation to total measured nerve volume. Also, clearing of samples is not necessary as the lead pigments in Microfil® provide high contrast compared to background tissue to acquire complete high resolution 3D images of the vessels.[17]

Our results indicate the significant correlation between the vascular volume and the vascular surface area measurements demonstrating that the methods could be used either complementary or separately, depending on the goals of the study. These methods will allow us to advance angiogenesis related research by improving the tools for studying and understanding vascular development and the mechanisms of neoangiogenesis.

CONCLUSION

This study provides accurate objective analysis of the newly formed vascular network of the sciatic nerve. The use of the micro CT and conventional photography provides many modalities for vascular exploration, allowing the exploration of the structure and organization of blood vessels. These imaging methods are easily reproducible and could be extrapolated to any other desired target organ ex vivo in small animals to investigate the vascular network.

REFERENCES

1. Weddell G. Axonal regeneration in cutaneous nerve plexuses. J Anat 1942: 77: 49-62 3.
2. Hobson MI, Green CJ, Terenghi G. VEGF enhances intraneural angiogenesis and improves nerve regeneration after axotomy. J Anat 2000: 197 Pt 4: 591-605.
3. Best TJ, Mackinnon SE. Peripheral nerve revascularization: a current literature review. J Reconstr Microsurg 1994: 10: 193-204.
4. Sondell M, Lundborg G, Kanje M. Vascular endothelial growth factor has neurotrophic activity and stimulates axonal outgrowth, enhancing cell survival and Schwann cell proliferation in the peripheral nervous system. J Neurosci 1999: 19: 5731-40.
5. Mompeo B, Engele J, Spanel-Borowski K. Endothelial cell influence on dorsal root ganglion cell formation. J Neurocytol 2003: 32: 123-9.
6. Skold MK, Svensson M, Tsao J, et al. Karolinska institutet 200-year anniversary. Symposium on traumatic injuries in the nervous system: injuries to the spinal cord and peripheral nervous system - injuries and repair, pain problems, lesions to brachial plexus. Front Neurol 2011: 2: 29.
7. Cattin AL, Burden JJ, Van Emmenis L, et al. Macrophage-Induced Blood Vessels Guide Schwann Cell-Mediated Regeneration of Peripheral Nerves. Cell 2015: 162: 1127-39.
8. Cui WL, Qiu LH, Lian JY, et al. Cartilage oligomeric matrix protein enhances the vascularization of acellular nerves. Neural Regen Res 2016: 11: 512-8.
9. Brindle NP, Saharinen P, Alitalo K. Signaling and functions of angiopoietin-1 in vascular protection. Circ Res 2006: 98: 1014-23.
10. Connolly DT, Heuvelman DM, Nelson R, et al. Tumor vascular permeability factor stimulates endothelial cell growth and angiogenesis. J Clin Invest 1989: 84: 1470-8.
11. Hu DE, Fan TP. Suppression of VEGF-induced angiogenesis by the protein tyrosine kinase inhibitor, lavendustin A. Br J Pharmacol 1995: 114: 262-8.
12. Norrby K. Vascular endothelial growth factor and de novo mammalian angiogenesis. Microvasc Res 1996: 51: 153-63.
13. Perrien DS, Saleh MA, Takahashi K, et al. Novel methods for microCT-based analyses of vasculature in the renal cortex reveal a loss of perfusable arterioles and glomeruli in eNOS-/- mice. BMC Nephrol 2016: 17: 24.
14. Kline TL, Knudsen BE, Anderson JL, et al. Anatomy of hepatic arteriolo-portal venular shunts evaluated by 3D micro-CT imaging. J Anat 2014: 224: 724-31.
15. Zagorchev L, Oses P, Zhuang ZW, et al. Micro computed tomography for vascular exploration. J Angiogenes Res 2010: 2: 7.
16. Bell MA, Weddell AG. A descriptive study of the blood vessels of the sciatic nerve in the rat, man and other mammals. Brain 1984: 107 (Pt 3): 871-98.
17. Ghanavati S, Yu LX, Lerch JP, Sled JG. A perfusion procedure for imaging of the mouse cerebral vasculature by X-ray micro-CT. J Neurosci Methods 2014: 221: 70-7.
18. Kotsougiani D, Hundepool CA, Bulstra LF, et al. Bone vascularized composite allotransplantation model in swine tibial defect: Evaluation of surgical angiogenesis and transplant viability. Microsurgery 2019: 39: 160-66.
19. Willems WF, Kremer T, Friedrich P, Bishop AT. Surgical revascularization induces angiogenesis in orthotopic bone allograft. Clin Orthop Relat Res 2012: 470: 2496-502.
20. Willems WF, Kremer T, Friedrich P, Bishop AT. Surgical revascularization in structural orthotopic bone allograft increases bone remodeling. Clin Orthop Relat Res 2014: 472: 2870-7.
21. Lee S, Barbe MF, Scalia R, Goldfinger LE. Three-dimensional reconstruction of neovasculature in solid tumors and basement membrane matrix using ex vivo X-ray microcomputed tomography. Microcirculation 2014: 21: 159-70.
22. Deshpande SS, Donneys A, Farberg AS, et al. Quantification and characterization of radiation-induced changes to mandibular vascularity using micro-computed tomography. Ann Plast Surg 2014: 72: 100-3.

23. Giusti G, Lee JY, Kremer T, et al. The influence of vascularization of transplanted processed allograft nerve on return of motor function in rats. Microsurgery 2014.
24. Wongtrakul S, Friedrich PF, Bishop AT. Vascular endothelial growth factor promotion of neoangiogenesis in conventional nerve grafts. J Hand Surg [Am] 2002: 27: 277-85.
25. Kumta S, Yip K, Roy N, Lee SK, Leung PC. Revascularisation of bone allografts following vascular bundle implantation: an experimental study in rats. Arch Orthop Trauma Surg 1996: 115: 206-10.
26. Hudson TW, Zawko S, Deister C, et al. Optimized acellular nerve graft is immunologically tolerated and supports regeneration. Tissue Eng 2004: 10: 1641-51.
27. Best TJ, Mackinnon SE, Midha R, Hunter DA, Evans PJ. Revascularization of peripheral nerve autografts and allografts. Plast Reconstr Surg 1999: 104: 152-60.
28. Adair TH, Montani JP. Angiogenesis. In Angiogenesis. San Rafael (CA), 2010.
29. Cutting CB, McCarthy JG. Comparison of residual osseous mass between vascularized and nonvascularized onlay bone transfers. Plastic & Reconstructive Surgery 1983: 72: 672-5.
30. Parrinello S, Napoli I, Ribeiro S, et al. EphB signaling directs peripheral nerve regeneration through Sox2-dependent Schwann cell sorting. Cell 2010: 143: 145-55.

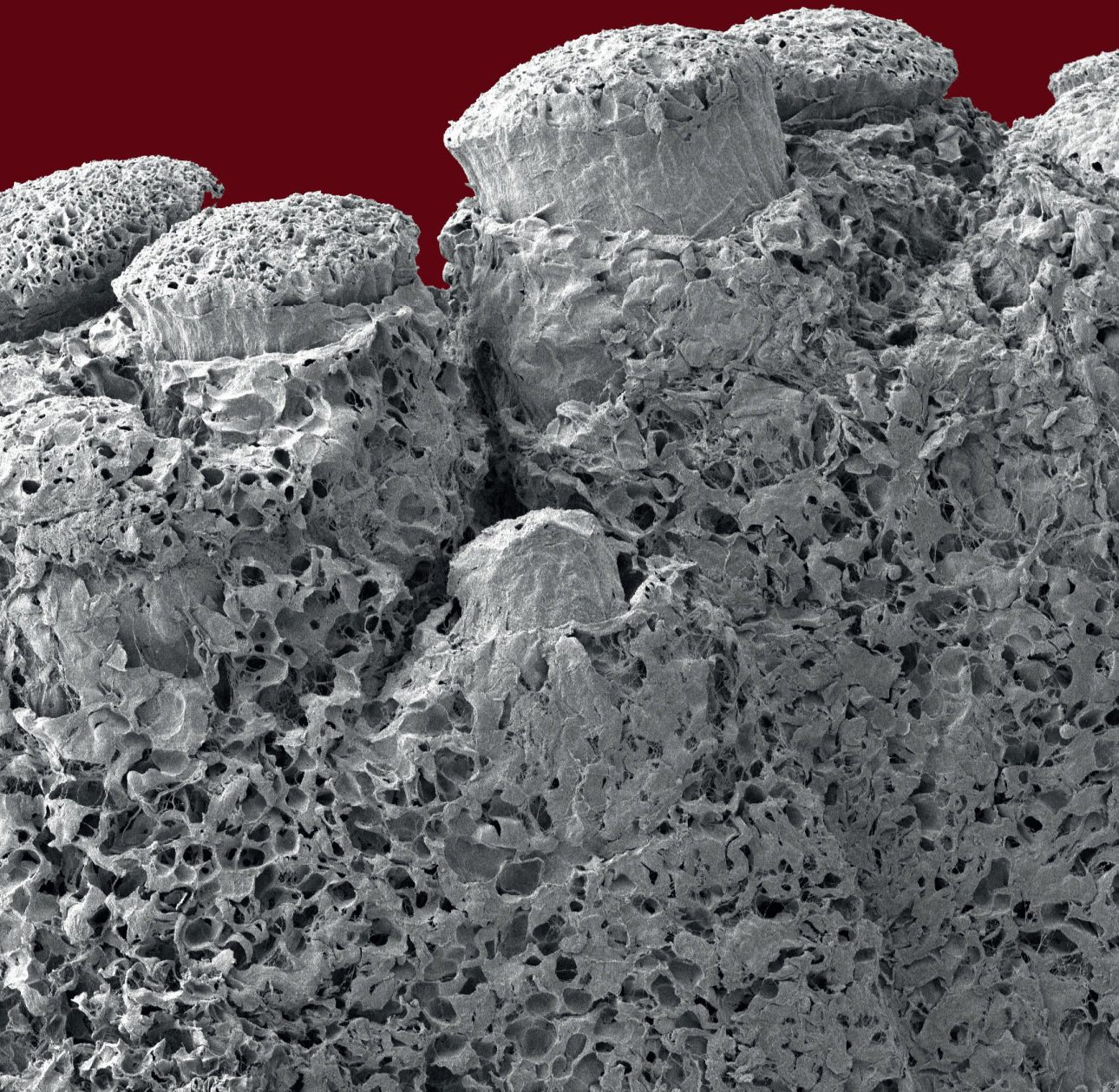

Chapter 6

Adipose derived mesenchymal stem cells seeded onto a decellularized nerve allograft enhances angiogenesis in a rat sciatic nerve defect model

Femke Mathot, Nadia Rbia, Allen T. Bishop,
Steven E.R. Hovius, Alexander Y. Shin

Microsurgery. 2020 July;40(5): 585-592

ABSTRACT

Purpose

Adipose derived mesenchymal stem cells (MSCs) are hypothesized to supplement tissues with growth factors essential for regeneration and neovascularization. The purpose of this study was to determine the effect of MSCs with respect to neoangiogenesis when seeded onto a decellularized nerve allograft in a rat sciatic defect model.

Methods

Allograft nerves were harvested from Sprague-Dawley rats and decellularized. MSCs were obtained from Lewis rats. 10mm sciatic nerve defects in Lewis rats were reconstructed with reversed autograft nerves, decellularized allografts, decellularized allografts seeded with undifferentiated MSC or decellularized allografts seeded with differentiated MSCs. At 16 weeks, the vascular surface area and volume were evaluated.

Results

The vascular surface area in normal nerves (34.9±5.7%.), autografts (29.5±8.7%), allografts seeded with differentiated (38.9±7.0%) and undifferentiated MSCs (29.2±3.4%) did not significantly differ from each other. Unseeded allografts (21.2±6.2%) had a significantly lower vascular surface area percentage than normal non-operated nerves (13.7%, $p=0.001$) and allografts seeded with differentiated MSCs (17.8%, $p=0.001$). Although the vascular surface area was significantly correlated to the vascular volume ($r=0.416$; $p=0.008$), no significant differences were found between groups concerning vascular volumes. The vascularization pattern in allografts seeded with MSCs consisted of an extensive non-aligned network of micro-vessels with a centripetal pattern, while the vessels in autografts and normal nerves were more longitudinally aligned with longitudinal inosculation patterns.

Conclusions

Neoangiogenesis of decellularized allograft nerve was enhanced by stem cell seeding, in particular by differentiated MSCs. The pattern of vascularization was different between processed allograft nerves seeded with MSCs compared to autograft nerves.

INTRODUCTION

Compared to decellularized allografts or bioabsorbable synthetic conduits, autograft nerves continue to result in superior functional outcomes after peripheral nerve repair. One hypothesis for autografts superiority is the ability of autografts to revascularize.[1-3] Revascularization of injured tissue is an essential process in tissue regeneration as it relieves injury-induced hypoxia at the regeneration site while facilitating the delivery of nutrients and cells essential for the regeneration process.[4] Revascularization occurs as early as 2 days after nerve injury and precedes the axonal regeneration.[5, 6] Hypoxia in peripheral nerves causes macrophages to secrete vascular endothelial growth factor (VEGF), which induces (neo)angiogenesis and facilitates trophic factors to arrive at the regeneration site.[7] The endothelial cells of newly formed blood vessels have a directional function by guiding Schwann cells across the nerve-gap, which direct the regenerating axons in the correct direction.[6, 8] A sufficient volume of well-organized newly formed vessels in both nerve stumps is requisite for a functional outcome after peripheral nerve repair and has been confirmed in several animal-models.[3, 9, 10] Improved revascularization and diminished duration of avascularity has been suggested to prevent central fibrosis or necrosis in autografts compared to decellularized allografts, especially in large nerve gaps.[11-14] Improved vascularization could therefore lead to improved nerve regeneration in decellularized allografts.

In order to improve vascularization, numerous studies have evaluated the addition of VEGF to nerve reconstructions. Although some studies demonstrated improved vascularization by the addition of VEGF, they failed to prove any benefit of VEGF with respect to functional outcomes demonstrating that the addition of a single growth factor was insufficient to replicate the complex angiogenesis cascade.[15-19]

Adipose derived Mesenchymal Stem Cells (MSCs), when seeded onto decellularized allograft nerves, result in the production of neurotrophic and angiogenic factors, one of which is VEGF.[20] While the exact role of MSCs (structural vs immunomodulatory) continues to be defined, it has been demonstrated that MSCs have a finite lifespan, stimulate tissue repair via release of trophic factors and produce proteins and cytokines that stimulate tissue regeneration with immunomodulatory effects.[20-25] MSCs differentiated into Schwann-like cells (differentiated MSCs) in vitro lead to increased gene expressions of angiogenic (VEGF) and neurotrophic genes when compared to undifferentiated MSCs[20, 22, 26, 27] and are considered nerve regeneration catalysts.[19] The disadvantages of differentiating MSC include the extra preparation time, expense and extra handling of the cells. The effect of differentiation thus needs to be carefully investigated.

In order to equal the results of nerve autografts, efforts have been recently made to optimize the quality of decellularized allografts.[28] To improve their outcomes a non-traumatic dynamic seeding strategy has been developed to seed undifferentiated and differentiated MSCs to the allograft surfaces, which survive up to a month in vivo.[29-31] Furthermore, differences in gene expression levels (and thus growth factors produced) have been elucidated between differentiate and undifferentiated MSCs, and demonstrated that differentiated MSCs in

particular showed enhanced expressions of VEGF after interacting with the outer surface of the decellularized allografts.[25, 32]

The purpose of this study was to either substantiate or invalidate the hypothesis whether the previously demonstrated different gene expression profiles of differentiated and undifferentiated MSCs would lead to different levels and patterns of vascularization when dynamically seeded onto processed/decellularized nerve allografts, in comparison to unseeded allografts and autografts.

METHODS

This study was approved by the IACUC institutional review committee and our Institutional Review Board (IACUC protocol A2464-00). A 10 mm segment of the right sciatic nerve of 20 Lewis rats (Envigo, USA) was excised and was replaced with either (i) a reversed autograft, (ii) a processed/decellularized nerve allograft, (iii) a processed/decellularized nerve allograft seeded with undifferentiated MSCs or (iv) a processed/decellularized nerve allograft seeded with differentiated MSCs. All four groups were sacrificed after 16 weeks to determine and compare degree and patterns of revascularization of the nerves. The 16 week survival period was chosen based on previous research indicating 16 weeks is the time period in which nerve regeneration matures.[33]

Nerve allograft harvest and processing

Ten Sprague-Dawley rats (Envigo, Madison, WI, USA) weighing 250-350 grams served as donors of 20 sciatic nerve segments of approximately 15 mm each. Sprague-Dawley rats were used to obtain a major histocompatibility complex mismatch with the recipient Lewis rats, in order to mimic a clinical setting in which allogenous donor nerves will be used.[34, 35] The rats were anesthetized in an isoflurane induction chamber and euthanized with an overdose of pentobarbital once asleep. Both sciatic nerves were carefully dissected with sharp dissecting scissors under an operating microscope (Zeiss OpMi6, Carl Zeiss Surgical GmbH, Oberkochen, Germany). Directly after their harvest, the obtained sciatic nerve segments were processed/decellularized according to a previously published five-day protocol that includes multiple washing steps and emerging in elastase.[28] Sterilization of the nerve segments was obtained with γ-irradiation.

Stem cell preparation and differentiation

In accordance with a future clinical trial in which the MSCs will be harvested from a patient, MSCs were harvested from the inguinal fat pad of an inbred Lewis rat and processed per Kingham and colleagues protocol.[36] The obtained MSCs were cultured in previously described cell culture conditions.[37-39] The MSCs complied with the criteria for MSCs, defined by the International Society for Cellular Therapy previously: they were plastic adherent and multi-potent and expressed canonical MSC-markers like CD44 (88.2%) and CD90 (88.3%) while markers such as CD34 and CD45 were absent.[30, 40]

Cell culture

The obtained MSCs were cultured in growth medium that contained α-MEM (Advanced MEM (1x); Life Technologies Corporation, NY, USA), 5% platelet lysate (PLTMax®; Mill Creek Life Sciences, MN, USA), 1% Penicillin/Streptomycin (Penicillin-Streptomycin (10.000 U/mL; Life Technologies Corporation, NY, USA), 1% GlutaMAX (GlutaMAX Supplement 100X; Life Technologies Corporation, NY, USA) and 0.2% Heparin (Heparin Sodium Injection, USP, 1.000 USP units per mL; Fresenius Kabi, IL, USA).

Differentiation of MSCs

The differentiation of MSCs into Schwann cell-like cells was performed and verified according to a previously described protocol. This protocol has shown to morphologically change 81.5% of the MSCs exposed to the differentiation medium into a typical spindle-like shape and lets approximately 40-45% of the exposed MSCs express glial cell marker GFAP, Schwann cell marker S100 and neurotrophin receptor p75.36 After two preparatory steps with ß-mercaptoethanol (Sigma-Aldrich corp., MO, USA) and all-trans-retinoic acid (1:1000, dilution of stock; Sigma-Aldrich Corp., MO, USA), a differentiation cocktail was introduced to their growth medium. This differentiation cocktail consisted of Forskolin (Sigma-Aldrich corp., MO, USA), basic fibroblast growth factor (bFGF; PeproTech, NJ, USA), platelet derived growth factor (PDGF-AA; PeproTech, NJ, USA), and neuregulin-1 ß1 (NRG1-b1; R&D systems Inc, MN, USA).

According to the protocol, MSCs differentiation was verified by immunocytochemistry for S100, GFAP and neurotrophin receptor p75 (Rabbit anti-S100, mouse anti-GFAP and rabbit anti-p75 NTR; all ThermoFisher Scientific, MA, USA). Secondary antibodies goat-anti rabbit FITC and goat anti-mouse Cyanine-3 (both ThermoFisher Scientific, MA, USA) were used to visualize the expression of the before-mentioned markers in differentiated MSCs. Undifferentiated MSC and Schwann cells were used as respectively negative and positive control.

Stem cell seeding

The decellularized allografts were dynamically seeded with 1x10^6 undifferentiated or differentiated MSCs for 12 hours at 37°C. Previous testing has shown that this is the most efficient seeding duration, leading to a seeding efficiency of 80% to 95% respectively.[30, 31]

Surgical procedure

Twenty male inbred Lewis rats (Envigo, Madison, WI, USA) weighing 250-300 gram, served as recipient rats. The surgical procedure was performed as previously described.[41] The 10 mm section of the sciatic nerve was reversed in the autograft group. The processed allografts, either unseeded, seeded with undifferentiated MSC or seeded with differentiated MSCs, were used to reconstruct a 10 mm sciatic nerve gap in the other three groups. No immunosuppression was administered postoperatively.

Non-survival procedure – measurements

During the non-survival procedures after 16 weeks, all rats (n=5) of each group were

anesthetized in an isoflurane induction chamber. Once asleep, the rats were euthanized with an overdose of pentobarbital.

Vascular preservation
A longitudinal incision over the abdomen exposed the abdominal organs. The aorta and inferior vena cava were dissected carefully. A catheter was placed and fixed inside the aorta over which 10 cc of saline was administered to flush the vasculature. Yellow Microfil® (Flow Tech inc., Carver, Massachusetts, USA) was administered by aortic infusion until both toenail matrixes were colored, which required at least 19 mL of Microfil®.[15] After 90 minutes of curing, the sciatic nerves were dissected and cleared in 5 days by immersing them in graded series of ethyl alcohol (25% - 50% - 75% - 95%) and a final day in methyl salicylate.

Vascular surface area
To optimize the accuracy of the measured level of revascularization, the vascular surface area and the vascular volume were obtained. The nerve samples were stretched by suturing both ends onto a solid holder. While in a petri dish with methyl salicylate, detailed pictures of the nerve were obtained with a Canon 5D Mark III camera, a Canon 65 mm Macro lens and a Canon Twin Lite Macro strobe light source. Polarized light was used to reduce reflections and a 1:1 magnification was used to ensure consistency of the pictures. To correct for the 3D structure of the nerve sample and the surface area that alters depending on the angle of observation, two pictures of each nerve sample were obtained 180 degrees rotated (i.e. front and back of nerve). The solid holder provided a clear distinction between the front and the back of the nerve sample. The pictures were blinded before analysis. Using Image Pro Plus Software, the total nerve area and the total vessel area were marked and measured and a vessel/nerve area ratio was calculated of each picture taken. The ratios of the two pictures (i.e. front and back of the nerve) were averaged. The obtained photographs also enabled the subjective assessment of the alignment of the preserved vasculature.[42]

Vascular volume
With a micro-CT (Inveon Multiple Modality PET/CT scanner, Siemens Medical Solutions USA, Inc., Knoxville, TN), a CT scan was obtained from the nerve samples with an effective pixel size of 9.91μm. As the microfil was more radiopaque than the rest of the nerve, the volume of the total nerve and the volume of the vasculature could be measured with Analyze 12.0 software (AnalyzeDirect, Inc., Overland Park, KS, USA). Eventually, vessel/nerve volume ratios were calculated for each scan.[42]

Correlations
The correlation between the vascular surface area and volume measurements was obtained to determine whether the methods are complementary to each other.

Statistical analysis
The outcome measures were analyzed with one-way ANOVA, with Bonferroni correction for post-hoc multiple comparisons. Correlations were analyzed with the Pearson's correlation test.

Data are expressed as the mean ±SD. The level of statistical significance was set at α=0.05.

RESULTS

Differentiation of MSCs into Schwann-like cells

Differentiated MSCs all adjusted morphologically to a spindle-like shape and demonstrated expression of Schwann cell markers S100, GFAP and NTR p75, which is in accordance with Schwann cells (**figure 1**) and previous studies.

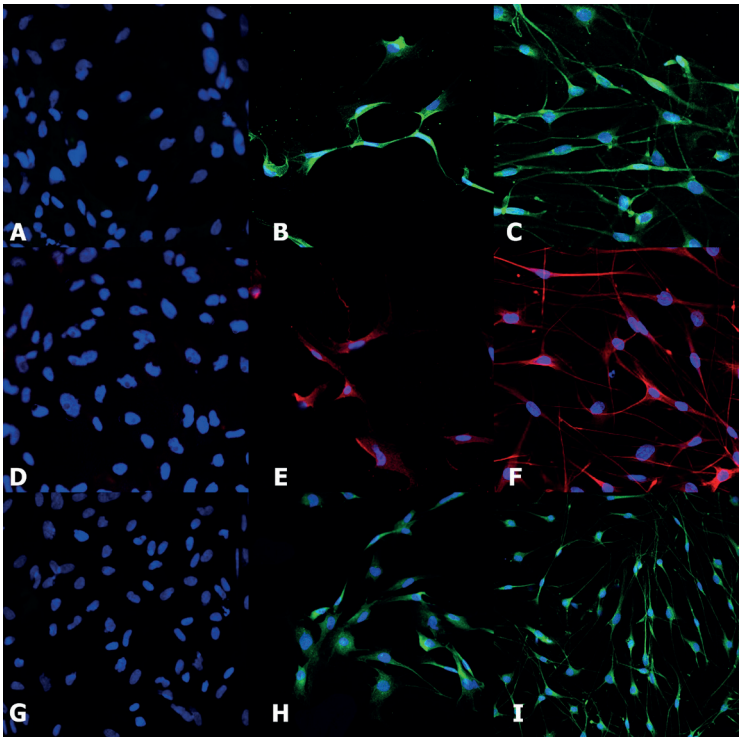

Figure 1. Differentiation of MSCs into Schwann-like cells was confirmed by comparing the expression of Schwann cell markers S100 (A-B-C), GFAP (D-E-F) and NTR p75 (G-H-I) in the differentiated MSCs (B-E-H) to the expression in Schwann cells (C-F-I) and undifferentiated MSCs (A-D-G).

Vascular surface area

Non-operated nerves had a vascular surface area percentage of 34.9±5.7%. Of the four studied groups, the vascular surface area was highest in the group that received allografts seeded with differentiated MSCs (38.9±7.0%), followed by the group with autografts (29.5±8.7%) and the group with allografts seeded with undifferentiated MSC (29.2±3.4%). Unseeded allografts (21.2±6.2%) had a significantly lower mean vascular surface area percentage than normal non-operated nerves (13.7%, p=0.001) and allografts seeded with differentiated MSCs (17.8%, p=0.001) (**figure 2 and 3**).

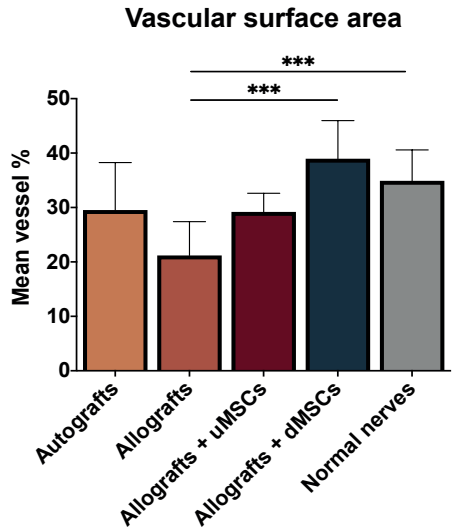

Figure 2. The vascular surface area outcomes of autografts, allografts, allografts seeded with undifferentiated MSC and allografts seeded with differentiated MSCs. The unseeded allografts showed a significantly lower mean vascular surface percentage than allografts seeded with differentiated MSCs and normal nerves (both p<0.001).
**** = p<0.001, Error bars = standard deviation of the mean.*
uMSC = undifferentiated Mesenchymal Stem Cells, dMSCs = differentiated Mesenchymal Stem Cells

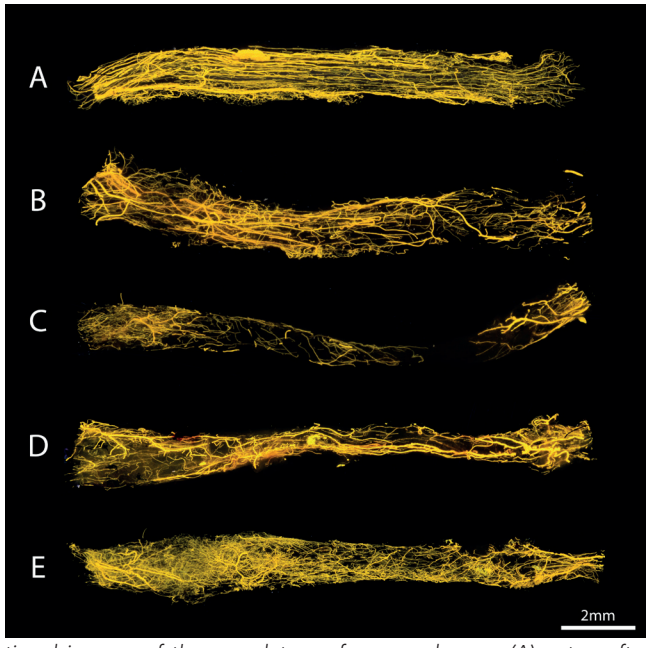

Figure 3. Conventional images of the vasculature of a normal nerve (A) autografts (B), allografts (C), allografts seeded with undifferentiated MSC (D) and allografts seeded with differentiated MSCs (E). The nerves were positioned from proximal (left) to distal (right). The ingrowth of vessels seem to occured from both nerve ends, but from proximal in particular. The structuring of the vessels was clearly less organized in our study groups compared to the control nerve.

Revascularization pattern

The vessels of normal, non-operated nerves aligned in the same longitudinal direction as the axons and the vasculature is equally distributed among the entire length of the nerve. The preserved vessels in autograft nerves seemed to be largely longitudinally aligned consistent with inosculation pattern of revascularization, but were less extensively present than in normal nerves. Unseeded allografts had less vascularization in general and demonstrated minimal if any vascularization in their mid-segment. In both MSC-seeded allograft groups, an extensive, non-aligned network of micro-vessels extended from the very proximal to the very distal graft end with a centripetal pattern of revascularization. In all groups, the ingrowth of vessels occurs from both nerve ends, but particularly from the proximal stump.

Vascular volume

The vascular volume measurements showed the same trend as the vascular surface area measurements; the allografts seeded with differentiated MSCs contained the highest vascular volume (4.6±3.6%), the outcomes of the autografts (3.78±0.7%) and the allografts seeded with undifferentiated MSC (3.4±0.2%) did not differ and the unseeded allografts scored the least (2.7±1.0%). ANOVA analysis between groups showed no statistically significant differences between the groups (F=0.916; p=0.455) (**figure 4 and 5**).

The vascular surface area and the vascular volume measurements were significantly correlated (r=0.416; p=0.008).

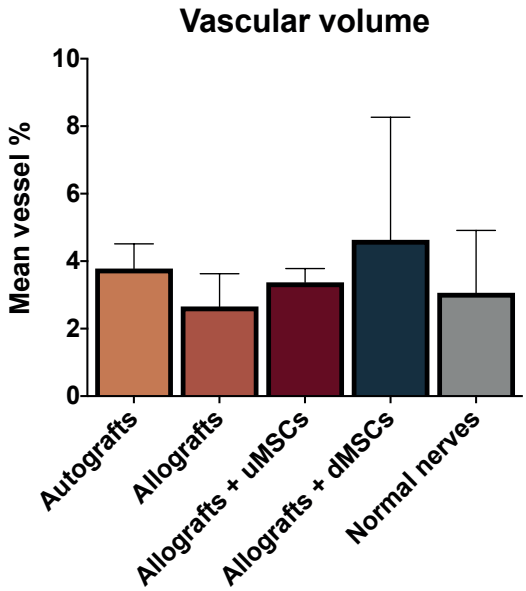

Figure 4. The vascular volume outcomes of autografts, allografts, allografts seeded with undifferentiated MSC and allografts seeded with differentiated MSCs. None of the differences between the groups was statistically significant.
Error bars = standard deviation of the mean
uMSC = undifferentiated Mesenchymal Stem Cells, dMSCs = differentiated Mesenchymal Stem Cells

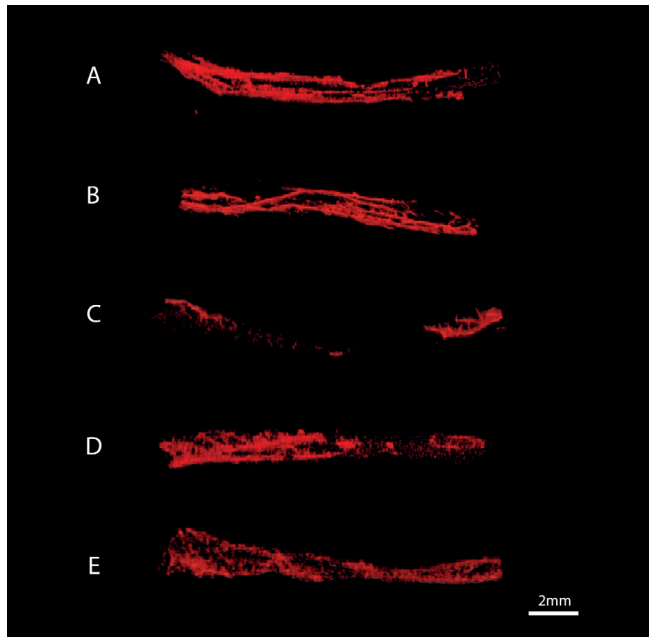

Figure 5. *Snapshots of the obtained micro-CT scans that served for the volume measurements of normal nerves (A) autografts (B), allografts (C), allografts seeded with undifferentiated MSCs (D) and allografts seeded with differentiated MSCs (E). The nerves are positioned from proximal (left) to distal (right). The smallest vessels are not detected by the micro-CT due to its effective pixel size.*

DISCUSSION

The purpose of this study was to determine whether the previously demonstrated different gene expression profiles of differentiated and undifferentiated MSCs would lead to different levels and patterns of vascularization when dynamically seeded onto processed/decellularized nerve allografts. Digital photography and micro-CT imaging allowed for the quantification and comparison of vascularity.

Neoangiogenesis has been previously quantified by counting of RECA-1 positive structures (immunohistochemical staining) and histomorphometric evaluation or the measurement of capillary density.[20, 43-45] These methods unfortunately fall short when aiming to precisely quantify and describe vascularity volumes and vascularization patterns. An evaluation strategy in which both 2D and 3D measures can be reliably obtained was used in the current study in order to compare the effect of undifferentiated versus differentiated MSCs.[42]

With respect to vascularization, there was an increase in the vascular surface area of processed allografts when seeded with undifferentiated and differentiated MSCs. However, only the effect of differentiated MSCs was statistically significant, suggesting that differentiated MSCs enhance (neo)angiogenesis to a greater extent than undifferentiated MSC. The enhanced expression of neurotrophic and angiogenic genes of MSCs when

differentiated into Schwann-like cells is the most likely mechanism of the superior degree of (neo)angiogenesis in processed nerve allografts seeded with differentiated MSCs.[19, 20, 22, 25-27, 32, 36, 46] The role of the growth factors in the differentiation medium that might become embedded in the extracellular matrix of the cells cannot be ruled out, but they are not specifically known to stimulate neoangiogenesis.[25] The vascularization in autograft nerves and normal non-operated nerves did not significantly differ from both stem-cell groups.

Revascularization in nerves is hypothesized to occur via two mechanisms: centripetal neovascularization (vessels sprouting into the graft from the surrounding tissues) and inosculation (vessels sprouting into the graft from both stump ends into the existing vascular tree).[47] In autografts, there is still an existing vascular tree surrounded by endothelial cells which is likely to increase the vascularization speed and improve the alignment of vessels which was demonstrated in this study.[1] In processed allografts, all cellular debris has been removed, leaving no directions for ingrowing vessels.[28] In contrast to the longitudinal alignment of vessels in normal non-operated and autograft nerves, the vascularization of the stem cell-seeded nerve allografts consisted of an extensive network of micro-vessels distributed among the entire nerve that were not in line with the expected direction of axon regeneration (**figure 3**). Combining the described differences in revascularization pattern, we hypothesize the predominant mechanism of revascularization in autografts is inosculation, leading to well-aligned and accelerated revascularization. Centripetal neovascularization was hypothetically the predominant mechanism of vascularization or at least had a greater share in the revascularization of allografts seeded with MSCs. Based on the timeline of angiogenic gene expression profiles in previous research[32] and the known limited survivability of MSCs in vivo, [29] both type of MSCs are expected to accelerated revascularization mainly in the first few days after seeding with a slowly diminishing effect up to 29 days.

The purpose of this study was to determine the effect of type of MSCs on enhancing vascularization of processed nerve allografts and to compare degree and pattern of vascularization to autograft and allograft nerves. It is thus underpowered to perform functional or histological analysis. Despite the small group size however, we were able to clearly demonstrate the effect of MSCs on vascularity. We successfully evaluated the vasculature of nerves in an accurate manner and were able to objectively quantify the amount of (neo)angiogenesis. A future study should focus on functional outcomes.

The effective pixel size of the used micro-CT may have caused a loss in the detection of the smallest vessels, particularly present in both stem cell groups. The CT-scans enabled us to fairly compare the volume of the bigger vessels in the operated nerve to that of the bigger vessels in the non-operated side, but it sub-optimally displayed the smaller vessels. This could partially mask the effect of stem cell seeding, as the MSCs seem to lead to the formation of small vessels in particular. For future research, it is advised to use a micro-CT scanner with a smaller effective pixel size. This is likely to increase the correlation between the vascular volume and the vascular surface area.

Although not part of the current study, the presented concept of seeding either differentiated or undifferentiated MSCs on the surface of decellularized nerve allografts is hypothesized to be clinically applicable. Off the shelve nerve allografts are already clinically available and potentially can be seeded with autologous MSCs, which are easily obtainable from the patient with peripheral nerve injury. If the hypothesized improved vascularity and functional outcome outweigh the extra delay in nerve repair that is necessary for cell-culture (1.5 week) has yet to be determined.

This study demonstrated that the vascularization of nerve grafts can be quantified and that both undifferentiated and differentiated MSCs enhance revascularization of processed nerve allografts.

CONCLUSION

The degree of vascularization of the processed/decellularized allograft nerves were improved by the addition of undifferentiated and differentiated MSCs, of which only the effect of differentiated MSCs was statistically significant. Revascularization of processed/decellularized allograft nerves with or without MSC was mainly via centripetal revascularization compared to revascularization in autograft nerves, which occurred via inosculation.

REFERENCES

1. Zhu Z, Huang Y, Zou X, et al. The vascularization pattern of acellular nerve allografts after nerve repair in Sprague-Dawley rats. Neurol Res 2017: 39: 1014-21.
2. Niu X, Liu X, Hu J, Jiang L. [Experimental research on revascularization of chemically extracted acellular allogenous nerve graft]. Zhongguo Xiu Fu Chong Jian Wai Ke Za Zhi 2009: 23: 235-8.
3. Donzelli R, Capone C, Sgulo FG, Mariniello G, Maiuri F. Vascularized nerve grafts: an experimental study. Neurol Res 2016: 38: 669-77.
4. Wynn TA, Vannella KM. Macrophages in Tissue Repair, Regeneration, and Fibrosis. Immunity 2016: 44: 450-62.
5. Ferretti A, Boschi E, Stefani A, et al. Angiogenesis and nerve regeneration in a model of human skin equivalent transplant. Life Sci 2003: 73: 1985-94.
6. Cutting CB, McCarthy JG. Comparison of residual osseous mass between vascularized and nonvascularized onlay bone transfers. Plastic & Reconstructive Surgery 1983: 72: 672-5.
7. Caillaud M, Richard L, Vallat JM, Desmouliere A, Billet F. Peripheral nerve regeneration and intraneural revascularization. Neural Regen Res 2019: 14: 24-33.
8. Parrinello S, Napoli I, Ribeiro S, et al. EphB signaling directs peripheral nerve regeneration through Sox2-dependent Schwann cell sorting. Cell 2010: 143: 145-55.
9. Zhu Y, Liu S, Zhou S, et al. Vascularized versus nonvascularized facial nerve grafts using a new rabbit model. Plast Reconstr Surg 2015: 135: 331e-9e.
10. Iijima Y, Ajiki T, Murayama A, Takeshita K. Effect of Artificial Nerve Conduit Vascularization on Peripheral Nerve in a Necrotic Bed. Plast Reconstr Surg Glob Open 2016: 4: e665.
11. D'Arpa S. Vascularized nerve "grafts": just a graft or a worthwhile procedure? Plast Aesthet Res 2016: 2: 183-92.
12. Sunderland S. Nerves and Nerve Injuries. Churchill Livingstone, 1978.
13. Brooks D. The place of nerve-grafting in orthopaedic surgery. J Bone Joint Surg Am 1955: 37-A: 299-305; passim.
14. Seddon HJ. Nerve Grafting. J Bone Joint Surg Br 1963: 45: 447-61.
15. Giusti G, Lee JY, Kremer T, et al. The influence of vascularization of transplanted processed allograft nerve on return of motor function in rats. Microsurgery 2014.
16. Wongtrakul S, Bishop AT, Friedrich PF. Vascular endothelial growth factor promotion of neoangiogenesis in conventional nerve grafts. J Hand Surg Am 2002: 27: 277-85.
17. Zor F, Deveci M, Kilic A, et al. Effect of VEGF gene therapy and hyaluronic acid film sheath on peripheral nerve regeneration. Microsurgery 2014: 34: 209-16.
18. Nishida Y, Yamada Y, Kanemaru H, et al. Vascularization via activation of VEGF-VEGFR signaling is essential for peripheral nerve regeneration. Biomed Res 2018: 39: 287-94.
19. Hoben G, Yan Y, Iyer N, et al. Comparison of acellular nerve allograft modification with Schwann cells or VEGF. Hand (N Y) 2015: 10: 396-402.
20. Kingham PJ, Kolar MK, Novikova LN, Novikov LN, Wiberg M. Stimulating the neurotrophic and angiogenic properties of human adipose-derived stem cells enhances nerve repair. Stem Cells Dev 2014: 23: 741-54.
21. Orbay H, Uysal AC, Hyakusoku H, Mizuno H. Differentiated and undifferentiated adipose-derived stem cells improve function in rats with peripheral nerve gaps. J Plast Reconstr Aesthet Surg 2011.
22. Tomita K, Madura T, Sakai Y, et al. Glial differentiation of human adipose-derived stem cells: implications for cell-based transplantation therapy. Neuroscience 2013: 236: 55-65.
23. Caplan AI. Adult Mesenchymal Stem Cells: When, Where, and How. Stem Cells Int 2015: 2015: 628767.
24. Liu Y, Zhang Z, Qin Y, et al. A new method for Schwann-like cell differentiation of adipose derived stem cells. Neurosci Lett 2013: 551: 79-83.
25. Mathot F, Shin AY, Van Wijnen AJ. Targeted stimulation of MSCs in peripheral nerve repair.

Gene 2019.
26. Zhao Z, Wang Y, Peng J, et al. Repair of nerve defect with acellular nerve graft supplemented by bone marrow stromal cells in mice. Microsurgery 2011: 31: 388-94.
27. Zhang Y, Luo H, Zhang Z, et al. A nerve graft constructed with xenogeneic acellular nerve matrix and autologous adipose-derived mesenchymal stem cells. Biomaterials 2010: 31: 5312-24.
28. Hundepool CA, Nijhuis TH, Kotsougiani D, et al. Optimizing decellularization techniques to create a new nerve allograft: an in vitro study using rodent nerve segments. Neurosurg Focus 2017: 42.
29. Rbia N, Bulstra LF, Thaler R, et al. In Vivo Survival of Mesenchymal Stromal Cell-Enhanced Decellularized Nerve Grafts for Segmental Peripheral Nerve Reconstruction. J Hand Surg Am 2019: 44: 514.e1-14.e11.
30. Mathot F, Rbia N, Bishop AT, et al. Adhesion, distribution, and migration of differentiated and undifferentiated mesenchymal stem cells (MSCs) seeded on nerve allografts. J Plast Reconstr Aesthet Surg 2019.
31. Rbia N, Bulstra LF, Bishop AT, van Wijnen AJ, Shin AY. A simple dynamic strategy to deliver stem cells to decellularized nerve allografts. Plast Reconstr Surg 2018.
32. Mathot F, Rbia N, Thaler R, et al. Gene expression profiles of differentiated and undifferentiated adipose derived mesenchymal stem cells dynamically seeded onto a processed nerve allograft. Gene 2020: 724: 144151.
33. Tang P, Whiteman DR, Voigt C, Miller MC, Kim H. No Difference in Outcomes Detected Between Decellular Nerve Allograft and Cable Autograft in Rat Sciatic Nerve Defects. J Bone Joint Surg Am 2019: 101: e42.
34. Hudson TW, Zawko S, Deister C, et al. Optimized acellular nerve graft is immunologically tolerated and supports regeneration. Tissue Eng 2004: 10: 1641-51.
35. Kumta S, Yip K, Roy N, Lee SK, Leung PC. Revascularisation of bone allografts following vascular bundle implantation: an experimental study in rats. Arch Orthop Trauma Surg 1996: 115: 206-10.
36. Kingham PJ, Kalbermatten DF, Mahay D, et al. Adipose-derived stem cells differentiate into a Schwann cell phenotype and promote neurite outgrowth in vitro. Exp Neurol 2007: 207: 267-74.
37. Crespo-Diaz R, Behfar A, Butler GW, et al. Platelet lysate consisting of a natural repair proteome supports human mesenchymal stem cell proliferation and chromosomal stability. Cell Transplant 2011: 20: 797-811.
38. Mader EK, Butler G, Dowdy SC, et al. Optimizing patient derived mesenchymal stem cells as virus carriers for a phase I clinical trial in ovarian cancer. J Transl Med 2013: 11: 20.
39. Mahmoudifar N, Doran PM. Osteogenic differentiation and osteochondral tissue engineering using human adipose-derived stem cells. Biotechnol Prog 2013: 29: 176-85.
40. Dominici M, Le Blanc K, Mueller I, et al. Minimal criteria for defining multipotent mesenchymal stromal cells. The International Society for Cellular Therapy position statement. Cytotherapy 2006: 8: 315-7.
41. Hundepool CA, Bulstra LF, Kotsougiani D, et al. Comparable functional motor outcomes after repair of peripheral nerve injury with an elastase-processed allograft in a rat sciatic nerve model. Microsurgery 2018: 38: 772-79.
42. Saffari TM, Mathot F, Bishop AT, Shin AY. New methods for objective angiogenesis evaluation of rat nerves using microcomputed tomography scanning and conventional photography. Microsurgery 2019.
43. Perrien DS, Saleh MA, Takahashi K, et al. Novel methods for microCT-based analyses of vasculature in the renal cortex reveal a loss of perfusable arterioles and glomeruli in eNOS-/- mice. BMC Nephrol 2016: 17: 24.
44. Kline TL, Knudsen BE, Anderson JL, et al. Anatomy of hepatic arteriolo-portal venular shunts evaluated by 3D micro-CT imaging. J Anat 2014: 224: 724-31.
45. Giusti G, Lee JY, Kremer T, et al. The influence of vascularization of transplanted processed allograft nerve on return of motor function in rats. Microsurgery 2016: 36: 134-43.

46. Ladak A, Olson J, Tredget EE, Gordon T. Differentiation of mesenchymal stem cells to support peripheral nerve regeneration in a rat model. Exp Neurol 2011: 228: 242-52.
47. Best TJ, Mackinnon SE, Midha R, Hunter DA, Evans PJ. Revascularization of peripheral nerve autografts and allografts. Plast Reconstr Surg 1999: 104: 152-60.

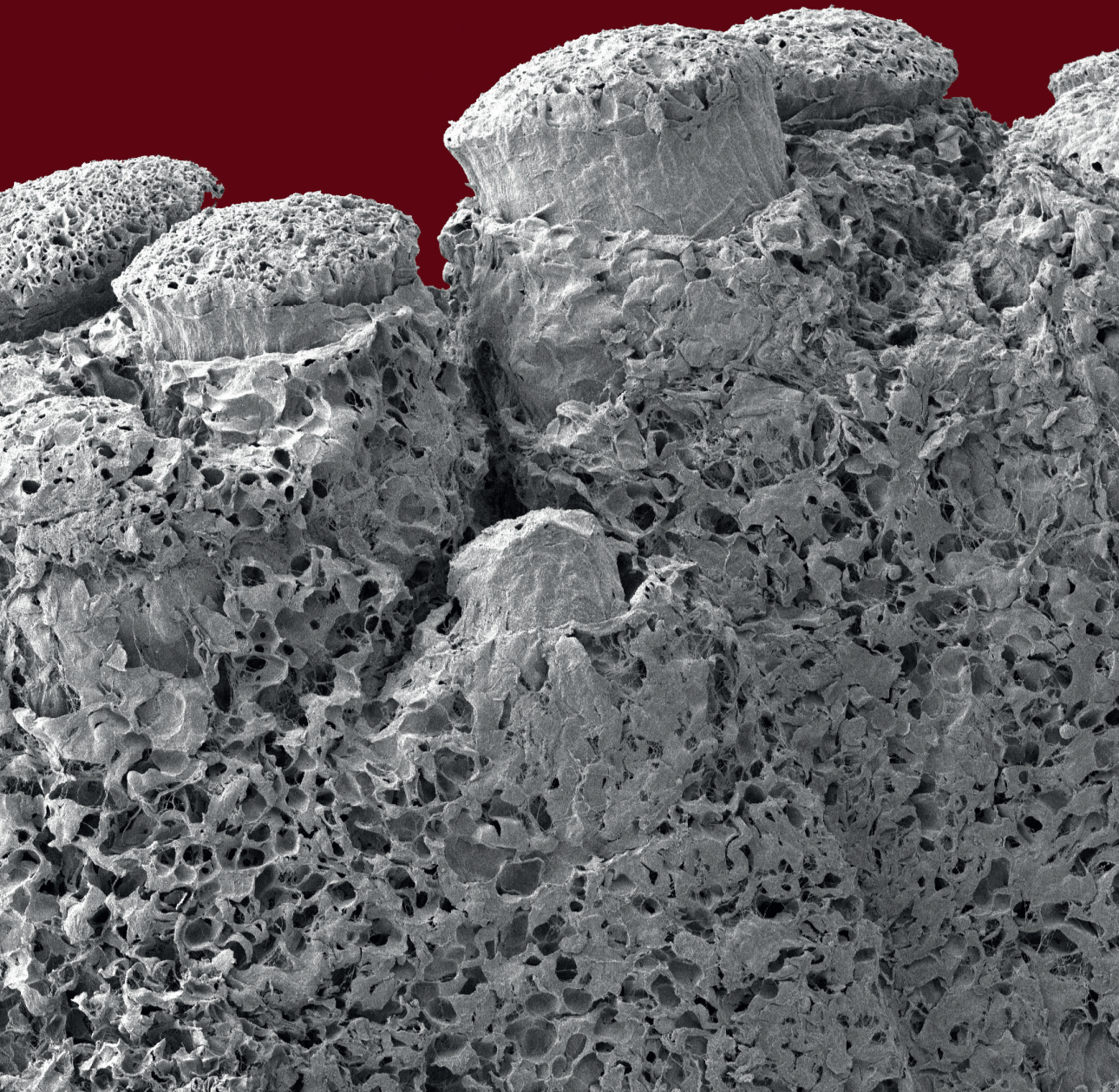

Chapter 7

Functional outcomes of nerve allografts seeded with undifferentiated and differentiated mesenchymal stem cells in a rat sciatic nerve defect model

Femke Mathot, Tiam M. Saffari, Nadia Rbia, Tim H.J. Nijhuis, Allen T. Bishop, Steven E.R. Hovius, Alexander Y. Shin

Plastic and Reconstructive Surgery. 2021 June; Online ahead of print

ABSTRACT

Background

Mesenchymal stem cells (MSCs) have the potential to produce neurotrophic growth factors and establish a supportive micro-environment for neural regeneration. The purpose of this study was to determine the effect of undifferentiated and differentiated MSCs dynamically seeded onto decellularized nerve allografts on functional outcomes when used in peripheral nerve repair.

Methods

In 80 Lewis rats a ten millimeter sciatic nerve defect was reconstructed with (i) autograft, (ii) decellularized allograft (iii) decellularized allograft seeded with undifferentiated MSCs, or (iv) decellularized allograft seeded with MSCs differentiated into Schwann cell-like cells. Nerve regeneration was evaluated over time by cross sectional tibial muscle ultrasound measurements, and at 12 and 16 weeks by isometric tetanic force measurements (ITF), compound muscle action potentials (CMAP), muscle mass, histology and immunofluorescence analyses.

Results

At 12 weeks, undifferentiated MSCs significantly improved ITF and CMAP outcomes compared to decellularized allograft alone, while differentiated MSCs significantly improved CMAP outcomes. The autografts outperformed both stem-cell groups histologically at 12 weeks. At 16 weeks, functional outcomes normalized between groups. At both time points, the effect of undifferentiated versus differentiated MSCs was not significantly different.

Conclusions

Undifferentiated and differentiated MSCs significantly improved functional outcomes of decellularized allografts at 12 weeks and were similar to autograft results in the majority of measurements. At 16 weeks, outcomes normalized as expected. Although differences between both cell-types were not statistically significant, undifferentiated MSCs improved functional outcomes of decellularized nerve allografts to a greater extent and have practical benefits for clinical translation by limiting preparation time and costs.

INTRODUCTION

Peripheral nerve defects not amendable to direct end-to-end neurorrhaphy require reconstruction with interposition nerve graft which could be accomplished with autograft, allograft or synthetic bioabsorbable conduits, each with their benefits and controversies.[1-3] Decellularized nerve allografts have been proposed as an ideal alternative to overcome donor site morbidity and limited supply of autografts.[1, 4-7] Improvement of outcomes of decellularized allografts by addition of host derived mesenchymal stem cells (MSCs) has been proposed to overcome the limitations of decellularized allograft nerves by producing trophic factors resulting in a favorable micro-environment for tissue regeneration.[8-14] MSCs are hypothesized to not only stimulate tissue regeneration, but potentially form extracellular matrix components, enhance angiogenesis, inhibit scar formation and control immune responses.[15] Adipose derived MSCs are easily accessible and proliferate faster than bone marrow derived MSCs, while having a similar effect on nerve regeneration and are thus ideal for translation to clinical use.[16-18]

In comparison to undifferentiated MSCs, MSCs differentiated into Schwann cell-like cells express neurotrophic and angiogenic genes to a greater extent than undifferentiated MSCs in vitro.[16, 19-21] Several in vivo studies using different MSC-delivery strategies did not demonstrate clear differences between the outcomes of undifferentiated and differentiated MSCs.[22, 23] Others reported that differentiated MSCs led to longer regenerating axon distance in vivo [19, 21, 24, 25], without resulting in improved functional outcomes.[21] The differentiation process of MSCs requires additional preparation time and expensive differentiation factors, which should be considered in translating bench work to clinical application.[16]

Recent studies have reported a non-traumatic strategy to adhere undifferentiated and differentiated MSCs to the surface of decellularized allografts, leading to a 29-day in vivo survival of seeded MSCs.[26-28] The adherence of MSCs to the decellularized allograft has demonstrated an interaction between MSCs and the extracellularly matrix leading to enhanced expression of neurotrophic, angiogenic, extracellular matrix and regulatory cell cycle genes in the first three (differentiated MSCs) to seven (undifferentiated MSCs) days after seeding in vitro, implying a direct effect of differentiated MSCs after implementation while undifferentiated MSCs require time to interact with the environment.[14]

A comparative study focusing on functional outcomes can elucidate the effect of different cells and their different effective phases on motor nerve regeneration. The purpose of this study was to determine the effect of dynamically seeding undifferentiated and differentiated MSCs onto decellularized nerve allografts[7] with respect to functional and histologic outcomes in a rat sciatic nerve defect model.

METHODS

Experimental design

After IACUC institutional review committee and our Institutional Review Board approval

(IACUC protocol A2464-00), a 10 mm segmental defect of the sciatic nerve of 80 male Lewis rats weighing 250-300 grams (Envigo, Madison, WI, USA) was repaired with a 10 mm (i) reversed autograft, (ii) decellularized allograft (iii) decellularized allograft seeded with undifferentiated MSCs, or (iv) decellularized allograft seeded with differentiated MSCs. The decellularized allografts originated from Sprague-Dawley rats and were specifically chosen for their histocompatibility mismatch to Lewis rats.[29, 30] This simulates the clinical setting where an allogenic processed nerve graft is seeded with autologous MSCs. After 12 and 16 weeks, functional, histological and immunofluorescence outcomes were evaluated.

Nerve allograft collection, processing and seeding

Sixty sciatic nerve segments from 30 Sprague-Dawley rats (Envigo, Madison, WI, USA) weighing 250-350 grams served as nerve allografts. After anesthesia with isoflurane, rats were euthanized, shaved and sterilely prepped. The sciatic nerve was exposed, removed under an operating microscope (Zeiss OpMi6, Carl Zeiss Surgical GmbH, Oberkochen, Germany) and processed according to a previously published protocol.[7] After sterilization with γ-irradiation, nerves were stored at 4°C in Phosphate Buffered Saline (PBS) until surgery.

Stem cell preparation and differentiation

MSCs were derived from the inguinal fat pad of inbred Lewis rats according to protocol.16 Cells were previously characterized by plastic adherence, pluripotency towards mesodermal lineages, the expression of mesenchymal stem cell markers CD29 (88.2%) and CD90 (88.3%) and the absence of hematopoetic cell markers CD34 (91.1% absent) and CD45 (86.0% absent).[26-28] Both cell-types were cultured in an incubator at 37°C (5% CO2) and the growth medium was changed every 72 hours. Passage six MSCs were used in this experiment for both differentiated and undifferentiated MSCs.

MSCs-culture

The stromal cell pellet was re-suspended in normal growth medium consisting of α-MEM (Advanced MEM (1x); Life Technologies Corporation, NY, USA), 5% platelet lysate (PLTMax®; Mill Creek Life Sciences, MN, USA), 1% Penicillin/Streptomycin (Penicillin-Streptomycin (10.000 U/mL; Life Technologies Corporation), 1% GlutaMAX (GlutaMAX Supplement 100X; Life Technologies Corporation) and 0.2% Heparin (Heparin Sodium Injection, USP, 1.000 USP units per mL; Fresenius Kabi, IL, USA).

MSC differentiation

MSCs were differentiated into Schwann cell-like cells using a differentiation cocktail containing 0.14% Forskolin (Sigma-Aldrich corp., MO, USA), 0.01% basis fibroblast growth factor (bFGF; PeproTech, NJ, USA), 0.005% platelet-derived growth factor (PDGF-AA; PeproTech) and 0.02% Neuregulin-1 ß1 (NRG1-b1; R&D systems Inc, MN, USA).[16] Differentiation was assessed by immunocytochemistry for the expression of S100 (S100; ThermoFisher Scientific, MA, USA), Glial fibrillary acidic protein (GFAP, mouse anti-GFAP; ThermoFisher Scientific) and neurotrophin receptor p75 (p75 NTR, rabbit anti-p75 NTR; ThermoFisher Scientific). Goat anti-rabbit fluorescein isothiocyanate (FITC) and goat anti-mouse cyanine 3 (CY3, both

ThermoFisher Scientific) were used as secondary antibodies. Cell nuclei were labeled with 4',6-diamidino-2-phenylindole (DAPI).

Seeding Protocol for Allograft Nerves
To attach the undifferentiated and differentiated MSCs to the decellularized nerve allografts they were dynamically seeded according to a previously described protocol.[28] Either 1x10^6 undifferentiated MSCs or 1x10^6 differentiated MSCs in 10mL growth medium were placed in a conical tube containing a decellularized nerve allograft. The conical tube was then placed on a bioreactor that was positioned in an incubator at 37°C (5% CO2). After the bioreactor had rotated for 12 consecutive hour, the nerve grafts with the attached MSCs were taken out of the tubes and directly implemented in the Lewis rats. The dynamic seeding strategy previously resulted in 80% and 95% adherence of cells on the surface of the processed allografts for undifferentiated and differentiated MSCs respectively.[27, 28]

Surgical procedure of the recipient animals
Under isoflurane anesthesia the right sciatic nerve of the Lewis rat was exposed. A 10 mm segment of the sciatic nerve was excised and reconstructed with a 10 mm graft under an operating microscope (Zeiss OpMi6, Carl Zeiss Surgical GmbH, Oberkochen, Germany). The epineurium was sutured with six 10-0 sutures (10-0 Ethilon, Ethicon Inc., USA), the muscle was approximated (6-0 Vicryl Rapide, Ethicon Inc.) and the skin was closed with a continuous subcutaneous suture (5-0 Vicryl Rapide, Ethicon Inc.). All rats received 5mL of 0.9% saline solution, 0.6mg/kg Buprenorphine and one dose of 30mg/kg diluted trimethoprim/sulfadiazine subcutaneously (Tribissen, Five Star Compounding Pharmacy, Clive, IA). Postoperatively, the rats were individually housed and provided with food and water ad libitum with a 12-hour light-dark cycle.

Ultrasound measurements
The cross-sectional tibial muscle area of six randomly selected rats per group was evaluated with ultrasound measurements of both sides at baseline and at two, four, eight, twelve and sixteen weeks after surgery as previously described using a GE Vivid 7 Ultrasound system (General Electric, Fairfield, CT, USA).[31, 32] Cross-sectional area was calculated with Adobe Photoshop CC 2018 (Adobe Systems Incorporated, San Jose, CA, USA).

Nonsurvival procedure
At 12 and 16 weeks, ten rats of each group underwent a non-survival procedure. Anesthesia was induced by isoflurane, followed by intraperitoneal injection of Ketamine (80mg/kg) and Xylazine (10mg/kg) and maintained by additional doses of Ketamine (40mg/kg).

Compound Muscle Action Potentials (CMAP) - A miniature bipolar electrode was clamped around the sciatic nerve proximal to the nerve graft. One ground electrode was placed in surrounding musculature and two recording electrodes were superficially placed in the anterior tibial muscle. The CMAP was measured using a VikingQuest portable electromyelogram (Nicolet Biomedical, Madison, WI). A non-recurrent single stimulation with a duration of

0.02ms at an intensity level of 2.7mA was applied. Maximal amplitude measurements were obtained bilaterally.[33, 34]

Isometric Tetanic Force (ITF) - The ITF was measured bilaterally per the protocol of Shin and colleagues.[35] The peroneal nerve and tibial muscle were exposed and the hind limb was secured to a testing platform with K-wires through the femur and ankle. The tibial tendon was secured to a clamp in anatomical position and attached to a force transducer (MDB-50; Transducer Techniques, Temecula, CA, USA) whose signals were processed using LabView (National instruments, Austin, Texas). A miniature electrode (Harvard Apparatus, Holliston, MA, USA), stimulated by a bipolar stimulator (Medtronic, Minneapolis, MN, USA) was clamped around the peroneal nerve branch of the sciatic nerve. The muscle tension and the stimulator frequency were optimized after which the maximal ITF was obtained. The tibial muscle was kept moist with warm saline.

Wet tibial muscle mass - Rats were euthanized with an overdose of pentobarbital (Fatal Plus, 390 mg/mL, Vortech, Dearborn, MI, USA) intraperitoneally. Tibial muscles were harvested bilaterally and wet muscle mass was determined after removing the tendon.

Histology - A three millimeter segment of both peroneal nerves of all rats were collected and placed into Trumps solution. Specimens were processed with 0.1M Phosphate Buffer, 1% Osmium tetroxide in buffer, graded series of alcohol and acetone. The samples were infiltrated in a 50%, 75% and finally 100% epoxy resin and polymerized at 65°C for 12-18 hours. Samples were cut in sections at 0.6 microns, placed on slides and stained on a warming plate with Toluidine blue for 2-2.5 minutes. The total tissue cable area (nerve area), axon area, axon count and myelin area were obtained using a Nikon Eclipse 50i microscope and Image Pro Plus Software. The N-ratio was calculated by dividing the myelinated fiber area (axon area and myelin area) by the tissue cable area.[36]

Immunofluorescence - Both sciatic nerves of five randomly selected rats per group were dissected and fixed in 10% formalin for 48 hours. Nerves samples were vertically embedded in paraffin and sections from the exact middle were stained for Schwann cell marker S100 and protein gene product 9.5 (PGP9.5), a pan neuronal marker. Immunohistochemical staining was performed at the Pathology Research Core (Mayo Clinic, Rochester, MN, USA) using the Leica Bond RX stainer (Leica, Buffalo Grove, IL, USA). The S100 (rabbit polyclonal; Dako, Agilent Technologies Inc., Carpinteria, CA, USA) and PGP9.5 primary antibody (rabbit polyclonal; Dako, Agilent Technologies Inc.) were diluted to 1:5000 in Background Reducing Diluent (Dako, Agilent Technologies Inc.) and incubated for 60 minutes with the samples, prior to staining with the appropriate secondary antibody (Alexa Goat-Anti-Rabbit 488, 1:300, for S100 and Alexa Goat-Anti-Rabbit 568, 1:200 for PGP9.5) and counterstained with Hoechst 33342 (all ThermoFisher Scientific, MA, USA). Images of the stained slides were obtained with a fluorescence laser confocal microscope (Zeiss LSM 780, Carl Zeiss Surgical GmbH, Oberkochen, Germany). The mean fluorescent density of both stains was measured using ImageJ software.

Statistical analysis

All obtained images were blinded and all outcomes were expressed as a percentage of the contralateral side to correct for biological variability between rats. Non-physiologic outcomes were excluded from analysis after review by a statistician and an independent researcher. Two-way analysis of variance (ANOVA) was used for the cross-sectional tibial area measurements. One-way ANOVA was used to compare all other outcome measures between groups. Post-hoc Bonferroni was used to correct for multiple comparisons. Outcomes were expressed as the mean and the standard error of the mean (SEM). Outcomes of cross-sectional tibial muscle area were expressed as mean difference and the standard error of the mean difference. The level of significance was set at α>0.05.

RESULTS

MSC differentiation

Differentiated MSCs showed immunofluorescence for the markers S100, GFAP and p75 NTR, corresponding to Schwann cells that served as positive controls. Undifferentiated MSCs did not show expression of these markers (**figure 1**).

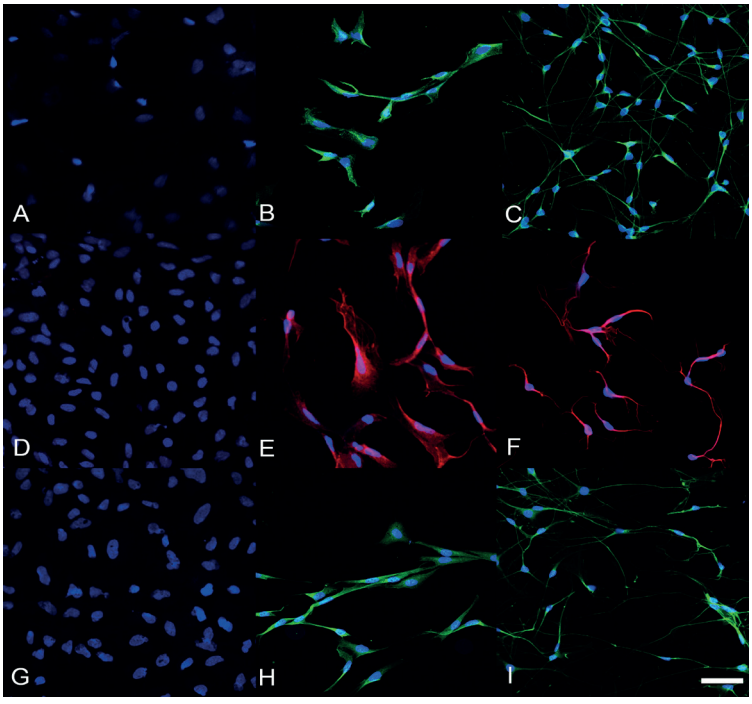

Figure 1. *Differentiation of MSCs into Schwann-like cells. Comparison of immunocytochemistry between undifferentiated MSCs (A-D-G), differentiated MSCs (B-E-H) and Schwann cells (C-F-I). Cells are tested for the presence of Schwann cell marker S100 (green, A-B-C), glial cell marker GFAP (red, D-E-F) and neurotrophin Receptor p75 (green, G-H-I). Cell nuclei are DAPI-stained (blue). 40X magnificantion, white scale bar = 40μm.*

Functional outcome measurements

Cross-sectional tibial muscle area (figure 2)

No significant differences between the groups were found. Within group comparisons only showed significant differences between the consecutive time points zero and two weeks after surgery for autografts, allografts and allografts seeded with differentiated MSCs. The lowest tibial muscle area in all groups was reached at two weeks (40-60% of the unoperated side) and improved up to 16 weeks, with a cross-sectional tibial muscle area ratio of approximately 75%.

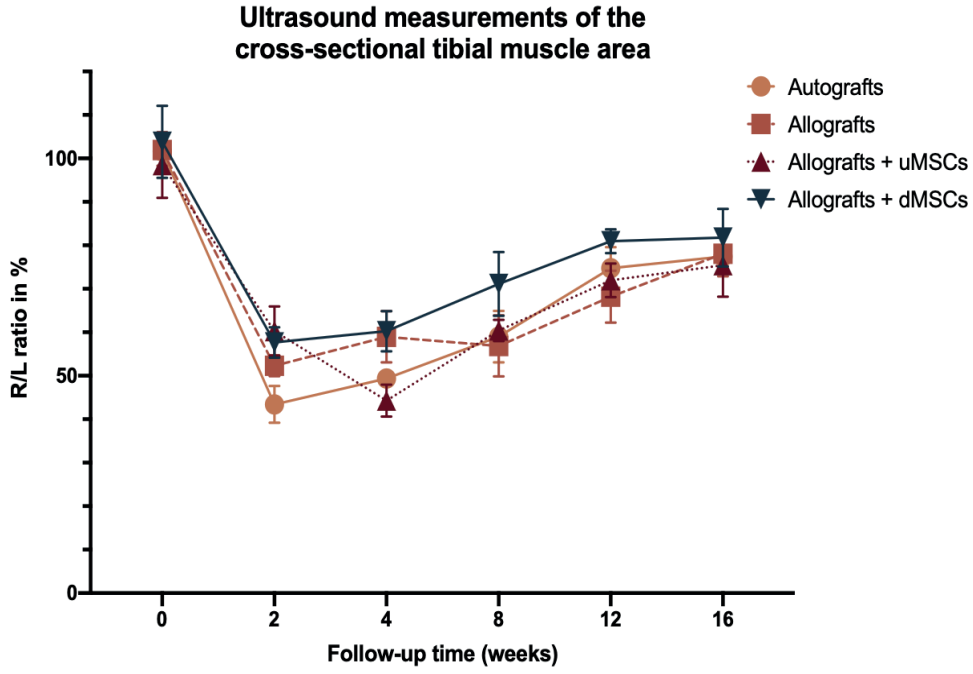

Figure 2. Cross-sectional tibial muscle area ratios (R/L) over time. No significant differences were found between groups. Autografts (+15.77 ±6.56%) and unseeded allografts (+11.33 ±9.22%) had the strongest increase in muscle area between 8 and 12 weeks, while allografts seeded with undifferentiated MSCs (+16.13 ±3.83%) and differentiated MSCs (+10.87 ±9.29%) experienced their strongest increase between 4 and 8 weeks after surgery. uMSCs = undifferentiated Mesenchymal Stem Cells; dMSCs = differentiated Mesenchymal Stem Cells. Error bars = Standard error of the mean

Compound Muscle Action Potential (CMAP) (figure 3)

At 12 weeks, CMAP ratio of unseeded allografts (13.48 ±5.00%) was significantly inferior to autografts (53.78 ±5.82%) ($p<0.001$), allografts seeded with undifferentiated MSCs (44.32 ±7.20%) ($p=0.004$) and differentiated MSCs (48.89 ±5.37%) ($p<0.001$). At 16 weeks, CMAP ratio was normalized between all groups, with 57.51 ±7.54% for autografts, 52.26 ±5.80% for allografts, 66.04 ±7.28% for allografts with undifferentiated MSCs and 61.49±8.16% for allografts with differentiated MSCs.

Isometric Tetanic Force (ITF) (figure 4)

The ITF ratio of allografts seeded with undifferentiated MSCs (49.74 ±6.80%) was significantly higher compared to unseeded allografts (26.32 ±4.36%) (p=0.017) at 12 weeks. The ratio in autografts (44.16 ±3.32%) and allografts seeded with differentiated MSCs (43.10 ±4.59%) did not demonstrate significant differences with any of the other groups. At 16 weeks, the ITF ratio of autografts (51.11 ±4.98%), allografts (56.22 ±4.44%), allografts with undifferentiated MSCs (56.12 ±6.51%) and allografts with differentiated MSCs (53.86 ±4.47%) did not significantly differ.

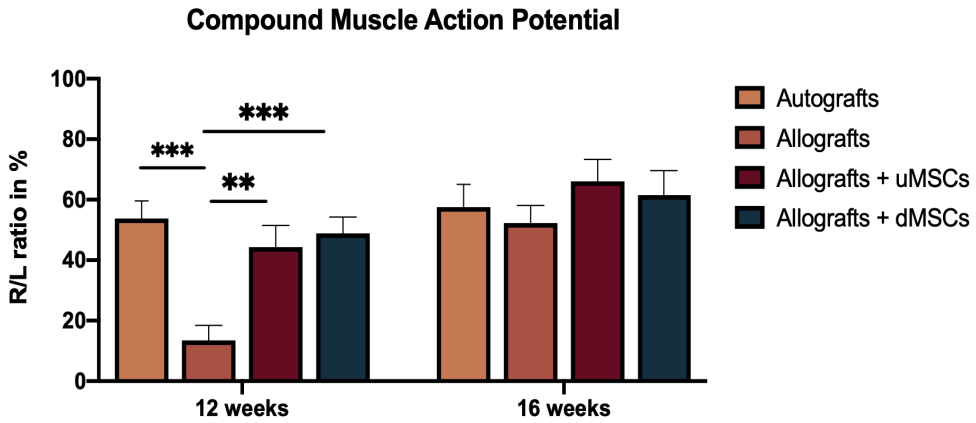

Figure 3. Compound muscle action potential ratios (CMAP, R/L) at 12 and 16 weeks. CMAP recovery of unseeded allografts was significantly inferior compared to all other groups at 12 weeks
uMSCs = undifferentiated Mesenchymal Stem Cells; dMSCs = differentiated Mesenchymal Stem Cells
** = p<0.05, ** = p<0.01, *** = p<0.001. Error bars = Standard error of the mean*

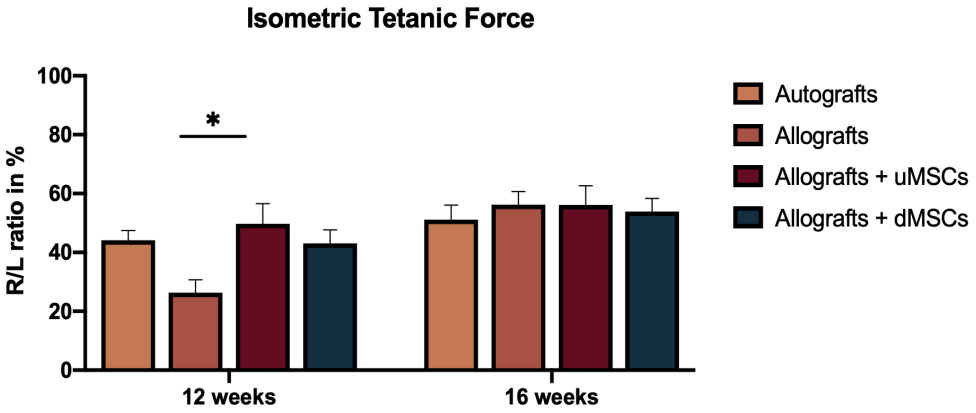

Figure 4. Isometric Tetanic Force ratios (R/L) at 12 and 16 weeks. ITF recovery of unseeded allografts were significantly inferior compared to allografts seeded with undifferentiated MSCs at 12 weeks
uMSCs = undifferentiated Mesenchymal Stem Cells; dMSCs = differentiated Mesenchymal Stem Cells
** = p<0.05, ** = p<0.01, *** = p<0.001. Error bars = Standard error of the mean*

Muscle mass (figure 5)

At 12 weeks, unseeded allografts measured a significantly lower tibial muscle mass ratio (49.54 ±2.30%) compared to autografts (59.84 ±1.64%) (p=0.021). Allografts with undifferentiated and differentiated MSCs measured a muscle mass ratio of 57.68 ±2.87% and 55.21 ±2.36% respectively. At 16 weeks, the muscle mass ratio of allografts seeded with undifferentiated MSCs was 59.96 ±3.79%, which significantly differed from autografts (74.13 ±1.90%) (p=0.002). Unseeded allografts and allografts seeded with differentiated MSCs had a muscle mass ratio of 69.09 ±1.54% and 70.09 ±2.60% respectively.

Histology

All obtained histology and immunofluorescence values are displayed in **table 1**. **Figure 6** provides representative nerve sections of the different groups. At 12 weeks, autografts had a significant larger axon area ratio compared to unseeded allografts (p<0.001), allografts seeded with undifferentiated MSCs (p<0.001) and allografts seeded with differentiated MSCs (p=0.004). At 16 weeks, no significant differences in axon area ratio between groups were found. The axon count, myelin area and nerve area measures did not demonstrate any significant differences between groups at any of the time points. Autografts had a significant higher N-ratio compared to unseeded allografts (p=0.023) and allografts seeded with undifferentiated MSCs (p=0.040) at 12 weeks. At 16 weeks, autografts had a significantly better N-ratio compared to unseeded allografts (p=0.003), allografts with undifferentiated MSCs (p=0.025) and allografts with differentiated MSCs (p=0.002) (**figure 7**).

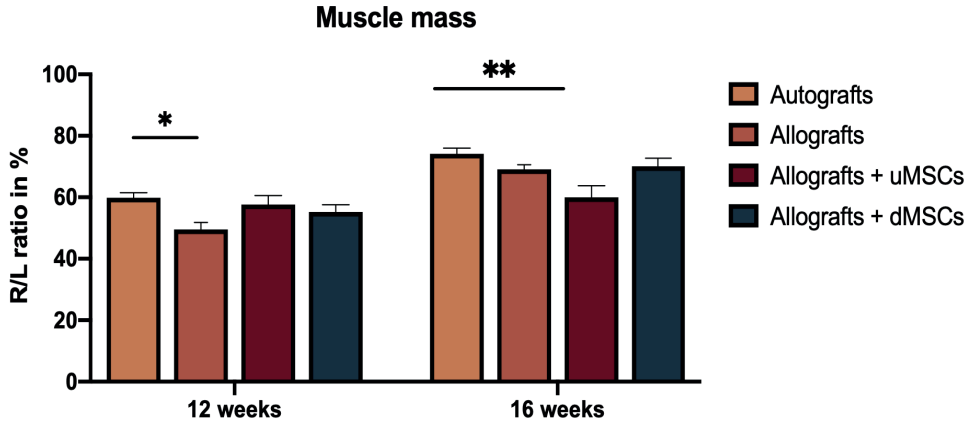

Figure 5. *Wet tibial muscle mass ratios (R/L) at 12 and 16 weeks. Autografts showed a significantly higher muscle mass recovery compared to unseeded allografts at 12 weeks, and allografts seeded with undifferentiated MSCs at 16 weeks. uMSCs = undifferentiated Mesenchymal Stem Cells; dMSCs = differentiated Mesenchymal Stem Cells. * = p<0.05, ** = p<0.01, *** = p<0.001. Error bars = Standard error of the mean*

	Autografts	Allografts	Allografts + undifferentiated MSCs	Allografts + differentiated MSCs
Axon area				
• 12 weeks	27.58 ±2.93%	10.14 ±1.89%	11.76 ±1.62%	15.48 ±2.27%
• 16 weeks	35.95 ±4.63%	21.90 ±3.41%	20.07 ±3.18%	20.84 ±5.65%
Axon count				
• 12 weeks	56.87 ±7.47%	32.42 ±5.38%	39.61 ±5.11%	47.39 ±5.55%
• 16 weeks	50.93 ±7.20%	38.94 ±2.67%	42.04 ±6.91%	43.37 ±13.49%
Myelin area				
• 12 weeks	57.12 ±4.77%	38.43 ±7.18%	40.11 ±3.58%	46.86 ±4.06%
• 16 weeks	69.63 ±8.12%	57.53 ±6.25%	50.69 ±5.72%	41.93 ±7.33%
Nerve area				
• 12 weeks	77.97 ±7.58%	63.77 ±5.74%	61.58 ±3.53%	71.09 ±6.23%
• 16 weeks	77.37 ±8.55%	79.18 ±8.09%	66.27 ±7.40%	60.74 ±8.77%
N-ratio				
• 12 weeks	59.06 ±2.48%	42.62 ±5.89%	46.58 ±3.59%	46.58 ±3.59%
• 16 weeks	72.22 ±2.93%	53.57 ±3.04%	57.53 ±2.74%	51.71 ±5.34%
S100 density				
• 12 weeks	96.48 ±1.16%	97.84 ±1.65%	92.85 ±3.17%	94.88 ±3.11%
• 16 weeks	102.37 ±6.94%	93.54 ±2.38%	94.61 ±3.86%	95.92 ±5.90%
PGP9.5 density				
• 12 weeks	106.95 ±16.30%	105.26 ±4.88%	101.13 ±9.55%	98.62 ±7.97%
• 16 weeks	92.81 ±5.15%	101.89 ±12.22%	98.13 ±13.88%	76.68 ±6.25%

Table 1. Histology and immunofluorescence outcomes obtained at 12 and 16 weeks for all groups. Outcomes are displayed as the mean and the standard error of the mean (SEM).
uMSCs = undifferentiated Mesenchymal Stem Cells; dMSCs = differentiated Mesenchymal Stem Cells
** = p<0.05, ** = p<0.01, *** = p<0.001. Error bars = Standard error of the mean*

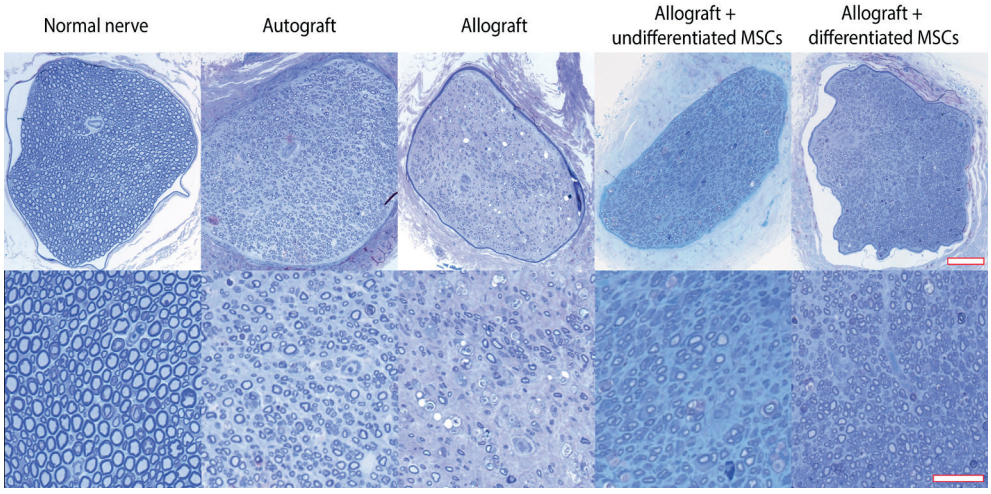

Figure 6. Examples of obtained images of peroneal nerve sections stained with toluidine blue at 12 weeks of follow-up. Scale bar upper images = 1mm, lower images = 0.5mm.

Immunofluorescence

S100 and PGP9.5 density outcomes are displayed in **table 1**. Examples of obtained immunofluorescence images are displayed in **figure 8**. Between group comparisons showed no significant differences in S100 and PGP9.5 density ratio at both time points.

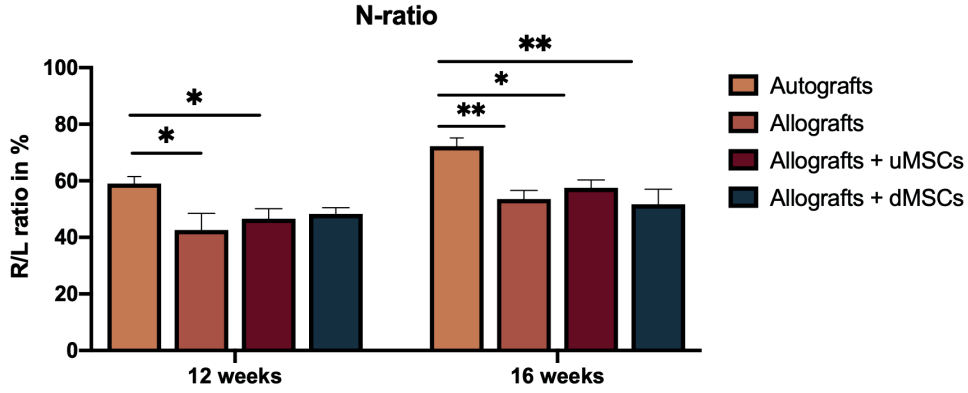

*Figure 7. N- ratios (R/L) at 12 and 16 weeks. Autografts had a significant higher N-ratio than unseeded allografts and allografts seeded with undifferentiated MSCs at 12 weeks and compared to other groups at 16 weeks. uMSCs = undifferentiated Mesenchymal Stem Cells; dMSCs = differentiated Mesenchymal Stem Cells. * = p<0.05, ** = p<0.01, *** = p<0.001. Error bars = Standard error of the mean*

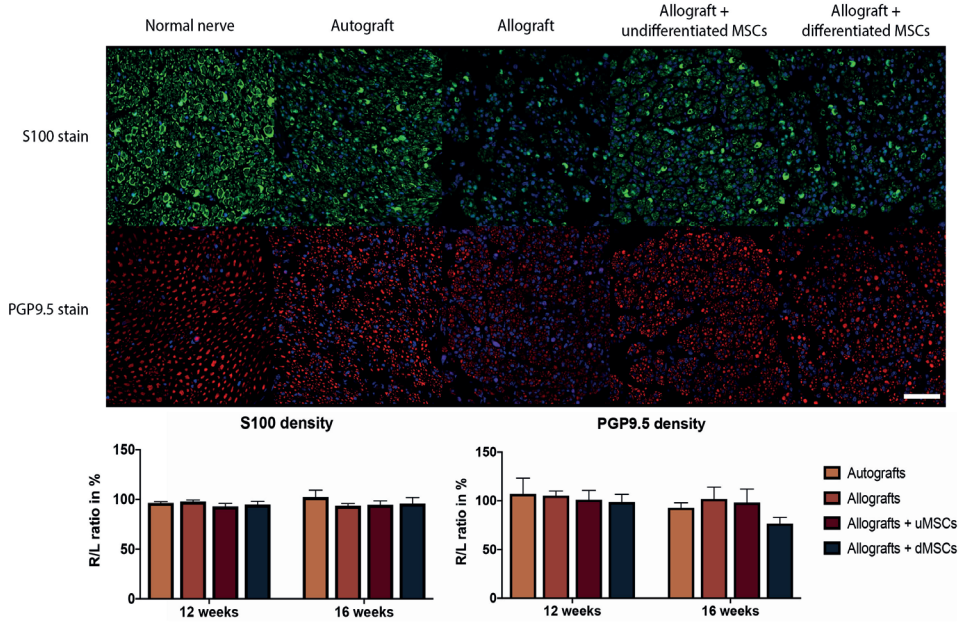

Figure 8. An overview of examples of the obtained images of nerve sections stained with S100 (Schwann cells, green) or PGP9.5 (axons, red) (both immunohystochemistry) at 12 weeks. Cell nuclei are DAPI stained and displayed in blue. The displayed images are obtained with 20X magnification, white error bar = 0.2mm.

DISCUSSION

Despite advances in decellularization techniques for allograft nerves, nerve autograft remain the gold standard for segmental defect reconstruction of critical motor or sensory nerves.[1, 6] To overcome the limitations of decellularized allograft nerves, MSCs have been hypothesized to improve outcomes of decellularized allograft nerves[7] by producing proteins and cytokines that establish a micro-environment favorable for neural regeneration.[8, 12-14, 37] Differentiated MSCs have been demonstrated to exert their neurotrophic effect immediately after implementation by expressing increased levels of neurotrophic genes, while undifferentiated MSCs require additional time to interact with the surrounding tissue prior to expressing neurotrophic genes.[14] The purpose of this study was to determine the effect of dynamically seeding undifferentiated and differentiated MSCs onto decellularized nerve allografts[7] with respect to functional and histologic outcomes in a rat sciatic defect model, in order to determine which cell-type has greatest clinical potential.

In this study, MSCs were successfully differentiated into Schwann cell-like cells[16] and dynamically seeded onto decellularized nerve allografts.[27] Compared to unseeded allografts, undifferentiated MSCs led to significant improvement of both ITF and CMAP ($p=0.017$ and $p=0.004$) outcomes at 12 weeks, while differentiated MSCs only led to significant improved CMAP outcomes ($p<0.001$). These findings correspond to the study of Hou and colleagues whom observed that (differentiated) MSC-seeded grafts recovered earlier than acellular grafts when measuring electrophysiology, with significant results at 12 weeks.[38] Differences between groups normalized at 16 weeks which is consistent with the study of Tang and colleagues, that demonstrated normalizing ITF measurements at 16 weeks of follow-up.[39] Functional assessment did not result in any significant differences between both cell-types for all functional outcome measures at 12 and 16 weeks, which is in line with published studies of Orbay and Watanabe.[22, 23] The hypothesized consequences of different effective phases of both cell-types could not be confirmed in this study.

At 16 weeks, no significant differences in functional outcomes between groups were found, except for muscle mass recovery that was significantly better in autografts than in allografts seeded with differentiated MSCs ($p=0.002$). Although muscle mass is easily obtainable, it is an indirect measurement of motor outcome as enlarged muscle fibers do not neccesarily feature improved contractility.[36] ITF has been described to objectively quantify contractility of muscle fibers and is easily reproducible.[36] The vulnerability of CMAP measurements, which is affected by the placement of all individual electrodes, may explain why the CMAP outcomes are greater than the ITF measures.[40]

Histologically, the autografts had significantly better N-ratios in the peroneal nerves at both time points compared to all other groups. Although not examined, this could be explained by less formation of fibrosis in autografts.[41] Due to small groups and insufficient sensitivity of density measures, the histology outcomes could not be significantly confirmed by immunofluorescence outcomes, but unseeded nerve allografts subjectively seem to contain less Schwann cells and axons compared to all other groups.

Autografts were used as control group to test whether MSCs could improve outcomes of decellularized allografts up to a level equal to that of autografts. While an additional control group in which sham surgery is performed would also be interesting to have, it would require the undesirable and precious use of additional animals. Alternatively, outcomes of the operated side were normalized to the unoperated control side in order to relate the test-outcomes to normal nerve and muscle function.

The significant differences between groups presented at 12 weeks and normalized after 16 weeks, insinuates that nerve regeneration in motor nerves in rats will occur after 12 weeks independently from the type of nerve repair. This finding might be correlated to the demonstrated finite survival of MSCs up to 29 days in vivo; it is suggested that MSCs significantly enhance nerve regeneration up to 12 weeks after which the superlative neuroregenerative capacity of rats takes over, due to the apoptosis of the MSCs.[42] The superlative neuroregenerative capacity of rats is a commonly described explanation and can be mitigated in a larger animal model.[26, 39] Absent significant differences when comparing cross-sectional tibial muscle areas is also a likely consequence of using a small animal model with small cross-sectional nerve areas, relatively leading to larger standard errors and less significant differences between groups.[31, 32] Future research should be performed on multiple time points in larger animal models with larger nerve gaps to potentially translate outcomes to humans.

Considering the overall goal to improve outcomes of decellularized nerve allografts in clinical practice, clinical applicability should be considered when interpretating results. The use of autologous differentiated MSCs requires approximately 4-5 weeks of preparation time, against 2-3 weeks for undifferentiated MSCs.[16] Moreover, the costs of the differentiation cocktail required to differentiate MSCs into Schwann Cell-like cells are high and add to the costs of extended cell culture. Differences between undifferentiated an differentiated MSCs were not statistically significant in light of the analyzed factors, but undifferentiated MSCs improved functional outcomes of decellularized nerve allografts to a greater extent than differentiated MSCs. Taking all this in consideration, undifferentiated MSCs have the greatest potential for bench-to-bedside application. Hypothetically, at the day of presentation in a clinical setting, adipose tissue can be obtained using minimally invasive techniques from the patient with nerve injury, MSCs can then be derived from this tissue and cultured for approximately 2 weeks after which the MSCs can be dynamically seeded onto an off-the-shelf commercially available nerve allografts, 12 hours in advance of the nerve repair. Translation to a larger animal model to ensure the enhanced functional outcomes, study of the capacity of human MSCs to be seeded on clinically available nerve allografts and FDA approval are potential hurdles that need to be addressed prior to application of the presented strategy in clinical practice.

CONCLUSION

Undifferentiated and differentiated MSCs significantly improved functional outcomes of decellularized allografts at 12 weeks in motor nerves and equaled the autograft results in the majority of outcome measurements. At 16 weeks, outcome measures normalized as expected. Considering clinical applicability, undifferentiated MSCs are more attractive as outcomes did not significantly differ between both cell-types, and differentiation requires increased time and cost.

Acknowledgements

We thank Roman Thaler, PhD, for assisting with cell culture and differentiation of the Mesenchymal Stem Cells.

We thank Patricia F. Friedrich for assistance with the preparations of the experiments.

REFERENCES

1. Giusti G, Willems WF, Kremer T, et al. Return of motor function after segmental nerve loss in a rat model: comparison of autogenous nerve graft, collagen conduit, and processed allograft (AxoGen). J Bone Joint Surg Am 2012: 94: 410-7.
2. Millesi H. Progress in peripheral nerve reconstruction. World J Surg 1990: 14: 733-47.
3. Mackinnon SE, Hudson AR, Falk RE, Hunter DA. The nerve allograft response--an experimental model in the rat. Ann Plast Surg 1985: 14: 334-9.
4. Whitlock EL, Tuffaha SH, Luciano JP, et al. Processed allografts and type I collagen conduits for repair of peripheral nerve gaps. MUSCLE NERVE 2009: 39: 787-99.
5. Cho MS, Rinker BD, Weber RV, et al. Functional outcome following nerve repair in the upper extremity using processed nerve allograft. J Hand Surg Am 2012: 37: 2340-9.
6. Rbia N, Shin AY. The Role of Nerve Graft Substitutes in Motor and Mixed Motor/Sensory Peripheral Nerve Injuries. J Hand Surg Am 2017: 42: 367-77.
7. Hundepool CA, Nijhuis TH, Kotsougiani D, et al. Optimizing decellularization techniques to create a new nerve allograft: an in vitro study using rodent nerve segments. Neurosurg Focus 2017: 42.
8. Caplan AI. Adult Mesenchymal Stem Cells: When, Where, and How. Stem Cells Int 2015: 2015: 628767.
9. Mushtaq M, DiFede DL, Golpanian S, et al. Rationale and design of the Percutaneous Stem Cell Injection Delivery Effects on Neomyogenesis in Dilated Cardiomyopathy (the POSEIDON-DCM study): a phase I/II, randomized pilot study of the comparative safety and efficacy of transendocardial injection of autologous mesenchymal stem cell vs. allogeneic mesenchymal stem cells in patients with non-ischemic dilated cardiomyopathy. J Cardiovasc Transl Res 2014: 7: 769-80.
10. Shen H, Wang Y, Zhang Z, et al. Mesenchymal Stem Cells for Cardiac Regenerative Therapy: Optimization of Cell Differentiation Strategy. Stem Cells Int 2015: 2015: 524756.
11. Nam HY, Karunanithi P, Loo WC, et al. The effects of staged intra-articular injection of cultured autologous mesenchymal stromal cells on the repair of damaged cartilage: a pilot study in caprine model. Arthritis Res Ther 2013: 15: R129.
12. Castro-Manrreza ME, Montesinos JJ. Immunoregulation by mesenchymal stem cells: biological aspects and clinical applications. J Immunol Res 2015: 2015: 394917.
13. Rbia N, Bulstra LF, Saffari TM, Hovius SER, Shin AY. Collagen Nerve Conduits and Processed Nerve Allografts for the Reconstruction of Digital Nerve Gaps: A Single-Institution Case Series and Review of the Literature. World Neurosurg 2019: 127: e1176-e84.
14. Mathot F, Rbia N, Thaler R, et al. Gene expression profiles of differentiated and undifferentiated adipose derived mesenchymal stem cells dynamically seeded onto a processed nerve allograft. Gene 2020: 724: 144151.
15. Mathot F, Shin AY, Van Wijnen AJ. Targeted stimulation of MSCs in peripheral nerve repair. Gene 2019.
16. Kingham PJ, Kalbermatten DF, Mahay D, et al. Adipose-derived stem cells differentiate into a Schwann cell phenotype and promote neurite outgrowth in vitro. Exp Neurol 2007: 207: 267-74.
17. Yoshimura H, Muneta T, Nimura A, et al. Comparison of rat mesenchymal stem cells derived from bone marrow, synovium, periosteum, adipose tissue, and muscle. Cell Tissue Res 2007: 327: 449-62.
18. di Summa PG, Kingham PJ, Raffoul W, et al. Adipose-derived stem cells enhance peripheral nerve regeneration. J Plast Reconstr Aesthet Surg 2010: 63: 1544-52.
19. Kingham PJ, Kolar MK, Novikova LN, Novikov LN, Wiberg M. Stimulating the neurotrophic and angiogenic properties of human adipose-derived stem cells enhances nerve repair. Stem Cells Dev 2014: 23: 741-54.
20. Tomita K, Madura T, Sakai Y, et al. Glial differentiation of human adipose-derived stem cells: implications for cell-based transplantation therapy. Neuroscience 2013: 236: 55-65.
21. Ladak A, Olson J, Tredget EE, Gordon T. Differentiation of mesenchymal stem cells to support peripheral nerve regeneration in a rat model. Exp Neurol 2011: 228: 242-52.

22. Orbay H, Uysal AC, Hyakusoku H, Mizuno H. Differentiated and undifferentiated adipose-derived stem cells improve function in rats with peripheral nerve gaps. J Plast Reconstr Aesthet Surg 2012: 65: 657-64.
23. Watanabe Y, Sasaki R, Matsumine H, Yamato M, Okano T. Undifferentiated and differentiated adipose-derived stem cells improve nerve regeneration in a rat model of facial nerve defect. J Tissue Eng Regen Med 2017: 11: 362-74.
24. Keilhoff G, Goihl A, Stang F, Wolf G, Fansa H. Peripheral nerve tissue engineering: autologous Schwann cells vs. transdifferentiated mesenchymal stem cells. Tissue Eng 2006: 12: 1451-65.
25. Kappos EA, Engels PE, Tremp M, et al. Peripheral Nerve Repair: Multimodal Comparison of the Long-Term Regenerative Potential of Adipose Tissue-Derived Cells in a Biodegradable Conduit. Stem Cells Dev 2015: 24: 2127-41.
26. Rbia N, Bulstra LF, Thaler R, et al. In Vivo Survival of Mesenchymal Stromal Cell-Enhanced Decellularized Nerve Grafts for Segmental Peripheral Nerve Reconstruction. J Hand Surg Am 2018.
27. Mathot F, Rbia N, Bishop AT, et al. Adhesion, distribution, and migration of differentiated and undifferentiated mesenchymal stem cells (MSCs) seeded on nerve allografts. J Plast Reconstr Aesthet Surg 2019.
28. Rbia N, Bulstra LF, Bishop AT, van Wijnen AJ, Shin AY. A simple dynamic strategy to deliver stem cells to decellularized nerve allografts. Plast Reconstr Surg 2018.
29. Hudson TW, Zawko S, Deister C, et al. Optimized acellular nerve graft is immunologically tolerated and supports regeneration. Tissue Eng 2004: 10: 1641-51.
30. Kumta S, Yip K, Roy N, Lee SK, Leung PC. Revascularisation of bone allografts following vascular bundle implantation: an experimental study in rats. Arch Orthop Trauma Surg 1996: 115: 206-10.
31 Hundepool CA, Nijhuis TH, Rbia N, et al. Noninvasive Ultrasound of the Tibial Muscle for Longitudinal Analysis of Nerve Regeneration in Rats. Plast Reconstr Surg 2015: 136: 633e-9e.
32. Bulstra LF, Hundepool CA, Friedrich PF, et al. Motor Nerve Recovery in a Rabbit Model: Description and Validation of a Noninvasive Ultrasound Technique. J Hand Surg Am 2016: 41: 27-33.
33. Hundepool CA, Bulstra LF, Kotsougiani D, et al. Comparable functional motor outcomes after repair of peripheral nerve injury with an elastase-processed allograft in a rat sciatic nerve model. Microsurgery 2018: 38: 772-79.
34. Giusti G, Lee JY, Kremer T, et al. The influence of vascularization of transplanted processed allograft nerve on return of motor function in rats. Microsurgery 2016: 36: 134-43.
35. Shin RH, Vathana T, Giessler GA, et al. Isometric tetanic force measurement method of the tibialis anterior in the rat. Microsurgery 2008: 28: 452-7.
36. Vleggeert-Lankamp CL. The role of evaluation methods in the assessment of peripheral nerve regeneration through synthetic conduits: a systematic review. Laboratory investigation. J Neurosurg 2007: 107: 1168-89.
37. Ma S, Xie N, Li W, et al. Immunobiology of mesenchymal stem cells. Cell Death Differ 2014: 21: 216-25.
38. Hou SY, Zhang HY, Quan DP, Liu XL, Zhu JK. Tissue-engineered peripheral nerve grafting by differentiated bone marrow stromal cells. Neuroscience 2006: 140: 101-10.
39. Tang P, Whiteman DR, Voigt C, Miller MC, Kim H. No Difference in Outcomes Detected Between Decellular Nerve Allograft and Cable Autograft in Rat Sciatic Nerve Defects. J Bone Joint Surg Am 2019: 101: e42.
40. S. Saffari TMS, A.M. Moore, A.Y. Shin. Peripheral Nerve Basic Science Research – What is important for hand surgeons to know? Submitted to Journal of Hand Surgery 2019.
41. den Dunnen WF, van der Lei B, Schakenraad JM, et al. Poly(DL-lactide-epsilon-caprolactone) nerve guides perform better than autologous nerve grafts. Microsurgery 1996: 17: 348-57.
42. Rbia N, Bulstra LF, Thaler R, et al. In Vivo Survival of Mesenchymal Stromal Cell-Enhanced Decellularized Nerve Grafts for Segmental Peripheral Nerve Reconstruction. J Hand Surg Am 2019: 44: 514.e1-14.e11.

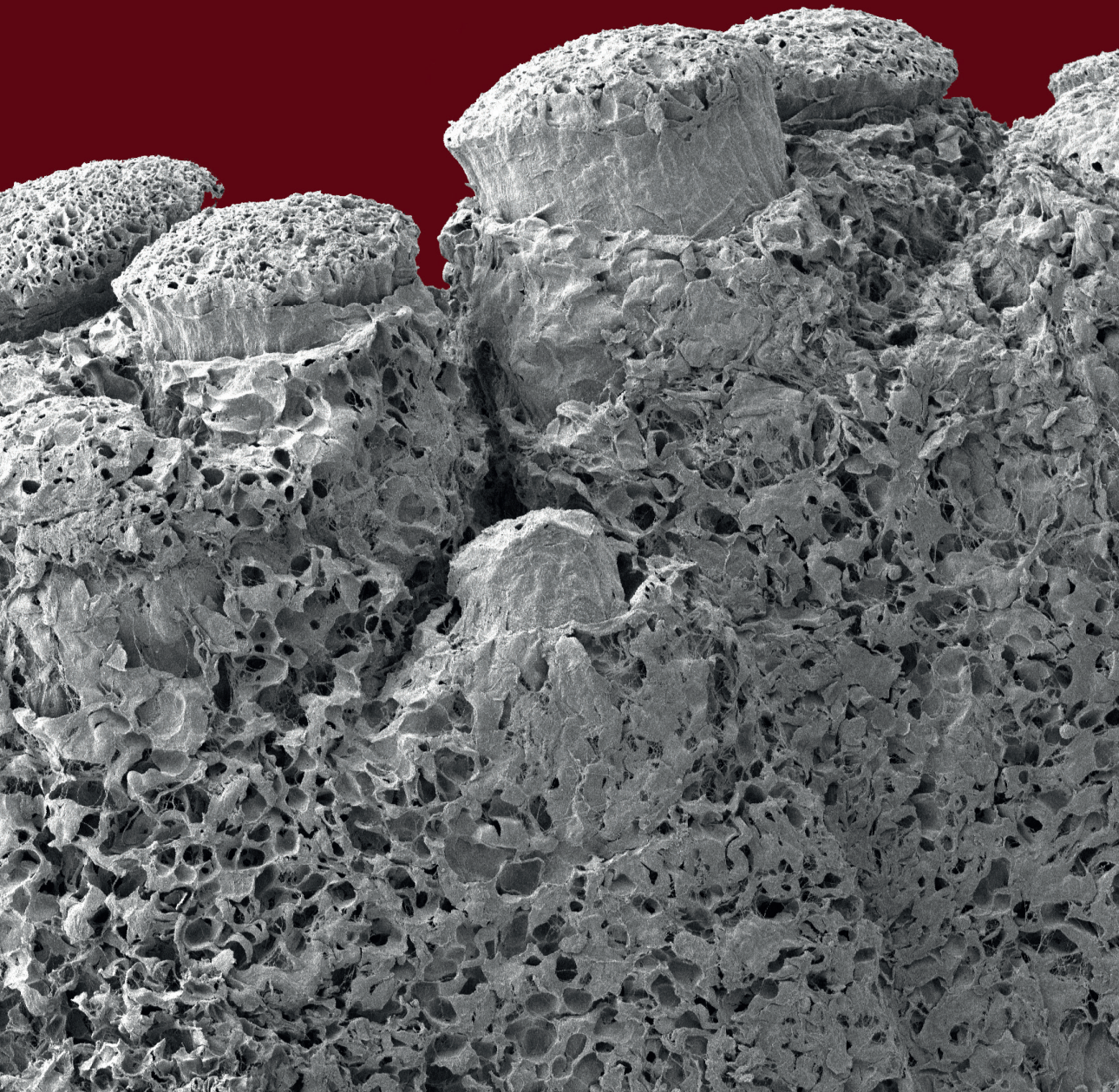

Chapter 8

Introducing human adipose-derived mesenchymal stem cells to Avance® nerve grafts and NeuraGen® nerve guides

Femke Mathot, Nadia Rbia, Roman Thaler, Allen T. Bishop, Andre J. van Wijnen, Alexander Y. Shin

Journal of plastic, reconstructive & aesthetic surgery: JPRAS. 2020 August; 73(8):1473-1481

ABSTRACT

Background

When direct nerve coaptation is impossible after peripheral nerve injury, autografts, processed allografts or conduits are used to bridge the nerve gap. The purpose of this study was to examine if human adipose derived Mesenchymal Stromal/Stem Cells (MSCs) could be introduced to commercially available nerve graft substitutes and to determine cell distribution and seeding efficiency of a dynamic seeding strategy.

Methods

MTS assays examined the viability of human MSCs after introduction to the Avance® Nerve Graft and the NeuraGen® Nerve Guide. MSCs were dynamically seeded on nerve substitutes for either 6, 12 and 24 hours. Cell counts, live/dead stains, Hoechst stains and Scanning Electron Microscopy (SEM) revealed the seeding efficiency and the distribution of MSCs after seeding.

Results

The viability of MSCs was not affected by the nerve substitutes. Dynamic seeding led to uniformly distributed MSCs over the surface of both nerve substitutes and revealed MSCs on the inner surface of the NeuraGen® Nerve Guides. The maximal seeding efficiency of NeuraGen® Nerve Guides (94%), obtained after 12 hours was significantly higher than that of Avance® Nerve Grafts (66%) ($p=0.010$).

Conclusion

Human MSCs can be dynamically seeded on Avance® Nerve Grafts and NeuraGen® Nerve Guides. The optimal seeding duration was 12 hours. MSCs were distributed in a uniform fashion on the exposed surfaces. This study demonstrates that human MSCs can be effectively and efficiently seeded onto commercially available nerve autograft substitutes in a timely fashion and sets the stage for clinical application of MSC seeded nerve graft substitutes.

INTRODUCTION

Peripheral nerve discontinuities that cannot be restored by direct end-to-end coaptation of nerve ends remain a clinical challenge. Despite many efforts to find an equivalent replacement, autologous nerve graft, which results in donor site morbidity, remains the gold standard in peripheral nerve reconstruction. To minimize donor site morbidity, increase the number of reconstructive options and improve the outcomes of peripheral nerve repair, further improvement of the commercially available 'off-the-shelf' nerve graft substitutes is essential.

Two commercially available nerve autograft substitutes are the NeuraGen® Nerve Guide (approved by the Food and Drug Administration in 2001) and the Avance® Nerve Graft (approved by the FDA in 2007). The NeuraGen® Nerve Guide is an artificial bioabsorbable hollow conduit made of purified bovine type I collagen. It has demonstrated effective nerve regeneration in small diameter, short (<3cm) sensory nerves defects, but evidence for its effective use in sensory nerve defects of longer size and/or larger diameter, or in motor nerve defects, remains scarce and inconsistent.[1-3]

The Avance® Nerve Graft is a decellularized human nerve allograft that has been processed to remove cellular debris. This process includes decellularization with chondroitinase and gamma-irradiation, leading to a natural human product with a remaining ultrastructure that does not necessitate the use of immunosuppression. While clinical outcomes have been mostly with case reports and series [1, 4-6], there has been a lack of prospective clinical trials and valid comparisons to autografts. Their application in large motor-nerve defects remains controversial.[1, 4, 7, 8]

The hypothesis that the addition of a cells that deliver growth factors at the nerve regeneration site could result in enhanced nerve regeneration has been confirmed by studies reporting a synergistic effect of mesenchymal stromal/stem cells (MSCs) added to a nerve conduit, leading to improved functional outcomes in various types of nerve gaps.[9-14] Similarly, the enhancing effect of added MSCs or Schwann cells to processed nerve allografts has also been demonstrated on a gene expression and functional outcome level.[15-20]

A variety of non-validated delivery methods have been reported. Micro-injection has been extensively described to deliver the MSCs. Acute micro-injection is known to be traumatic to MSCs even though cells remain metabolically active.[21] Micro-injection also damages the ultrastructure of the allograft and when placed in the center of a hollow conduit, leakage occurs which may alter the effective dose of MSCs in an unpredictable manner.[22-27] Dynamic seeding is a novel, recently described delivery method that successfully adheres MSCs in a uniform matter on the surface of processed nerve grafts.[27, 28]

Application and validation of this dynamic seeding strategy when applied to commercially available products like the Avance® Nerve Graft and the NeuraGen® Nerve Guide could enhance the clinical applicability of the described method and would enable a valid comparison of the two products and their capability to enhance nerve regeneration when

supported by MSCs.

In order to determine the clinical potential of dynamic seeding of MSCs, this study was designed to examine the interaction between MSCs and two commercially available nerve graft substitutes; the Avance® Nerve Graft and the NeuraGen® Nerve Guide. The purpose of this study was to determine (I) if the interaction of human adipose derived MSCs with the NeuraGen® Nerve Guide and the Avance® Nerve Graft influences cell viability, (II) if human adipose derived MSCs can be dynamically seeded and distribute uniformly onto these nerve substitutes, and (III) if dynamic seeding and optimized timing improves the efficiency of MSC-seeding.

METHODS

General design

Two experiments were designed to ascertain the interaction of the nerve graft substitutes with human adipose derived MSCs and to determine the optimal seeding times, survivability and distribution of MSCs.

Adipose Derived Mesenchymal Stem Cell Collection and Preparation

Passage five human MSCs, isolated from abdominal lipo-aspirates of a male donor were used in this experiment. Cells were provided by the Mayo Clinical Human Cellular Therapy Laboratory (Rochester, Minnesota, USA). These MSCs have been tested extensively for multi-lineage potential, cell surface markers (CD73, CD90, CD105, CD44, CD14, CD45) and RNA-sequence transcriptome profiles previously.(23-25) For MSC culture, growth media consisting of a-MEM (Advanced MEM (1x); Gibco by Life TechnologiesTM, Cat #12492013), 5% platelet lysate (PLTMax®; Mill Creek Life Sciences), 1% penicillin/streptomycin (Penicillin-Streptomycin (10.000 U/mL); Gibco by Life TechnologiesTM Cat #15140148), 1% GlutaMAX (GlutaMAXTM Supplement 100X; Gibco by Life Technologies, Cat #35050061) and 0.2% heparin (Heparin Sodium Injection, USP, 1.000 USP units per mL; NOVAPLUS®) was used and media was changed every 72 hours. [29-31]

Experimental Design and Measurement of Mesenchymal Stem Cell Viability

To test whether the chemical products used during processing of the Avance® Nerve Graft and the NeuraGen® Nerve Guide are harmful to MSCs, cell metabolic activity was measured using (3-(4,5-dimethylthiazol-2-yl)-5-(3-carboxymethoxyphenyl)-2-(4-sulfophenyl)-2H-tetrazolium) (MTS) assays that were performed according to the manufacturer's protocol (CellTiter 96® AQueous One Solution Cell Proliferation Assay, Promega®). Twenty-four 2mm-segments of the Avance® Nerve Graft and the NeuraGen® Nerve Guide were soaked in a-MEM for two hours prior to the MTS assay. The soaked nerve substitute segments and 5,000 MSCs dissolved in 100µL growth medium were placed into wells which were coated with pHEMA (Poly 2-hydroxyethyl methacrylate; Sigma Cat # P3932) to prevent migration of the MSCs to the plastic well. Any influence of the pHEMA coating on cell viability, was

eliminated by measuring the viability of two extra groups (MSCs + Avance® Nerve Graft and MSCs + NeuraGen® Nerve Guide) at each time point. After 1, 2, 3 and 7 days of incubation at 37°C the metabolic activity of three samples of each group were measured with the Infinite® 200 Pro TECAN Reader (Tecan Trading AG, Switzerland) at an absorbance wavelength of 490nm. The metabolic activity of group I (pHEMA + MSCs + Avance® Nerve Graft) and group II (pHEMA + MSCs + NeuraGen® Nerve Guide) were expressed as a ratio of the metabolic activity of the control group (pHEMA + MSCs) and compared to each other.

Experimental Design and Measurement of Cell distribution, Migration and Seeding Efficiency

In total, 20 Avance® Nerve Grafts and 20 NeuraGen® Nerve Guides of 10mm in length were used in this experiment. 18 samples per group were dynamically seeded according to the dynamic seeding strategy described by Rbia and colleagues.[27] Prior to seeding, all nerve substitute segments were soaked in a-MEM for two hours as an equilibration step to restore the salt balance. Conical tubes containing the nerve samples and one million MSCs per nerve sample in growth medium were rotated in a bioreactor placed in an incubator (37°C) for 6, 12 and 24 hours (n=6 per group per seeding duration).

The viability of adherent MSCs was evaluated by live/dead Cell Viability Assays (Invitrogen, Life Technologies Corporation, NY, USA) after each of the different seeding durations. Hoechst staining was performed according to standard protocols (Hoechst stain solution; Sigma-Aldrich Corp., MO, USA) on the surface of the nerve substitutes to show the distribution and migration of cells after dynamic seeding. Both Live/Dead and Hoechst stains were performed on three samples per group per seeding duration and were visualized directly after seeding with a confocal microscope (Zeiss LSM 780 confocal microscope).

To study cell distribution, Scanning Electron Microscopy (SEM) (n=3 per group per seeding duration) was performed. Samples were fixed in 2% Trump's fixative solution (37% formaldehyde and 25% glutaraldehyde) directly after seeding. After 24 hours, samples were washed with phosphate buffer, rinsed in water, processed through graded series of ethanol (final 100% ethanol), critical point dried with carbon and mounted on an aluminum stub. After sputter-coating for 60 seconds using gold-palladium, sample-images were taken with a Hitachi S-4700 cold field emission SEM (Hitachi High Technologies America, Inc., IL, USA) at 5kV accelerating voltage. After obtaining images of the graft surface, samples were cut longitudinally and imaged to reveal cell distribution on the inside of the nerve substitutes.

To reinforce the SEM-findings, two extra 10mm samples per group were seeded with 1 million MSCs according to the estimated optimal seeding duration, fixed in 10% formalin and processed and embedded in paraffin. Three sections of 5µM of the proximal- and mid-nerve substitutes were taken and Hoechst stained to evaluate for cells that migrated inside the nerve substitute (i.e. within the nerve allograft or nerve conduit material itself). The cells were visualized with a confocal microscope (Zeiss LSM 780 confocal microscope; Zeiss, Germany).

To quantify seeding efficiency, cell counts of the cell supernatant after the rotation duration was completed, provided the number of MSCs that remained free floating in the media. This indirectly led to the number and percentages of MSCs that were attached to the nerve sample, in this manuscript expressed as seeding efficiency.[32]

In addition to cell counts in the supernatant, seeding efficiency of MSCs after the various seeding durations was further evaluated by Hoechst fluorescence staining of the seeded nerve substitutes using the Infinite® 200 Pro TECAN Reader (Tecan Trading AG, Switzerland) at an absorbance wavelength of 340/458nm.

Statistical analysis

Cell counts were performed in triplicate per sample and are expressed as the mean percentage ± standard deviation (SD). The different measurements were analyzed using a two-way ANOVA. When ANOVA indicated a significant interaction, both within and between group comparisons were analyzed with the Kruskal-Wallis test, followed by pairwise comparisons using Wilcoxon rank-sum tests with Bonferroni correction. Significance was set at α>0.05.

RESULTS

Cell Viability upon interaction of MSCs with Nerve Graft Substitute:

Analysis revealed no significant effect on cell viability of the pHEMA coating that was used in this experiment. The viability of MSCs when in presence with the Avance® Nerve Graft or the NeuraGen® Nerve Guide, expressed as a ratio of the viability of MSCs without either of the nerve substitutes in **figure 1**, was not affected by the presence of both nerve substitutes indicating that there was no detrimental interaction of the manufacturing process to MSCs. There were no significant differences in cell-viability between and within the two groups over time as well (p=0.450).

Cell distribution, migration and seeding efficiency of MSCs on Nerve Graft Substitute

Live/dead staining and nuclear staining using Hoechst dye revealed a uniform distribution of viable MSCs over the entire surface of both nerve substitutes after all seeding durations. **Figure 2 and 3** demonstrate example images after 12 hours of seeding of live/dead staining and Hoechst staining respectively. Hoechst fluorescent measurements demonstrated increased fluorescence as seeding duration time increases (**figure 4**) (p=0.001), but there were no significant differences in Hoechst fluorescence between groups.

Despite the different composition of the surfaces of the Avance® Nerve Graft and the NeuraGen® Nerve Guide, SEM images revealed a similar distribution of cells among their surface (**figure 5**). Manual quantification could not be carried out reliably due to cell aggregation, but assessment of the samples showed a marked increase in cell coverage of both nerve substitutes between 6 and 12 hours of seeding. Between 12 and 24 hours of dynamic seeding, there were no appreciable differences in cell coverage. The morphology of

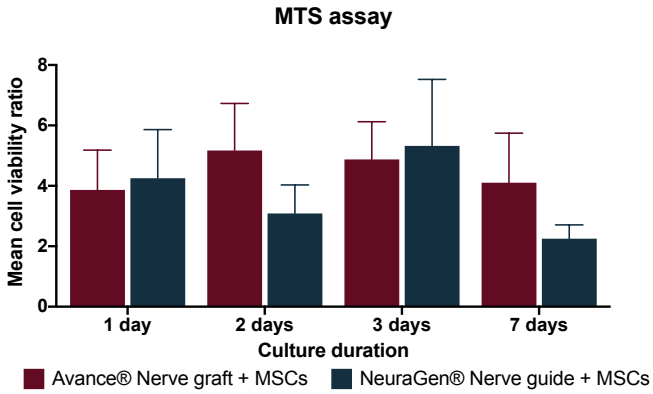

Figure 1. Cell-viability over time of MSCs when combined with the Avance® Nerve Graft and the NeuraGen® Nerve Guide (n=3 per group per time point). Viability of MSCs in presence of the Avance® Nerve Graft and the NeuraGen® Nerve Guide is expressed as a ratio of the viability of MSCs without any of the nerve substitutes. pHEMA coating was used in all groups presented in this figure. There were no significant differences between and within groups in 7 days of follow-up. Error bars: SEM. SEM = standard error of the mean

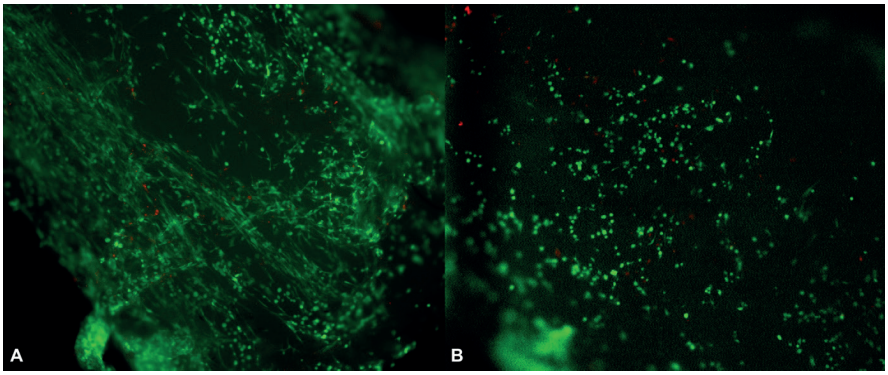

Figure 2. Live/Dead stains of a seeded Avance® Nerve Graft (A) and a seeded NeuraGen® Nerve Guide (B) after 12 hours of seeding with MSCs, show mainly living cells (green) mixed with only a few dead cells (red) on the surface of both nerve substitutes.

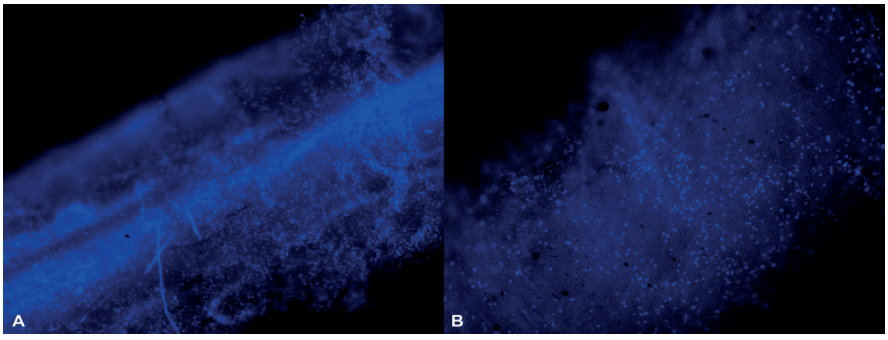

Figure 3. Hoechst stained Avance® Nerve Graft (A) and NeuraGen® Nerve Guide (B) after 12 hours of dynamic seeding with MSCs show a uniform distribution of cell nuclei among both nerve substitutes (10X). Cell nuclei are displayed in bright blue.

cells did not change over time. SEM images of longitudinally cut segments of the Avance® Nerve Graft did not show any MSCs in the inner ultrastructure of the graft after 6, 12 and 24 hours of seeding (**figure 6**, left side). MSCs were present throughout the inner surface of the NeuraGen® Nerve Guides after 6, 12 and 24 hours, although the coverage of MSCs was clearly less than on the outside of the Nerve Guide (Figure 6, right side). Additionally, the MSC did not migrate into the substrate of the NeuraGen® Nerve Guides. These findings were confirmed by Hoechst staining of cross-sectional images of both groups, that revealed no staining of nuclei in cells inside of the Avance® Nerve Grafts but detectable nuclear staining of cells within the NeuraGen® Nerve Guides (**figure 7**).

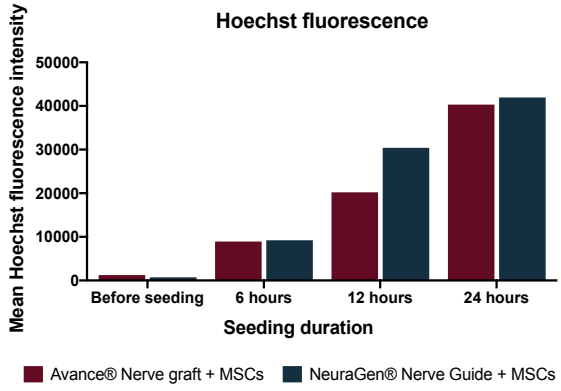

Figure 4. Hoechst fluorescence intensity of the Avance® Nerve Graft and the NeuraGen® Nerve Guide when seeding with MSCs according to increasing seeding durations (n=3 per group per time point). ANOVA analysis did not demonstrate a significant interaction between seeding duration and Hoechst fluorescence (p=0.001) when merging the groups, but within groups analysis did not demonstrate any significant increases between time points (p>0.221 for the Avance® Nerve Grafts and p>0.083 for the NeuraGen® Nerve Guides).

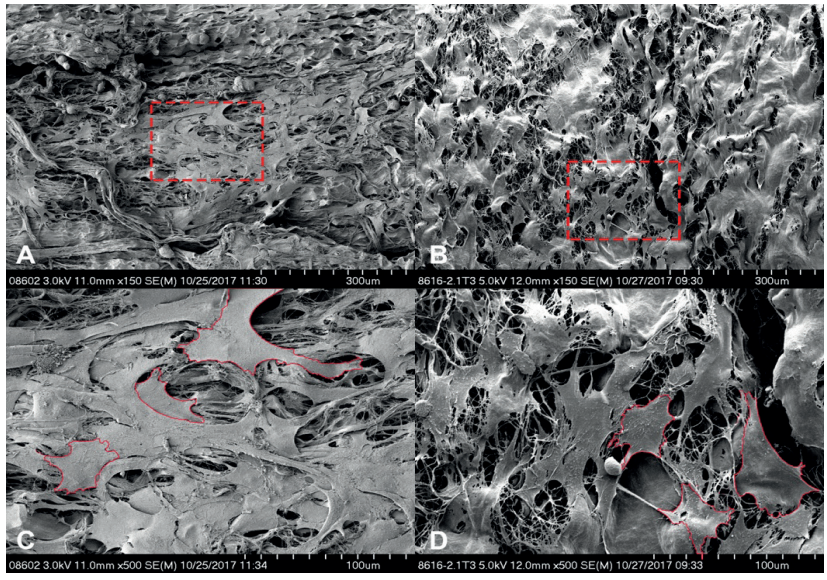

Figure 5. Scanning electron microscopy images showing the cell-coverage of the Avance® Nerve Graft (A and C) and the NeuraGen® Nerve Guide (B and D) after being dynamically seeded with human MSCs for 12 hours. Images A and B display overview images with 150X magnification. Images C and D display the areas that are encircled in red in images A and B, 500X magnification. Shown is a uniform distribution of partly aggregating MSCs on the porous surface of both nerve substitutes. Examples of cell contours are displayed in red in C and D.

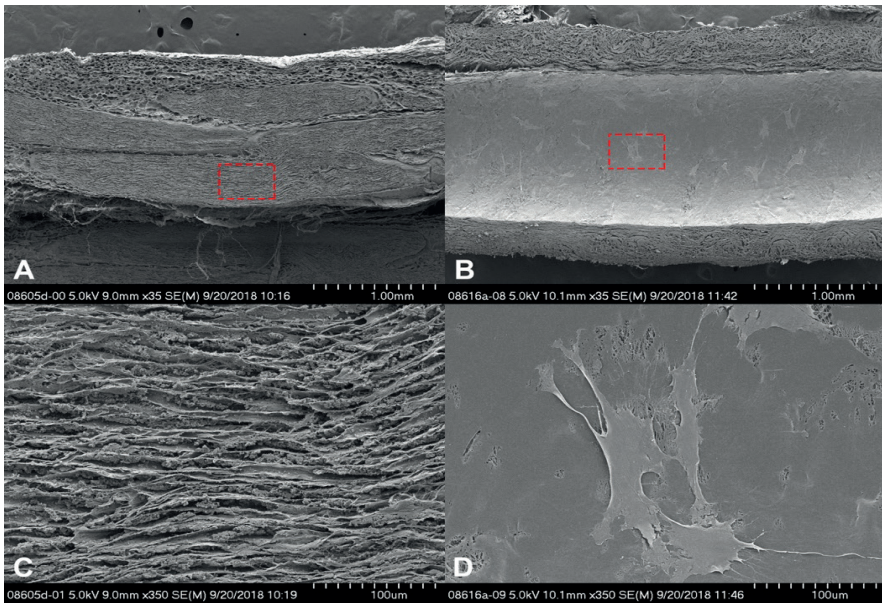

Figure 6. Cross-sectional scanning electron microscopy images of the Avance® Nerve Graft (A and C) and the NeuraGen® Nerve Guide (B and D) after 12 hours of dynamic seeding with human MSCs. Both nerve substitutes were cut longitudinally. The cross-section of the Avance® Nerve Graft shows aligned fascicles without the presence of any cells. The cross-section of the NeuraGen® Nerve Guide demonstrates the smooth inner surface of the hollow conduit, with MSCs spread out among the entire length of the nerve guide.

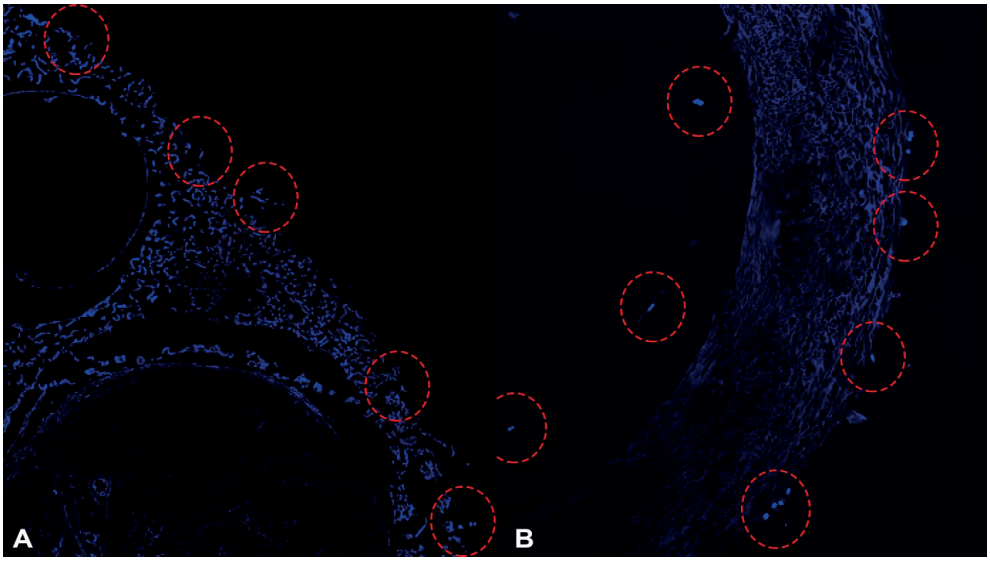

Figure 7. Hoechst-stained cross-sectional segments of the Avance® Nerve Graft (A) and the NeuraGen® Nerve Guide (B) after 12 hours of dynamic seeding with human MSCs. Cell nuclei, labeled in bright blue, are displayed among the outer surface of the Avance® Nerve Graft (left) and on both the inner and outer surface of the NeuraGen® Nerve Guide (right).

Seeding efficiency

With the Avance® Nerve Graft, a seeding efficiency of 18.23% (± 28.12) was obtained after 6 hours, reaching a maximum of 66.46% (± 16.01) after 12 hours that was sustained at 59.90% (± 28.81) after 24 hours of dynamic seeding. With the NeuraGen® Nerve Guide, the seeding efficiency increased from 52.08% (± 14.81) after 6 hours to 94.17% (± 4.03) after 12 hours but decreased to 52.50% (± 19.27) after 24 hours.

Two-way ANOVA showed a significant interaction between seeding duration, the different groups and the seeding efficiency (p=0.004). Kruskal-Wallis analysis of within-group differences for the Avance® Nerve Grafts was significant (p=0.007). Pairwise comparisons showed that the increase in seeding efficiency between the first (6hr) and second (12hr) time points was statistically significant (p=0.006), but that the decrease between the second (12hr) and third (24 hr) time points was not (p=0.589). The Kruskal-Wallis analysis of within-group differences of the NeuraGen® Nerve Guide showed a significant interaction (p=0.024). Pairwise comparisons revealed a significant increase in seeding efficiency between time point 1 and 2 (p=0.029) and a significant decrease between time point 2 and 3 (P=0.029).

Seeding efficiencies obtained with the NeuraGen® Nerve Guide were significantly higher than the seeding efficiencies obtained with the Avance® Nerve Graft after 12 hours of seeding (p=0.010). No significant differences were found at time point 1 (p=0.055) and time point 3 (p=0.522). The seeding efficiency over time for both groups is depicted in **figure 8**.

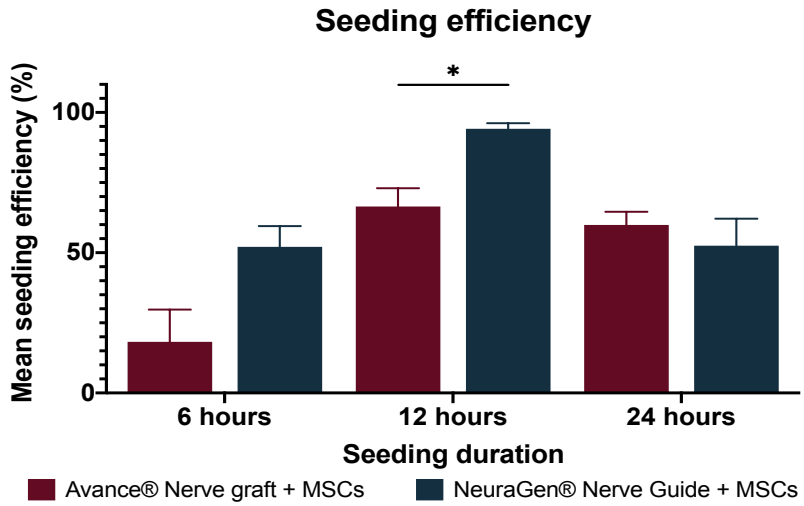

*Figure 8. Seeding efficiencies of the Avance® Nerve Graft and the NeuraGen® Nerve Guide after completion of 6, 12 and 24 hours of dynamic seeding with human MSCs (n=6 per group per time point). Both groups obtained an optimal seeding efficiency after 12 hours of dynamic seeding; the Avance® Nerve Graft reached a seeding efficiency of 66.46% (± 16.01), the NeuraGen® Nerve Guide reached a seeding efficiency of 94.17% (± 4.03). Error bars: SEM. * = significant difference, with α >0.05. SEM = standard error of the mean*

DISCUSSION

We examined the clinical potential of dynamic seeding of MSCs onto commercially available nerve graft substitutes by testing whether (I) the NeuraGen® Nerve Guide and the Avance® Nerve Graft affect the viability of human MSCs, (II) human MSCs can be dynamically seeded and distribute uniformly onto these nerve substitutes, and (III) dynamic seeding and optimized timing improves the efficiency of MSC-seeding.

MTS assays demonstrated that both the Avance® Nerve Graft and the NeuraGen® Nerve Guide did not affect the metabolic activity or survivability of human adipose derived MSCs. The human MSCs were able to adhere in a uniform manner of the surfaces of both nerve substitutes, with an optimal dynamic seeding duration of 12 hours. The significantly better seeding efficiency of NeuraGen® Nerve Guides after 12 hours of seeding is most likely due to their hollow conduit configuration, enabling MSCs to adhere on the outer and inner surface of the conduit. The MSCs did not migrate inside the Avance® Nerve Graft or into the substrate of the NeuraGen® Nerve Guides. It is hypothesized that the decrease in seeding efficiency after 12 hours of dynamic seeding is related to cell damage due to the rotational forces of the seeding process, leading to a decreased ability of cells to adhere to the surfaces of the nerve substitutes.

The concept that MSCs inside a nerve substitute support the regeneration of axons is relevant for the applicability of the dynamic seeding strategy. MSCs used in peripheral nerve repair potentially differentiate into Schwann cells in vivo, and may have a structural function by replacing injured tissue. However, studies supporting that MSCs need to be delivered inside nerve substitutes are limited and most papers show that only a fraction of the added MSCs are differentiated into actual Schwann cells and survive on the long term.[33, 34] Other studies reported trophic effects of MSCs, producing proteins and molecules that stimulate tissue regeneration, form extracellular matrix components, enhance angiogenesis, inhibit scar formation, and attenuate inflammation without the MSCs actually being physically integrated into the regenerating tissue.[35-39] Robust expression of secreted proteins including growth factors and morphogens by MSCs when introduced to injured tissues supports the concept that MSCs may be more effective as tissue repair catalysts rather than architectural participants.[40, 41]

The trophic concept forms the basis of the proposed delivery method of MSCs. Considering the shown mismatch in size between the axon fascicules and the MSCs (**figure 6**), delivery of MSCs inside a graft may block the ingrowth of regenerating axons. As MSCs do not need to be delivered inside the nerve graft to produce growth factors and cytokines that support nerve regeneration, it is preferred that MSCs are added in a simple, efficient and systematic manner that is non-traumatic and avoids damage to the nerve substitute. In contrast to microinjection and soaking methods, the dynamic seeding strategy of Rbia and colleagues meets these requirements.[22, 26-28] This strategy has demonstrated to enhance the neuroregenerative gene expression in the MSCs [19, 20] and revealed an in vivo survival of the MSCs up to 29 days.[42] The absence of MSCs on the inner surface of the Avance® Nerve Graft therefore does not

implicate that this combination by definition results in less nerve regeneration enhancement that the combination of MSCs and the NeuraGen® Nerve Guide. In vivo studies using the described techniques should indicate whether MSC-seeding location (inner or outer surface) has implications for their effect on nerve regeneration.

Seeding efficiency was indirectly determined by cell-counts in the supernanent after the seeding duration time passed. Although multiple cell counts were performed with small standard errors and subjective assessment of the obtained live/dead and Hoechst images imply high seeding efficiencies, seeding efficiency could theoretically be overestimated by this indirect strategy as MSCs might have attached to the conical tube or have clumped together.[32] Group sizes were limited due to the costs associated with the use of the various products. Another limitation is that we did not test our chimeric cell/graft models yet in animal models.

Despite the limitations, this study is a preliminary but essential step towards considering the use of dynamic seeding in a clinical setting. This study clearly demonstrates that MSCs can be seeded on the Avance® Nerve Graft and the NeuraGen® Nerve Guide. MSCs more efficiently adhered to the inner and outer surface of the NeuraGen® Nerve Guide than to the Avance® Nerve Graft, MSCs are evenly distributed on the surface and do not migrate into the nerve or substrate.

CONCLUSION

The NeuraGen® Nerve Guide and the Avance® Nerve Graft do not negatively influence the viability of human MSCs. After 12 hours of dynamic seeding, 66% (Avance) to 94% (NeuraGen) of the administered dose of MSCs adhered to the nerve substitutes, with a statistically significant higher efficiency for the NeuraGen Nerve Guide. The vast majority of adhered MSCs survived and were distributed in a uniform manner among the surface of both nerve substitutes and did not migrate into the nerve or collagen material. Future human or animal studies will permit determination of the effects of MSCs seeded on nerve graft substitutes on motor regeneration or sensory re-innervation in large nerve deficits.

Conflicts of interest

The authors have nothing to disclose. This study was funded by the NIH R01, 'Bridging the gap: angiogenesis and stem cell seeding of processed nerve allograft'. 1 RO1 NS102360-01A1

The Avance® Nerve Grafts used in this study were provided by AxoGen Inc., Alachua, Florida, USA. The NeuraGen® Nerve Guides used in this study were provided by Integra LifeSciences Holdings Corporation, Plainsboro, New Jersey, USA.

REFERENCES

1. Lin MY, Manzano G, Gupta R. Nerve allografts and conduits in peripheral nerve repair. Hand Clin 2013: 29: 331-48.
2. Moore AM, Kasukurthi R, Magill CK, et al. Limitations of conduits in peripheral nerve repairs. Hand (N Y) 2009: 4: 180-6.
3. Isaacs J, Browne T. Overcoming short gaps in peripheral nerve repair: conduits and human acellular nerve allograft. Hand (N Y) 2014: 9: 131-7.
4. Brooks DN, Weber RV, Chao JD, et al. Processed nerve allografts for peripheral nerve reconstruction: A multicenter study of utilization and outcomes in sensory, mixed, and motor nerve reconstructions. MICROSURGERY 2012: 32: 1-14.
5. Cho MS, Rinker BD, Weber RV, et al. Functional outcome following nerve repair in the upper extremity using processed nerve allograft. J Hand Surg Am 2012: 37: 2340-9.
6. Karabekmez FE, Duymaz A, Moran SL. Early clinical outcomes with the use of decellularized nerve allograft for repair of sensory defects within the hand. Hand (N Y) 2009: 4: 245-9.
7. Rbia N, Shin AY. The Role of Nerve Graft Substitutes in Motor and Mixed Motor/Sensory Peripheral Nerve Injuries. J Hand Surg Am 2017: 42: 367-77.
8. Rinker B, Zoldos J, Weber RV, et al. Use of Processed Nerve Allografts to Repair Nerve Injuries Greater Than 25 mm in the Hand. Ann Plast Surg 2017: 78: S292-s95.
9. Whitlock EL, Tuffaha SH, Luciano JP, et al. Processed allografts and type I collagen conduits for repair of peripheral nerve gaps. Muscle Nerve 2009: 39: 787-99.
10. Pfister LA, Papaloizos M, Merkle HP, Gander B. Nerve conduits and growth factor delivery in peripheral nerve repair. J Peripher Nerv Syst 2007: 12: 65-82.
11. Cui Y, Yao Y, Zhao Y, et al. Functional collagen conduits combined with human mesenchymal stem cells promote regeneration after sciatic nerve transection in dogs. J Tissue Eng Regen Med 2018: 12: 1285-96.
12. Hsueh YY, Chang YJ, Huang TC, et al. Functional recoveries of sciatic nerve regeneration by combining chitosan-coated conduit and neurosphere cells induced from adipose-derived stem cells. Biomaterials 2014: 35: 2234-44.
13. Ao Q, Fung CK, Tsui AY, et al. The regeneration of transected sciatic nerves of adult rats using chitosan nerve conduits seeded with bone marrow stromal cell-derived Schwann cells. Biomaterials 2011: 32: 787-96.
14. di Summa PG, Kingham PJ, Campisi CC, Raffoul W, Kalbermatten DF. Collagen (NeuraGen(R)) nerve conduits and stem cells for peripheral nerve gap repair. Neurosci Lett 2014: 572: 26-31.
15. Brenner MJ, Lowe JB, 3rd, Fox IK, et al. Effects of Schwann cells and donor antigen on long-nerve allograft regeneration. Microsurgery 2005: 25: 61-70.
16. Ogden MA, Feng FY, Myckatyn TM, et al. Safe injection of cultured schwann cells into peripheral nerve allografts. Microsurgery 2000: 20: 314-23.
17. Hess JR, Brenner MJ, Fox IK, et al. Use of cold-preserved allografts seeded with autologous Schwann cells in the treatment of a long-gap peripheral nerve injury. Plast Reconstr Surg 2007: 119: 246-59.
18. Wang Y, Zhao Z, Ren Z, et al. Recellularized nerve allografts with differentiated mesenchymal stem cells promote peripheral nerve regeneration. Neurosci Lett 2012: 514: 96-101.
19. Rbia N, Bulstra LF, Lewallen EA, et al. Seeding decellularized nerve allografts with adipose-derived mesenchymal stromal cells: An in vitro analysis of the gene expression and growth factors produced. J Plast Reconstr Aesthet Surg 2019: 72: 1316-25.
20. Mathot F, Rbia N, Thaler R, et al. Gene expression profiles of differentiated and undifferentiated adipose derived mesenchymal stem cells dynamically seeded onto a processed nerve allograft. Gene 2020: 724: 144151.
21. Onishi K, Jones DL, Riester SM, et al. Human Adipose-Derived Mesenchymal Stromal/Stem Cells Remain Viable and Metabolically Active Following Needle Passage. Pm r 2016: 8: 844-54.

22. Jesuraj NJ, Santosa KB, Newton P, et al. A systematic evaluation of Schwann cell injection into acellular cold-preserved nerve grafts. J Neurosci Methods 2011: 197: 209-15.
23. Garvican ER, Cree S, Bull L, Smith RK, Dudhia J. Viability of equine mesenchymal stem cells during transport and implantation. Stem Cell Res Ther 2014: 5: 94.
24. Agashi K, Chau DY, Shakesheff KM. The effect of delivery via narrow-bore needles on mesenchymal cells. Regen Med 2009: 4: 49-64.
25. Mamidi MK, Singh G, Husin JM, et al. Impact of passing mesenchymal stem cells through smaller bore size needles for subsequent use in patients for clinical or cosmetic indications. J Transl Med 2012: 10: 229.
26. Thompson MJ, Patel G, Isaacs J, et al. Introduction of neurosupportive cells into processed acellular nerve allografts results in greater number and more even distribution when injected compared to soaking techniques. Neurol Res 2017: 39: 189-97.
27. Rbia N, Bulstra LF, Bishop AT, van Wijnen AJ, Shin AY. A simple dynamic strategy to deliver stem cells to decellularized nerve allografts. Plast Reconstr Surg 2018.
28. Mathot F, Rbia N, Bishop AT, et al. Adhesion, distribution, and migration of differentiated and undifferentiated mesenchymal stem cells (MSCs) seeded on nerve allografts. J Plast Reconstr Aesthet Surg 2019.
29. Crespo-Diaz R, Behfar A, Butler GW, et al. Platelet lysate consisting of a natural repair proteome supports human mesenchymal stem cell proliferation and chromosomal stability. Cell Transplant 2011: 20: 797-811.
30. Mader EK, Butler G, Dowdy SC, et al. Optimizing patient derived mesenchymal stem cells as virus carriers for a phase I clinical trial in ovarian cancer. J Transl Med 2013: 11: 20.
31. Mahmoudifar N, Doran PM. Osteogenic differentiation and osteochondral tissue engineering using human adipose-derived stem cells. Biotechnol Prog 2013: 29: 176-85.
32. Villalona GA, Udelsman B, Duncan DR, et al. Cell-seeding techniques in vascular tissue engineering. Tissue Eng Part B Rev 2010: 16: 341-50.
33. Orbay H, Uysal AC, Hyakusoku H, Mizuno H. Differentiated and undifferentiated adipose-derived stem cells improve function in rats with peripheral nerve gaps. J Plast Reconstr Aesthet Surg 2011.
34. Tomita K, Madura T, Sakai Y, et al. Glial differentiation of human adipose-derived stem cells: implications for cell-based transplantation therapy. Neuroscience 2013: 236: 55-65.
35. Caplan AI, Hariri R. Body Management: Mesenchymal Stem Cells Control the Internal Regenerator. Stem Cells Transl Med 2015: 4: 695-701.
36. Caplan AI. Adult Mesenchymal Stem Cells: When, Where, and How. Stem Cells Int 2015: 2015: 628767.
37. Castro-Manrreza ME, Montesinos JJ. Immunoregulation by mesenchymal stem cells: biological aspects and clinical applications. J Immunol Res 2015: 2015: 394917.
38. Ma S, Xie N, Li W, et al. Immunobiology of mesenchymal stem cells. Cell Death Differ 2014: 21: 216-25.
39. Mathot F, Shin AY, Van Wijnen AJ. Targeted stimulation of MSCs in peripheral nerve repair. Gene 2019.
40. Kingham PJ, Kolar MK, Novikova LN, Novikov LN, Wiberg M. Stimulating the neurotrophic and angiogenic properties of human adipose-derived stem cells enhances nerve repair. Stem Cells Dev 2014: 23: 741-54.
41. Liu Y, Zhang Z, Qin Y, et al. A new method for Schwann-like cell differentiation of adipose derived stem cells. Neurosci Lett 2013: 551: 79-83.
42. Rbia N, Bulstra LF, Thaler R, et al. In Vivo Survival of Mesenchymal Stromal Cell-Enhanced Decellularized Nerve Grafts for Segmental Peripheral Nerve Reconstruction. J Hand Surg Am 2019: 44: 514.e1-14.e11.

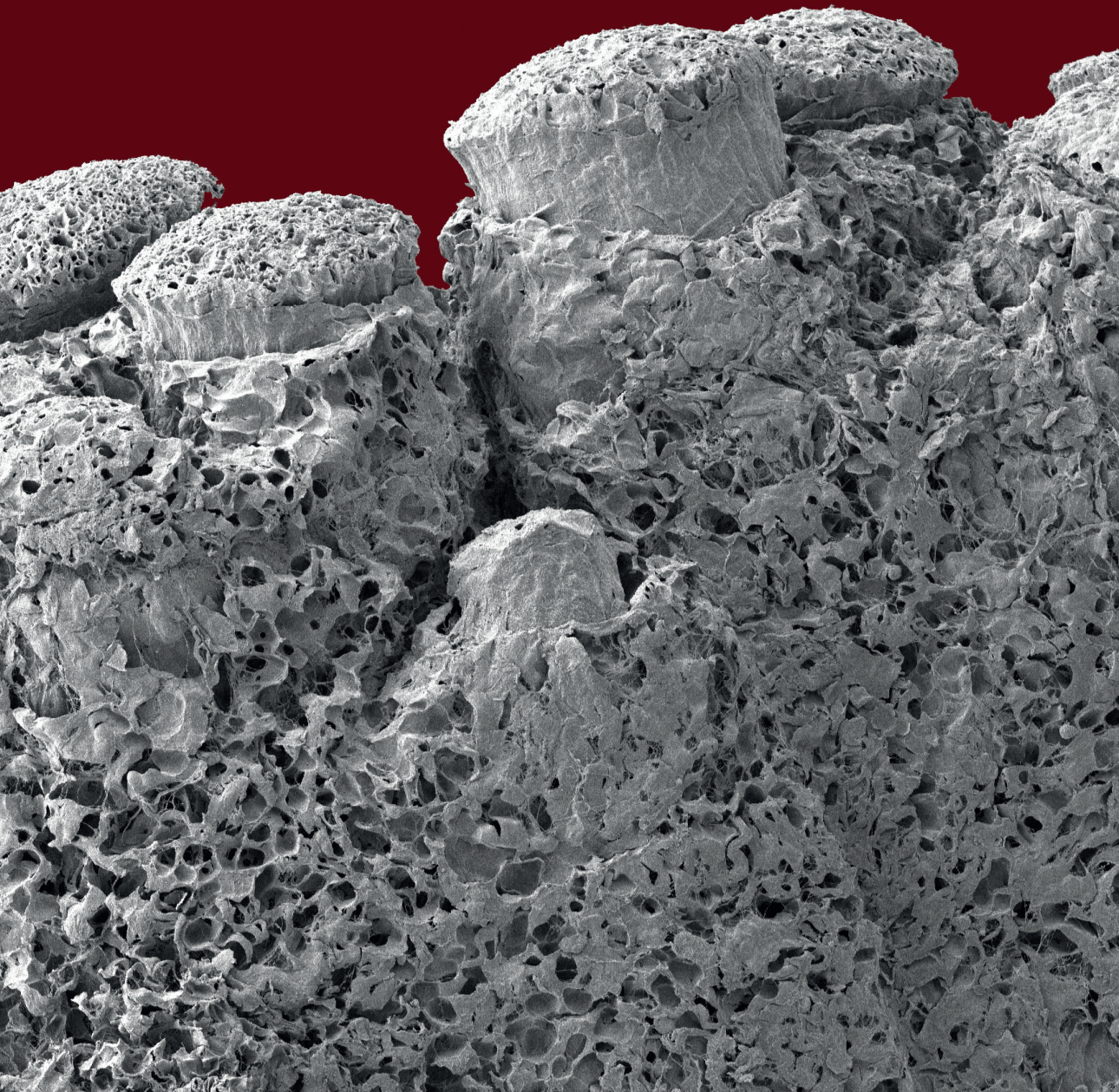

Chapter 9

Gene expression profiles of human adipose-derived mesenchymal stem cells dynamically seeded on clinically available processed nerve allografts and collagen nerve guides

Femke Mathot, Nadia Rbia, Roman Thaler, Allan B. Dietz, Andre J. van Wijnen, Allen T. Bishop, Alexander Y. Shin

Neural Regeneration Research.
2021 August; 16(8):1613-1621

ABSTRACT

Background

As the functional outcome of clinically available nerve graft substitutes remains inadequate to replace the use of autograft nerves in peripheral nerve injuries, it was hypothesized that Mesenchymal Stem Cells (MSCs) could provide the necessary trophic factors when seeded onto the surfaces of these commonly used nerve graft substitutes. We aimed to determine the gene expression of MSCs when influenced by Avance® Nerve Grafts or NeuraGen® Nerve Guides.

Methods

Human adipose derived MSCs were cultured and dynamically seeded onto 30 Avance® Nerve Grafts and 30 NeuraGen® Nerve Guides for 12 hours. At 6 different time points after seeding, qPCR analyses were performed for 5 samples per group. Neurotrophic (NGF, GDNF, PTN, GAP43, BDNF), myelination (PMP22 and MPZ), angiogenic (VEGF-a and PECAM1/CD31), extracellular matrix (ECM) (COL1A1, COL3A1, FBLN1, LAMB2) and cell surface marker (CD96) gene expressions were quantified. Unseeded Avance® Nerve Grafts and NeuraGen® Nerve Guides were used to evaluate the baseline gene expression, and unseeded MSCs provided the reference gene expression of MSCs.

Results

The interaction of MSCs with the Avance® Nerve Grafts led to a short-term upregulation of neurotrophic (NGF, GDNF and BDNF), myelination (PMP22 and MPZ) and angiogenic genes (CD31 and VEGF-a) and a long-term upregulation of BDNF, VEGF-a and COL1A1. The interaction between MSCs and the NeuraGen® Nerve Guide led to short term upregulation of neurotrophic (NGF, GDNF and BDNF) myelination (PMP22 and MPZ), angiogenic (CD31 and VEGF-a), ECM (COL1A1) and cell surface (CD96) genes and long-term upregulation of neurotrophic (GDNF and BDNF), angiogenic (CD31 and VEGF-a), ECM genes (COL1A1, COL3A1, FBLN1) and cell surface (CD96) genes. Analysis demonstrated MSCs seeded onto NeuraGen® Nerve Guides expressed significantly higher levels of neurotrophic (PTN), angiogenic (VEGF-a) and ECM (COL3A1, FBLN1) genes on the long term compared to MSCs seeded onto Avance® Nerve Grafts.

Conclusion

The interaction between human MSCs and Avance® Nerve Grafts and NeuraGen® Nerve Guides resulted in a significant upregulation of the expression of numerous genes important for nerve regeneration over time. The in vitro interaction of MSCs with the NeuraGen® Nerve Guide was more pronounced, particularly in the long term (>14 days after seeding). These results suggest that MSC-seeding has potential to be applied in a clinical setting, which needs to be confirmed in future in vitro and in vivo research.

INTRODUCTION

Peripheral nerve injuries result in a major social and economic burden by causing loss of function of target muscles.[1-3] In order to restore nerve function when the nerve gap is not suitable for direct end to end coaptation, (sensory) autografts, allografts and artificial guides can be used to bridge the gap. While resulting in optimal recovery rates, autograft nerve options are limited in diameter and length and associated with donor side morbidity.[4] Avance® Nerve Grafts and NeuraGen® Nerve Guides are commercially available nerve substitutes, approved for clinical use and are theoretically unlimited in supply. If their clinical outcome would be similar to autografts, these nerve graft substitutes may supplant autograft nerves.

Sensory nerve gaps (<2.5cm) can be effectively restored by either nerve conduits or processed nerve allografts [5], but their application in mixed or motor nerve defects with greater defect length and larger diameters results in varying outcomes.[6-9] In daily clinical practice, processed nerve grafts are described to only lead to good outcomes in mixed/motor nerves with maximal gap lengths of 6mm and diameters between 3 and 7mm.[10] In cases that exceed these dimensions, autograft nerves remain the gold standard by surpassing the results of nerve conduits and allografts.[10-12] However, particularly in nerve injuries with large gaps or multiple nerve injuries (i.e. brachial plexus injuries) there are often not enough autologous nerve graft sources to optimally reconstruct the defects.[13]

Seeding of mesenchymal stem cells (MSCs) on nerve graft substitutes may potentially reduce the outcome differences between nerve substitutes and nerve autografts. MSCs can interact with the extracellular matrix (ECM) of the nerve graft substitute to produce trophic factors necessary for tissue regeneration that supplement endogenous trophic sources.[14-18] To benefit from these trophic properties, dynamic seeding of MSCs is beneficial as it permits atraumatic introduction of MSCs to the ECM of graft substitutes prior to implantation while preventing damage to both the cells and the graft substitutes.

In peripheral nerve injury, a defined process occurs commencing from Wallerian degeneration to axonal regeneration and muscle reinnervation. This includes a nine step process from injury to regeneration: 1. response to stimulus (Schwann cells and neurons change their state and become activated, 3-7 days), 2. regional inflammation (macrophage infiltration, 3-7 days), 3. immune response (7 days), 4. cell proliferation (formation of Bunger bands, 3-7 days), 5. cell migration (Schwann cell migration, 7-14 days), 6. axon guidance (7-14 days), 7. myelination (initiated by Schwann Cells, 14 days), 8. extracellular matrix (7-14 days), 9. growth factor activity for axonal regeneration (3-14 days).[19]

To determine the exact potential of MSC-seeding in clinical practice and to understand its mode of action within the described regeneration process, it is essential to elucidate the interaction between human MSCs and the ECM of clinically available nerve substitutes. The purpose of this study was to examine this interaction by measuring expression of mRNA biomarkers for myelination, neurotrophic and angiogenic processes, ECM deposition

and immune responses in human MSCs as a function of time after dynamic seeding onto Avance® Nerve Grafts and NeuraGen® Nerve Guides.

MATERIALS AND METHODS

General design

Human adipose derived mesenchymal stem cells were cultured and seeded onto 30 Avance® Nerve Grafts (AxoGen, Inc., Alachua, Florida, USA) and 30 NeuraGen® Nerve Guides (Integra LifeSciences Corporation, Plainsboro, New Jersey, USA). At 6 different time points after seeding, quantitative polymerase-chain-reaction (qPCR) analyses were performed (5 samples per group). Five additional unseeded Avance® Nerve Grafts and 5 unseeded NeuraGen® Nerve Guides provided the baseline gene expression of the nerve substitutes; 5 samples of unseeded MSCs provided the reference gene expression of MSCs.

Human mesenchymal stem cells

The Mayo Clinical Human Cellular Therapy laboratory (Rochester, Minnesota, USA) provided the human MSCs used in this experiment. They complied with the criteria defined by the International Society for Cellular Therapy.[20] Multi-lineage potential, presence of cell surface markers (CD73, CD90, CD105, CD44, CD14 and CD45) and RNA-sequence transcriptome profiles have all been tested previously.(23-25) MSCs were cultured in growth media composed of Advanced MEM (a-MEM, 1x; Gibco by Life TechnologiesTM, Cat #12492013), 5% platelet lysate (PLTMax®; Mill Creek Life Sciences), 1% penicillin/streptomycin (Penicillin-Streptomycin (10.000 U/mL); Gibco by Life TechnologiesTM Cat #15140148), 1% GlutaMAX (GlutaMAXTM Supplement 100X; Gibco by Life Technologies, Cat #35050061) and 0.2% heparin (Heparin Sodium Injection, USP, 1.000 USP units per mL; NOVAPLUS®). The MSCs were cultured in an incubator at 37°C (5% CO2), growth medium was changed every 72 hours and cells were split at 80% confluence. Passage 5 MSCs were used in this study.[21-23]

Nerve allografts and guides

Avance® Nerve Grafts are human nerve allografts that have been decellularized and irradiated to obtain non-immunogenic, sterile human nerves with remaining ultrastructure. The NeuraGen® Nerve Guides are composed of purified bovine type I collagen and are empty conduits that do not contain any ultrastructure in the central portion of the guide.[24] Both the Avance® Nerve Graft and the NeuraGen® Nerve Guide have been approved by the Food and Drug Administration for human clinical use since 2007 and 2001, respectively.

A total of 35 Avance® Nerve Grafts and 35 NeuraGen® Nerve Guides of 15mm in length were voluntarily provided by Axogen® (Axogen Corporation, Alachua, Florida, USA) and Integra (Integra LifeSciences Corporation, Princeton, New Jersey, USA) respectively. Five samples of each group were used to determine the baseline gene expression and 30 of

each group were used to study the interaction with MSCs over time.

MSC seeding

To seed MSCs on nerve substitutes in a non-traumatic manner, a previously described seeding strategy was applied.[25, 26] Previous studies have demonstrated a 66% and 94% seeding efficiency for the Avance® Nerve Grafts and the NeuraGen® Nerve Guides, respectively.[27] Prior to seeding, the Avance® Nerve Grafts and the NeuraGen® Nerve Guides were soaked in a-MEM to restore the salt balance and to remove any harmful detergents. The nerve substitutes were placed in conical tubes containing 1 million MSCs in 10mL growth medium. The conical tubes were rotated for 12 consecutive hours on a bioreactor placed in a 37°C incubator.

Quantitative PCR analysis

Quantitative PCR analysis was performed on 5 duplicates per group before seeding (n=5 per group, baseline gene expression) and at 6 time points after seeding: directly after seeding, 1 day, 3 days, 7 days, 14 days and 21 days (n=5 per group per time point). Between seeding and qPCR analysis, the samples were placed in wells containing growth media. To determine the baseline gene expression of the MSCs, qPCR analysis was performed on 5 samples of MSCs only.

At each time point, the seeded nerve substitutes were removed from the wells, placed in Qiazol and frozen at -80°C. The seeded nerve substitutes were minced with a sterile needle to ensure the DNA of the MSCs was dissolved in the fluid. Ribonucleic acid (RNA) extraction took place according to the manufacturer's protocol (Direct-zolTM RNA MiniPrep Kit; Zymo Research, Irvine, CA, USA). RNA concentration was measured with the NanoDropTM 2000/2000c Spectrophotometer (ThermoFisher Scientific, Waltham, MA, USA). Subsequently, complementary deoxyribonucleic acid (cDNA) was obtained (SuperScript III, Invitrogen, Carlsbad, CA; 3 minutes at 65°C, 90 minutes at 37°C and 5 minutes at 95°C) and diluted to establish a concentration of 10ng/µL. The obtained cDNA was combined with the selected primers (all manufactured by Sigma, table 1) and real time-qPCR master mix (Qiagen, MD, USA) and amplified by real time-qPCR using a thermocycler (Bio-rad Laboratories, Inc., CA, USA) under the following parameters: 15 minutes at 95°C, followed by 50 cycles of 95°C for 20s, 60°C for 35s and 72°C for 35s. This provided the mRNA expression levels of the investigated genes.

Analysis of mRNA biomarkers

In relation to the described Wallerian degeneration and axon regeneration process, the neurotrophic effects of the interaction between MSCs and nerve substitutes were measured by assessing a panel of mRNA biomarkers, including nerve growth factor (NGF), glial cell line-derived neurotrophic factor (GDNF), pleiotrophin (PTN), growth associated protein 43 (GAP43) and brain-derived neurotrophic factor (BDNF). The expression of myelination marker genes peripheral protein 22 (PMP22) and myelin protein zero (MPZ) were measured. The angiogenic potential of the seeded MSCs was measured by the gene

expression of platelet endothelial cell adhesion molecule 1 (PECAM1/CD31) and vascular endothelial cell growth factor alpha (VEGF1). Establishment of the ECM was assessed by monitoring expression of collagen type I (COL1A1), collagen type III (COL3A1), Fibulin 1 (FBLN1) and laminin subunit beta 2 (LAMB2). Immunoglobulin expression was determined by quantification of cluster of differentiation 96 (CD96), a cell surface marker.

Both Glyceraldehyde-3-Phosphate Dehydrogenase (GAPDH) and AKT Serine/Threonine Kinase 1 (AKT1) were used as reference genes. Expression of the AKT1 gene was determined to be more stable and considered the most optimal housekeeping gene based on BestKeeper analysis and therefore was used as reference gene in the analysis.[28] The 2-ΔΔCT method was used to calculate the mRNA levels which were expressed as a ratio of AKT1.[29-31] Primer sequences for each of the genes that were analyzed are displayed in **table 1**.

Gene ID	Biology	Forward primer	Reverse primer
NGF	Neurotropic marker	ATACAGGCGGAACCACACTCAG	ATACAGGCGGAACCACACTCAG
GDNF	Neurotropic marker	CACCAGATAAACAAATGGCAGTGC	CACCAGATAAACAAATGGCAGTGC
PTN	Neurotropic marker	ACTGGAAGTCTGAAGCGAGC	CTTCTTCTTAGATTCTGCTTGAGGT
GAP43	Neurotropic marker	GTCCACTTTCCTCTCTATTTC	TGTTCATTCCATCACATTGA
BDNF	Neurotropic marker	AGAGGCTTGACATCATTGGCTG	CAAAGGCACTTGACTACTGAGCATC
PMP22	Myelination marker	GTTAAAGGGAACGCCAGGA	AGTTTCTGCAGCCCAAAGGA
MPZ	Myelination marker	GAGGAGGCTCAGTGCTATGG	GCCCGCTAACCGCTATTTCT
VEGF-a	Angiogenic marker	ATCTGCATGGTGATGTTGGA	GGGCAGAATCATCACGAAG
PECAM/ CD31	Angiogenic marker	AACAGTGTTGACATGAAGAGCC	AACAGTGTTGACATGAAGAGCC
COL1A1	ECM protein	GTAACAGCGGTGAACCTGG	CCTCGCTTTCCTTCCTCTCC
COL3A1	ECM protein	TTGAAGGAGGATGTTCCCATCT	ACAGACACATATTTGGCATGGTT
FBLN1	ECM protein	AGAGCTGCGAGTACAGCCT	CGACATCCAAATCTCCGGTCT
LAMB2	ECM protein	ACACGCAAGCGAGTGTATGA	AATCACAGGGCAGGCATTCA
CD96	Cell surface marker / immunoglobulin	AGATTGTGTGATGAAGGACATGG	AGATTGTGTGATGAAGGACATGG
AKT1	Household gene	ATGGCGCTGAGATTGTGTCA	CCCGGTACACCACGTTCTTC
GAPDH	Household gene	CCCGGTACACCACGTTCTTC	TGTGGTCATGAGTCCTTCCA

Table 1. mRNA primer sequences. ECM = extracellular matrix.
NGF = nerve growth factor, GDNF = glial cell line-derived neurotrophic factor, PTN = pleiotrophin, GAP43 = growth associated protein 43, BDNF = brain-derived neurotrophic factor, PMP22 = peripheral myelin protein 22, MPZ = myelin protein zero, VEGF-a = vascular endothelial cell growth factor alpha, PECAM = platelet endothelial cell adhesion molecule 1, COL1A1 = collagen tpe 1, COL3A1 = collagen type III, FBLN1 = fibulin 1, LAMB2 = laminin beta 2 subunit, CD96 = cluster of differentiation 96, AKT1 = threonine kinase 1, GAPDH = glyceraldehyde-3-phosphate dehydrogenase.

Statistical analysis

The gene expression profiles of the seeded MSCs on both nerve substitutes were expressed as a ratio of the average gene expression of unseeded MSCs (= reference group). Gene expression ratios of MSCs seeded onto Avance® Nerve Grafts were compared to gene expression ratios of MSCs seeded onto NeuraGen® Nerve Guides over time and were analyzed using a 2-factor ANOVA with repeated measures of one factor, with post-hoc Bonferroni correction. This analysis provided insight in the effects of the type of nerve substitute and the time passed after seeding. All results are expressed as the mean +/- SEM. A $\alpha<0.05$ was considered statistically significant.

RESULTS

Control experiments with nerve substitutes

The presence of RNA was examined in unseeded Avance® Nerve Grafts (n=5) and NeuraGen® Nerve Guides (n=5) and no RNA was detected.

Neurotrophic gene expression (Figure 1)

Expression of five neurotrophic factors (NGF, GDNF, PTN, GAP43 and BDNF) was measured by qPCR to assess whether nerve substitutes can induce neurotrophic factors in MSCs.

Nerve Growth factor (NGF)

NGF is endogenously produced by cells like neurons and Schwann cells and is crucial for neuroplasticity since it promotes neuron maturation and can induce cell repair and apoptosis.[32, 33] The factor time solely had a significant effect on NGF expression ($p<0.001$), while the type of nerve substitute did not ($p=0.228$). Directly after seeding, MSCs on Avance® Nerve Grafts expressed significantly increased levels of NGF compared to MSCs on NeuraGen® Nerve Guides (5.304 ±0.731 versus 2.530 ±0.419, $p<0.001$), while MSCs on NeuraGen® Nerve Guides expressed significantly increased NGF expression ratio 1 day after seeding (1.226 ±0.187 versus 3.868 ±1.379, $p=0.002$). After 1 to 3 days after seeding, the NGF expression of MSCs in both groups was comparable to the expression in unseeded MSCs. Thus, NGF expression is transiently elevated in MSCs seeded onto nerve substitutes shortly after seeding and subsides over time.

Glial cell line-derived neurotrophic factor (GDNF)

GDNF is described to have a crucial role in neuronal migration, proliferation and synaptogenesis.[34, 35] Enhanced GDNF delivery has demonstrated to result in earlier regeneration after nerve crush injuries [36] and its expression decreases coincidentally with the ingrowth of regenerating axons.[35] The GDNF expression ratio of seeded MSCs was significantly affected by culture duration after seeding ($p<0.001$); the expression slowly diminished over time with the exception of GDNF expression after 21 days in MSCs seeded onto Avance® Nerve Grafts. No significant differences were found in GDNF expression between both groups. The GDNF expression curves of both groups approximated the unseeded MSC expression from 1 day onwards.

Pleiotrophin (PTN)
PTN expression was measured as it is involved in neurite outgrowth and synaptogenesis after peripheral nerve injury.[37, 38] The expression ratio of PTN was modulated in MSCs by the type of nerve substitute ($p<0.001$) and by the time after seeding ($p=0.001$). PTN expression decreased up to 7 days after seeding for both groups, after which particularly the PTN expression of MSCs seeded on NeuraGen® Nerve Guides increased again up to 21 days after seeding. The MSCs on the NeuraGen® Nerve Guide expressed a significant higher PTN ratio than MSCs on Avance® Nerve Grafts after 14 (0.590 ±0.151 versus 0.174 ±0.037, $p=0.011$) and 21 days (0.718 ±0.29 versus 0.116 ±0.050, $p<0.001$). Although the PTN expression of MSCs on NeuraGen® Nerve Guides approximated the baseline gene expression of unseeded MSCs after 21 days, measures at all the other time points demonstrated downregulation of the baseline expression.

Growth associated protein 43 (GAP43)
GAP43 expression increases after axotomy, eventually leading to enhanced axon density in regenerating nerve fibers.[39] The GAP43 expression of seeded MSCs was significantly affected by the time after seeding ($p=0.008$) and the type of nerve substitute ($p=0.046$). The GAP43 expression of MSCs on both nerve substitutes increased over time, of which the expression of MSCs on Avance® Nerve Grafts most evenly increased over time. There were no significant differences in GAP43 expression between both nerve substitutes. All measured expression ratios were below 1, implicating downregulation of the baseline GAP43 expression.

Brain-derived Neurotrophic Factor (BDNF)
BDNF induces neuronal cell survival and differentiation and accelerates axonal outgrowth [40], but also is involved in synapse formation.[41, 42] The BDNF expression ratio of seeded MSCs was significantly affected by the time passed after seeding ($p<0.001$). The BDNF expression in MSCs seeded on Avance® Nerve Grafts (3.846 ±0.636) was significantly higher after 14 days compared to the expression in MSCs on NeuraGen® Nerve Guides (1.720 ±0.164)($p=0.020$). The expression ratio in both groups approximated 1 directly after seeding, and increased up to 4 (i.e. a fourfold of the baseline BDNF expression in unseeded MSCs) on various time points in later phases (1 day and 21 days after seeding for the NeuraGen® Nerve Guide, 7, 14 and 21 days after seeding for the Avance® Nerve Grafts).

Myelination gene expression (Figure 2)

Peripheral myelin protein 22 (PMP22)
The PMP22 gene is mainly expressed in Schwann cells and encodes a relatively minor but crucial component of the myelin sheeth.[43] Duplication or deletion of PMP22 leads to demyelination and axon loss, resulting in common demyelinating neuropathies.[44, 45] PMP22 expression ratio was significantly affected by the time after seeding ($p=0.0.26$), but not by the type of nerve substitute ($p=0.542$) on which the MSCs were seeded. The expression ratio started high for both groups (1.90 ±0.231 for Avance® Nerve Grafts, 1.78 ±0.663 for NeuraGen® Nerve Guides) and decreased to a level comparable to unseeded MSCs after 21 days (0.716 ±0.278 for Avance® Nerve Grafts, 0.928 ±0.102 for NeuraGen® Nerve Guides). There were no significant differences between groups over time.

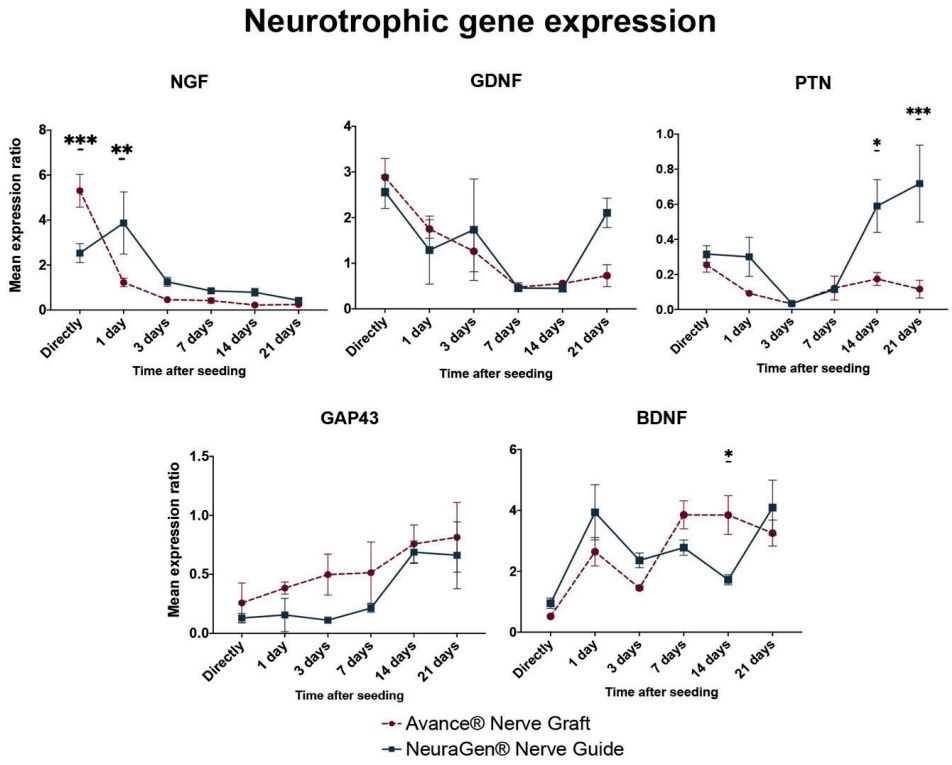

*Figure 1. Gene expression curves of human MSCs seeded onto Avance® Nerve Grafts and NeuraGen® Nerve Guides concerning neurotrophic genes NGF, GDNF, PTN, GAP43 and BDNF at 6 different time points after seeding. * = p<0.05, ** = p<0.01, *** = p<0.001. Error bars = Standard error of the mean*

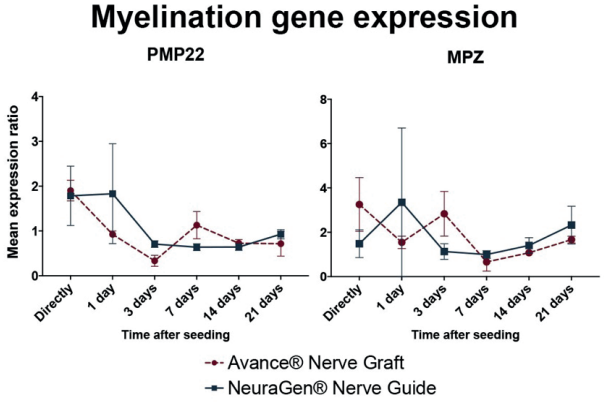

Figure 2. Gene expression curves of MSCs seeded onto Avance® Nerve Grafts and NeuraGen® Nerve Guides concerning myelination genes PMP22 and MPZ at 6 different time points after seeding. Error bars = Standard error of the mean

Myelin protein zero (MPZ)
MPZ is also expressed by Schwann cells and is the main protein of (compact) myelin. Reduced expression of MPZ results in instable myelination, leading to neuropathies and axonal loss. MPZ is therefore pivotal in successful nerve regeneration.[43] The MPZ gene expression ratio was not significantly affected by type of nerve substitute (p=0.936), nor by the time passed after seeding (p=0.650). Compared to the baseline MPZ expression in unseeded MSCs, the expression ratio in both groups was increased both at the beginning (up to 3 days after seeding) and at the end (21 days) of the experiment. There were no significant differences in MPZ expression over time between groups.

Angiogenic gene expression (Figure 3)

Vascular Endothelial Growth Factor alpha (VEGF-a)
Neoangiogenesis occurs from two days onwards after nerve injury and facilitates the delivery of trophic factors at the nerve stump and guides Schwann cells in the right direction.[46-48] Enhanced expression and production of VEGF-A induces local angiogenesis, playing an important role in the peripheral nerve regeneration process.[49] The type of nerve substitute had no significant effect on the VEGF-a expression of seeded MSCs (p=0.107). Time passing did have a significant effect on the VEGF-a expression of seeded MSCs (p<0.001). The VEGF-a expression in both groups was high (4 to 12 fold of the baseline expression) in the first 24 hours after seeding, equal to unseeded MSCs around 3 to 7 days after seeding and then increased again (3 to 8 fold of the baseline expression) up to 21 days after seeding. The VEGF-a expression was significantly higher in the MSCs seeded on NeuraGen® Nerve Guides directly after seeding (11.006 ±0.33 versus 6.698 ±1.502, p=0.020) and 21 days after seeding (8.690 ±2.062 versus 4.118 ±1.847, p=0.011).

Platelet Endothelial Cell Adhesion Molecule (PECAM-1/CD31)
CD31 regulates endothelial cell adhesion, being crucial in the process of angiogenesis.[50] The factor time significantly influenced the CD31 expression ratio (p<0.001), but the type of nerve substitute did not have a significant impact (p=0.77). When comparing groups over time, MSCs seeded onto NeuraGen® Nerve Guides had a significant higher CD31 expression ratio compared to MSCs seeded onto Avance® Nerve Grafts directly after seeding (3.016 ±0.364 versus 1.096 ±0.13, p=0.025) and 21 days after seeding (2.254 ±0.815 versus 0.244 ±0.123, p=0.017). The expression in the NeuraGen® Nerve Guide group was significantly lower than in the Avance® Nerve Graft group 1 day after seeding (p<0.001). With the exception of directly, 1 day and 21 days after seeding, all other time points demonstrated significant downregulation of the baseline CD31 expression of unseeded MSCs.

Extracellular matrix gene expression (Figure 4)

Collagenase type 1 (COL1A1)
The COL1A1 gene encodes for the main component of type 1 collagen. This ECM-component regulates Schwann cell proliferation and differentiation, but overexpression of COL1A1 could

impede axon sprouting by inducing scarring.[51] The time passed after seeding (p=0.014) and the type of nerve substitute (p=0.033) both had a significant effect on the COL1A1 gene expression ratio. Directly after seeding, MSCs on NeuraGen® Nerve Guides (2.468 ±0.064) had a significant higher COL1A1 expression ratio than MSCs on Avance® Nerve Grafts (1.152 ±0.332) (p=0.008). Aside from increased COL1A1 expression directly (NeuraGen® Nerve Guide), 14 (Avance® Nerve Graft) and 21 days (NeuraGen® Nerve Guides) after seeding, the COL1A1 expression in the NeuraGen® Nerve Guide group was comparable to the baseline COL1A1 expression of unseeded MSCs.

Collagenase type 3 (COL3A1)
Just like type 1, collagenase type 3 is a fibril forming collagen and an ECM component in the peripheral nervous system, regulating Schwann cell differentiation and axonal guidance.[51, 52] The COL3A1 gene expression ratio was significantly affected by time after seeding (p<0.001) and the type of nerve substitute (p=0.014). The expression curve of both groups was u-shaped and approximated a ratio of 1 (i.e. comparable to baseline COL3A1 expression), with a significant higher expression ratio of MSCs seeded onto NeuraGen® Nerve Guides after 21 days (1.696 ±0.132 versus 0.664 ±0.192, p<0.001).

Fibulin-1 (FBLN1)
FBLN-1 expression was assessed as it is a component of the perineurium of peripheral nerves and fulfills a axonal guiding and supporting function.[53] Time after seeding (p<0.001) and type of nerve substitute (p=0.002) both significantly affected the FBLN1 expression ratio. When comparing groups over time, the MSCs seeded onto NeuraGen® Nerve Guides had a significant higher FBLN1 expression ratio after 14 (0.760 ±0.193 versus 0.236 ±0.079, p=0.037) and 21 days (1.962 ±0.318 versus 0.340 ±0.183, p<0.001). The expression in the Avance® Nerve Graft group remained low over time, while the expression in the NeuraGen® Nerve Guide group seemed to arise from 7 days onwards, demonstrating significant upregulation of the baseline FBLN1 expression.

Laminin Beta 2 subunit (LAMB2)
LAMB2 is a basis laminin protein that is essential in proper synaptogenesis at neuromuscular junctions.[54] There was no significant effect of either the time passed after seeding (p=0.247) nor the type of nerve substitute (p=0.354). No significant differences between groups occurred over time, while the expression in both groups remained lower than the expression in unseeded MSCs.

Immunoglobulin expression (Figure 5)

Cluster of Differentiation 96 (CD96)
CD96 is an immunoglobulin family member that interferes in the adhesive interactions between cells, in the late phase immune response.[55] Only the factor time significantly affected the CD96 expression rate (p=0.011). 21 days after seeding, the expression in MSCs seeded onto NeuraGen® Nerve Guides (2.226 ±0.443) was significantly higher than the expression

in MSCs seeded onto Avance® Nerve Grafts (1.326 ±0.097, p=0.030). The expression curve of the NeuraGen® Nerve Guide group seemed to increase on the long term, while the expression curve of the Avance® Nerve Graft group remained stable on the long term. The obtained CD96 expressions demonstrated a slight upregulation in comparison to baseline gene expression of unseeded MSCs at most time points.

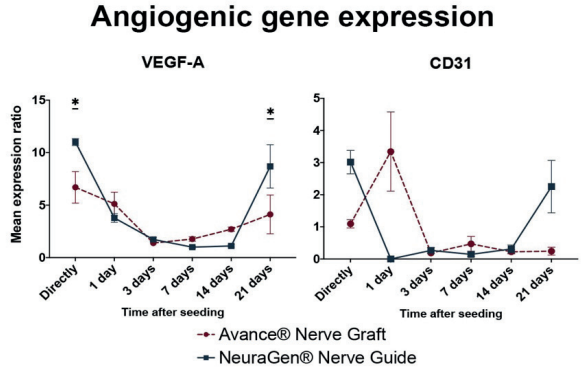

Figure 3. Gene expression curves of MSCs seeded onto Avance® Nerve Grafts and NeuraGen® Nerve Guides concerning angiogenic genes VEGF-a and CD31 at 6 different time points after seeding.
** = p<0.05, Error bars = Standard error of the mean*

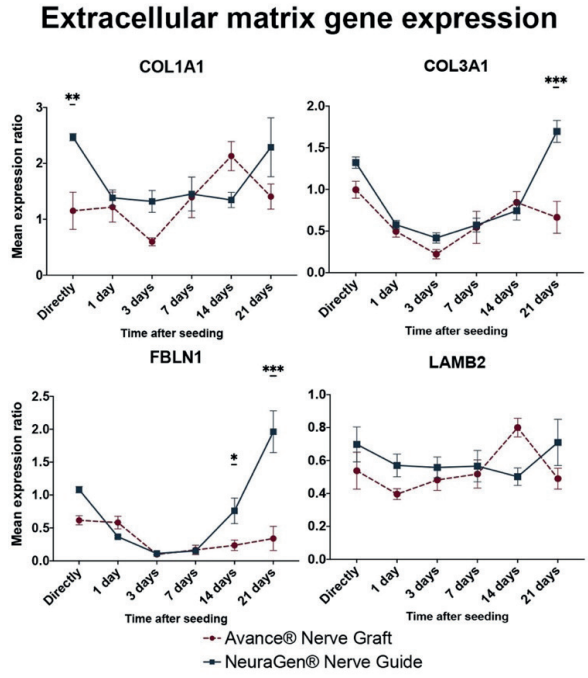

Figure 4. Gene expression curves of MSCs seeded onto Avance® Nerve Grafts and NeuraGen® Nerve Guides concerning extracellular matrix genes COL1A1, COL3A1, FBLN1 and LAMB2 at 6 different time points after seeding.
*** = p<0.01, *** = p<0.001, Error bars = Standard error of the mean*

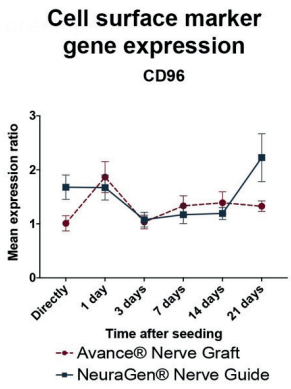

Figure 5. Gene expression curve of MSCs seeded onto Avance® Nerve Grafts and NeuraGen® Nerve Guides concerning the immunoglobulin marker CD96 at 6 different time points after seeding.
Error bars = Standard error of the mean

DISCUSSION

Secondary to their regenerative ability, MSCs are of broad biomedical relevance.[56-62] While differentiation of MSCs into specific cell types (i.e. differentiation into Schwann type cells) has been described as one mode of action [63, 64], secretion of essential trophic factors is a functionally different and possible more plausible explanation for their regenerative capacities.[14, 16, 65, 66] This putative tissue-specific trophic expression of MSCs occurs in response to cues from their micro-environment.[18, 67, 68]

In this study, gene expression profiles of human MSCs seeded onto Avance® Nerve Grafts and NeuraGen® Nerve Guides were examined over time in order to provide mechanistic insight in the interaction of MSCs seeded on nerve substitutes. Expression curves of a select panel of prominent neurotrophic, myelination, angiogenic, ECM and cell surface marker/immunoglobulin genes have been analyzed.

The displayed gene expressions of seeded MSCs are all expressed as a ratio of the gene expression in unseeded MSCs, the reference group. Considering a gene expression ratio of 1.0 meaning that the interaction between MSCs and the nerve substitutes did not result in changes in gene expression, one could argue that the interaction of MSCs with the Avance® Nerve Grafts leads to a clear upregulation in the first hours to days after seeding of neurotrophic genes NGF, GDNF and BDNF, myelination markers PMP22, MPZ and angiogenic genes CD31 and VEGF-a. In the long term, the interaction between MSCs and the Avance® Nerve Grafts causes an upregulation of BDNF, VEGF-a and COL1A1. The interaction between MSCs and the NeuraGen® Nerve Guide led on the short term to an upregulation of neurotrophic genes NGF, GDNF and BDNF, myelination markers PMP22 and MPZ, angiogenic genes CD31 and VEGF-a, ECM gene COL1A1 and cell surface marker CD96. In the long term, the expression of neurotrophic genes GDNF and BDNF,

angiogenic genes CD31 and VEGF-a, ECM genes COL1A1, COL3A1 and FBLN1 and cell surface marker CD96 were all upregulated by the interaction between the MSCs and the NeuraGen® Nerve Guide. Genes of which the expression was downregulated for both groups were PTN, GAP43 and LAMB2. A summary of the described gene expression trends and differences is displayed in **table 2**.

The described steps of Wallerian degeneration and axon regeneration in which the evaluated genes are hypothetically involved are illustrated in **figure 6**. It displays the proposed mechanism of MSC-seeding; MSCs are seeded on the outer surface, gene expression of the MSCs is changed by the ECM, resulting in production of trophic factors that are involved in Wallerian degeneration and axon regeneration inside the nerve substitutes.

Gene ID	Biology	Short term (0 - 24 hours)			Long term (14 - 21 days)		
		Avance®	NeuraGen®	Significance	Avance®	NeuraGen®	Signifi-cance
NGF	Neurotrophic marker	↑↑	↑↑	*** / **	↓↓	↓↓	- / -
GDNF	Neurotrophic marker	↑↑	↑↑	- / -	≈	↑↑	- / -
PTN	Neurotrophic marker	↓↓	↓↓	- / -	↓↓	≈	* / ***
GAP43	Neurotrophic marker	↓↓	↓↓	- / -	↓	↓	- / -
BDNF	Neurotrophic marker	↑	↑↑	- / -	↑↑	↑↑	* / -
PMP22	Myelination marker	↑	↑	- / -	≈	≈	- / -
MPZ	Myelination marker	↑	↑	- / -	↑	↑	- / -
VEGF-a	Angiogenic marker	↑↑	↑↑↑	* / -	↑↑	↑↑↑	- / *
PECAM/ CD31	Angiogenic marker	↑	↑	- / -	↓	↑	- / -
COL1A1	ECM protein	≈	↑	** / -	↑	↑	- / -
COL3A1	ECM protein	≈	↑	- / -	≈	↑	- / ***
FBLN1	ECM protein	↓	≈	- / -	↓	↑	* / ***
LAMB2	Extracellular matrix protein	↓	↓	- / -	↓	↓	- / -
CD96	Cell surface marker / immunoglobulin	↑	↑	- / -	≈	↑	- / -

Table 2. Summary of interaction-induced relative changes in gene expression of human MSCs on the short and long term. The signs under significance display whether there were significant differences between the groups at the first two (directly and 24 hours after seeding, separated by a forward slash) and the final two (14 days and 21 days after seeding, separated by a forward slash) time points.
↑↑↑ = extreme enhancement
↑↑ = moderate enhancement, ↓↓ = moderate reduction
↑ = slight enhancement, ↓ = slight reduction
≈ = no enhancement, no reduction
*- = no significant difference, * = p<0.05, **=p<0.01, ***=p<0.001*

As described NGF, GDNF, PTN, GAP43 and BDNF play a part in the stimulation of axonal outgrowth and the proliferation of neurons and Schwann cells (step 4 and 9, figure 6).[69-71] Previous in vivo research in a rat model demonstrated that particularly NGF is expressed in a significant higher manner in nerve autografts than in decellularized allografts.[72] In our study, NGF and GDNF expression was enhanced in the first 0-24 hours after seeding and the GDNF expression after 21 days seemed to increase again in the NeuraGen® Nerve Guide group. BDNF expression was enhanced in both groups among the entire follow-up period (up to 21 days), but PTN and GAP43 expressions did not increase in comparison to unseeded MSCs (ratio <1.0). The long-term low expression of PTN and GAP43 and the enhanced expression of BDNF after seeding was correspondingly described in in vitro research using human nerve allografts that were processed with elastase and stored at 4°C. In the study of Rbia and colleagues enhanced BDNF expression also led to enhanced levels of BDNF growth factor production. In contradiction to our findings, NGF and GDNF were not enhanced in that particular study, which might be due to differences in the ECM as a result of the different decellularization process.[73] Our results suggests that the interaction between MSCs and the ECM of nerve substitutes stimulates neural proliferation or may enhance neural outgrowth, particularly by upregulation of NGF, GDNF and BDNF.

MPZ and PMP22 are mainly expressed in Schwann cells, which initiate axon myelination, occurring approximately 2 weeks after injury (step 7, figure 6).[19] The short-term (first 24 hours) enhanced expression of PMP22 and MPZ demonstrated in this study corresponds to previous in vitro research using the same seeding strategy on different nerve allografts.[73] Since transdifferentiation into Schwann-like cells is unlikely to have occurred in the described time-span, the elevated level of PMP22 might be subscribed to its role in the development of intercellular junctions.[74] The PMP22 and MPZ expression was not significantly altered on the long term (from 7 days onwards) by the interaction with the nerve substitutes in the current study; this could be due to the absence of Schwann cells in this in vitro setting. Previously, rat autograft nerves did not express significantly different levels of PMP22 and MPZ in vivo than unseeded processed allografts, which could insinuate that these genes are not pivotal for improving nerve regeneration in processed nerve allografts to a level equal to autografts.[72]

VEGF-a functions particularly in axon regeneration and guidance (step 6 and 9, figure 6) by stimulating formation of blood vessels and enhancing Schwann cell and neuron survival.[71, 75] In vivo, rat autograft nerves previously demonstrated to express significantly higher levels of VEGF-a than unseeded processed nerve allografts.[72] The demonstrated upregulation of VEGF-a expression in this study in the first 24 hours and from two weeks onwards after seeding is in accordance with the described nerve regeneration cascade and with previous in vivo research, supporting the role that MSCs can play in revascularization.[72] CD31 is a platelet endothelial cell adhesion molecule (Pecam1) that is required for the motility and organization of endothelial cells, essential for angiogenesis (step 9, figure 6).[76] Autografts do not express significantly different levels of CD31 in vivo than processed nerve allografts.[72] Our data describes enhanced CD31 expression directly after seeding that diminishes after 1 to 3 days after seeding.

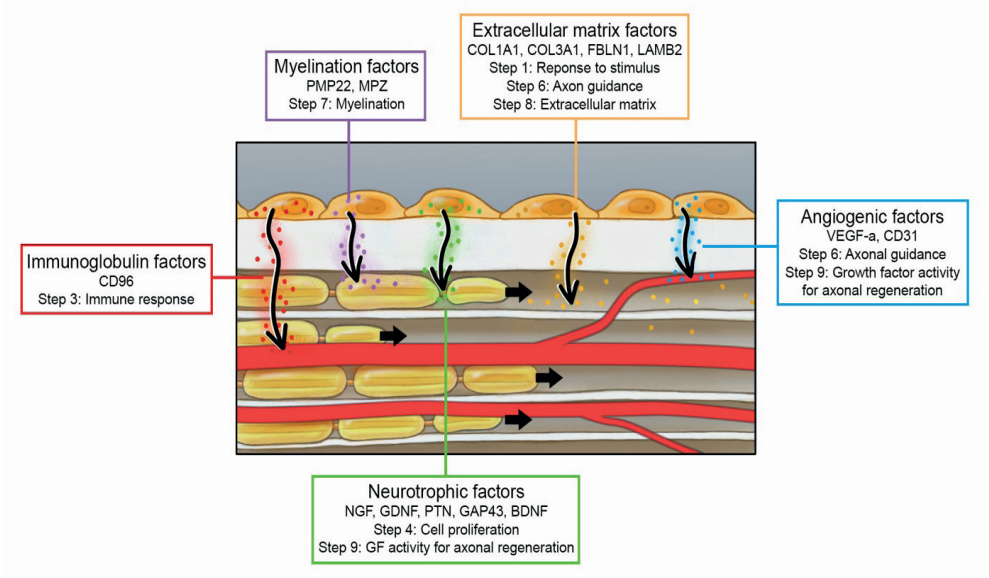

Figure 6. Proposed mechanism of MSC-seeding on nerve substitutes. The interaction between MSCs and the nerve substitute results in changes in gene expression profiles, leading to production of trophic factors that are involved in Wallerian degeneration and axon regeneration.
GF = growth factor

ECM components derived from genes like COL1A1, COL3A1, FBLN1 and LAMB2 are essential for creating a pro-regenerative environment in the early stages after nerve injury and facilitate reinnervation in later stages by guiding the growth cone in the right direction (figure 6).[19, 77] Although autografts previously demonstrated a trend of enhanced expression of these ECM markers in vivo compared to unseeded allografts, none of the differences were statistically significant.[72] In the current study, MSCs seeded onto NeuraGen® Nerve Guides demonstrated a U-shaped expression of COL1A1, COL3A1 and FBLN1, corresponding to the described cascade and previous in vitro studies.[73, 78] Considering the absence of detectable RNA levels of unseeded Avance® Nerve Grafts and NeuraGen® Nerve Guides, the influence of the material components of the nerve substitutes on itself on the ECM gene expression is estimated as negligibly small.

CD96 is a membrane protein that is involved in the late phase immune response by interfering in adhesive interactions between cells (step 3, figure 6), which potentially explains why its expression remains more or less stable over time.[55]

When studying the demonstrated expression curves, some inconsistent expression ratios can be identified. Measures were taken to minimize the vulnerabilities during the obtainment of the mRNA levels like using five replicates per time point, a stable reference gene and experienced researchers. Besides, not all these inconsistent ratios differ significantly from the measures before and after that specific time point. Studying the demonstrated expression

curves, we identified four general trends; a linear decline (NGF, GDNF, CD31) a linear increase (PTN, GAP43, BDNF), a stable curve (PMP22, MPZ, COL1A1, LAMB2, CD96) and a U-shaped curve (VEGF-a, COL3A1, FBLN1). We believe that those trends are more reliable and therefore a more important finding than the individual expression ratios at each of the time points.

The in vitro setting of our study does not provide the required micro-environmental signals that are essential to mimic the described regeneration cascade. Studying the effects on gene expression that is solely caused by the interaction between MSCs and nerve substitutes, does demonstrate the potential of MSCs to interfere in the previously mentioned cascade steps when dynamically seeded on the outer surface of clinically available nerve graft substitutes. It is recognized that corroborating the mRNA expression changes to protein expression changes could have contributed to the described findings. However, measuring protein levels is a costly technique, vulnerable to flaws and the absence of environmental regenerative signals in vitro would have resulted in outcomes that cannot per definition be related to in vivo protein expression and would still need translation to an in vivo model. Therefore, this study is used to demonstrate that interaction between MSCs and the nerve substitutes occurs, effects a wide range of genes and that it lasts on the long term, while limiting the costs and still preventing unnecessary sacrifices of extra animals in the future.

Although it was hypothesized that the biological composition of the Avance® Nerve Grafts (i.e. neural tissue) would lead to more expression of neurotrophic genes in MSCs, analysis demonstrated that the MSCs seeded onto NeuraGen® Nerve Guides expressed higher levels of neurotrophic (GDNF and PTN), angiogenic (CD31 and VEGF-a), ECM (COL3A1 and FBLN1) and immunoglobulin (CD96) genes. Higher seeding efficiency and a different composition of the guide may have resulted in improved sustainability of the graft/MSCs in vitro and better cell proliferation in the long-term, leading to the described enhanced gene expressions. Most neurotrophic factors mediate other processes that are not involved in nerve regeneration which could explain enhanced gene expression levels in the absence of any neural material in the NeuraGen® Nerve Guide group.[13]

While our data suggest that nerve autograft substitutes could benefit from the addition of MSCs, future studies are necessary to determine gene expression patterns and the resulting trophic factor production of MSCs in the presence of injured nerve tissue. Furthermore, the in vivo effects on functional outcomes of the described interactions need to be correlated and compared to determine the clinical relevance of our findings.

CONCLUSION

When human MSCs are dynamically seeded onto the surfaces of Avance® Nerve Grafts and NeuraGen® Nerve Guides, their interaction with the ECM of these nerve substitutes results in a change and mostly an upregulation of the expression of numerous genes important for nerve regeneration over time. The in vitro interaction of MSCs with the NeuraGen® Nerve

Guide is greater than the Avance® Nerve Grafts, particularly in the long-term (>14 days after seeding). Future studies should focus on translation to an in vivo model to confirm the potential of the described techniques and mRNA expression changes for clinical application.

REFERENCES

1. Hong TS, Tian A, Sachar R, et al. Indirect Cost of Traumatic Brachial Plexus Injuries in the United States. J Bone Joint Surg Am 2019: 101: e80.
2. Landers ZA, Jethanandani R, Lee SK, et al. The Psychological Impact of Adult Traumatic Brachial Plexus Injury. J Hand Surg Am 2018: 43: 950.e1-50.e6.
3. Karsy M, Watkins R, Jensen MR, et al. Trends and Cost Analysis of Upper Extremity Nerve Injury Using the National (Nationwide) Inpatient Sample. World Neurosurg 2019: 123: e488-e500.
4. FF IJ, Nicolai JP, Meek MF. Sural nerve donor-site morbidity: thirty-four years of follow-up. Ann Plast Surg 2006: 57: 391-5.
5. Rbia N, Bulstra LF, Saffari TM, Hovius SER, Shin AY. Collagen Nerve Conduits and Processed Nerve Allografts for the Reconstruction of Digital Nerve Gaps: A Single-Institution Case Series and Review of the Literature. World Neurosurg 2019: 127: e1176-e84.
6. Moore AM, Kasukurthi R, Magill CK, et al. Limitations of conduits in peripheral nerve repairs. Hand (N Y) 2009: 4: 180-6.
7. Safa B, Shores JT, Ingari JV, et al. Recovery of Motor Function after Mixed and Motor Nerve Repair with Processed Nerve Allograft. Plast Reconstr Surg Glob Open 2019: 7: e2163.
8. Brooks DN, Weber RV, Chao JD, et al. Processed nerve allografts for peripheral nerve reconstruction: a multicenter study of utilization and outcomes in sensory, mixed, and motor nerve reconstructions. Microsurgery 2012: 32: 1-14.
9. Safa B, Jain S, Desai MJ, et al. Peripheral nerve repair throughout the body with processed nerve allografts: Results from a large multicenter study. Microsurgery 2020.
10. Rbia N, Shin AY. The Role of Nerve Graft Substitutes in Motor and Mixed Motor/Sensory Peripheral Nerve Injuries. J Hand Surg Am 2017: 42: 367-77.
11. Lin MY, Manzano G, Gupta R. Nerve allografts and conduits in peripheral nerve repair. Hand Clin 2013: 29: 331-48.
12. Whitlock EL, Tuffaha SH, Luciano JP, et al. Processed allografts and type I collagen conduits for repair of peripheral nerve gaps. Muscle Nerve 2009: 39: 787-99.
13. Gordon T. The role of neurotrophic factors in nerve regeneration. Neurosurg Focus 2009: 26: E3.
14. Caplan AI. Adult Mesenchymal Stem Cells: When, Where, and How. Stem Cells Int 2015: 2015: 628767.
15. Cao F, Liu T, Xu Y, Xu D, Feng S. Culture and properties of adipose-derived mesenchymal stem cells: characteristics in vitro and immunosuppression in vivo. Int J Clin Exp Pathol 2015: 8: 7694-709.
16. Caplan AI, Hariri R. Body Management: Mesenchymal Stem Cells Control the Internal Regenerator. Stem Cells Transl Med 2015: 4: 695-701.
17. Salgado AJ, Reis RL, Sousa NJ, Gimble JM. Adipose tissue derived stem cells secretome: soluble factors and their roles in regenerative medicine. Curr Stem Cell Res Ther 2010: 5: 103-10.
18. Mathot F, Shin AY, Van Wijnen AJ. Targeted stimulation of MSCs in peripheral nerve repair. Gene 2019: 710: 17-23.
19. Pan B, Liu Y, Yan JY, et al. Gene expression analysis at multiple time-points identifies key genes for nerve regeneration. Muscle Nerve 2017: 55: 373-83.
20. Dominici M, Le Blanc K, Mueller I, et al. Minimal criteria for defining multipotent mesenchymal stromal cells. The International Society for Cellular Therapy position statement. Cytotherapy 2006: 8: 315-7.
21. Crespo-Diaz R, Behfar A, Butler GW, et al. Platelet lysate consisting of a natural repair proteome supports human mesenchymal stem cell proliferation and chromosomal stability. Cell Transplant 2011: 20: 797-811.
22. Mader EK, Butler G, Dowdy SC, et al. Optimizing patient derived mesenchymal stem cells as virus carriers for a phase I clinical trial in ovarian cancer. J Transl Med 2013: 11: 20.
23. Mahmoudifar N, Doran PM. Osteogenic differentiation and osteochondral tissue engineering

using human adipose-derived stem cells. Biotechnol Prog 2013: 29: 176-85.
24. Meek MF, Coert JH. US Food and Drug Administration /Conformit Europe- approved absorbable nerve conduits for clinical repair of peripheral and cranial nerves. Ann Plast Surg 2008: 60: 466-72.
25. Rbia N, Bulstra LF, Bishop AT, van Wijnen AJ, Shin AY. A simple dynamic strategy to deliver stem cells to decellularized nerve allografts. Plast Reconstr Surg 2018.
26. Mathot F, Rbia N, Bishop AT, et al. Adhesion, distribution, and migration of differentiated and undifferentiated mesenchymal stem cells (MSCs) seeded on nerve allografts. J Plast Reconstr Aesthet Surg 2020: 73: 81-89.
27. Mathot F, Rbia N, Thaler R, et al. Introducing Human Adipose Derived Mesenchymal Stem Cells to Avance® Nerve Grafts and NeuraGen® Nerve Guides. Journal of Plastic, Reconstructive & Aesthetic Surgery : JPRAS 2020: Accepted for publication.
28. Pfaffl MW, Tichopad A, Prgomet C, Neuvians TP. Determination of stable housekeeping genes, differentially regulated target genes and sample integrity: BestKeeper--Excel-based tool using pair-wise correlations. Biotechnol Lett 2004: 26: 509-15.
29. Dudakovic A, Camilleri E, Riester SM, et al. High-resolution molecular validation of self-renewal and spontaneous differentiation in clinical-grade adipose-tissue derived human mesenchymal stem cells. J Cell Biochem 2014: 115: 1816-28.
30. Jesuraj NJ, Santosa KB, Macewan MR, et al. Schwann cells seeded in acellular nerve grafts improve functional recovery. MUSCLE NERVE 2014: 49: 267-76.
31. Livak KJ, Schmittgen TD. Analysis of relative gene expression data using real-time quantitative PCR and the 2(-Delta Delta C(T)) Method. Methods 2001: 25: 402-8.
32. Manni L, Rocco ML, Bianchi P, et al. Nerve growth factor: basic studies and possible therapeutic applications. Growth Factors 2013: 31: 115-22.
33. Aarao TLS, de Sousa JR, Falcao ASC, Falcao LFM, Quaresma JAS. Nerve Growth Factor and Pathogenesis of Leprosy: Review and Update. Front Immunol 2018: 9: 939.
34. Paratcha G, Ledda F. GDNF and GFRalpha: a versatile molecular complex for developing neurons. Trends Neurosci 2008: 31: 384-91.
35. Yamada Y, Shimizu K, Nitta A, et al. Axonal regrowth downregulates the synthesis of glial cell line-derived neurotrophic factor in the lesioned rat sciatic nerve. Neurosci Lett 2004: 364: 11-5.
36. Magill CK, Moore AM, Yan Y, et al. The differential effects of pathway- versus target-derived glial cell line-derived neurotrophic factor on peripheral nerve regeneration. J Neurosurg 2010: 113: 102-9.
37. Jin L, Jianghai C, Juan L, Hao K. Pleiotrophin and peripheral nerve injury. Neurosurg Rev 2009: 32: 387-93.
38. Blondet B, Carpentier G, Lafdil F, Courty J. Pleiotrophin cellular localization in nerve regeneration after peripheral nerve injury. J Histochem Cytochem 2005: 53: 971-7.
39. Ceber M, Sener U, Mihmanli A, et al. The relationship between changes in the expression of growth associated protein-43 and functional recovery of the injured inferior alveolar nerve following transection without repair in adult rats. J Craniomaxillofac Surg 2015: 43: 1906-13.
40. Vogelin E, Baker JM, Gates J, et al. Effects of local continuous release of brain derived neurotrophic factor (BDNF) on peripheral nerve regeneration in a rat model. Exp Neurol 2006: 199: 348-53.
41. Zagrebelsky M, Korte M. Form follows function: BDNF and its involvement in sculpting the function and structure of synapses. Neuropharmacology 2014: 76 Pt C: 628-38.
42. Sendtner M, Holtmann B, Kolbeck R, Thoenen H, Barde YA. Brain-derived neurotrophic factor prevents the death of motoneurons in newborn rats after nerve section. Nature 1992.
43. Scherer SS, Wrabetz L. Molecular mechanisms of inherited demyelinating neuropathies. Glia 2008: 56: 1578-89.
44. Hui-Chou HG, Hashemi SS, Hoke A, Dellon AL. Clinical implications of peripheral myelin protein 22 for nerve compression and neural regeneration: a review. J Reconstr Microsurg 2011: 27:

67-74.
45. Taioli F, Cabrini I, Cavallaro T, Acler M, Fabrizi GM. Inherited demyelinating neuropathies with micromutations of peripheral myelin protein 22 gene. Brain 2011: 134: 608-17.
46. Caillaud M, Richard L, Vallat JM, Desmouliere A, Billet F. Peripheral nerve regeneration and intraneural revascularization. Neural Regen Res 2019: 14: 24-33.
47. Cutting CB, McCarthy JG. Comparison of residual osseous mass between vascularized and nonvascularized onlay bone transfers. Plastic & Reconstructive Surgery 1983: 72: 672-5.
48. Parrinello S, Napoli I, Ribeiro S, et al. EphB signaling directs peripheral nerve regeneration through Sox2-dependent Schwann cell sorting. Cell 2010: 143: 145-55.
49. Nishida Y, Yamada Y, Kanemaru H, et al. Vascularization via activation of VEGF-VEGFR signaling is essential for peripheral nerve regeneration. Biomed Res 2018: 39: 287-94.
50. DeLisser HM, Christofidou-Solomidou M, Strieter RM, et al. Involvement of endothelial PE-CAM-1/CD31 in angiogenesis. Am J Pathol 1997: 151: 671-7.
51. Koopmans G, Hasse B, Sinis N. Chapter 19: The role of collagen in peripheral nerve repair. Int Rev Neurobiol 2009: 87: 363-79.
52. Hubert T, Grimal S, Carroll P, Fichard-Carroll A. Collagens in the developing and diseased nervous system. Cell Mol Life Sci 2009: 66: 1223-38.
53. Miosge N, Gotz W, Sasaki T, et al. The extracellular matrix proteins fibulin-1 and fibulin-2 in the early human embryo. Histochem J 1996: 28: 109-16.
54. Maselli RA, Arredondo J, Ferns MJ, Wollmann RL. Synaptic basal lamina-associated congenital myasthenic syndromes. Ann N Y Acad Sci 2012: 1275: 36-48.
55. Georgiev H, Ravens I, Papadogianni G, Bernhardt G. Coming of Age: CD96 Emerges as Modulator of Immune Responses. Front Immunol 2018: 9: 1072.
56. Hare JM, Fishman JE, Gerstenblith G, et al. Comparison of allogeneic vs autologous bone marrow-derived mesenchymal stem cells delivered by transendocardial injection in patients with ischemic cardiomyopathy: the POSEIDON randomized trial. Jama 2012: 308: 2369-79.
57. Hare JM, DiFede DL, Rieger AC, et al. Randomized Comparison of Allogeneic Versus Autologous Mesenchymal Stem Cells for Nonischemic Dilated Cardiomyopathy: POSEIDON-DCM Trial. J Am Coll Cardiol 2017: 69: 526-37.
58. Mushtaq M, DiFede DL, Golpanian S, et al. Rationale and design of the Percutaneous Stem Cell Injection Delivery Effects on Neomyogenesis in Dilated Cardiomyopathy (the POSEIDON-DCM study): a phase I/II, randomized pilot study of the comparative safety and efficacy of transendocardial injection of autologous mesenchymal stem cell vs. allogeneic mesenchymal stem cells in patients with non-ischemic dilated cardiomyopathy. J Cardiovasc Transl Res 2014: 7: 769-80.
59. Shen H, Wang Y, Zhang Z, et al. Mesenchymal Stem Cells for Cardiac Regenerative Therapy: Optimization of Cell Differentiation Strategy. Stem Cells Int 2015: 2015: 524756.
60. Koga H, Muneta T, Nagase T, et al. Comparison of mesenchymal tissues-derived stem cells for in vivo chondrogenesis: suitable conditions for cell therapy of cartilage defects in rabbit. Cell Tissue Res 2008: 333: 207-15.
61. Sutton MT, Fletcher D, Ghosh SK, et al. Antimicrobial Properties of Mesenchymal Stem Cells: Therapeutic Potential for Cystic Fibrosis Infection, and Treatment. Stem Cells Int 2016: 2016: 5303048.
62. Sutton MT, Fletcher D, Episalla N, et al. Mesenchymal Stem Cell Soluble Mediators and Cystic Fibrosis. J Stem Cell Res Ther 2017: 7.
63. Orbay H, Uysal AC, Hyakusoku H, Mizuno H. Differentiated and undifferentiated adipose-derived stem cells improve function in rats with peripheral nerve gaps. J Plast Reconstr Aesthet Surg 2011.
64. Tomita K, Madura T, Sakai Y, et al. Glial differentiation of human adipose-derived stem cells: implications for cell-based transplantation therapy. Neuroscience 2013: 236: 55-65.
65. Castro-Manrreza ME, Montesinos JJ. Immunoregulation by mesenchymal stem cells: biological aspects and clinical applications. J Immunol Res 2015: 2015: 394917.

66. Ma S, Xie N, Li W, et al. Immunobiology of mesenchymal stem cells. Cell Death Differ 2014: 21: 216-25.
67. Kingham PJ, Kolar MK, Novikova LN, Novikov LN, Wiberg M. Stimulating the neurotrophic and angiogenic properties of human adipose-derived stem cells enhances nerve repair. Stem Cells Dev 2014: 23: 741-54.
68. Liu Y, Zhang Z, Qin Y, et al. A new method for Schwann-like cell differentiation of adipose derived stem cells. Neurosci Lett 2013: 551: 79-83.
69. Zhang R, Rosen JM. The role of undifferentiated adipose-derived stem cells in peripheral nerve repair. Neural Regen Res 2018: 13: 757-63.
70. Boyd JG, Gordon T. Neurotrophic factors and their receptors in axonal regeneration and functional recovery after peripheral nerve injury. Mol Neurobiol 2003: 27: 277-324.
71. Hoyng SA, De Winter F, Gnavi S, et al. A comparative morphological, electrophysiological and functional analysis of axon regeneration through peripheral nerve autografts genetically modified to overexpress BDNF, CNTF, GDNF, NGF, NT3 or VEGF. Exp Neurol 2014: 261: 578-93.
72. Rbia N, Bulstra LF, Friedrich PF, et al. Gene expression and growth factor analysis in early nerve regeneration following segmental nerve defect reconstruction with a mesenchymal stromal cell-enhanced decellularized nerve allograft. Plast Reconstr Surg Glob Open 2020: 8: e2579.
73. Rbia N, Bulstra LF, Lewallen EA, et al. Seeding decellularized nerve allografts with adipose-derived mesenchymal stromal cells: An in vitro analysis of the gene expression and growth factors produced. J Plast Reconstr Aesthet Surg 2019: 72: 1316-25.
74. Roux KJ, Amici SA, Notterpek L. The temporospatial expression of peripheral myelin protein 22 at the developing blood-nerve and blood-brain barriers. J Comp Neurol 2004: 474: 578-88.
75. Hobson MI, Green CJ, Terenghi G. VEGF enhances intraneural angiogenesis and improves nerve regeneration after axotomy. J Anat 2000: 197 Pt 4: 591-605.
76. Cao G, O'Brien CD, Zhou Z, et al. Involvement of human PECAM-1 in angiogenesis and in vitro endothelial cell migration. Am J Physiol Cell Physiol 2002: 282: C1181-90.
77. Allodi I, Udina E, Navarro X. Specificity of peripheral nerve regeneration: interactions at the axon level. Prog Neurobiol 2012: 98: 16-37.
78. Mathot F, Rbia N, Thaler R, et al. Gene expression profiles of differentiated and undifferentiated adipose derived mesenchymal stem cells dynamically seeded onto a processed nerve allograft. Gene 2020: 724: 144151.

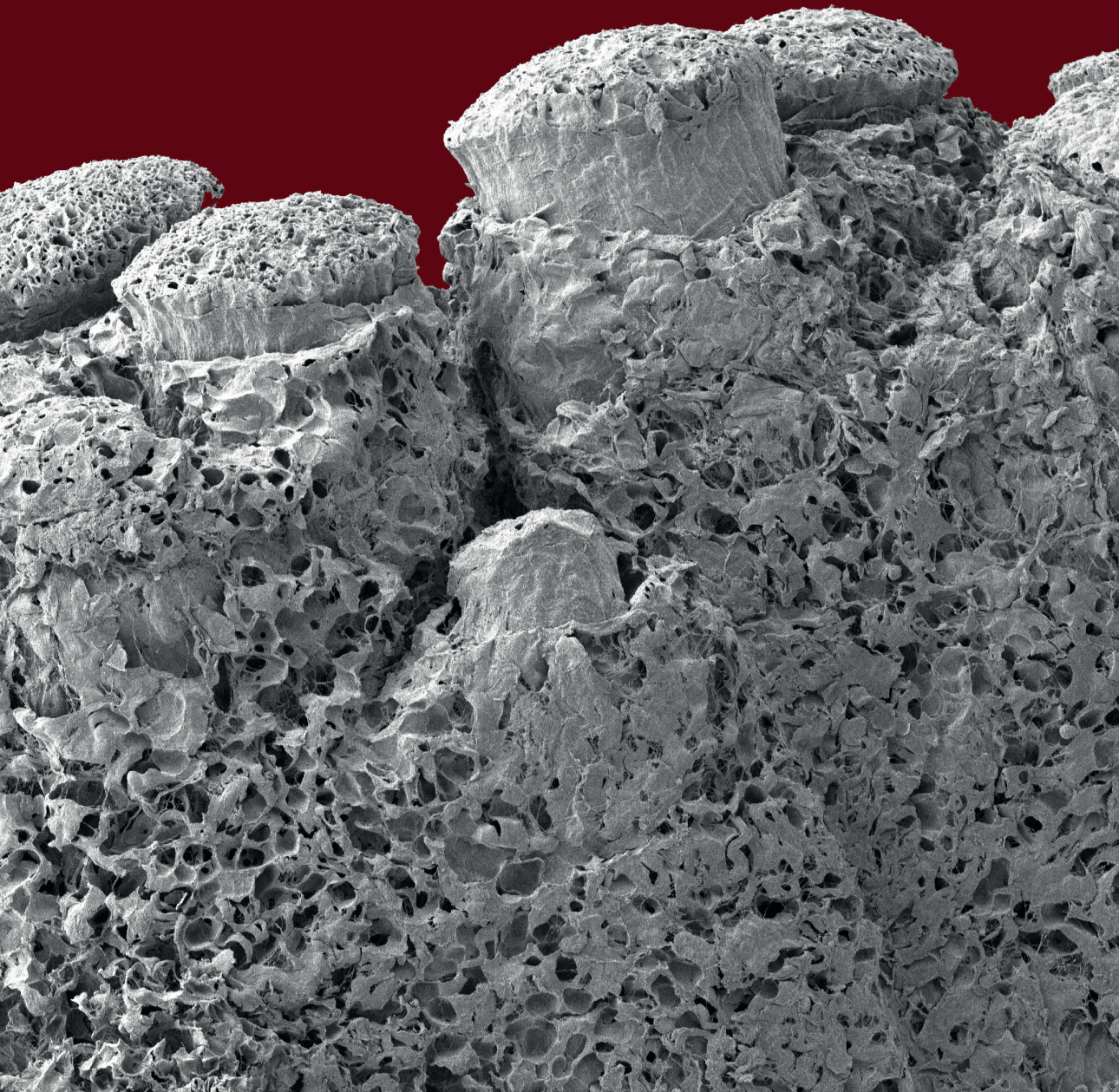

Chapter 10

General discussion and future perspectives

BACKGROUND

Peripheral nerve injuries that have led to nerve gaps not repairable by direct coaptation of both nerve ends need to be bridged by nerve grafts. Ideally these grafts are autografts as they are known to result in the best functional outcomes.[1] However, autografts are not endlessly available and donor site morbidity should be taken into account.[2, 3] The off-the-shelve available nerve allografts currently do not lead to equal results as autograft nerves, hypothetically due to the absence of essential elements like a proficient vascular bed and adequate intrinsic trophic factors. First the role of mesenchymal Stem Cells (MSCs) will be described as they possess trophic capacities and have been hypothesized to be able to fulfill a role in improving the outcomes of nerve allografts. Second our studies to assess vascularization of the allograft will be discussed.

The neural regenerative capacities of mesenchymal stem cells (MSCs) have been extensively tested in the past. Although some results were hopeful, their absence in current clinical practice reveals the continuing uncertainties regarding the ideal delivery strategy, their mechanism of action and perhaps most important their capacities to improve functional outcomes of peripheral nerve repair. This thesis aimed to get more insight in the mechanisms of action of MSCs when delivered to decellularized nerve allografts and conduits with a recently described innovative seeding strategy.[4] The effects on gene expression, vascularity and functionality of undifferentiated MSCs were compared to MSCs differentiated into Schwann cell-like cells and the clinical potential was explored using FDA approved nerve graft substitutes in a study model.

One of the first proposed mechanisms of the MSCs to aide in neural regeneration was their ability to transdifferentiate into cells essential in this process. An often used hypothesis was that MSCs could differentiate into Schwann Cells and thus support and regulate neural regeneration. Over the years, only a few research groups claimed to have proven that delivered MSCs have a structural function, by differentiating into Schwann cells in vivo and by replacing injured cells in the regenerated nerve.[5-7] However, the beneficial effects of delivered MSCs have not been convincingly demonstrated. When studying MSC-dimensions, one could consider that the MSCs are disproportionally big compared to the single nerve fiber/axon on which the MSCs are supposed to exert their effect. Blockage of ingrowing axons and damage to the inner ultrastructure of nerve substitutes are therefore not unthinkable consequences.[8-10] Also, in previous studies MSCs have been mostly delivered inside nerve substitutes by injection. The smaller the injection-needle diameter, the less harm is caused to the ultrastructure of the nerve substitutes. This is opposite to MSC viability: the smaller the needle, the more pressure is built up in the syringe resulting in a more impaired viability of the MSCs.[11-13] Inefficient delivery and fascicle blockage may explain the numerous studies that did not demonstrate a beneficial effect of MSCs delivered inside nerve substitutes despite their differentiational capacities.[14, 15]

Derived from other fields of research, the theory evolved that MSCs can have a trophic effect on regenerating tissues without being built into the new tissue.[16, 17] This trophic theory

is supported by in vitro studies demonstrating improved neurite outgrowth and enhanced levels of trophic factors in culture media in the presence of MSCs.[18-20] Furthermore, studies reported positive effects of MSCs in vivo without confirmed in vivo differentiation or long term survival.[18, 21] This trophic concept led to the insight that MSCs could influence nerve regeneration without being delivered inside nerve grafts. Trophic factors can theoretically penetrate the epineurium by diffusion, just like they do from surrounding vasculature. To avoid injection, dynamic seeding on nerve substitutes was proposed and led to a uniform distribution of MSCs on the outer surface of nerve grafts.[4] Drawbacks of this strategy are the minimal 12 hours needed to let the MSCS adhere to the nerve grafts and the potential vulnerability of the MSCs as they are on the outer surface of the graft during surgery. However, MSCs survived up to 29 days in vivo, implying that they can withstand the mechanical impacts during surgery.[22] Due to its practicability and efficient cell delivery, dynamic seeding is labeled as an effective strategy to non-traumatically adhere MSCs to nerve grafts, after which they ideally exert their trophic function.

IN VITRO RESEARCH

After nerve injury, Schwann cells change to a proliferating state[23, 24], producing trophic factors that contribute to formation of the growth cone, angiogenesis, bands of Büngner and axon regeneration.[25-32] Although undifferentiated MSCs possess trophic characteristics, it is uncertain if they meet up to the trophic levels of Schwann cells normally present at the side of nerve regeneration. Since Schwann cells are essential for nerve regeneration but require autologous nerve tissue, differentiating MSCs into Schwann cell-like cells has been suggested as required addition to processed nerve grafts to hopefully have even greater effects on nerve regeneration than undifferentiated MSCs.[20]

Compared to undifferentiated MSCs, MSCs differentiated into Schwann cell-like cells demonstrated to express enhanced levels of neurotrophic and angiogenic factors in vitro and led to comparable nerve regeneration in vivo in previous studies.[18, 20, 33-36] However, delivery strategies have never been tested on differentiated MSCs in specific. As this is fundamental to fairly compare effects of undifferentiated and differentiated MSCs in vitro and in vivo, both their capabilities to adhere to the surface of decellularized nerve allografts were analyzed in **chapter 3**. This revealed a seeding efficiency of 80% for undifferentiated and 95% for differentiated MSCs. Although not significant, the difference cannot be subscribed to laminin levels, previously described to improve cell attachment, since both cell types expressed comparable levels over time (**chapter 4**).[37] The difference might subjectively be attributed to the tendency of differentiated MSCs to cluster together. The fact that undifferentiated and differentiated MSCs can be equally seeded onto decellularized nerve grafts is essential preliminary knowledge to further fairly compare both cell-types in their capabilities to enhance angiogenesis and nerve regeneration.

In **chapter 4** the genes expressed by the different cell-types at multiple time points after

seeding on a decellularized allograft are described. Environmental signals are absent in this in vitro setting and the actual production of trophic factors was not quantified, but both gene expression profiles were altered by the extracellular matrix of the nerve allografts. The most striking suggestion described in this study, is the different effective phase of undifferentiated and differentiated MSCs. It seemed that undifferentiated MSCs needed some time to interact with the ECM to enhance expression of the appropriate genes, while differentiated MSCs directly expressed enhanced levels of genes essential for nerve regeneration. In accordance to our findings, previous studies also demonstrated that the ECM significantly enhances the neurotrophic characteristics of differentiated MSCs in particular on the short term, but these studies lack long term evaluation points or did not make direct comparisons to undifferentiated MSCs.[20, 37, 38] By all means, the enhanced short-term gene expression of differentiated MSCs and the enhanced long-term gene expression of undifferentiated MSCs perhaps suggest that a cocktail of both undifferentiated and differentiated MSCs together provide a better cover for the trophic factors needed during the entire Wallerian degeneration and axon regeneration process and deserves to be studied in future research.

IN VIVO EVALUATION STRATEGIES OF FUNCTIONAL OUTCOMES

Many measurements to evaluate functional outcome are possible, we however have chosen for compound muscle action potentials (CMAP), isometric tetanic force (ITF), muscle mass and cross-sectional tibial muscle area. Behavioral studies like walking track analysis were deliberately not used to evaluate nerve regeneration since they are very sensitive to several flaws. This includes dependency on walking velocity, weight shifts as a compensatory mechanism, difficulty to acquire representative paw prints and dependency on sensory feedback.[39] Likewise, CMAP and ITF outcomes are affected by electrode placement, manipulation of the nerve which can result in neuropraxia and overstimulation of the nerve and muscle leading to muscle fatigue.[40] However, muscle function was determined to represent the most relevant outcome factor for clinical practice and CMAP, ITF and muscle mass were rated to most optimally represent muscle function. Despite their flaws, we estimated CMAP and ITF to be less vulnerable than behavioral studies and our analyses resulted in significant differences with acceptable standard errors.

The rationale of the non-invasive ultrasound evaluation of cross-sectional tibial muscle area is logical, but it seems to be not sensitive enough to significantly demonstrate subtle cross-sectional muscle area differences within groups in the rat model. Due to its inability to detect differences between groups, it is questionable if the ultrasound technique should be used in future research in rat-models. However, ultrasound evaluation does not require the sacrifice of extra animals, it has great intra-rater and inter-rater reliabilities, it demonstrates regeneration curves and might reveal significant differences in bigger animal/muscle models.[41-43] For future studies in larger muscle models it is therefore still recommended to use this non-invasive muscle function evaluation strategy.

ANGIOGENESIS & GENE EXPRESSION

Our research was aimed to correlate the level of angiogenesis to the expression of angiogenic genes and to describe if the functional outcomes trace back to the demonstrated expression levels of the evaluated trophic genes. To answer these questions the correlations between each of the studied subjects (angiogenesis and gene expression, angiogenesis and functional outcomes, functional outcomes and gene expression) will be discussed sequentially.

Angiogenesis is crucial for the supply of nutrients and trophic factors, but also influences the alignment of bands of Büngner.[30, 31] VEGF-a has been extensively studied and demonstrated to be an indispensable factor in the angiogenesis process and therefore also for nerve regeneration.[31, 44-46] When studying the VEGF-a gene expression of differentiated and undifferentiated MSCs in **chapter 4**, it occurred that the VEGF-a expression of both cell-types was significantly enhanced after interacting with the extracellular matrix of the decellularized nerve graft. For undifferentiated MSCs, this was previously demonstrated in vitro and in vivo while using the same seeding strategy.[47, 48] The VEGF-a expression of differentiated MSCs was significantly higher than of undifferentiated MSCs directly after seeding ($p=0.003$), lower at the longer term time points and approached the expression of undifferentiated MSCs again at 21 days after seeding. Enhanced expression of VEGF-a directly after differentiating MSCs was demonstrated before[18], but longitudinal VEGF-a expression after seeding has not been compared to this extent. Translating these findings to a long-term in vivo model, it was hypothesized that undifferentiated MSCs would enhance vascularization to an equal or even augmented level compared to differentiated MSCs. Although there were no significant differences concerning the level of revascularization between undifferentiated and differentiated MSCs in **chapter 6**, only differentiated MSCs significantly improved vascularization of decellularized allografts. This partly contradicts the expectations based on the demonstrated VEGF-a expressions described in **chapter 4**.

In an attempt to explain the subjective discrepancy between the in vitro and in vivo findings one could argue that the time frame of both studies is completely different. The in vitro data suggested an increasing VEGF-a expression trend in differentiated MSCs from 14 days onwards, while the expression in undifferentiated MSCs slowly decreased from 7 days onwards. The hypothesis that VEGF-a expression of differentiated MSCs will overtake the expression of undifferentiated MSCs on the long term is supported by previous research reporting significantly higher VEGF-a expression in differentiated MSCs after 12 weeks in vivo, which matches our in vivo angiogenesis findings.[49]

The long term follow up in vivo might as well have minimized the between group differences due to the superlative nerve regeneration capacities of rats[50, 51] which could be based on superposed revascularization capacities.[52] Another hypothetical explanation is the absence of environmental signals in the in vitro setting, what might have caused the differentiated MSCs to lose their differentiational state, leading to different gene expression patterns. The differentiational state of MSCs is better preserved in vivo by signals from the surrounding regenerating nerve.[53] Therefore, in vivo outcomes are believed to represent the effects of

differentiated MSCs to a better extent than in vitro outcomes, resulting in the assumption that differentiated MSCs enhance angiogenesis in nerve allografts to a greater extent than undifferentiated MSC.

ANGIOGENESIS & FUNCTIONAL OUTCOMES

The used techniques to measure angiogenesis validated in **chapter 5**, are unique and innovative in describing 2D and 3D angiogenesis. Disadvantages of these techniques are the dependency on the effective pixel size of the used micro CT and adequate injection of the radiopaque compound. However, Microfil® has demonstrated before to reach even the smallest vessels, allowing analysis of the entire vascular network and adequate compound injection can be easily checked at the nailbeds of the rats.[54] Even if no micro CT is available, an impression of the vascular network and analysis of the vascular surface area can be readily obtained with the 2D technique. Although the 2D and 3D techniques cannot be combined with histological analysis of vessels since they require different processing techniques, histological evaluation falls short in quantifying and describing vascularity volumes and vascularization patterns and forms therefore no loss to the evaluation of angiogenesis. Vascular distribution and vessel sizes analyses on micro CT samples could add valuable information about neoangiogenesis in future studies in addition to vascular volume and surface area.

Compared to unseeded, decellularized nerve allografts, both MSC-groups enhanced functional outcomes, which could be allocated to their improved angiogenesis described in **chapter 6**. Since angiogenesis is granted a crucial role in axon guidance and nerve regeneration, it was expected that particularly differentiated MSCs would improve the functional outcomes of nerve allografts. There were no significant differences between the functional outcomes of undifferentiated and differentiated MSCs. However, compared to unseeded allografts, undifferentiated MSCs led to significantly improved CMAP and ITF outcomes, while differentiated MSCs only led to significantly enhanced CMAP outcomes. The small study groups and small animal model can be put forward as explanations that other significant differences were absent.

Although most motor outcomes of both MSC-groups equaled the motor outcomes of nerve autografts, autografts histologically outperformed MSC-seeded allografts despite the comparable or even enhanced level of neoangiogenesis in the MSC-groups. The alignment of the new vasculature can be a clarification to this subtle discrepancy between the level of angiogenesis, the histological outcomes and the functional outcomes, as measured by CMAP, ITF and muscle mass. The vasculature was significantly enhanced in nerve grafts seeded with differentiated MSC in particular, but it led to an extensive, non-aligned network of small vessels. Considering their guiding role, enhanced angiogenesis should lead to improved regeneration, but might be counterproductive if it extents a particular level or becomes less aligned. When subjectively comparing the angiogenesis samples of the MSC-groups and the autograft group, the mal-alignment of vasculature seems to be of greater

extent in the differentiated MSC-group in particular. This might explain the very subtle differences in functional and histological outcomes between both MSC-groups (in benefit for undifferentiated MSCs) and the autografts (in benefit for the autografts). Future studies should focus on ways to quantify vessel diameters and vessel alignment in order to confirm the hypothesis that alignment of vasculature is of major importance for nerve regeneration efficiency.

GENE EXPRESSION & FUNCTIONAL OUTCOMES

Differences in functional outcomes between groups cannot be completely traced back to the level of neoangiogenesis, so other processes and genes must have affected nerve regeneration as well. Since the baseline gene expression of both MSC-groups was significantly altered upon interaction with processed nerve allografts, leading to production of trophic factors, it is very plausible that the MSCs not only have caused enhanced angiogenesis, but improved axon regeneration in its entirety as well. It is impossible to solidly relate the barely differing functional outcomes of differentiated and undifferentiated MSCs to each of the individual gene expression curves. Expression curves of PTN, GAP43, NGF, FBLN1 and CCNB2 particularly differed between undifferentiated and differentiated MSCs in vitro, mostly in benefit for differentiated MSCs. Although these differences apparently do not lead to significantly enhanced nerve regeneration, one should not jump to the conclusion that these genes don't significantly affect nerve regeneration. The subtle discrepancies between in vitro gene expression and functional outcomes in vivo are the consequence of limited numbers per group, enormous differences in signals from surrounding tissues between in vitro and in vivo settings and the completely different time frames of both studies.

The different effective phases of both cell types suggested by their gene expression in **chapter 4**, might be relatable to the demonstrated tibial muscle area recovery over time. The degeneration of tibial muscles in the groups treated with differentiated MSCs only seems to occur in the first two weeks after surgery after which muscle area increases again, while in the undifferentiated MSC-group the muscle degeneration continued until four weeks after surgery. This might be due to differentiated MSCs being able to interact faster with the ECM than undifferentiated MSCs, although none of the muscle area differences between groups were significant.

In contradiction to undifferentiated MSCs[22], in vivo survivability of dynamically seeded differentiated MSCs has not been studied yet. Although differentiation of MSCs sensitizes MSCs to toxic effects[55], it has been suggested that differentiated MSCs possess even greater survivability than undifferentiated MSCs.[6] The significant improvement of functional outcomes of nerve allografts by both cell types and the absence of significant differences between undifferentiated and differentiated MSCs described in **chapter 7** are in accordance with these findings, suggesting at least sufficient survivability of both cell types to exert their effect. Nevertheless, it would be interesting to analyze the relation of vitality and survivability of both cell types and functional outcomes in future in vivo studies.

BENCH TO BEDSIDE TRANSLATION

Considering the discussed gene expression profiles and their effect on angiogenesis, nerve regeneration and functional outcome, no scientifically funded specific preference can be expressed for either undifferentiated or differentiated MSCs. Usage of undifferentiated MSCs requires approximately half of the preparation time and even less than half of the costs of differentiated MSCs. Like previously described, applying a combination of differentiated and undifferentiated MSCs to processed nerve allograft might have undiscovered potential, but will reduce the ease of MSC-seeding per definition since both culturing techniques would need to be combined. As clinical applicability is crucial when estimating future potential of both cell-types, usage of undifferentiated MSCs is advised for future studies.

Anticipatory to a clinical setting, we envision that adipose tissue is derived from patients with peripheral nerve injury as soon as possible after trauma, using a minimally invasive technique which can be performed on the ER or outpatient clinic. MSCs are obtained from this adipose tissue and cultured for approximately 2 weeks. Thereafter, the MSCs are dynamically seeded for 12 hours onto an off-the-shelf available nerve allograft, immediately prior to surgery. To test whether this would be technically possible in the future, we examined in **chapter 8** if human MSCs can be dynamically seeded onto nerve substitutes currently available in clinic; the NeuraGen® Nerve Guide and the Avance® Nerve Graft. Surprisingly, MSCs adhered significantly more efficient to the surface of NeuraGen® Nerve Guides. This is attributed to the adherence of MSCs to both the inner and the outer surface of the nerve guides, while MSCs only adhered to the outer surface of Avance® Nerve Grafts as expected. Although the adherence of MSCs on the inner surface of NeuraGen® Nerve Guides hypothetically leads to enhanced concentrations of trophic factors that reach the regeneration site in NeuraGen® Nerve Guides, in vivo studies should indicate whether the MSC adherence location truly has implications for their effect on axon regeneration.

The interaction between (undifferentiated) MSCs and both clinically available nerve substitutes resulted in an altered gene expression profile of the MSCs, described in **chapter 9**. Most trends of the expression curves were relatable to physiological Wallerian degeneration and axon regeneration processes, implying potential benefit of the addition of MSCs to regenerating nerves.[56] Contrary to expectations considering the biological material components of both nerve substitutes, MSCs on NeuraGen® Nerve Guides demonstrated most gene expression adjustments appropriate for nerve regeneration. These results are hopeful, but like demonstrated with the rat MSCs in chapters 4, 5 and 6, the in vitro findings might not be completely relatable to in vivo results. Due to the neural tissue composition of Avance® Nerve Grafts, the interaction with the MSCs and the micro-environment might be more significant than NeuraGen® Nerve Guides. Contrarily, effects of MSCs on NeuraGen® Nerve Guides might be more prominent since part of the adhered cells lie protected on the inner surface, being closer to the regenerating nerve and avoiding mechanical stress during surgery. Besides this in vitro analysis, the result of the interaction between MSCs and the Avance® Nerve Graft and the NeuraGen® Nerve Guide on a gene-expression level should therefore be analyzed in vivo as well.

FUTURE PERSPECTIVES

The presented thesis demonstrates cautious potential of MSC seeding in the repair of peripheral nerve injuries. As with all forms of basic science research, small research steps will have to follow to confirm this potential.

MSC optimization

MSC-function and viability has been described to significantly variate between donors.[57, 58] For example, proliferation capacities decreases with increasing donor age[59], female MSCs have more anti-inflammatory capacities than male MSCs[60] and auto-immune diseases reduce the immunosuppressive capacities of MSCs.[61] Efforts to select ideal MSC donors, either in light of allogenous MSC transplantation or in light of patient selection that are more prone to benefit from autologous MSC therapy, might extend the described enhancing effect of MSCs.

A big hurdle in translating MSC-seeding to a clinical trial, are safety concerns and with that FDA approval. However, with sufficient data from animal studies and extensive descriptions of the deriving, culture and implementation steps, usage of adipose derived MSCs might be allowed to be studied under an investigational new drug application (IND). As this allowance will be easier obtained for usage of autologous MSCs than for allogenous MSCs, this thesis focused on autologous MSC application.

Contrary to MSCs, stromal vascular fraction (SVF) does not need to be manipulated or cultured prior to use, which limits the risk of contamination, making it safer and subject to lesser regulatory criteria. Stromal vascular fraction is a heterogeneous collection of cells, including MSCs, macrophages and pericytes and has demonstrated regenerative capabilities in multiple clinical settings like neurodegenerative disorders[62], alopecia areata[63] and perianal fistulizing Crohn's disease.[64] SVF can be easily and quickly derived from autologous adipose tissue, contains high concentrations of stromal cells and can be directly used after its acquisition.[65] SVF has demonstrated comparable effects as MSCs in other fields of research, but they have not been thoroughly compared in peripheral nerve repair yet.[66, 67] It would therefore be interesting to test if and at what efficiency SVF can be dynamically seeded onto nerve substitutes, to be able to fairly compare its effect on peripheral nerve regeneration to that of MSCs.

In vivo gene expression and growth factor production

The in vivo gene expression and the release of trophic factors of MSCs when seeded on nerve grafts should be studied to get a complete mechanistic insight in the effect of MSCs. This is preferably done at multiple time points, particularly short term, in an in vivo model to get the most reliable outcomes. Unfortunately this does require the use of many animals since qPCR analysis and trophic factor release analysis is preferably performed on five replicates per group per time point. To bypass the need for extra animals, one could consider another in vitro study, in which the micro-regenerative environment is simulated by presence of an unprocessed cut nerve segment in the same culture dish as the MSC-seeded decellularized nerve grafts. Although suboptimal, presence of a nerve segment in an in vitro culture, might simulate an in vivo setting while exposing the MSCs to trophic signals of the cut nerve segment.

Translation to bigger nerve gap models

Rats are often used as animal-model to perform fundamental studies prior to translation to a bigger animal. We choose to do so as well as they can be easily housed, are relatively cheap, they can endure anesthesia and surgery quite well, plenty of rat-specific reagents (needed for qPCR analysis for example) are available and most nerve studies have been performed in rats making results easy comparable to other studies. The major disadvantage of using a rat-model is their described superposed neuroregenerative capacities compared to humans, particularly due to the limited nerve gap that can be obtained.[50, 51] After fundamental studies have been performed to clarify details of the neuroregenerative capacity of MSCs in vivo, we suggest to translate studies to a bigger animal model like the rabbit. Needless to say, considering alternative animal-free study options and critically assessing the necessity and size of another animal-study must precede future animal-studies.

Surgical angiogenesis

As described in several chapters of this thesis, MSCs demonstrated to improve functional outcomes of peripheral nerve repair due to release of trophic factors that, among other things, enhance angiogenesis. Angiogenesis is postulated to be a crucial element in nerve regeneration and therefore other or complementing strategies to enhance angiogenesis are estimated to be valuable future research subjects. A vital, well vascularized wound bed has shown to be essential for regenerating tissues, providing trophic factors and enhancing outgrowth of blood vessels.[68, 69] A vascularized fat flap that envelopes an implanted decellularized nerve allograft is hypothesized to improve axon regeneration. The blood vessels and the stromal cells (MSC relatives) that are present in the fat tissue might lead to less fibrosis, enhanced vascularization and improved regeneration. Moreover, it would be interesting to study whether this surgical angiogenesis technique can work synergistic with the MSC-seeding technique presented in this thesis. One could hypothesize that a vascularized wound bed leads to more extensive delivery of trophic factors to the MSCs, resulting in extended survival times or enhanced activity/vitality of MSCs. On their turn, the trophic factors of the MSCs might decrease the immune response resulting in less fibrosis of the fat flap and potentially stimulate the outgrowth of blood vessels from the flap inside the nerve graft. Perhaps this also influences the distribution and orientation of vessels inside the nerve. The hypothesized synergistic effect of MSCs and surgical angiogenesis is illustrated in **figure 1**. The effect on peripheral nerve regeneration of stem-cell therapy combined with surgical angiogenesis deserves to be studied in future in vitro and in vivo settings.

Immunomodulation

Adjuvant therapies like immunomodulation have also demonstrated future potential to improve outcomes of peripheral nerve regeneration. Tacrolimus (FK506) is a regularly used immunosuppressant, often chronically systemically administered after organ transplantation. Besides, it demonstrated to have neuroprotective characteristics by influencing pathways that lead to enhanced GAP43 and NGF synthesis, which hypothetically results in accelerated Wallerian degeneration and axon regeneration.[70] Although this suggests a role for Tacrolimus in peripheral nerve regeneration, substantial systemic doses of Tacrolimus not only results in undesirable immunosuppression, but also in neurotoxicity, inducing peripheral neuropathy.

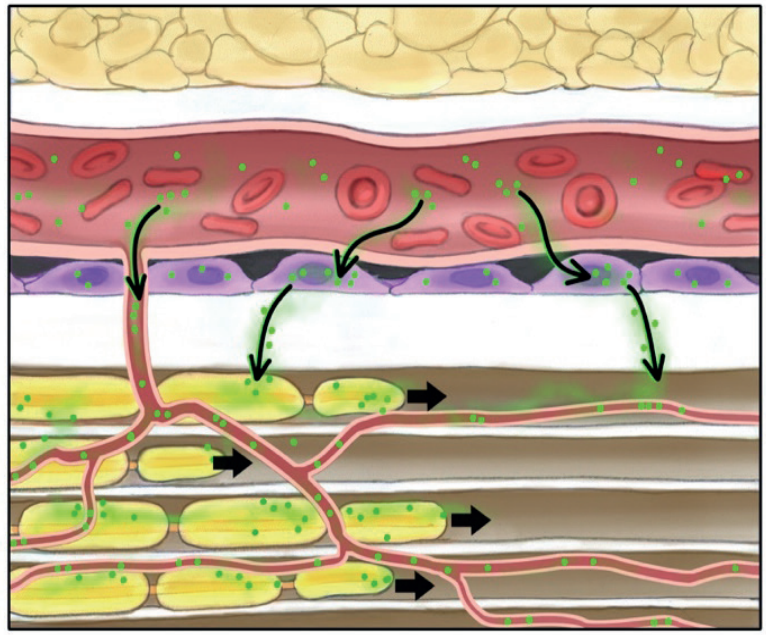

Figure 1. Illustration of the hypothesized synergistic effect on axon regeneration between surgical angiogenesis and MSC-seeding.

Local delivery of Tacrolimus would therefore be ideal.[71] Hydrogel is described to facilitate this local delivery, containing microspheres that encapsulate Tacrolimus.[72] Hydrogel delivery of Tacrolimus has resulted in improved in vitro and in vivo outcomes after peripheral nerve repair [73], but uncertainties like its mechanism of action, ideal dosage, duration of treatment and their interaction with MSCs remain to be studied before clinical translation can be considered.[74]

Cell delivery

Besides factors like Tacrolimus, NGF and BDNF[75], microspheres have shown to be able to encapsulate MSCs[76], potentially facilitating local delivery of MSCs to regenerating nerves. Since MSC-delivery in peripheral nerve repair is a rather underexposed research topic, it would be interesting to directly compare delivery efficiencies of different strategies like MSC-injection and microsphere encapsulation to that of dynamic seeding.

IN CONCLUSION

Contemplating the described outcomes, correlations and limitations, the chapters of this thesis have demonstrated that undifferentiated and differentiated MSCs can be efficiently seeded onto processed nerve allografts. Both cell types can interact with the extracellular matrix of processed nerve allografts, mostly leading to an upregulation of neurotrophic, angiogenic and extracellular matrix genes. Compared to unseeded processed nerve

allografts, the angiogenic factors resulting from the interaction between MSCs (differentiated MSCs in particular) and processed nerve allografts, led to enhanced neoangiogenesis in an in vivo model. Together with multiple enhanced neurotrophic and extracellular matrix factors, the enhanced angiogenesis caused by the MSCs results in improved functional outcomes of processed nerve allografts. There were no significant differences between the functional outcomes of undifferentiated and differentiated MSCs, resulting in a preference for the use of undifferentiated MSCs due to practical benefits. The dynamic seeding technique is applicable to human MSCs and nerve graft substitutes available in clinical practice and results in an interaction between the MSCs and the extracellular matrix of the grafts. Ideally, MSC seeding with all its beneficial effects on nerve regeneration will be combined in future studies with other initiatives to improve nerve regeneration like optimization of MSC quality, immunomodulation and surgical angiogenesis.

REFERENCES

1. Rbia N, Shin AY. The Role of Nerve Graft Substitutes in Motor and Mixed Motor/Sensory Peripheral Nerve Injuries. J Hand Surg Am 2017: 42: 367-77.
2. FF IJ, Nicolai JP, Meek MF. Sural nerve donor-site morbidity: thirty-four years of follow-up. Ann Plast Surg 2006: 57: 391-5.
3. Hallgren A, Bjorkman A, Chemnitz A, Dahlin LB. Subjective outcome related to donor site morbidity after sural nerve graft harvesting: a survey in 41 patients. BMC Surg 2013: 13: 39.
4. Rbia N, Bulstra LF, Bishop AT, van Wijnen AJ, Shin AY. A simple dynamic strategy to deliver stem cells to decellularized nerve allografts. Plast Reconstr Surg 2018.
5. Orbay H, Uysal AC, Hyakusoku H, Mizuno H. Differentiated and undifferentiated adipose-derived stem cells improve function in rats with peripheral nerve gaps. J Plast Reconstr Aesthet Surg 2011.
6. Tomita K, Madura T, Sakai Y, et al. Glial differentiation of human adipose-derived stem cells: implications for cell-based transplantation therapy. Neuroscience 2013: 236: 55-65.
7. Wang D, Liu XL, Zhu JK, et al. Bridging small-gap peripheral nerve defects using acellular nerve allograft implanted with autologous bone marrow stromal cells in primates. Brain Res 2008: 1188: 44-53.
8. Sunderland S, Lavarack JO, Ray LJ. The caliber of nerve fibers in human cutaneous nerves. J COMP NEUROL 1949: 91: 87-101.
9. Ryu YJ, Cho TJ, Lee DS, Choi JY, Cho J. Phenotypic characterization and in vivo localization of human adipose-derived mesenchymal stem cells. Mol Cells 2013: 35: 557-64.
10. Ge J, Guo L, Wang S, et al. The size of mesenchymal stem cells is a significant cause of vascular obstructions and stroke. Stem Cell Rev 2014: 10: 295-303.
11. Garvican ER, Cree S, Bull L, Smith RK, Dudhia J. Viability of equine mesenchymal stem cells during transport and implantation. Stem Cell Res Ther 2014: 5: 94.
12. Agashi K, Chau DY, Shakesheff KM. The effect of delivery via narrow-bore needles on mesenchymal cells. Regen Med 2009: 4: 49-64.
13. Mamidi MK, Singh G, Husin JM, et al. Impact of passing mesenchymal stem cells through smaller bore size needles for subsequent use in patients for clinical or cosmetic indications. J Transl Med 2012: 10: 229.
14. Jesuraj NJ, Santosa KB, Newton P, et al. A systematic evaluation of Schwann cell injection into acellular cold-preserved nerve grafts. J Neurosci Methods 2011: 197: 209-15.
15. Thompson MJ, Patel G, Isaacs J, et al. Introduction of neurosupportive cells into processed acellular nerve allografts results in greater number and more even distribution when injected compared to soaking techniques. Neurol Res 2017: 39: 189-97.
16. Caplan AI, Hariri R. Body Management: Mesenchymal Stem Cells Control the Internal Regenerator. Stem Cells Transl Med 2015: 4: 695-701.
17. Caplan AI. Adult Mesenchymal Stem Cells: When, Where, and How. Stem Cells Int 2015: 2015: 628767.
18. Kingham PJ, Kolar MK, Novikova LN, Novikov LN, Wiberg M. Stimulating the neurotrophic and angiogenic properties of human adipose-derived stem cells enhances nerve repair. Stem Cells Dev 2014: 23: 741-54.
19. Lattanzi W, Geloso MC, Saulnier N, et al. Neurotrophic features of human adipose tissue-derived stromal cells: in vitro and in vivo studies. J Biomed Biotechnol 2011: 2011: 468705.
20. Kingham PJ, Kalbermatten DF, Mahay D, et al. Adipose-derived stem cells differentiate into a Schwann cell phenotype and promote neurite outgrowth in vitro. Exp Neurol 2007: 207: 267-74.
21. Zhao Z, Wang Y, Peng J, et al. Repair of nerve defect with acellular nerve graft supplemented by bone marrow stromal cells in mice. Microsurgery 2011: 31: 388-94.
22. Rbia N, Bulstra LF, Thaler R, et al. In Vivo Survival of Mesenchymal Stromal Cell-Enhanced Decellularized Nerve Grafts for Segmental Peripheral Nerve Reconstruction. J Hand Surg Am

2019: 44: 514.e1-14.e11.
23. Stoll G, Muller HW. Nerve injury, axonal degeneration and neural regeneration: basic insights. Brain Pathol 1999: 9: 313-25.
24. Parkinson DB, Bhaskaran A, Arthur-Farraj P, et al. c-Jun is a negative regulator of myelination. J Cell Biol 2008: 181: 625-37.
25. Bosse F. Extrinsic cellular and molecular mediators of peripheral axonal regeneration. Cell Tissue Res 2012: 349: 5-14.
26. Kidd GJ, Ohno N, Trapp BD. Biology of Schwann cells. Handb Clin Neurol 2013: 115: 55-79.
27. Fu SY, Gordon T. The cellular and molecular basis of peripheral nerve regeneration. Mol Neurobiol 1997: 14: 67-116.
28. Lowery LA, Van Vactor D. The trip of the tip: understanding the growth cone machinery. Nat Rev Mol Cell Biol 2009: 10: 332-43.
29. Geraldo S, Gordon-Weeks PR. Cytoskeletal dynamics in growth-cone steering. J Cell Sci 2009: 122: 3595-604.
30. Jessen KR, Mirsky R. The repair Schwann cell and its function in regenerating nerves. J Physiol 2016: 594: 3521-31.
31. Cattin AL, Burden JJ, Van Emmenis L, et al. Macrophage-Induced Blood Vessels Guide Schwann Cell-Mediated Regeneration of Peripheral Nerves. Cell 2015: 162: 1127-39.
32. Gordon T. The role of neurotrophic factors in nerve regeneration. Neurosurg Focus 2009: 26: E3.
33. Orbay H, Uysal AC, Hyakusoku H, Mizuno H. Differentiated and undifferentiated adipose-derived stem cells improve function in rats with peripheral nerve gaps. J Plast Reconstr Aesthet Surg 2012: 65: 657-64.
34. Watanabe Y, Sasaki R, Matsumine H, Yamato M, Okano T. Undifferentiated and differentiated adipose-derived stem cells improve nerve regeneration in a rat model of facial nerve defect. J Tissue Eng Regen Med 2017: 11: 362-74.
35. Ladak A, Olson J, Tredget EE, Gordon T. Differentiation of mesenchymal stem cells to support peripheral nerve regeneration in a rat model. Exp Neurol 2011: 228: 242-52.
36. Ching RC, Wiberg M, Kingham PJ. Schwann cell-like differentiated adipose stem cells promote neurite outgrowth via secreted exosomes and RNA transfer. Stem Cell Res Ther 2018: 9: 266.
37. di Summa PG, Kalbermatten DF, Raffoul W, Terenghi G, Kingham PJ. Extracellular matrix molecules enhance the neurotrophic effect of Schwann cell-like differentiated adipose-derived stem cells and increase cell survival under stress conditions. Tissue Eng Part A 2013: 19: 368-79.
38. Han IH, Sun F, Choi YJ, et al. Cultures of Schwann-like cells differentiated from adipose-derived stem cells on PDMS/MWNT sheets as a scaffold for peripheral nerve regeneration. J Biomed Mater Res A 2015: 103: 3642-8.
39. Wood MD, Kemp SW, Weber C, Borschel GH, Gordon T. Outcome measures of peripheral nerve regeneration. Ann Anat 2011: 193: 321-33.
40. Shin RH, Vathana T, Giessler GA, et al. Isometric tetanic force measurement method of the tibialis anterior in the rat. Microsurgery 2008: 28: 452-7.
41. Bulstra LF, Hundepool CA, Friedrich PF, et al. Functional Outcome after Reconstruction of a Long Nerve Gap in Rabbits Using Optimized Decellularized Nerve Allografts. Plast Reconstr Surg 2020.
42. Bulstra LF, Hundepool CA, Friedrich PF, et al. Motor Nerve Recovery in a Rabbit Model: Description and Validation of a Noninvasive Ultrasound Technique. J Hand Surg Am 2016: 41: 27-33.
43. Hundepool CA, Nijhuis TH, Rbia N, et al. Noninvasive Ultrasound of the Tibial Muscle for Longitudinal Analysis of Nerve Regeneration in Rats. Plast Reconstr Surg 2015: 136: 633e-9e.
44. Caillaud M, Richard L, Vallat JM, Desmouliere A, Billet F. Peripheral nerve regeneration and intraneural revascularization. Neural Regen Res 2019: 14: 24-33.
45. Hillenbrand M, Holzbach T, Matiasek K, Schlegel J, Giunta RE. Vascular endothelial growth factor gene therapy improves nerve regeneration in a model of obstetric brachial plexus palsy.

Neurol Res 2015: 37: 197-203.
46. Hobson MI, Green CJ, Terenghi G. VEGF enhances intraneural angiogenesis and improves nerve regeneration after axotomy. J Anat 2000: 197 Pt 4: 591-605.
47. Rbia N, Bulstra LF, Friedrich PF, et al. Gene expression and growth factor analysis in early nerve regeneration following segmental nerve defect reconstruction with a mesenchymal stromal cell-enhanced decellularized nerve allograft. Plast Reconstr Surg Glob Open 2020: 8: e2579.
48. Rbia N, Bulstra LF, Lewallen EA, et al. Seeding decellularized nerve allografts with adipose-derived mesenchymal stromal cells: An in vitro analysis of the gene expression and growth factors produced. J Plast Reconstr Aesthet Surg 2019: 72: 1316-25.
49. Fan L, Yu Z, Li J, Dang X, Wang K. Schwann-like cells seeded in acellular nerve grafts improve nerve regeneration. BMC Musculoskelet Disord 2014: 15: 165.
50. Gordon T, Borschel GH. The use of the rat as a model for studying peripheral nerve regeneration and sprouting after complete and partial nerve injuries. Exp Neurol 2017: 287: 331-47.
51. Scheib J, Höke A. Advances in peripheral nerve regeneration. Nat Rev Neurol 2013: 9: 668-76.
52. Zhu Z, Huang Y, Zou X, et al. The vascularization pattern of acellular nerve allografts after nerve repair in Sprague-Dawley rats. Neurol Res 2017: 39: 1014-21.
53. Kingham PJ, Reid AJ, Wiberg M. Adipose-derived stem cells for nerve repair: hype or reality? Cells Tissues Organs 2014: 200: 23-30.
54. Zagorchev L, Oses P, Zhuang ZW, et al. Micro computed tomography for vascular exploration. J Angiogenes Res 2010: 2: 7.
55. Faroni A, Rothwell SW, Grolla AA, et al. Differentiation of adipose-derived stem cells into Schwann cell phenotype induces expression of P2X receptors that control cell death. Cell Death Dis 2013: 4: e743.
56. Pan B, Liu Y, Yan JY, et al. Gene expression analysis at multiple time-points identifies key genes for nerve regeneration. Muscle Nerve 2017: 55: 373-83.
57. Lo Surdo JL, Millis BA, Bauer SR. Automated microscopy as a quantitative method to measure differences in adipogenic differentiation in preparations of human mesenchymal stromal cells. Cytotherapy 2013: 15: 1527-40.
58. Sen A, Lea-Currie YR, Sujkowska D, et al. Adipogenic potential of human adipose derived stromal cells from multiple donors is heterogeneous. J Cell Biochem 2001: 81: 312-9.
59. Stenderup K, Justesen J, Clausen C, Kassem M. Aging is associated with decreased maximal life span and accelerated senescence of bone marrow stromal cells. Bone 2003: 33: 919-26.
60. Sammour I, Somashekar S, Huang J, et al. The Effect of Gender on Mesenchymal Stem Cell (MSC) Efficacy in Neonatal Hyperoxia-Induced Lung Injury. PLoS One 2016: 11: e0164269.
61. Serena C, Keiran N, Madeira A, et al. Crohn's Disease Disturbs the Immune Properties of Human Adipose-Derived Stem Cells Related to Inflammasome Activation. Stem Cell Reports 2017: 9: 1109-23.
62. Duma C, Kopyov O, Kopyov A, et al. Human intracerebroventricular (ICV) injection of autologous, non-engineered, adipose-derived stromal vascular fraction (ADSVF) for neurodegenerative disorders: results of a 3-year phase 1 study of 113 injections in 31 patients. Mol Biol Rep 2019: 46: 5257-72.
63. Stevens HP, Donners S, de Bruijn J. Introducing Platelet-Rich Stroma: Platelet-Rich Plasma (PRP) and Stromal Vascular Fraction (SVF) Combined for the Treatment of Androgenetic Alopecia. Aesthet Surg J 2018: 38: 811-22.
64. Serrero M, Grimaud F, Philandrianos C, et al. Long-term Safety and Efficacy of Local Microinjection Combining Autologous Microfat and Adipose-Derived Stromal Vascular Fraction for the Treatment of Refractory Perianal Fistula in Crohn's Disease. Gastroenterology 2019: 156: 2335-37.e2.
65. Bora P, Majumdar AS. Adipose tissue-derived stromal vascular fraction in regenerative medicine: a brief review on biology and translation. Stem Cell Res Ther 2017: 8: 145.
66. Nguyen A, Guo J, Banyard DA, et al. Stromal vascular fraction: A regenerative reality? Part 1:

Current concepts and review of the literature. J Plast Reconstr Aesthet Surg 2016: 69: 170-9.
67. Mohammadi R, Mehrtash M, Mehrtash M, Sajjadi SS. Nonexpanded Adipose Stromal Vascular Fraction Local Therapy on Peripheral Nerve Regeneration Using Allografts. J Invest Surg 2016: 29: 149-56.
68. Coert JH. Pathophysiology of nerve regeneration and nerve reconstruction in burned patients. Burns 2010: 36: 593-8.
69. Hovius SE, Ultee J. Volkmann's ischemic contracture. Prevention and treatment. Hand Clin 2000: 16: 647-57.
70. Labroo P, Shea J, Sant H, Gale B, Agarwal J. Effect Of combining FK506 and neurotrophins on neurite branching and elongation. Muscle Nerve 2017: 55: 570-81.
71. Zuo KJ, Saffari TM, Chan K, Shin AY, Borschel GH. Systemic and Local FK506 (Tacrolimus) and its Application in Peripheral Nerve Surgery. J Hand Surg Am 2020.
72. Tajdaran K, Shoichet MS, Gordon T, Borschel GH. A novel polymeric drug delivery system for localized and sustained release of tacrolimus (FK506). Biotechnol Bioeng 2015: 112: 1948-53.
73. Tajdaran K, Chan K, Shoichet MS, Gordon T, Borschel GH. Local delivery of FK506 to injured peripheral nerve enhances axon regeneration after surgical nerve repair in rats. Acta Biomater 2019: 96: 211-21.
74. Saffari TM, Bedar M, Zuidam JM, et al. Exploring the neuroregenerative potential of tacrolimus. Expert Rev Clin Pharmacol 2019: 12: 1047-57.
75. Zhao Q, Li ZY, Zhang ZP, et al. Polylactic-co-glycolic acid microspheres containing three neurotrophic factors promote sciatic nerve repair after injury. Neural Regen Res 2015: 10: 1491-7.
76. Li YY, Cheng HW, Cheung KM, Chan D, Chan BP. Mesenchymal stem cell-collagen microspheres for articular cartilage repair: cell density and differentiation status. Acta Biomater 2014: 10: 1919-29.

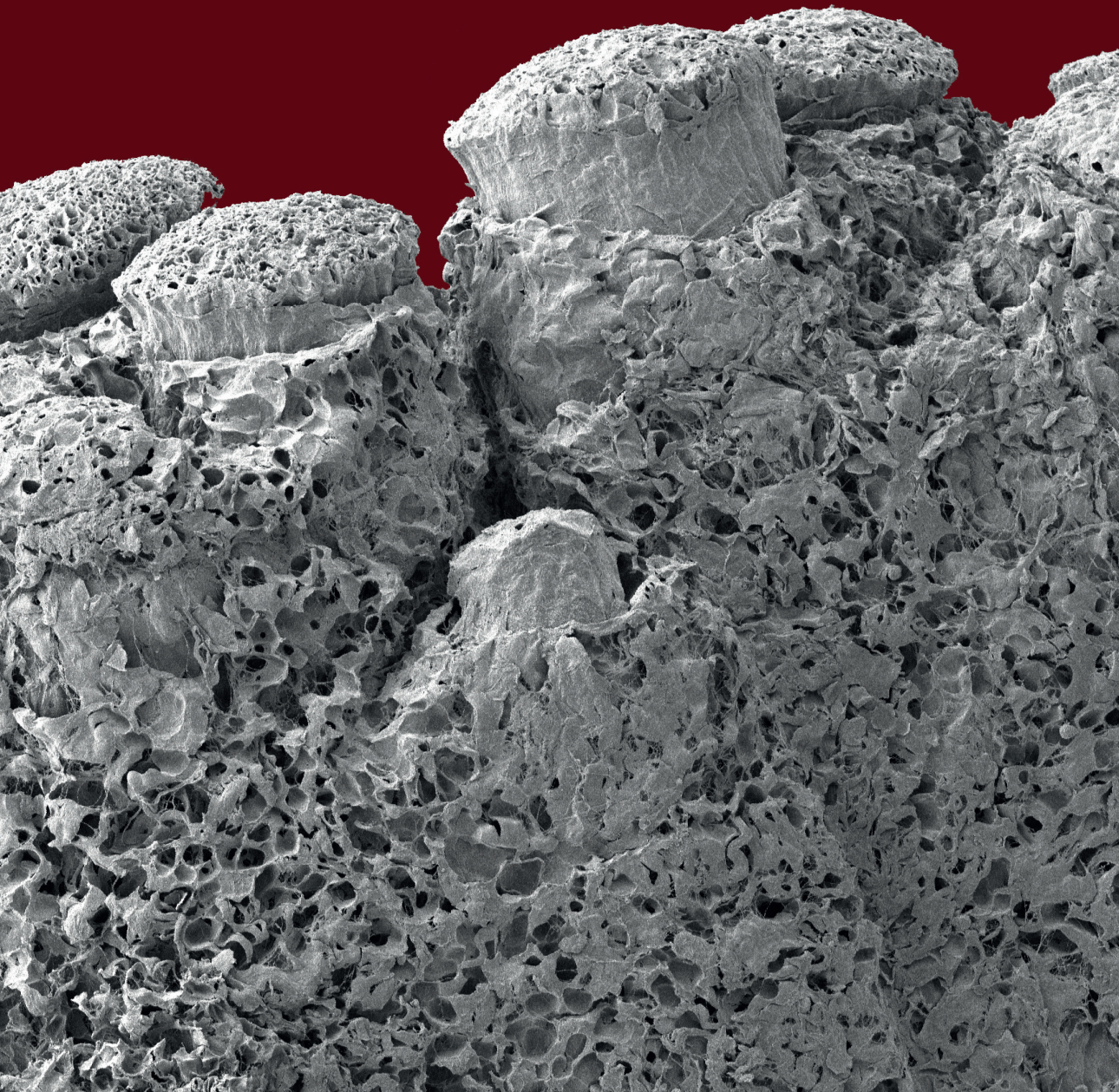

Chapter 11

Summary
Dutch summary

SUMMARY

In the general introduction, **chapter 1**, the aims and scope of this thesis are elucidated. The overall goal of this thesis is to improve the results of autograft substitutes like processed nerve allografts and nerve conduits when used in peripheral nerve repair. MSCs are hypothesized to possess regenerative capacities beneficial for nerve regeneration in these nerve substitutes, which is most plausibly caused by their secretion of trophic factors. As Schwann cells are essential for the function and regeneration of nerves by excreting numerous trophic factors, MSCs differentiated into Schwann cell-like cells might excrete enhanced levels of trophic factors leading to improved nerve regeneration. With this thesis, we literally strained every nerve to determine if the addition of differentiated and undifferentiated adipose derived MSCs to nerve substitutes could provoke the desired improvement in peripheral nerve regeneration.

In **chapter 2** a review of the currently available literature was performed to create the fundament for our experimental research. An overview of the current available MSC-differentiating methods is provided, delivery strategies and cell dosing are discussed and previous in vitro and in vivo outcomes of naïve and differentiated MSCs are described. Optimal delivery and dosing of (differentiated) MSCs has not been explored extensively, but dynamic seeding seems to deliver undifferentiated MSCs in a timely and non-traumatic manner. The neural induction of MSCs by chemicals combined with growth factors is the preferred and most extensively described method to obtain Schwann cell-like differentiation. Although differentiated MSCs demonstrated more potential in vitro compared to undifferentiated MSCs, their beneficial effect has not been convincingly confirmed in previous in vivo studies. Since differentiation of MSCs requires extra preparation time and costs, convincing in vivo results are required to determine which type of MSCs has most clinical potential.

Chapter 3 focuses on the development of a delivery strategy that is applicable to both undifferentiated and differentiated MSCs. To test whether differentiated MSCs could be dynamically seeded comparable to undifferentiated MSCs, the experimental set-up of the described study comprised multiple samples of 1x10^6 (undifferentiated or differentiated) MSCs that were placed in a conical tube containing a processed nerve graft, which was rotated for either 6, 12 or 24 hours. Viability, seeding efficiency and cell distribution on the outer surface of the nerve allografts were evaluated. We concluded that differentiated MSCs can be dynamically seeded, leading to a similar cell-distribution as seeded undifferentiated MSCs. Twelve hours of seeding was estimated to provide the most efficient cell adherence for both cell-types, but differentiated MSCs had a significantly higher cell adherence than undifferentiated MSCs (95% versus 80%). This might indicate that differentiation of MSCs improves in vitro cell adherence to processed nerve allografts.

To understand the biological differences of undifferentiated and differentiated MSCs before and after seeding onto processed nerve allografts, the gene expression profiles of both cell-types are compared in **chapter 4**. Gene expression of both cell-types was quantified by quantitative polymerase chain reaction (qPCR) analysis of neurotrophic, angiogenic,

extracellular matrix and cell cycle genes at multiple time points after seeding. The gene expression profile of both cell-types changed significantly upon interaction with processed nerve allografts. Undifferentiated MSCs demonstrated enhanced expressions of neurotrophic (NGF, GDNF, PMP22), extracellular matrix (FBLN1, LAMB2) and regulatory cell cycle genes (CCNB2) 7 days after seeding. Differentiated MSCs expressed enhanced levels of neurotrophic (NGF, GDNF, GAP43), angiogenic (VEGF1), extracellular matrix (FBLN1) and regulatory cell cycle genes (CASP3, CCNB2) in the first 72 hours after seeding. The differences in gene-profiles and effective phases suggests that both cell-types can affect nerve regeneration in different ways and at different time points, which should be confirmed in vivo.

Vascularization has been postulated to be essential for nerve regeneration by guiding regenerating nerves and providing the supply of necessary trophic factors. As tools to visualize and quantify vascularization patterns in transplanted nerves are lacking, the study described in **chapter 5** focusses on the development of a technique that provides a three-dimensional visualization and quantification of the peripheral neural vascularity in a rodent model. Vascularization in autografts (n=12) and untreated nerves (n=12) was quantified by the vascular surface area using conventional photography (2D) and the vascular volume was calculated using micro-computed tomography (3D). Combining both methods accurately reflects the degree of vascularization in rat nerves. This easily reproducible strategy allows objective assessment of the level and the organization of vascularization in nerves and could be extrapolated to any other desired organ ex vivo.

In **chapter 6**, the technique validated in chapter 5 is used to determine the beneficial effect on vascularization when seeding undifferentiated and differentiated MSCs onto a decellularized nerve allograft in a rat sciatic nerve defect model. The vascularization of normal nerves, autografts, allografts seeded with differentiated MSCs and allografts seeded with undifferentiated MSCs was quantified and compared at 16 weeks after surgery. Unseeded allografts had a significantly lower vascular surface area percentage than normal non-operated nerves and allografts seeded with differentiated MSCs. Although it was significantly correlated to the vascular surface area, no significant differences in vascular volume were obtained between groups. The vascularization pattern in MSC-seeded allografts consisted of an extensive non-aligned network of micro-vessels with a centripetal pattern, while the vessels in autografts and normal nerves were more aligned with longitudinal patterns. The more extensive network might facilitates better oxygen and nutrient supply throughout the graft, but can be detrimental for the alignment of sprouting axons considering the directional function of vasculature.

The study in **chapter 7** aimed to determine whether the previous elucidated rationale of MSC-seeding onto nerve allografts could be confirmed by in vivo evaluation of functional outcomes. Autografts (n=20), allografts (n=20), allografts seeded with undifferentiated MSCs (n=20) and allografts seeded with differentiated MSCs (n=20) were used to reconstruct a ten millimeter sciatic nerve defect in a rodent model. Cross sectional tibial muscle ultrasound measurements evaluated functional recovery over time. At 12 and 16 weeks after surgery (n=10 per group

per time point) isometric tetanic force, compound muscle action potentials, muscle mass, histology and immunofluorescence analyses were performed. Both cell-types significantly improved part of the functional outcomes of processed allografts and equaled the majority of autograft results at 12 weeks of follow-up. Differences between undifferentiated and differentiated MSCs were not statistically significant. Considering the increased preparation time and costs of differentiated MSCs, undifferentiated MSCs are more clinically applicable.

In **chapter 8** a preliminary but essential step towards translating the use of dynamic seeding into a clinical setting is described. The purpose of the study was to examine if human adipose derived MSCs could be dynamically seeded onto the clinically available Avance® Nerve Graft (processed nerve allograft) and the NeuraGen® Nerve Guide (hollow collagen conduit). Viability of MSCs, seeding efficiency and cell distribution were determined for both nerve substitutes. The viability of MSCs was not negatively affected by the composition of the nerve substitutes. The optimal seeding duration was 12 hours, leading to a significant higher seeding efficiency of NeuraGen® Nerve Guides compared to Avance® Nerve Grafts (94% versus 65% of the administered dose of MSCs). This was hypothetically related to the cell distribution on both nerve substitutes; dynamic seeding led to a uniform distribution of MSCs over the surfaces of both nerve substitutes, but only to adherence of MSCs on the inner surface of the NeuraGen® Nerve Guide. These results demonstrate that human MSCs can be effectively and efficiently seeded on commercially available nerve autograft substitutes in a timely fashion.

The interaction between human adipose derived MSCs and the extracellular matrix of the clinically available Avance® Nerve Grafts and NeuraGen® Nerve Guides was assessed in **chapter 9.** Quantitative PCR analyses on multiple time points (up to 21 days) after MSC-seeding demonstrated the course of the expression of neurotrophic (NGF, GDNF, PTN, GAP43, BDNF), myelination (PMP22, MPZ), angiogenic (VEGF-a, CD31), extracellular matrix (COL1A1, COL3A1, FBLN1, LAMB2) and immunoglobulin (CD96) genes. The interaction resulted in a change and mostly an upregulation of the expression of numerous genes important for nerve regeneration over time. Despite the absence of micro-environmental signals in this in vitro study, the (timing of) upregulation of most genes could be correlated to processes occurring during Wallerian degeneration and axon regeneration of injured peripheral nerves. It was hypothesized that the biological composition of the Avance® Nerve Grafts (i.e. neural tissue) would lead to more expression of neurotrophic genes, but the in vitro interaction of MSCs with the NeuraGen® Nerve Guide was greater, particularly in the long-term results. These outcomes suggest that clinically available nerve autograft substitutes could benefit from the addition of MSCs.

In **chapter 10**, the main findings of this thesis are described and placed in a broader perspective. Suggestions for future research are illustrated and substantiated. By enhanced expression of trophic factors leading to increased vascularization and axon regeneration, dynamic seeding of MSCs leads to improved functional outcomes of decellularized allografts. Seeding of undifferentiated MSCs is more cost-efficient than differentiated MSCs and can be applied to clinically available nerve graft substitutes.

NEDERLANDSE SAMENVATTING

In de algemene inleiding, **hoofdstuk 1**, worden de doelen van dit proefschrift uiteengezet. Het algemene doel is het verbeteren van de uitkomsten van gedecellulariseerde allogene zenuwtransplantaten die gebruikt worden in het geval van perifeer zenuw letsel. Mesenchymale stamcellen bevatten regeneratieve eigenschappen die mogelijk gunstige effecten hebben op zenuw regeneratie wanneer ze gebruikt worden in combinatie met zenuwtransplantaten. Deze regeneratieve eigenschappen van stamcellen zijn het gevolg van de productie en excretie van trofische (groei) factoren. Omdat schwann-cellen essentieel zijn voor functionerende, maar zeker ook voor regenererende zenuwen, zou het differentiëren van stamcellen in schwann-cell achtige cellen mogelijk leiden tot nog meer excretie van trofische factoren die van belang zijn bij zenuw regeneratie. In dit proefschrift hebben we gepoogd te analyseren of het toevoegen van stamcellen, al dan niet in een gedifferentieerde vorm, de gewenste verbetering van de uitkomsten van zenuwtransplantaten kan bewerkstelligen.

Hoofdstuk 2 beschrijft de rationale van dit proefschrift, waarin relevante beschikbare literatuur wordt samengevat. Hierin komen differentiatie-technieken, strategieën om cellen in of op zenuwen te bezorgen en eerder beschreven uitkomsten van ongedifferentieerde en gedifferentieerde stamcellen aan de orde. Het induceren van een neurale differentiatiestaat van stamcellen wordt in voorgaande studies voornamelijk op een efficiënte manier bereikt door de cellen te kweken in een mengsel van chemicaliën en groeifactoren. Cel-doseringen en optimale toedieningstechnieken zijn onvoldoende onderzocht, maar het dynamisch zaaien van ongedifferentieerde stamcellen lijkt een efficiënte en atraumatische methode om stamcellen gelijkmatig te verdelen over het oppervlak van een zenuwtransplantaat. Hoewel gedifferentieerde cellen in vitro meer zenuw-regeneratie potentie lijken te hebben, hebben eerdere onderzoeken dit voordeel nog niet kunnen bevestigen in vivo. Het differentiëren van stamcellen vergt extra tijd en materiaalkosten. Het is derhalve essentieel om overtuigende in vivo resultaten te verkrijgen om te bepalen welk celtype de meeste potentie heeft om in de toekomst in de kliniek toegepast te worden.

Hoofdstuk 3 focust op de ontwikkeling van een stamcel-toedieningsstrategie die toepasbaar is op zowel ongedifferentieerde als gedifferentieerde stamcellen. Om te bepalen of de eerder beschreven dynamische zaaiings-strategie vergelijkbaar toepasbaar is op gedifferentieerde stamcellen, werden samples van 1x10^6 stamcellen (ongedifferentieerd of gedifferentieerd) samen met een gedecellulariseerd zenuwtransplantaat in een reageerbuis geplaatst. Deze reageerbuizen werden vervolgens geroteerd voor 6, 12 of 24 uur. Cel-vitaliteit, bezaaiings-efficiëntie en cel-distributie over de oppervlakte van de zenuwtransplantaten werden geëvalueerd. Gedifferentieerde cellen konden gezaaid worden, leidend tot een vergelijkbare cel-distributie als het zaaien van ongedifferentieerde cellen. Twaalf uur zaaien leidde tot de meest optimale cel bedekking voor zowel ongedifferentieerde en gedifferentieerde cellen, maar gedifferentieerde stamcellen hadden een significant hogere bedekking dan ongedifferentieerde stamcellen (95% versus 80%). De bevindingen wijzen erop dat het differentiëren van stamcellen de in vitro aantrekkingskracht op gedecellulariseerde zenuwtransplantaten vergroot.

Om de biologische verschillen tussen ongedifferentieerde en gedifferentieerde stamcellen voor en na het zaaien op gedecellulariseerde, allogene zenuwtransplantaten beter te begrijpen, werden in **hoofdstuk 4** de genexpressie profielen van beide celtypes in kaart gebracht en met elkaar vergeleken. De genexpressie werd gekwantificeerd door middel van 'quantitative polymerase chain reaction' (qPCR) analyse van neurotrofe, angiogene, extracellulaire matrix en celproliferatie genen op meerdere tijdstippen na het bezaaien. De genexpressieprofielen van ongedifferentieerde en gedifferentieerde stamcellen veranderden significant na de blootstelling aan het oppervlak van de gedecellulariseerde zenuwtransplantaten. Ongedifferentieerde stamcellen toonden een toename in de expressie van neurotrofe (NGF, GDNF, PMP22), extracellulaire matrix (FBLN1, LAMB2) en celproliferatie genen (CCBN2) vanaf 7 dagen na het zaaien. Gedifferentieerde stamcellen toonden een verhoogde expressie van neurotrofe (NGF, GDNF, GAP43), angiogene (VEGF1-a), extracellulaire matrix (FBLN1) en celproliferatie genen (CASP3, CCNB2) in de eerste 72 uur na het zaaien. De beschreven interacties en verschillen tussen de celtypes suggereren dat beide type stamcellen een positief effect kunnen hebben op zenuw regeneratie, maar dat ze op verschillende manieren en tijdspunten effectief zijn.

Vascularisatie wordt als essentieel geacht voor zenuwregeneratie omdat het regenererende axonen kan voorzien van de benodigde trofische factoren en als leidraad werkt voor de regeneratie richting. Adequate methodes om de hoeveelheid vascularisatie in zenuwen te kwantificeren ontbreken. Derhalve wordt in **hoofdstuk 5** een techniek beschreven waarin de vascularisatie zowel in 2D (vascularisatie oppervlakte door middel van conventionele fotografie) als in 3D (vascularisatie volume door middel van 'micro-computed tomography', micro-CT) kan worden gekwantificeerd. Deze technieken worden geverifieerd met behulp van 12 autogene zenuwtransplantaten en 12 normale zenuwen. De beschreven technieken zijn makkelijk te reproduceren en faciliteren een objectieve beoordeling van de vascularisatie in zenuwen.

In **hoofdstuk 6** worden de in hoofdstuk 5 geverifieerde technieken gebruikt om het effect van ongedifferentieerde en gedifferentieerde stamcellen te analyseren betreffende de vascularisatie van zenuwtransplantaten. De vascularisatie van normale zenuwen, autologe zenuwtransplantaten, gedecellulariseerde allogene zenuwtransplantaten, en allogene zenuwtransplantaten bezaaid met ongedifferentieerde of gedifferentieerde stamcellen werden met elkaar vergeleken 16 weken na de implementatie van de zenuwen in een rat-model. Onbezaaide allogene zenuwtransplantaten hadden een significant kleinere vascularisatie oppervlakte dan normale zenuwen en allogene zenuwen bezaaid met gedifferentieerde stamcellen. Ondanks een significante correlatie tussen het vasculaire oppervlakte en het vasculaire volume, werden er geen significante verschillen vastgesteld tussen de groepen wat betreft het vasculaire volume. Het vascularisatie-patroon van met stamcellen bezaaide zenuwtransplantaten was anders (uitgebreider maar minder georganiseerd) dan dat in autologe zenuwtransplantaten en normale zenuwen.

In **hoofdstuk 7** werd onderzocht of de hiervoor uiteengezette rationale van het gebruik van

stamcellen in perifeer zenuwherstel ook bevestigd kon worden in een in vivo evaluatie van de functionele uitkomsten. Autologe zenuwtransplantaten (n=20), allogene zenuwtransplantaten (n=20), allogene zenuwtransplantaten bezaaid met ongedifferentieerde stamcellen (n=20) en allogene zenuwtransplantaten met gedifferentieerde stamcellen (n=20) werden gebruikt om een 10mm zenuw defect in een ratmodel te reconstrueren. Echografie van spieren werd gebruikt om tussentijds het zenuwherstel te meten. 12 en 16 weken na de operatie (n=10 per groep per tijdspunt) werden elektrofysiologie, isometrische tetanische kracht, spiermassa, histologie en immunofluorescentie gebruikt om de zenuwregeneratie te beoordelen. Na 12 weken zorgden beide cel-varianten voor significante verbetering van een groot deel van de functionele uitkomsten van allogene zenuwtransplantaten en bereikten grotendeels resultaten die vergelijkbaar waren met die van autologe zenuwtransplantaten. De verschillen tussen de uitkomsten van ongedifferentieerde en gedifferentieerde stamcellen waren niet significant. Gezien de extra tijd en materiaalkosten die het gebruik van gedifferentieerde stamcellen met zich mee brengt, hebben ongedifferentieerde stamcellen een hogere klinische toepasbaarheid.

In **hoofdstuk 8** wordt een preliminaire maar essentiële stap naar het toepassen van het bezaaien van zenuwtransplantaten met stamcellen in de kliniek beschreven. Humane stamcellen werden bezaaid op de commercieel beschikbare Avance® Nerve Graft (gedecellulariseerd zenuwtransplantaat) en NeuraGen® Nerve Guide (holle, collagene buis). Vitaliteit, bezaaiings-efficiëntie, en cel-verdeling werden voor beide zenuwvervangers beoordeeld na 6, 12 en 24 uur zaaien. De vitaliteit van stamcellen werd niet negatief beïnvloed door de extracellulaire matrix van beide zenuwvervangers. Optimale bezaaiings-efficiëntie werd bereikt na 12 uur zaaien en leidde tot 94% bezaaiings-efficiëntie op de NeuraGen® Nerve Guide en 65% op de Avance® Nerve Graft (significant verschil). Dit verschil komt waarschijnlijk doordat stamcellen zowel aan de buitenkant als aan de binnenkant van de NeuraGen® Nerve Guide vast kleefden. Beide zenuwvervangers kunnen effectief en efficiënt bezaaid worden met humane stamcellen.

De interactie tussen humane stamcellen en de extracellulaire matrix van de in hoofdstuk 8 beschreven klinisch beschikbare zenuwvervangers werd onderzocht in **hoofdstuk 9**. Opnieuw werd qPCR op verschillende tijdspunten na het bezaaien ingezet om de expressie van neutrotrofe (NGF, GDNF, PTN, GAP43, BDNF), myelinisatie (PMP22, MPZ), angiogene (VEGF-a, CD31), extracellulaire matrix (COL1A1, COL3A1, FBLN1, LAMB2) en immunoglobuline (CD96) genen te kwantificeren. De interactie resulteerde in beide groepen in een verandering en voornamelijk een verhoging van de expressie van verscheidene genen die belangrijk zijn voor zenuwregeneratie. Hoewel de normaal aanwezige signalen uit de micro-omgeving van een regenererende zenuw ontbraken in deze in vitro studie, konden de meeste veranderingen in genexpressie en de timing daarvan worden gerelateerd aan processen die optreden tijdens Wallerse degeneratie en axon regeneratie. Ondanks dat de Avance® Nerve Graft uit natuurlijk zenuw-materiaal bestaat, lijkt de interactie tussen stamcellen en de NeuraGen® Nerve Guide groter, voornamelijk op de lange termijn. Deze bevindingen suggereren dat klinisch beschikbare zenuwvervangers voordeel kunnen ondervinden van het bezaaien met humane stamcellen.

In **hoofdstuk 10** worden de voornaamste bevindingen uit dit proefschrift beschreven en in een breder perspectief geplaatst. Hierin worden suggesties voor toekomstig onderzoek belicht en onderbouwd. Dynamisch zaaien van stamcellen op allogene zenuwtransplantaten leidt tot een toegenomen vascularisatie en axon regeneratie door een toegenomen expressie en productie van trofische factoren. Het zaaien van ongedifferentieerde stamcellen is meer kosteneffectief dan gedifferentieerde stamcellen en heeft dus een hogere klinische toepasbaarheid.

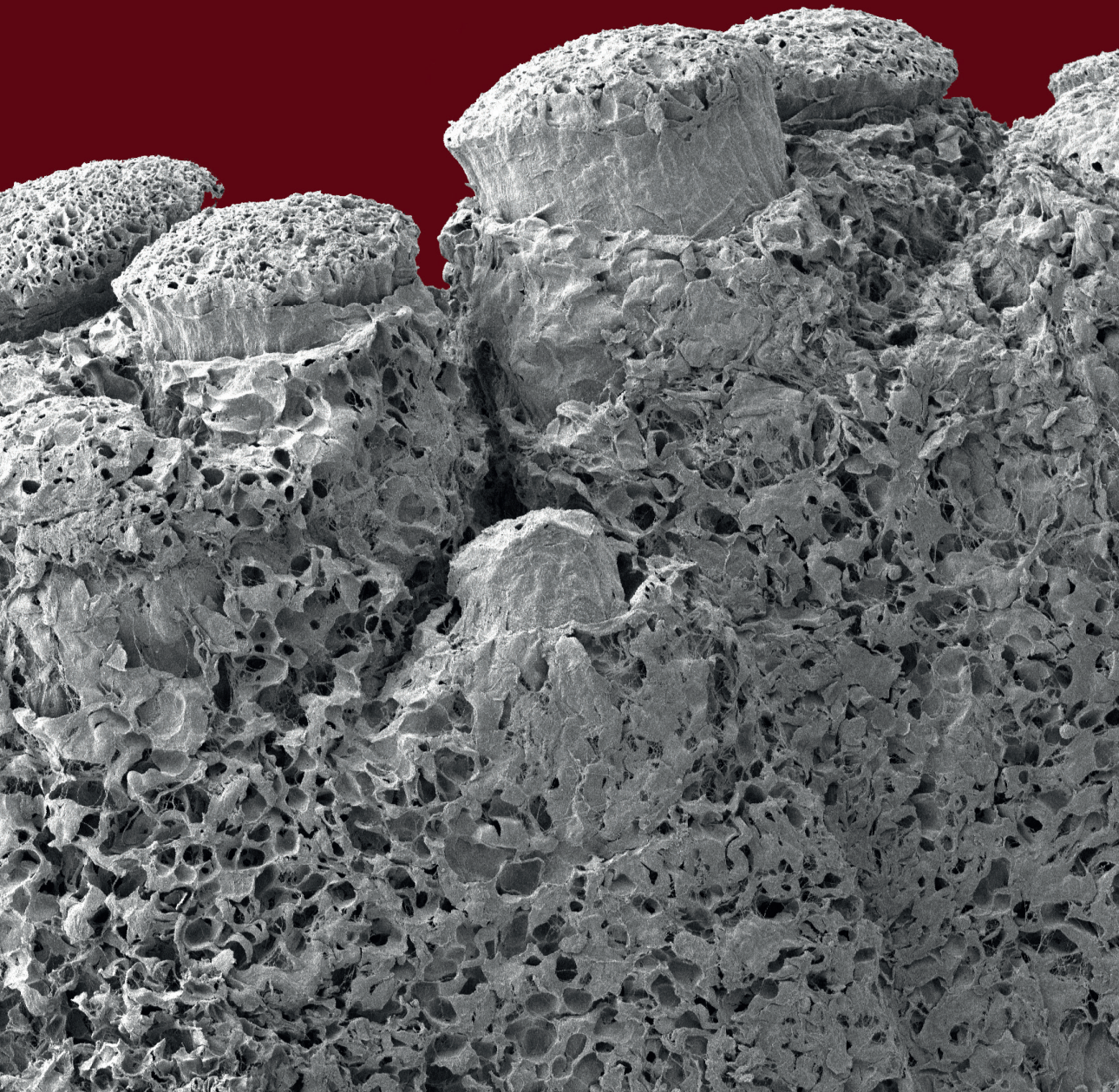

Appendices

Research data management
List of publications
PhD Portfolio
Curriculum Vitae
Dankwoord

RESEARCH DATA MANAGEMENT

All data obtained during my PhD research trajectory at the Radboudumc have been stored in secured files at the department drive on the Radboudumc server and in the secured Digital Research Environment (DRE) of the Radboudumc. The rat studies described in Chapter 3, 4, 5, 6 and 7 were approved by the Institutional Animal Care and Use Committee of the Mayo Clinic (Rochester, Minnesota, USA) (IACUC protocol A2464-00 and IACUC protocol A3348-18). The Mayo Clinical Human Cellular Therapy laboratory (Rochester, Minnesota, USA) provided the human Mesenchymal Stem Cells used in chapter 8 and 9. These Mesenchymal Stem Cells were obtained and used with approval of local institutional review boards (IRB #07-008842). Experimental primary and secondary data and analysis are available from the associated corresponding authors on request.

LIST OF PUBLICATIONS

1. **Bacteremia and pneumonia in a tertiary PICU: an 11-year study.** Mathot F, Duke T, Daley AJ, Butcher T. Pediatr Crit Care Med. 2015 Feb;16(2):104-13.

2. **Targeted stimulation of MSCs in peripheral nerve repair.** Mathot F, Shin AY, van Wijnen AJ. Gene. 2019 Aug 20;710:17-23.

3. **Adhesion, distribution, and migration of differentiated and undifferentiated mesenchymal stem cells (MSCs) seeded on nerve allografts.** Mathot F, Rbia N, Bishop AT, Hovius SER, van Wijnen AJ, Shin AY. J Plast Reconstr Aesthet Surg. 2020 Jan;73(1):81-89.

4. **Gene expression profiles of differentiated and undifferentiated adipose derived mesenchymal stem cells dynamically seeded onto a processed nerve allograft.** Mathot F, Rbia N, Thaler R, Bishop AT, van Wijnen AJ, Shin AY. Gene. 2020 Jan 15;725:144151.

5. **New methods for objective angiogenesis evaluation of rat nerves using microcomputed tomography scanning and conventional photography.** Saffari TM, Mathot F, Bishop AT, Shin AY. Microsurgery. 2020 Mar;40(3):370-376

6. **Revascularization patterns of nerve allografts in a rat sciatic nerve defect model.** Saffari TM, Mathot F, Friedrich PF, Bishop AT, Shin AY. J Plast Reconstr Aesthet Surg. 2020 Mar;73(3):460-468

7. **Adipose derived mesenchymal stem cells seeded onto a decellularized nerve allograft enhances angiogenesis in a rat sciatic nerve defect model.** Mathot F, Rbia N, Bishop AT, Hovius SER, Shin AY. Microsurgery. 2020 Jul;40(5):585-592.

8. **Introducing human adipose-derived mesenchymal stem cells to Avance® nerve grafts and NeuraGen® nerve guides.** Mathot F, Rbia N, Thaler R, Bishop AT, van Wijnen AJ, Shin AY. J Plast Reconstr Aesthet Surg. 2020 Aug;73(8):1473-1481

9. **Surgical angiogenesis modifies the cellular environment of nerve allografts in a rat sciatic nerve defect model.** Saffari TM, Badreldin A, Mathot F, Bagheri L, Bishop AT, van Wijnen AJ, Shin AY. Gene. 2020 Aug 15;751:144711.

10. **Microcomputed analysis of nerve angioarchitecture after combined stem cell delivery and surgical angiogenesis to nerve allograft.** Saffari TM, Mathot F, Thaler R, van Wijnen AJ, Bishop AT, Shin AY. J Plast Reconstr Aesthet Surg. 2020 Dec 24;S1748-6815(20)30714-2. Online ahead of print.

11. **Gene expression profiles of human adipose-derived mesenchymal stem cells dynamically seeded on clinically available processed nerve allografts and collagen nerve guides.** Mathot F, Rbia N, Thaler R, Dietz AB, van Wijnen AJ, Bishop AT, Shin AY. Neural Regen Res. 2021 Aug;16(8):1613-1621.

12. **Functional outcomes of nerve allografts seeded with undifferentiated and differentiated mesenchymal stem cells in a rat sciatic nerve defect model.** Mathot F, Saffari TM, Rbia N, Nijhuis THJ, Bishop AT, Hovius SER, Shin AY. Plast Reconstr Surg. 2021 Jun 21. Online ahead of print.

13. **Surgical Angiogenesis of Decellularized Nerve Allografts Improves Early Functional Recovery in a Rat Sciatic Nerve Defect Model.** Saffari TM, Mathot F, Friedrich PF, Bishop AT, Shin AY. Accepted for publication in Plastic and Reconstructive Surgery.

PHD PORTFOLIO

Institute for Health Sciences
Radboudumc

Name PhD candidate: F. Mathot Department: Plastic Surgery Graduate School: Radboud Institute for Health Sciences	PhD period: • 31-10-2016 – 10-09-2021 Promotor(s): • Prof. dr. S.E.R. Hovius • Prof. dr. D.J.O. Ulrich Co-promotor(s): • Dr. T.H.J. Nijhuis	
	Year(s)	ECTS
TRAINING ACTIVITIES		
Courses & Workshops		
• Microsurgery course (Mayo Clinic)	2016	1.5
• Microsurgery course (Erasmus MC)	2016	1.5
• IACUC: the care and use of Animals in Research at Mayo Clinic	2016	0.5
• RST Infection Prevention and control – Annual required training	2016	0.2
• HIPAA Privacy Module and your role in Protecting Patient Information	2016	0.2
• 2016 Integrity and Compliance Annual Training	2016	1
• Distal Radial Ulnar Joint Arthroplasty Lab, Aptis Medical	2016	0.4
• Mayo Clinic Brachial Plexus Dissection Course	2017	1
• CTSC 5600 Statistics in clinical research	2017	2
• 2017 Integrity and Compliance Annual Training	2017	1
• TriMed Orthopedics Distal Radius Surgical Approaches and Fragment Specific Fixation	2017	0.4
• Integra Total Wrist Arthroplasty	2017	0.4
• Small Joint Arthroplasty Lab, Integra	2017	0.4
• Synthes Orthopedics Small Bone Fixation Lab	2017	0.4

Symposia & congresses		
• Mayo Hand Club Meeting, May 2017 • 1x Oral presentation	2017	1.35
• ASSH Annual Meeting, September 2017 • 1x Oral presentation	2017	1.25
• NVPC dagen, May 2018 • 2x Oral presentation	2018	1
• FESSH, June 2018 • 1x Oral and 1x Poster presentation	2018	2
• ASSH Annual Meeting, September 2018 • 1x Oral and 2x Poster presentation	2018	2.5
• SEOHS 2018, December 2018 • 1x Oral presentation	2018	0.5
• ASPN Annual Meeting, February 2019 • 2x Oral presentation	2019	1.75
• FESSH, June 2019 • 2x Oral presentation	2019	2.25
Other		
• NIH R01 Grant proposal: Bridging the gap: Angiogenesis and stem cell seeding of processed nerve allograft (awarded with $1.250.000)	2016-2017	3
• Catharine van Tussenbroek Fonds (awarded with €1250)	2016	1
• Michael van Vloten fonds (awarded with €9.500)	2016	1.5
TEACHING ACTIVITIES		
Lecturing		
• Cadaver lab lecture on hand anatomy for medical students	2018	0.2
• Training my successor in person at Mayo Clinic	2018	2
Supervision of internships / other		
• Research collaborator at Mayo Clinic (supervising experimental designs, experimental execution and statistical analysis of results and reviewing manuscripts)	2018-present	6.5

CURRICULUM VITAE

Femke Mathot was born on November 5th , 1991 in Boskoop, The Netherlands, where she grew up with her parents and her two brothers. After graduating high school in 2009, she attended medical school at the Erasmus Medical Center in Rotterdam. For her master thesis she went to Melbourne, Australia to perform a study which eventually resulted in her first scientific publication. A minor on reconstructive surgery from head to hands in her fourth year of medical school, introduced her to plastic and reconstructive surgery and caused her growing interest into this medical field. After completing her senior internship at the plastic and reconstructive surgery department of the Erasmus Medical Center, she obtained her medical degree in 2016 and started working as a resident not in training at the general surgery department of the Maasstad Hospital in Rotterdam. In October 2016, she was invited for a research fellowship at the Mayo Clinic in Rochester, Minnesota, USA. Until November 2017 she worked in the microvascular research lab of the Mayo Clinic as a research fellow under the supervision of Dr. A.Y. Shin, Dr. A.T. Bishop and Prof. Dr. S.E.R. Hovius. The basic science studies she performed during that time laid the foundation of this PhD thesis. During her research fellowship she contributed to a NIH grant application, which was granted to the microvascular research lab just before her return to the Netherlands. This grant enabled the continuation of the research on peripheral nerve regeneration. Upon her return in the Netherlands, she combined her PhD trajectory with clinical work as a resident not in training at the plastic surgery department at the Radboudumc, under the supervision of prof. dr. D.J.O. Ulrich. In October 2018 she was admitted to the residency program of this department. She started residency at the general surgery department at the IJsselland Hospital under the supervision of dr. P.G. Doornebosch in April 2019. In October 2020 she returned to the Radboudumc for the continuation of the final 4 years of her residency in plastic surgery.

DANKWOORD

Velen hebben een bijdrage geleverd aan de totstandkoming van dit proefschrift; een aantal mensen zou ik graag expliciet willen bedanken.

Geachte **professor Hovius**, beste prof; als promotor heeft u mij de kans gegeven om het onderzoeksavontuur aan te gaan dat tot dit proefschrift heeft geleid. U heeft mij de vrijheid gegeven om mijzelf wetenschappelijk te ontwikkelen en was te allen tijde beschikbaar voor advies. Relativeren, op z'n tijd wat water bij de wijn doen en gesprekstechnieken tijdens 'onderhandelingen' (voor gevorderden) zijn dingen die ik van u heb mogen leren waar ik de rest van mijn carrière profijt van ga hebben. Gedurende mijn fellowship in Amerika, maar ook tijdens mijn klinische werkzaamheden heb ik heel duidelijk uw onvoorwaardelijke steun mogen ervaren (en die ervaar ik nog steeds!) en daar ben ik u enorm dankbaar voor. Wat een geluk dat ik nu op de valreep ook nog van uw chirurgische expertise mag leren.

Geachte **professor Ulrich**, beste prof; bedankt dat u mij heeft opgenomen in uw team. Ik ben trots dat ik me bij deze ambitieuze club heb mogen aansluiten waarvan u absoluut de aanvoerder bent. Patiëntenzorg, onderwijs en onderzoek; u neemt op al deze gebieden alleen genoegen met het uiterste en daarmee tilt u de kwaliteit van de gehele afdeling tot een hoger niveau. Dat het harde werken wordt afgewisseld met gezellige afdelingsuitjes en heerlijke skitrips maakt dat ik me geen betere opleidingsplek had kunnen wensen. Bedankt voor het vertrouwen en dat u van mij de beste versie van mijzelf als plastisch chirurg wilt maken.

Dear **dr. Shin**; thank you so much for the many opportunities you gave me while working in your renown lab at the Mayo Clinic. You gave me the freedom to develop new research techniques, to work on many of your innovative research projects and to present our studies at meetings throughout the United States. You never hesitated to invite me to all sorts of hands-on labs and courses and introduced me to many other inspiring nerve researchers and surgeons. Some professional, fruitful discussions were required to finish the final papers, for which I am very grateful as they led to the best versions of the manuscripts. Thank you for everything!

Dr. Nijhuis, beste Tim, bedankt voor jouw rotsvaste vertrouwen! Vanaf het allereerste moment heb je mij gesteund en zonder die steun had ik hier nu zeker niet gestaan. Jouw aansporingen ('strooi met je talent') en oneindige positivisme zijn aanstekelijk. Wat een mooie eigenschap om toekomstige collega's mee te nemen in je eigen succes zodat ook zij succesvol kunnen zijn. Een echte teamplayer; bedankt dat je daarmee zo'n goed voorbeeld voor me bent. Ik vind het ontzettend leuk dat onze samenwerking zich heeft voortgezet in Nijmegen en ik nu de fijne kneepjes van de plastische chirurgie van je mag leren.

Dear **dr. Bishop,** I am so grateful that I got to work in your inspiring lab and learn from the best! Not only am I impressed by your intellect and surgical skills; together with your modesty

and hospitality you set high standards as a role model. Needless to say, Gail was a great contributor to this hospitality. I will always remember decorating the (giant) Christmas tree, curving pumpkins for Halloween and all the other lovely dinners we had with your family. Thank you for making me feel at home in Rochester!

Geachte **prof. dr. Bartels**, **prof. dr. Coert** en **dr. van Alfen**; veel dank voor het willen lezen en beoordelen van dit proefschrift als leescommissie. **Prof. dr. van Osch**, **dr. Ruigrok** en **dr. de Ruiter;** bedankt dat jullie bereid zijn om plaats te nemen in de promotiecommissie. Ik kijk uit naar jullie inzichten.

Dear **Pat,** you were absolutely indispensable during the experiments. I would especially like to thank you for thinking along when I brought up another strange idea (I still remember you sitting on one of the counters of the lab taking pictures of nerves hidden under a selfmade box). Thank you for all those nice memories!

Dear **dr. van Wijnen**, dear Andre. Thank you for giving me the opportunity to use all the facilities of your impressive lab. You always stimulated me to critically evaluate our outcomes and you were really helpful during the writing process of the papers.

Dear **Roman,** it was ideal to have a 'supervisor' in the lab that was always around. Many times I have bothered you with questions and you always took the time to help me. Not to mention that you took care of my babies (my cells) when I was away; thank you for that.

Beste **Elisa,** wat hebben we veel mee gemaakt samen gedurende de vele uurtjes in (maar ook buiten) het lab. Het was fijn om iemand te hebben waarmee ik lief en leed kon delen, eindeloos kon kletsen en uren kon doorbrengen in de bioscoop. En ook jij **Dolph**, bedankt voor alle nodige afleiding binnen en buiten het lab. Ik ben zo blij dat we nu allemaal plastisch chirurg in wording zijn!

Beste **Nadia,** als mijn directe voorganger heb je veel voorwerk voor mijn onderzoeken verzet. Bovendien was je altijd bereid me te helpen en mee te denken voor een zo goed mogelijk resultaat. Bedankt!

Beste **Mana,** bang dat mijn onderzoek niet goed opgevolgd zou worden ben ik nooit geweest. Vanaf moment één ben je doortastend en ambitieus en een gouden match met dr. Shin. Ik ben onder de indruk van je netwerk-vaardigheden en heb er vertrouwen in dat je gaat bereiken wat je wilt bereiken.

Beste **Caroline**, **Liselotte**, **Maiwand** en **Tara**; ook jullie zijn allemaal onderdeel van de 'nerve research mafia' (aldus dr. Shin), ieder met z'n eigen kwaliteiten. Bedankt voor het uitvoeren van de experimenten die voorafgingen en zullen volgen op de studies beschreven in dit proefschrift. Het zou toch mooi zijn als we uiteindelijk met elkaar een klinische verandering teweeg kunnen brengen in de behandeling van perifeer zenuwletsel.

Beste **Hanneke Tielemans**, **Pieter Hupkens**, **Till Wagner**, **Franz Pronk**, **Erik Walbeehm**, **Tim de Jong**, **Brigitte van der Heijden, Marielle Vehmeijer** en **Stefan Hummelink**; bedankt voor jullie interesse in mijn onderzoek en jullie bereidheid mij alle ins en outs van ons mooie vak te leren.

Lieve collega assistenten; **Claire, Nicholas, Vera, Anne Sophie, Tycho, Lennart, Kaj, Bo, Harm, Saskia** en **Vivian**, lieve oud-collega's; **Marijn, Inge, Pepijn** en **Laura** en onderzoekers van de afdeling; wat is het top om met zulke leuke, enthousiaste en ambitieuze collega's samen te mogen werken. Bedankt voor jullie collegialiteit en gezelligheid.

Erik de Laat, **Nienke Gort, Yasmille Winnen** en **Stephan van Raay**; jullie hebben allemaal je eigen rol binnen de afdeling en vervullen die met verve. Bedankt daarvoor!

Alle poli-assistenten, OK-assistenten, medewerkers van het secretariaat en verpleegkundigen van de afdeling; zonder jullie natuurlijk geen goede patiëntenzorg. Bedankt voor jullie inzet en het verhogen van mijn werkplezier.

Alle lieve ijsvogels en in het bijzonder **dr. Doornebosch**; bedankt voor de mooie eerste jaren van mijn opleiding. Het fundament van mijn chirurgische loopbaan is bij jullie gelegd.

Lieve vrienden en vriendinnen;

Lieve **meiden**; wat voel ik me rijk met jullie vriendschap! Het is een geruststellend idee dat we elkaar nooit echt uit het oog zullen verliezen, want hoewel ik daar al serieuze pogingen voor heb gedaan (ik noem een half jaar Australië of een jaar Amerika); jullie springen gewoon in het vliegtuig om me op te komen zoeken. **Yvet**, jouw zorgzaamheid en interesse zorgen altijd voor goede gesprekken en ons matchende DNA geeft een speciale band. **Liek**, ik ken niemand zo creatief als jij en je droge humor heeft voor zeer ontspannende lach-sessies gezorgd. **Manon**, of eigenlijk Kuijf, jij bent overal voor in en met jouw eindeloze hoeveelheid energie ben je een echt organisatietalent, maar ook een heerlijk feestnummer. **Merel**, je bent ondernemend en enthousiast en we delen onze 'passie' voor lekker eten, wat fijn! **Britt**, onze knapste vriendin; ik kan altijd zo enorm met (en soms ook om) jou lachen, maar bovenal ben je ondernemend, altijd in voor gezelligheid en zorg je er ook nog voor dat onze wenkbrauwen 'on fleek' zijn. De vroegere stapvakanties hebben inmiddels plaats gemaakt voor volwassen (wijn)tripjes en de vele thee/wijn-avondjes zijn een zeer welkome afwisseling geweest op het zwoegen aan dit proefschrift. Onwijs bedankt voor alle afleiding en voor wie jullie zijn! Het is heerlijk dat ook onze leuke mannen zo'n goede match zijn; ik kijk met veel plezier uit naar alle toekomstige mooie momenten met jullie!

Lieve **kratjes**, jullie zorgen er met elkaar voor dat iedere activiteit, barbecue of feest memorabel is en daarom ben ik altijd graag van de partij. De skitrips, en dan in het bijzonder die van vorig jaar, zijn hier zeker een voorbeeld van. Dankzij jullie inzet hebben we er niet alleen voor gezorgd dat Boskoop en Reeuwijk voorop liepen in het ontwikkelen van groepsimmuniteit,

maar ook hebben de twee weken in quarantaine een significante bijdrage geleverd in het afronden van de laatste manuscripten van dit proefschrift. Bedankt!

Lieve **laaiblikkers**, hoewel de frequentie van gezamelijke uitjes is afgenomen nu we allemaal in andere levensfases zitten, weet ik dat ik op jullie kan rekenen als er iets te vieren valt.

Lieve **Tahnee** en **Karlijn**, de basis die we in Australië hebben gelegd zorgt nu nog steeds voor mooie middagen, avondjes en zelfs hele weekendjes weg. Bedankt voor jullie fijne vriendschap.

Lieve familie;

Lieve **Piet**, **José**, **Bas** en **Déwy**, bedankt dat ik vanaf het begin in een warm bad bij jullie terecht ben gekomen. Ik ben wellicht niet de ideale schoondochter/zus met mijn regelmatige afwezigheid door diensten/reizen/onderzoek, maar jullie interesse bleef onverminderd aanwezig en de spelletjesavonden en de gezamenlijke weekendjes weg koester ik.

Lieve **Martine**, ik ben vrij selectief als het gaat om potentiële vriendinnetjes voor mijn broers, maar jij was vanaf moment één door de selectie. Naast je liefde voor Vin en Novée ben je onwijs sportief, enthousiast, lief en altijd geïnteresseerd in mijn carrière-ontwikkelingen en daarmee ben je een zeer welkome aanvulling voor ons gezin.

Lieve **Rens** en **Vin**, mijn broers en nu ook mijn paranimfen! Hoewel ik wist dat mama ontroerd zou zijn van het feit dat ik jullie als paranimfen zou vragen, is dat niet mijn (enige) motivatie geweest. Rens, ik kijk op tegen jouw welbespraaktheid, je snelle humor en je intelligentie. Tijdens de vele discussies aan de keukentafel zijn we aan elkaar gewaagd en dat maakt het nooit saai. Vin, het enthousiasme waarmee je over werk, vakanties of jouw nieuwe kleine liefde Novée kunt vertellen is een jaloersmakend mooie eigenschap. Je nuchterheid en ondernemingsdrang maken van jou een grote broer om trots op te zijn. Wie denkt dat ik na het afleveren van dit proefschrift misschien naast mijn schoenen zou gaan lopen, kent mijn broers nog niet. Zij zullen er met veel liefde en aandacht voor zorgen dat ik lekker met beide voetjes op de vloer blijf staan. Bedankt daarvoor en voor het feit dat jullie op de grote dag naast mij willen staan!

Lieve **pap** en **mam**, wat fijn dat ik op deze manier de gelegenheid krijg om jullie te vertellen hoe dankbaar ik jullie ben voor de zorgeloze jeugd die jullie mij hebben bezorgd, voor het stimuleren om het beste uit mezelf te willen halen zonder mij druk op te leggen, voor het leggen van de basis van mijn zelfvertrouwen (en voor het voorkomen van het doorslaan daarvan), voor jullie nuchterheid, voor jullie onvoorwaardelijke steun, voor het altijd willen luisteren naar mijn verhalen en dan ook nog eens de moeite doen om de namen te onthouden (mama dan), voor al jullie warmte en liefde. Wat een voorbeeld zijn jullie voor mij. Ik had me oprecht geen betere ouders kunnen wensen!

Lieve **Sjelle**, als er iemand is die met name tijdens de jaren waarin ik werkte aan dit proefschrift heeft afgezien, ben jij het wel. Je hebt bewezen dat je geduld onuitputtelijk is en ik ben je eeuwig dankbaar dat je altijd als mijn rots in de branding hebt willen fungeren. Met je humor, je zorgzaamheid, je vrolijkheid, je nuchterheid en je liefde maak je ook van mij een leuker mens. Ik kijk enorm uit naar alle mooie en fijne avonturen die we samen zullen gaan beleven.

Printing of this thesis was financially supported by:

Radboudumc

ChipSoft

Aleamed

BAPMEDICAL
MEDICAL CARE FOR THE SKIN

JVPC
Junior Vereniging
Plastische Chirurgie

QuaMedical
for reconstructive surgery products

NVPC
Nederlandse Vereniging
voor Plastische Chirurgie
HANDCHIRURGIE, RECONSTRUCTIEVE EN ESTHETISCHE CHIRURGIE